The effects of environmental and microbiota manipulation on myelination in the YAC128 and BACHD models of Huntington disease

Thesis submitted in September 2017 for the

Degree of Doctor in Philosophy

By

Carola Izabela Radulescu

Department of Psychology

The University of Sheffield

Thesis abstract

White matter (WM) deterioration is increasingly being recognised as a hallmark of Huntington disease (HD) and is correlated to disease severity. Environmental experience has also been shown to alter white matter structure and function, and microbiota-gut-brain bidirectional communication has been implicated in the regulation of oligodendrocyte differentiation and myelination. This suggests that environmental and microbiota manipulations can be used as assays to interrogate white matter plasticity in HD. This could provide new insights into the mechanisms and role of white matter changes in HD pathogenesis, and inform discovery of novel biomarkers and therapeutic approaches in the disorder.

This thesis describes three studies that address this question directly. In the first study, we examined the effects of environmental enrichment on white matter characteristics and behaviour in the YAC128 mouse model of HD and wild-type (WT) controls. This was followed by a second study in which the same outcomes were examined in response to environmental deprivation through social isolation in identical mouse genotypes. Finally, we examined the effect of microbiota on white matter in BACHD mouse models of HD and WT controls, housed under germ-free (GF) and specific pathogen free (SPF) conditions. White matter plasticity was examined using a range of techniques including transmission electron microscopy, immunohistochemistry, and immunoblotting, and behaviour and motor function evaluated using a battery of targeted tests.

Our findings provide evidence that environmental and microbiota manipulation has differential and complex effects on white matter in WT and HD mice, including alterations in axonal diameter, myelin thickness, as well as oligodendrocytes cell populations. The work described herein therefore offers new insights into white matter plasticity and abnormalities in HD and lays the foundation for future studies.

I would like to dedicate this thesis to my partner and best supporter, Sam Harris, and to my amazing friend and inspiration, Barbora Nováková.

Acknowledgements

I would like to express my special appreciation and thanks to my TLGM supervisor, Asst Prof Mahmoud Pouladi. It has been a short but intense two years in his lab. Mahmoud is one of the friendliest and most approachable people I have worked with, and that was of considerable help when transitioning from Sheffield to Singapore. I admire his love for science, his brave attitude towards collaborations, and his high ambitions to always achieve more. I appreciate that over the last two years he has pushed me hard to always aim higher in science, and running (#first10K) related goals. This PhD journey would have not even started if it was not for my Sheffield supervisor, Dr Nicolas Vautrelle (Nico). While working together, I learnt three important skills that I will hope to carry with me throughout my career, and life: patience, persistence and 'build your own equipment' sort of skill. I would like to give my very special thanks for supporting me for all these (too many) years, throughout my undergraduate and MSc dissertation projects, as well as for the first two years of my PhD in Sheffield. I would like to wish him the best of luck in the next steps of his career in New Zealand. I would also like to thank super Prof Peter Redgrave (Pete), who accepted to take me in his lab as an unexperienced psychology student. Pete's passion for the study of the basal ganglia and all its intricate and complex connections, as well as his ideas that often go beyond science, and into the realm of philosophy, have always inspired me. And finally, I would like to thank my supervisor Dr Enrico Bracci for giving me the opportunity to learn the multi-electrode array technique, for all the lab meeting conversations and advice.

Throughout my PhD journey I had the opportunity to work in two great labs, with some exceptional people. I want to start by thanking the whole TLGM NDD lab in Singapore, as they have showed me the joys of working in a team – Kagistia, Xiaohong, Ruizhu, Bernice. Special thanks to those who directly supported the projects presented in this thesis: Marta Garcia Miralles, for teaching me the (too many to list here) technical skills, and for always standing up for me; Harwin Sidik, for being my electron microscopy

buddy, and for all the brilliant and useful science related advice; Costanza Ferrari Bardile, for all the help in the lab, and the friendship outside the lab; Amberlyn Tan, for setting up the mice colonies, genotyping, and for the tissue collection help; Yihui Huang and Bryan Ng, for teaching me all about western blots; Amirah Yusof, for all the great help you offered over the last few months of my thesis write up; Amanda Chern and Rachel Tan, for helping with the final blots and cell counting. I would like to thank my undergraduate students who helped greatly with these projects: Hannah Low and Eveline Shevin. I would also like to thank our collaborators: Dr. Paola Flórez De Sessions, Eliza Ho Xin Pei, Collins Wenhan Chu and Emma Layton (GIS, A*STAR); Dr Florent Ginhoux and Donovan Low, (SigN, A*STAR); and Prof Sven Pettersson, Dr Lee Hae Ung (Leon), and Llanto Elma Faylon (MHINM, NTU). For technical support I would like to thank Laytin (Bronjo Medi) and her team, and special thanks for their patience and perseverance in teaching me the ‘dark science’ of electron microscopy (EM) to Micky Leong Lo Ngah, and the team from the EM Unit at NUS, Singapore.

Everyone in the Sheffield Alfred Denny neuroscience groups has kindly offered their support during my PhD journey there. This support was manifested either through sharing of scientific knowledge and skills, or funny stories over a pint at Uni Arms: Mariana, Rasha, Martin, Paul, Luke, Aneurin, Jason, Clare, Myles, Kevin, Tim, and of course the lovely Shef neuro-girls – Kira, Rebecca, Priya. Special thanks to the rodent room: Kam, Kendra and Brandon. For technical support I would like to thank Michael, Andy and Len.

I would like to thank my examiners for taking their time to read this thesis, and offer me their critical consideration. My regards also go to my postgraduate tutors, Pete Totterdale and Liz Milne for pushing me to finish writing up, and to Josie Cassidy, Pauline Low and April Tan for all the admin related support.

Among the main perks of doing an intercontinental PhD is building beautiful, long-lasting, multi-cultural friendships. This journey would have not been as adventurous and enjoyable if not for the new and old friends I have had along the way. Special thanks to my PhD buddies in Sheffield: Chloe, Carla, James, David, and Jovin, I have always had good laughs with you. I am

forever grateful to Kira for all the help she offered in my transition to Singapore. To my Botannia flatmates, in Singapore: the 41 crew - Claudia, Rebecca, James, and Dorin, and the 42 crew - Costanza, Maria, Kat, and Kortessa, I loved every single adventure of our #phdatthetropics life. The Fantastics (four), Marta, Harwin and Bryan, offered me the perfect package of helpful lab mates, and the most supportive, reliable and fun friends. Yihui and Madeline, I greatly enjoyed all the fantastic Singaporean food adventures, and I will forever crave for chilli crab, xiao long bao, durian and mangostene. I would also like to thank my close friends who made the long journey from Europe, as well as other parts of Asia, to Singapore, and came to visit - Patricia, Catalin, Hanna, Rafet, Rachel, Barbora, Pin, Ashwini, and Fiona.

Finally, I would like to thank my parents, Aurora and Gheorghe, and my grandparents, Eva and Ilie. I would definitely not be here if it was not for the upbringing and opportunities you offered, and for the sacrifice you made to help me through school and (too many years of) university. I know it has not been easy being away from home for over 10 years, and for that I am grateful for your understanding, support and for respecting the choices I have made. *Dragi părinți și bunici, vă mulțumesc din suflet pentru tot.*

And last, but not least, I would like to thank my biggest supporter, and wonderful partner in (neuro)science and in life, Samuel Sebastian Harris (not to be confused with the other Sam Harris!). Thank you for instigating in me an even greater love for science and discovery, for critical thinking and for ethical consideration (and, of course, for first edition books!). You are truly and forever an inspiration.

Table of contents

List of figures

List of tables

Index of abbreviations

ABC	.....	ABC Vectastain Kit
AD	.....	Alzheimer disease
BAC	.....	Bacterial artificial chromosome
BrdU	.....	5-bromo-2-deoxyuridine
BSA	.....	Bovine serum albumin
CAG	.....	Cytosine-adenine-guanine
CC	.....	Corpus callosum
ChR2	.....	Channelrhodopsin
CNP	.....	2',3'-cyclic-nucleotide 3'-phosphodiesterase
CNS	.....	Central nervous system
DAB	.....	Diaminobenzidine
DARPP-32	.....	Dopamine-regulated neuronal phosphoprotein
DDSA	.....	Dodecenylsuccinic anhydride
DH	.....	Deprived housing
DMP-30	.....	2,4,6-Tris(dimethylaminomethyl)phenol
DNA	.....	Deoxyribonucleic acid
DT-MRI	.....	Diffusion tensor magnetic resonance imaging
DTI	.....	Diffusion tensor imaging
EH	.....	Enriched housing
ENS	.....	Enteric nervous system
EPM	.....	Elevated plus maze
FA	.....	Fractional anisotropy
FAD	.....	flavin adenine dinucleotide
fmiCC	.....	Forceps minor of corpus callosum
FST	.....	Forced swim test
GABA	.....	Gamma-Aminobutyric acid
GI	.....	Gastrointestinal
gCC	.....	Genu of corpus callosum
GFP	.....	Green fluorescent protein
GST-π/pi	.....	Glutathione S-transferase π
GlutAH	.....	glutaraldehyde
GPe	.....	globus pallidus pars externa
GPi	.....	globus pallidus pars interna
HCl	.....	hydrochloric acid

HCN	.....	hyperpolarization-activated cyclic nucleotidegated
HD	.....	Huntington disease
HTT	.....	Huntingtin protein
HTT	.....	Huntingtin gene
IB	.....	Immunoblotting
ID	.....	Inner diameter
IHC	.....	Immunohistochemistry
IF	.....	Immunofluorescence
M	.....	Molar (for concentrations)
MAG	.....	Myelin-associated glycoprotein
MBP	.....	Myelin basic protein
mHTT	.....	Mutant huntingtin
MOBP	.....	Myelin-associated oligodendrocytic basic protein
MOG	.....	Myelin oligodendrocyte glycoprotein
MRI	.....	Magnetic resonance imaging
MS	.....	Multiple sclerosis
MSN	.....	Medium spiny neuron
MW	.....	Molecular weight
N	.....	Normal (for concentrations)
NaN3	.....	Sodium aside
NGS	.....	Normal goat serum
NMDA	.....	N-methyl-d-aspartic acid
OCT	.....	Optimum cutting temperature
OF	.....	Open field (test)
Olig1	.....	Oligodendrocyte transcription factor 1
Olig2	.....	Oligodendrocyte transcription factor 2
OPC	.....	Oligodendrocyte precursor / progenitor cell
OsO4	.....	Osmium tetroxide
PBS	.....	Phosphate buffered saline
PBS-T	.....	Phosphate buffered saline + Tween
PCR	.....	Polymerase chain reaction
PD	.....	Parkinson disease
pf	.....	Parafascicular nucleus
PFA	.....	Paraformaldehyde
PFC	.....	Prefrontal cortex
pH	.....	Potential of Hydrogen
pn	.....	Post-natal

polyQ	.....	Polyglutamine
PV	.....	Parvalbumin
qRT-PCR	.....	Quantitative real-time PCR
RNA	.....	Ribonucleic acid
rpm	.....	rotations per minute
RR	.....	Rotarod (test)
RT	.....	Room temperature
SA	.....	Spontaneous activity (test)
SH	.....	Standard housing
SNc	.....	Substantia nigra pars compacta
SNr	.....	Substantia nigra pars reticulata
TEM	.....	Transmission electron microscopy
TH	.....	Tyrosine hydroxylase
UV	.....	Ultraviolet
WB	.....	Western blot
WM	.....	White matter
WT	.....	Wild-type
YAC	.....	Yeast artificial chromosome

Chapter 1. General introduction

1.1. Huntington Disease

Huntington disease (HD) is a fatal autosomal-dominant neurodegenerative disorder that affects approximately 5-10 in 100,000 individuals, and is particularly prominent amongst those of Caucasian European descent (Fisher & Hayden, 2014; Morrison, 2012; Wexler et al., 2016). HD was first characterised by George Huntington in the late 19th century (Huntington, 1872), and it is now well established to be associated with a triad of clinical features such as progressive motor, cognitive, and psychiatric, decline. Disease onset is inferred from the manifestation of perceptible motor signs, such as chorea, dystonia and bradykinesia, and occurs on average at 40 years of age, with death normally following within 15-20 years (Ross & Tabrizi, 2011). The period prior to a formal diagnosis of manifest HD is normally referred to as the pre-manifest, or pre-symptomatic, period, although these terms may be somewhat of a misnomer, given that neuropathological changes, particularly in the striatum, and cognitive and psychiatric disturbances, may precede motor onset by several years (Cha et al., 1998; Gutekunst et al., 1999; Hobbs et al., 2010; Marder et al., 2000; Tabrizi et al., 2013). HD is caused by the expansion of the cytosine-adenine-guanine (CAG) triplet repeat in the huntingtin (*HTT*) gene, located on the short arm of chromosome 4, that encodes the 350kDa huntingtin (HTT) protein with a polyglutamine (polyQ) stretch located at the N-terminus (Macdonald, 1993). HD is associated with CAG repeats greater than 36, with *HTT* CAG repeat length being inversely correlated to age of motor onset (Andrew et al., 1993; Duyao et al., 1993; Snell et al., 1993).This relationship accounts for approximately 50-70% of the observed variance in clinical onset, with greater onset variance associated with lower CAG repeats, potentially due to a greater influence of genetic and environmental modifiers, and lower variance with larger repeat sizes greater than 44 (Langbehn et al., 2004). A parametric survival model predicts that a 40-year old individual with 42 CAG repeats has a 91% chance to present with motor symptoms by the age of 65 (i.e the disease is essentially fully penetrant), whilst that with 36 repeats has a

14% chance of onset before the age of 75 (Langbehn et al., 2004). Importantly, many patients possessing CAG repeats less than 41 may not present with clinical symptoms during their lifetime (i.e. the disease is partially penetrant) (Langbehn et al., 2004).

The HTT protein is composed of approximately 50 recurring amino-acids, known as HEAT (Huntingtin, Elongation factor 3 (EF3), protein phosphatase 2A (PP2A), yeast kinase TOR1) repeats, that form a superhelical structure with a hydrophobic core (Andrade & Bork, 1995; Li et al., 2006). HTT is predominantly cytoplasmic, normally palmitoylated at cysteine 218 (Yanai et al., 2006), and is expressed in cells throughout the human body, although more preponderantly in the brain and testes (DiFiglia et al., 1995). HTT appears to be important for early embryonic development (Ross & Tabrizi, 2011) and is thought to play a key role in neurogenesis (Nguyen et al., 2013). It is considered to be a scaffolding protein that can coordinate complexes of other proteins.

While the pathogenesis of HD is still poorly understood, it is well established that the presence of a polyQ expansion forms an abnormal conformation of mutant HTT (mHTT) and confers a so-called gain in toxic function (Poirier, Jiang, & Ross, 2005; Ross & Tabrizi, 2011). Mutant HTT is also more susceptible to proteolysis, relative to the wild-type HTT protein, and its truncation is known to promote generation and aggregation of N-terminal fragments (Lunkes & Mandel, 1998; Walker, 2007; Wellington, Leavitt, & Hayden, 2000). These fragments may be generated via a variety of proteases such as caspase-3 and 6 (Wellington et al., 2002), calpains (Kim et al., 2001) and matrix metalloproteinase-10 (Miller & Bezprozvanny, 2010), and/or abnormal splicing of HTT (Sathasivam et al., 2013). Accumulation and aggregation of N-terminal fragments in neuronal nuclei has been shown to be promoted by phosphorylation of the N-terminal S16 in HTT (Havel et al., 2011). Furthermore, polyQ expansion in HTT is associated with reduced palmitoylation, which promotes the formation of intra-nuclear inclusion bodies (i.e. large abnormal HTT aggregates (Yanai et al., 2006). Intra-cellular mutant HTT aggregates, a

pathological signature of HD, are not only confined to cell nuclei, but have also been observed in dendrites, axonal terminals, in addition to the cytoplasm (DiFiglia, 1997; Gutekunst et al., 1999; Ross & Tabrizi, 2011). However, whether mutant HTT aggregation, in of itself, promotes cytotoxicity, or provides neuroprotection, or is simply an epiphenomenon, remains a topic of intense debate (Hackam et al., 1998; Bjørkøy et al., 2005). Moreover, the effect of cellular location of these inclusions has only recently been revealed, suggesting that nuclear inclusions are well tolerated, but cytoplasmic peri-nuclear inclusions are correlated with cell death (Liu et al., 2014).

1.1.1. Neurodegeneration and pathogenic mechanisms in HD

HD is associated with profound and selective loss of striatal cells, particularly GABAergic medium spiny neurons (MSNs), which project to the globus pallidus (GP) and substantia nigra (SN). Of these, enkephalin-containing MSNs that project to the external area of the GP (GPe) appear to be particularly susceptible to degeneration compared to substance P-containing MSNs that project to the internal area of the GP (GPi); in turn, the latter neurons projecting to the pars reticulata portion of the SN (SNr) are more vulnerable than those which project to the compacta portion of the SN (SNc) (Reiner et al., 1988; Sapp et al., 1995). Interestingly, large interneurons are spared from degeneration. These neuropathological changes are consistent with the observation of chorea in the early stages of HD due to dysregulation of basal ganglia-thalamocortical circuitry. Other areas that undergo atrophy in HD include the cerebral cortex, thalamus, hypothalamic lateral tuberal nuclei, and notably, sub-cortical white matter, and can be even more widespread in cases of juvenile HD onset (Ross & Tabrizi, 2011).

Mutant HTT disrupts normal (i.e. wild-type HTT regulated) vesicle transport and recycling (Caviston & Holzbaur, 2009), partly through interaction with Huntingtin-Associated Protein 1 (Hap1), leading to

inhibition of cortical trafficking/release of pro-survival brain derived neurotrophic factor (BDNF), and thus diminished neurotrophic support for striatal cells (Gauthier et al., 2004). Mutant HTT also disrupts fast axonal transport of organelles (Gunawardena et al., 2003; Szebenyi et al., 2003), and can reduce mitochondrial trafficking to synapses, affecting production of ATP (Orr et al., 2008; Shirendeb et al., 2011). Furthermore, mutant HTT also disrupts the mitochondrial protein import complex TIM23, to impair transport of proteins into mitochondria, leading to mitochondrial dysfunction and neuronal cell death (Yano et al., 2014).

Mutant HTT may also impair the autophagy-lysosome and ubiquitin-proteasome systems (UPS) that form two of the major pathways of degradation of intracellular proteins. Specifically, mutant HTT was found to diminish the ability of autophagic vacuoles to recognise cytosystolic cargo, thus compromising autophagic clearance (Martinez-Vicente et al., 2010). In turn, dysfunctional proteasome activity, possibly due to sequestration of UPS components into inclusion bodies, was also reported by early studies (Bence, 2001; Bennett et al., 2005). However, other work did not report a dysfunctional UPS in HD (Maynard et al., 2009), although this was later reconciled by UPS impairment being found to be restricted to a time-window preceding the presentation of inclusion bodies (Mitra, Tsvetkov, & Finkbeiner, 2009). Dysregulation of these protein degradation pathways may therefore lead to impaired clearance and toxic intra-cellular protein accumulation.

Another aspect believed to play a key role in HD pathogenesis pertains to the effect of mutant HTT on gene transcription. Microarray studies have demonstrated that several genes exhibit altered expression patterns in HD (Hodges, 2006; Luthi-Carter, 2000; Sipione et al., 2002). Mutant HTT has been shown to interact with a number of regulators of transcription, including cyclic adenosine monophosphate (cAMP) response element binding (CREB) protein, and CREB-binding protein (CBP) (Nucifora, 2001; Steffan et al., 2001), associated with cell proliferation and survival, peroxisome proliferator-activated receptor gamma coactivator 1-alpha

(PGC-1α) (Cui et al., 2006), associated with energy metabolism, and others such as Sp1 transcription factor (Dunah et al., 2002) and basal transcription factors (Ross & Tabrizi, 2011). Importantly, decreased transcription of brain derived neurotrophic factor (BDNF) in HD may underpin the increased relative susceptibility of the striatum to neurodegeneration (Zuccato & Cattaneo, 2009).

Since MSNs are innervated by glutamatergic axons, a long-standing hypothesis is that over-stimulation of glutamate, particularly N-methyl-D-aspartate (NMDA), receptors may lead to excitotoxicity and death in these cells (Coyle & Schwarcz, 1976; Flint Beal, 1994; Zeron et al., 2002). Changes in NMDA receptor subunits early in HD (Ali & Levine, 2006); (Benn et al., 2007), as well as impaired trafficking of NMDAR due to mutant HTT (Fan et al., 2007), may thus selectively predispose MSNs to excitotoxicity. Alternatively, glutamate clearance by glia may also be diminished in the presence of mutant HTT, that could also result in excitotoxicity (Shin et al., 2005).

1.1.2. The role of glial cells in HD pathogenesis

Little is known about the role of glia, comprising of astrocytes, microglia and oligodendrocytes, on HD pathogenesis. However, reactive gliosis has been observed in a number of HD animal models as well as patients (Reddy et al., 1998). Expression of mutant HTT in astrocytes was correlated to disease severity, reduced the expression of the glutamate transporters, GLT-1 and GLAST, in HD mouse models and patients, thus decreasing glutamate uptake, and suggesting this mechanism could play a key role in HD neurodegeneration through promotion of excitotoxicity (Bradford et al., 2009; Faideau et al., 2010; Shin et al., 2005). A recent study has highlighted the likely causal role for glia in HD, by demonstrating striatal transplantation of normal glia in transgenic HD mice slowed patho-progression and increased survival (Benraiss et al., 2016). Expression of mutant HTT in astrocytes was also seen to suppress release of BDNF, vital for cell proliferation and survival (Hong et al., 2016; Wang et al.,

2012). Kir4.1 K+ ion channel expression was found to be decreased in a HD mouse model, and associated with increased MSN excitability; viral delivery of Kir4.1 channels to striatal astrocytes subsequently diminished MSN dysfunction, decreased motor deficits, and increased survival (Tong et al., 2014). In addition, neuroinflammation may also play a key role in HD neuro-degeneration, since microglia have been demonstrated to be robustly activated in pre-symptomatic and early stages of HD (Sapp et al., 2001; Tai et al., 2007), in a manner correlated to disease severity, and leading to increased release of pro-inflammatory cytokines and chemokines (Björkqvist et al., 2008; Wild et al., 2011). Furthermore, expression of mutant HTT in microglia was shown to facilitate pro-inflammatory transcriptional activation, and that such microglia were more predisposed to inducing neurodegeneration (Crotti et al., 2014).

Lastly, recent studies have begun to elucidate the effect of mutant HTT on oligodendrocytes, and the roles of such glia on HD pathogenesis; this forms a central theme to this thesis, and is described in detail in the following sections.

1.1.3. Current treatment for HD

HD is a single-gene disease and as such is an ideal model to study neurodegenerative diseases as a whole, and test for possible therapeutic interventions that can slow or suppress disease onset. However, despite this, and numerous clinical trials, there are currently no disease-modifying drugs available to stop or reverse HD. Therapeutic strategies are limited to ameliorating motor, behavioural and psychiatric symptoms only, for which there are only two FDA-approved pharmacological agents available. These consist of tetrabenazine, also licensed in the UK, and its deuterium altered milder cousin deutetrabenazine, to treat chorea, a common symptom in HD. Neuroleptics, also, may be beneficial in patients that have concurrent psychosis, and selective serotonin reuptake inhibitors (SSRIs) may help to manage depression and suicidal ideation - symptoms that can be compounded by identical side-effects of tetrabenazine. Furthermore, as described earlier, not all the variability in onset and progression of HD can

be explained by CAG repeat length and much of this variability may be underpinned by environmental factors. This suggests that disease onset, progression, and symptomatology, can be modulated, to some extent, by lifestyle factors and multi-disciplinary interventions. Accordingly, this possibility forms another central theme to this thesis.

1.1.4. Mouse models of HD

Much of the knowledge we have on the pathogenesis of HD has derived from the use of model systems, the most common of which being that of the mouse. Mouse models of HD are generated using knock-in or transgenic approaches (see Table 1.1 for a summary of common mouse models of HD).

Knock-in mouse models probably recapitulate the genetic insult more faithfully than transgenic models, have normal life-span, and display a relatively slow and mild behavioural and neurodegenerative phenotype. Full-length mutant HTT knock-in mouse models, which include the CAG140, HdhQ111 and HdhQ150 lines, have been largely generated through knock-in of a CAG tract-expanded *HTT* exon 1 into the endogenous *Htt* gene locus, with CAG repeat sizes ranging 5-200, and can be homozygous or heterozygous for the mutation (Pouladi, Morton, & Hayden, 2013a).

Another class of genetic mouse models includes transgenic lines, which express N-terminal fragments of human *HTT* and include the R6/2 (the first transgenic mouse of HD), R6/1 and N171-Q82 lines. These mice are associated with a fast disease onset, motor, cognitive and behavioural deficits, and loss of body weight and reduced life-span. The N171-82Q shows motor deficits from 11 weeks of age, while in the R6/1 model behavioural deficits appear around 6-8 weeks of age and in the juvenile R6/2 HD model, deficits were seen as early as 3.5 weeks (Lione et al., 1999).

Finally, and of direct relevance to this thesis, transgenic models have been created that express the full-length mutant HTT using yeast artificial chromosome (YAC) (Hodgson et al., 1999) and bacterial artificial chromosome (BAC) (Gray et al., 2008) technology. BACHD and YAC128 models express the entire human *HTT* locus with 125 and 97 CAG repeats, respectively (Hodgson et al., 2008; Gray et al., 2008). These models are well known to display progressive motor, cognitive and psychiatric abnormalities, increases in body weight, as well as relatively late-onset selective striatal atrophy.

Table 1.1 Commonly used mouse models of HD

Model	Transgene Product	Promoter	CAG Length	Behavioural Phenotype	Neuropathology Phenotype
Full length knock-in models					
CAG140	Full-length chimeric human *HTT* exon 1:mouse *Htt*	Endogenous mouse *Htt* promoter	140	Hyperactivity at 4 weeks then hypo-activity by 12 weeks. Gait deficits by 48 weeks. Body weight loss.	Neuronal loss. Intra-nuclear inclusions and neuropil aggregates by 8 months.
HdhQ111	As above	As above	111	Gait deficits by 24 months.	Nuclear inclusions at 48 weeks, neuropil aggregates at 68 weeks. Astrogliosis by 96 weeks.
HdhQ150	As above	As above	150 & 200	Gait and locomotor deficits, clasping, between 4-10 months	Intra-nuclear aggregates, gliosis, axonal dysfunction at 14 months.
Hdh4/Q72 & Hdh4/Q80	As above	As above	72 & 80	Aggressive behaviour. Impaired rotarod performance	Aggregates by 28 weeks with nuclear inclusions by 96 weeks
zQ175	As above	As above	188	Hypo-activity at 8 weeks and impaired rotarod performance at 30 weeks	Decreased cortico-striatal volume, and neuronal density at 4 months.
Truncated N-terminal fragment models					
R6/1	67 amino acids of N-terminal fragment (human HTT)	Human *HTT* promoter	116	Body weight loss at 22 weeks. Motor deficits at 4-5 months	Neuronal atrophy and loss. Aggregates at 2 months. Decreased brain volume by 18 weeks.
R6/2	As above	As above	144-150	Rotarod impairments by 5 weeks. Dystonia with clasping by 6	Gross brain atrophy by 60 days with neuronal loss and astrogliosis by 90

				weeks. Body weight loss by 9 weeks.	days. Aggregates from day 1
N171-Q82	171 amino acids of N-terminal fragment (human *HTT* cDNA)	Mouse *Prp* promoter	82	Motor deficits and clasping at 11 weeks. Body weight loss.	Gross brain atrophy with striatal neuron loss. Aggregates at 16 weeks
Full length transgenic models					
YAC128	Full-length human *HTT*	Human *HTT* promoter and regulatory elements	128	Motor performance abnormalities at 3 months and rotarod impairment by 6 months. Increase in body weight at 2 months.	Striatal and cortical neuron loss and decreased cortical and striatal volume by 12 months. Macroaggregates at 12 months.
YAC72	As above	As above	77	Hyperactivity at 7 months. Body weight loss.	Selective striatal neurodegeneration at 12 months.
BACHD	As above	As above	97	Rotarod impairment at 8 weeks. Gain in body weight.	Decreased cortico-striatal volume and gross brain atrophy at 12 months. Cortical inclusions 12-18 months.

Prp, prion protein; *HTT,* huntington.

1.2. Oligodendroglial populations dynamics and adaptive myelination

1.2.1. Overview of glial cells in the central nervous system

Four major types of glial cells populate the central nervous system (CNS): astrocytes, microglia, oligodendrocytes, and oligodendrocytes precursor cells (OPCs) or neuron-glia 2 (NG2) cells. Historically, glial cells were viewed as forming the glue or connective tissue of the brain. However, more recent work has demonstrated each type of glial cell to be highly specialized and plays supportive roles in the function and plasticity of the CNS, including response to injury, homeostatic function and trophic support, as well as modulation of signal propagation along axons (Domingues et al., 2016; Zuchero & Barres, 2015). Astrocytes have critical roles in supporting the blood-brain barrier, contributing to neuronal survival and synapse maintenance (Barres, 2008; Graeber, Li, & Rodriguez, 2011). Microglia, in turn, are the principal resident immune cells of the brain, and are involved in defense against pathogens and clearance of dead cells (Chan, Kohsaka, & Rezaie, 2007). NG2 cells are oligodendrocyte precursor cells (OPCs), and generate myelinating oligodendrocytes in the post-natal brain, and participate in maintaining CNS homeostasis and tissue repair (Hughes et al., 2013; Nishiyama et al., 2016; Raff, Miller, & Noble, 1983). Critical roles for oligodendrocytes include myelination (Tomassy, Dershowitz, & Arlotta, 2016), trophic (Bankston, Mandler, & Feng, 2013), and metabolic, support for axons (Fünfschilling et al., 2012; Lee et al., 2012), and modulation of neuroplasticity (Bechler, Swire, & Ffrench-Constant, 2017; Osso & Chan, 2017).

1.2.2. Oligodendroglial lineage – from OPCs to mature myelinating oligodendrocytes

Oligodendrocytes precursor cells (OPCs)

OPCs, also known as polydendrocytes, or as neuron-glia 2 (NG2) cells, are bipolar, highly proliferative cells that have the ability to migrate and differentiate into oligodendrocytes (Nishiyama et al., 2009; Nishiyama et al., 2016). Adult OPCs remain in a constant and slow proliferative state (Clarke et al., 2012; Hughes et al., 2013; Kang et al., 2010) and generate oligodendrocytes continuously throughout life (Yeung et al., 2014). This process takes place at a much slower rate in adulthood relative to development (Dimou et al., 2008; Rivers et al., 2008). However, it is still unclear whether all OPCs cells differentiate into oligodendrocytes, or whether a proportion of these lose their capacity to do so with age (Nishiyama et al., 2016). OPCs are homogenously distributed throughout the brain, in both gray and white matter regions, such as the corpus callosum, the cerebellum, the cortex and the optic nerve (Clarke et al., 2012; Hughes et al., 2013; Levine, Stincone, & Lee, 1993; Shi, Marinovich, & Barres, 1998). The capacity for OPCs to generate oligodendrocytes in the adult brain is greater and faster in white, compared to gray, matter, where they also exhibit faster differentiation and high proliferation rate, as well as a faster cell cycle (Dimou et al., 2008; Hill et al., 2013; Rivers et al., 2008; Viganò & Dimou, 2016; Viganò et al., 2013; Yeung et al., 2014; Young et al., 2013; Zhu et al., 2011). These regional differences in OPC proliferation and differentiation could therefore explain the observed variation in myelination in the adult brain (Osso & Chan, 2017).

Oligodendrocytes development

Cell-intrinsic, extrinsic, and environmental, factors regulate oligodendrocyte differentiation from OPCs (reviewed in Mitew et al. (2014) and Viganò et al. (2013)). When cells become committed to oligodendroglial lineage, the transcription factor *Olig2* (oligodendrocyte lineage transcription factor 2) is expressed (Lu et al., 2002; Novitch, Chen, & Jessell, 2001). This is followed

by the onset of *Sox10* (SRY (sex determining region Y)-box 10) expression, a transcription factor that precedes PDGFRα (platelet-derived growth factor receptor A) and NG2 expression (Noble et al., 1988; Stolt et al., 2002; Stolt, 2004; Takada, Kucenas, & Appel, 2010). *Sox10* is expressed throughout all developmental stages (Küspert et al., 2011), whereas *Olig2* was shown to be downregulated with oligodendrocyte maturation (Ligon et al., 2006). *Olig2* is established to have an important role in differentiation, but its potential role in modulating myelination in the long-term remains unclear (Mei et al., 2013; Mitew et al., 2014). Myelin Regulatory Factor (*Myrf*) is a recently discovered membrane-associated transcription factor, which is not only critical for mediating oligodendrocytes differentiation, mature oligodendrocyte identity, and promotion of new oligodendrocytes in adulthood, but also for myelin generation, and myelin related gene maintenance (Bujalka et al., 2013; Emery et al., 2009; Koenning et al., 2012; Liu & Zhou, 2013; McKenzie et al., 2014). Other transcription factors required for oligodendrocyte differentiation (reviewed by Mitew et al., (2014)) are *Olig1* (Xin et al., 2005), *Nkx2.2* (Qi et al., 2001), *Zfp191* (Howng et al., 2010)) and *Ascl1/Mash1* (Nakatani et al., 2013; Parras et al., 2007; Sugimori et al., 2008).

Extracellular cues such as chemotactic proteins, growth factors, nuclear receptor ligands, and intracellular signaling, are also required for OPC differentiation into oligodendrocytes (Nave & Werner, 2014; Valny et al., 2017). Other mechanisms revealed to regulate different stages of oligodendrocyte differentiation and maturation include chromatin remodeling and histone modification (Copray et al., 2009; Marin-Husstege et al., 2002; Shen, Li, & Casaccia-Bonnefil, 2005), DNA methylation (Coelho et al., 2009), and post-translational-modifications through regulation of microRNAs (Svaren, 2014).

Oligodendroglial lineage markers

Several immunohistochemical markers are used for identification of each stage of oligodendroglial development. OPCs express high levels of gangliosides, which bind to PDGFRα (Pringle & Richardson, 1993) and

proteoglycan NG2 (Levine et al., 1993; Nishiyama et al., 1996), whereas these markers are not expressed in neural stem cells. As OPCs mature and undergo differentiation they can be detected by the oligodendrocyte antigen O4 and O1 (Sommer & Schachner, 1981), and cease to express NG2 and PDGFRα. As they begin to differentiate into premyelinating, or immature, oligodendrocytes, 2',3'-cyclic-nucleotide 3'-phosphodiesterase (CNP) and the myelin lipid galactocerebroside are amenable to detection (Pfeiffer, Warrington, & Bansal, 1993; Zhang & Jiao, 2015). Premyelinating oligodendrocytes further mature into myelinating oligodendrocytes that express Glutathione S-transferase (GST-pi), and myelin membrane proteins, such as myelin basic protein (MBP), proteolipid protein (PLP), myelin-oligodendrocyte glycoprotein (MOG), and myelin-associated glycoprotein (MAG) (Nishiyama et al. (2009); Figure 1.1)

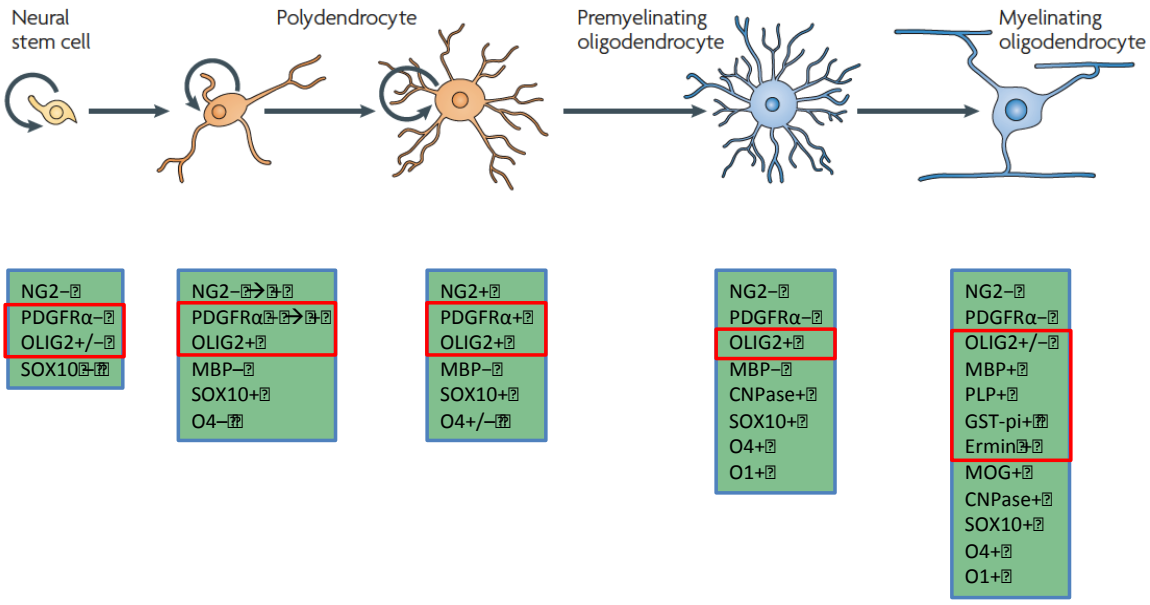

Figure 1.1 Development stages of oligodendrocytes

Adapted from Nishiyama et al. (2009), Nature Reviews Neuroscience

Multiple roles of oligodendrocytes

Newly developed fate-mapping techniques investigate proliferation and differentiation of oligodendrocytes from OPCs using transgenic mice expressing inducible Cre, under the regulation of OPC or oligodendrocyte specific genes, including *Ng2*, *Pdgfrα*, *Plp*, *Cnp*, *Myrf* (Clarke et al., 2012; Kang et al., 2010; Rivers et al., 2008; Young et al., 2013; Zhu et al., 2011). Recent studies from the Richardson lab have provided evidence that production of new myelinating oligodendrocytes and active myelination is required during adulthood for skill learning (McKenzie et al., 2014; Xiao et al., 2016). Other work has recently revealed that oligodendrocytes also provide crucial trophic support through the production of brain derived neurotrophic factor (BDNF), glial-derived neurotrophic factor (GDNF), insulin-like growth factor (IGF-1), nerve growth factor (NGF) and neutrotrophin-3 (NT-3) (Dai et al., 2003; Nave, 2010; Wilkins et al., 2003). Finally, oligodendrocytes also provide metabolic support via the lactate monocarboxylate transporter 1 (MCT1) which maintains axonal mitochondrial energy metabolism (Fünfschilling et al., 2012; Lee et al., 2012; Saab, Tzvetanova, & Nave, 2013).

1.2.3. Myelin and adaptive myelination

Structure of myelin

Approximately 70-85% of myelin membrane by dry-weight is composed of lipids, while the remaining 15-30% being protein. Lipid composition is not myelin specific, and consists of a high content of cholesterol, galactolipids, and other lipids, such as glycosphingolipids, and plasmalogens (Chrast et al., 2011). The compact myelin proteins MBP and PLP are among the most abundant specific myelin related proteins (Boggs, 2006). MBP is localized on the intracellular surface of the membrane, and is critical for myelin formation, compaction and stability (Min et al., 2009). PLP, in turn, is a more preponderant transmembrane protein, and is involved in consolidating adjacent myelin layers during the myelin wrapping process (Klugmann et al., 1997), as well as the enrichment of cholesterol in myelin (Werner et al.,

2013). The uncompacted myelin proteins, MOG, MAG, and CNP account for most of the remaining proteins. In the myelin membrane, MAG is located in the periaxonal layer, while MOG is present on the external surface; however, both proteins are also expressed in oligodendrocytes (Pham-Dinh et al., 1993). MOG is believed to play a key role in modulating stability of microtubules (Johns & Bernard, 1999), while MAG is crucially involved in myelinated axon maintenance (Yin et al., 1998). Myelin lipids are critical for regulating conduction along axons, whereas proteins have important roles in production and maintenance of myelin itself, as well as mediating axon-glial interaction (Simons & Nave, 2015).

Transcription factors of myelination

In terms of transcription factors required for myelination, OLIG1 was shown to be critical for the initial myelination onset, since *Olig1* knock out (KO) mice were capable of generating highly branched CNP+O4+ oligodendrocytes (Li et al., 2007; Xin et al., 2005). SOX10 is also critical for myelination as it acts at the MBP promoter (Li et al., 2007; Stolt et al., 2002) similarly to OLIG1, and interacts directly with *Myrf* (Hornig et al., 2013). MYRF drives immature, premyelinating oligodendrocytes to a maturation and myelination stage (Emery et al., 2009), whereas absence of *Myrf* leads to loss of myelin genes, and subsequent demyelination (Koenning et al., 2012). Additional transcription factors for myelin gene expression and myelination include the zinc finger proteins, ZFP488 (Soundarapandian et al., 2011) and ZFP191 (Howng et al., 2010), although their mechanisms of action have not yet been elucidated (Mitew et al., 2014).

Axonal cues to myelin formation and OPCs differentiation

Myelin thickness, and length between each myelin segment (i.e. internode), varies markedly within a single axon, and across axons (Micheva et al., 2016; Tomassy et al., 2014). Axonal diameter (i.e. caliber), which also varies greatly across axons in the CNS, has been identified as a key property influencing myelin sheath length, thickness and internode length characteristics (Butt, Ibrahim, & Berry, 1998; Hildebrand et al., 1993; Almeida

et al., 2011), all of which play a crucial role is shaping the conduction velocity of each axon (Rushton, 1951). This variability in myelin organization suggests there to be an inherently wide range of axonal conduction velocities in the CNS, which may be important to the timing and regulation of neuronal networks (Bechler et al., 2017; de Hoz & Simons, 2014).

Oligodendrocytes have been shown, using microfiber cultures, to have an intrinsic program for generation of myelination, where newly generated myelin sheaths exhibited similar properties to myelin sheaths present in the brain. These properties included increased sheath length with increased axonal fiber diameter, generation of compact and multilamellar membranes of similar lengths to those observed in vivo, and, notably, a minimal axonal diameter threshold of 300nm for myelination to be initiated (Bechler, Byrne, & Ffrench-Constant, 2015; Lee et al., 2012; Rosenberg et al., 2008). Additionally, Pten knock-out (KO) from cerebellar granule cells, and thus ablation of PTEN signaling inhibition, led to altered gene expression in-vivo, and an increase in diameter size of axons previously under this myelination threshold, resulting in these axons being myelinated (Goebbels et al., 2017). Increased proliferation and differentiation of OPCs was also observed, suggesting newly differentiated oligodendrocytes may have contributed to this myelination (Goebbels et al., 2017). Taken together, these studies suggest a minimal axonal diameter required for oligodendrocytes to sense and initiate myelination, but fall short of explaining why many axons in the CNS with supra-threshold diameters for myelination remain unmyelinated (Almeida et al., 2011). This could be partly due to a cell-type specific dependency in myelination-related characteristics, with recent work in the mouse showing parvalbumin-expressing cells to be the only GABAergic interneuron population to be myelinated in the cortex (Micheva et al., 2016). Interestingly, differential cell-type specific myelination could represent a trade-off between space and energy demands with signal transduction benefits of myelination (Harris & Attwell, 2012; Osso & Chan, 2017).

OPCs and oligodendrocytes can also be receptive of axonal cues and promote selection of that axon through differentiation and myelination,

respectively (Osso & Chan, 2017). OPCs express a number of neurotransmitter receptors, including glutamate and GABA receptors, and receive synaptic input from neurons (Larson, Zhang, & Bergles, 2016; Maldonado & Angulo, 2015). In turn, increased neuronal activity promotes OPC proliferation and oligodendrocytes differentiation (Gibson et al., 2014), and modulates myelin sheath characteristics (Hines et al., 2015; Gautier et al., 2015; Gibson et al., 2014; Wake et al., 2015). Furthermore, oligodendrocytes processes that enwrap non-active axons are more likely to retract their processes compared to those enveloping highly active axons (Hines et al., 2015).

Adaptive and plastic myelination

Elegant studies have demonstrated that myelination is a highly adaptive and plastic process, and undergoes substantial remodeling throughout life as a result of combination between intrinsic and extrinsic factors (Bechler et al., 2017; Bercury & Macklin, 2015; Snaidero & Simons, 2014). Most of the evidence available to support adaptive myelination is from studies investigating myelination during brain development (Wake, Lee, & Fields, 2011; Hines et al., 2015; Mensch et al., 2015). In humans, intra-cortical myelination persists until the third decade of life, and is stable until the fifth decade of life, after which it begins to decline (Grydeland et al., 2013). Contrastingly, in mice, most of the myelination process takes place during the first two postnatal months, although it also occurs later in life (Young et al., 2013). A newly proposed property of adult myelination in the CNS is that myelin synthesized in adulthood is associated with thinner sheaths relative to axon diameter and shorter internodes, compared to myelin synthesized in adolescence (Young et al., 2013). However, others have suggested that this observation may be more simply explained by the protracted and on-going process of myelin production (Karttunen et al., 2017).

An interesting model for CNS myelination proposed by (Bechler et al., 2017) suggests that initiation of myelin is enacted by an oligodendrocyte intrinsic program, while later adaptations and alterations are driven by environmental cues and neuronal activity. In keeping with this, optogenetic activation of

neurons has been shown to promote increased myelination (Gibson et al., 2014). Furthermore, neuronal signaling related factors such as matrix receptors of the integrin family, Neuregulin-1 (NRG1), or NMDA glutamate receptors in the myelin sheath, all contribute to myelination and its maintenance, and, while these may not be required for its initiation, they may serve important roles in adaptive myelination (Brinkmann et al., 2008; Câmara et al., 2009; Saab et al., 2013); also discussed in (Bechler et al., 2017). Neuronal NRG1 is a member of the NRG superfamily of epidermal growth factor-like ligands and it binds to the cell surface ErbB receptor on oligodendrocytes (Taveggia et al., 2007). Conditional KO mice lacking neuronal NRG1 were not associated with differences in myelination formation, but overexpression of neuronal NRG1 led to thicker myelination, particularly in small diameter axons that are not usually myelinated (Brinkmann et al., 2008; Taveggia et al., 2007). Interestingly, reduced expression of NRG1 during social isolation in juvenile mice was shown to result in hypomyelination and thinner myelin sheaths in axons of the PFC (Makinodan et al., 2012). These findings suggest that while NRG1 signaling may not be required for establishing myelination in CNS, it likely plays an important role in behavioural-dependent myelination.

Interestingly, several new findings suggest a small window of time for newly differentiated oligodendrocytes to myelinate, such as ~5 hours in the zebrafish, and ~12 hours in rodent-derived myelinating cultured cells (Watkins et al., 2008; Czopka, Ffrench-Constant, & Lyons, 2013). A window of myelination was also described in relation to the capacity of myelin to respond to environmental manipulation and behavioural experience, with more flexibility during adolescence, but not young adulthood, in rodents (Makinodan et al., 2012). Others, however, have demonstrated myelin alterations in adulthood with longer periods of environmental manipulation (Liu et al., 2012). Further effects of environmental manipulation on myelination are described in greater detail in the following sections.

1.2.4. Imaging tools for myelin characterisation

Myelination can be visualized and characterised through high-resolution imaging of ultra-thin sections of brain tissue using electron microscopy (EM). Properties such as myelinated and unmyelinated axonal population distribution, myelin thickness, and ultrastructure, can be obtained using EM. Myelin thickness can be quantified and compared using the g-ratio measure, which is calculated as the inner axonal diameter divided by the outer diameter (axonal diameter plus myelin lamellae; Friede & Miyagishi, 1972). Accordingly, smaller g-ratios are associated with thicker myelin sheaths and the g-ratio of unmyelinated axons is equal to unity. The optimal g-ratio for the rat CNS has been suggested to be around 0.77 (Chomiak & Hu, 2009), although values can vary in the literature.

Imaging white matter microstructure in humans is achieved using diffusion-weighed imaging (DWI) and diffusion-tensor imaging (DTI) magnetic resonance imaging (MRI) (Bihan et al., 1986). These imaging techniques rely on fractional anisotropy (FA) to infer axonal fiber density, axonal diameter and myelination. Several studies have reported myelination plasticity by observing increased FA values, associated with an increase in axonal diameter and myelin thickness, as a result of skill training (Scholz et al., 2009).

1.2.5. White matter of the CNS – with focus on the corpus callosum (CC) and prefrontal cortex (PFC)

The white matter of the CNS consists of myelinated and unmyelinated axons, and glial cells. Axons are most abundant, followed by oligodendrocytes, astrocytes, OPCs, and microglia (Walhovd, Johansen-Berg, & Káradóttir, 2014). Myelination in white matter tracts is not homogenous and not all axons are myelinated (Dangata, Findlater, & Kaufman, 1996; Sturrock, 1980; Young et al., 2013). Furthermore, as described previously, many axons are known to possess non-uniform myelin distributions along their length, termed ‘intermittent myelination’ (Micheva et al., 2016; Tomassy et al., 2014).

Human white matter volume increases during childhood, adolescence, and into adulthood (Westlye et al., 2010).

Myelinated tracts ensheathe the axons of the cortex, and the inter- and intra-hemispheric connecting fibres of the corpus callosum (CC), internal and external capsule, the cingulum, and the anterior commissure (Zatorre, Fields, & Johansen-Berg, 2012). The CC is the largest white-matter structure of the brain, and it facilitates inter-hemispheric communication, playing a critical role in the relay of cognitive, motor and sensory information between cortical regions. Callosal fibers arise from cortical pyramidal neurons and are topographically structured as they project through the CC (Innocenti, 1994). The human CC is segmented into five regions based on functional and anatomical connectivity: the lamina rostralis, the genu, the body, the isthmus, and the splenium, from frontal to caudal (Hofer & Frahm, 2006; Raybaud, 2010). In rodents, however, different regions of the CC are typically classified according to three main areas, the genu, mid-body and splenium. The genu and the body of the CC transfer information from the prefrontal cortex, the premotor, primary motor and supplemental motor cortex, whereas the splenium integrates connections from posterior parietal cortex, and the temporal and occipital lobes (Raybaud, 2010). Interestingly, despite the CC being one of the most highly myelinated structures in the brain, it also contains a high proportion of unmyelinated axons following the developmental peak in myelination (Sturrock, 1980; Young et al., 2013). Some of these unmyelinated axons become myelinated in adulthood, possibly leaving room for plasticity required for skill learning (Fields, 2008; Zatorre et al., 2012). Indeed, of the total number of oligodendrocytes in the CC of 8 month old mice, about 30% are generated after 7 weeks of age (Rivers et al., 2008; Zhu et al., 2011).

In addition, the PFC is also highly enriched in myelinated fibres, and myelinates late into adulthood in both humans and animals (Fuster, 1996; McKenzie et al., 2014; Miller et al., 2012). The PFC has been linked to higher cognitive functions, such as planning, executive tasks and working memory, and plays a key role in personality expression and social behaviour

(McEwen, 2013; Miller & Cohen, 200); Yang et al., 2009; Yuan & Raz, 2014). Interestingly, the rate of OPCs differentiation into oligodendrocytes is faster in the cortex than other white matter regions, such as the spinal cord and optic nerve (Young et al., 2013), highlighting the potential importance of myelination in this brain region. Particularly during development, myelination in the PFC is more plastic and sensitive than other regions, to experience, environmental and social factors (Hoban et al., 2016a; Liu et al., 2012; Makinodan et al., 2012; Tomlinson, Leiton, & Colognato, 2016a).

1.2.6. White matter abnormalities in Huntington disease

Oligodendrocytes and myelin are vital for axonal function and survival, while dysfunction of this population, along with defects in myelination, may play important roles in the development and severity of neurodegenerative diseases (NDDs) such as HD (Ettle, Schlachetzki, & Winkler, 2016; Huang et al., 2015a; Liu & Zhou, 2013).

Accompanying the well-studied neuronal degeneration in the basal ganglia, white matter (WM) atrophy and myelination defects have been identified as an early feature of the HD phenotype in both patients and animal models (Bartzokis et al., 2007; Ciarmiello et al., 2006; Fennema-Notestine et al., 2004; Novak et al., 2014; Rosas et al., 2003; Tabrizi et al., 2009; Xiang et al., 2011). Progressive reduction in WM volume and alterations in WM tracts have been reported by longitudinal studies in pre-symptomatic HD gene carriers (Tabrizi et al., 2009; Tabrizi et al., 2013; Shaffer et al., 2017), and indicate loss of connectivity between cortical and sub-cortical regions, which may underpin early clinical symptoms. White matter alterations were found in the corpus callosum (CC) and prefrontal cortex (PFC) of pre-symptomatic and symptomatic HD gene carriers (Bourbon-Teles et al., 2017; Matsui et al., 2013; Matsui et al., 2015; Rosas et al., 2006). Furthermore, striatal cell death follows a dorsal-to-ventral progression in HD (Hedreen, 2003; Vonsattel, 2007), and, similarly, altered diffusivity in WM of the dorsal PFC-striatal pathway was observed in a pre-symptomatic HD group (Matsui et al., 2015).

HD animal models recapitulate WM related alterations in humans. Our group has explored the molecular and ultrastructural features of WM abnormalities in HD mouse and rat models (Garcia-Miralles et al., 2016; Teo et al., 2016). Using diffusor tensor imaging (DTI) imaging, WM microstructural abnormalities were revealed prior to neuronal loss in the CC of the YAC128 mouse model and the BACHD rat model (Teo et al., 2016). In addition, thinner myelin sheaths and lower levels of myelin related gene transcripts were seen in these animals compared to healthy animals (Teo et al., 2016). Others have also reported microstructural abnormalities in the R6/2 and HdhQ250 mouse model, and reduction in myelin sheaths thickness, as well as decreased expression of myelin related genes in the BACHD and HdhQ250 mouse models (Jin et al., 2015; Xiang et al., 2011).

While HTT expression in glial cells has long been recognised (Hebb, Denovan-Wright, & Robertson, 1999), more recent studies have observed mutant HTT aggregates in glial cells, including astrocytes, in addition to neuronal cells (Faideau et al., 2010; Shin et al., 2005). *Myrf* knock-out in adult mice, and selective expression of mutant HTT in oligodendrocytes of transgenic mice, led to similar oligodendroglia related impairments, such as demyelination, reduction in myelin gene expression, along with progressive motor impairments, seizures, metabolic impairments and reduced survival (Koenning et al., 2012; Huang et al., 2015a). Furthermore, mutant HTT was found to be spatially restricted to oligodendrocyte-rich brain regions such as the CC (Huang et al., 2015a).

1.3. Environmental manipulation

Through molecular, cellular, structural and functional alterations, the plastic brain responds to cognitive, sensory, physical or social stimulation, in interaction with the enriched or deprived environment (Galani et al., 2007; Keiner et al., 2017; Okuda et al., 2009; Qiu et al., 2012; Segovia et al., 2008; Viola et al., 2009). Environmental manipulation by either enrichment or deprivation was shown to be involved in modulation of myelination and

oligodendroglia population and precursor cells (Komitova et al. 2006; Liu et al., 2012; Liu et al., 2016; Magalon et al., 2007; McKenzie et al., 2014; Tomlinson, Leiton, & Colognato, 2016a; Wang & Young, 2014).

1.3.1. What is a standard housing condition in rodents

Laboratory animals, with particular reference to rodents, are generally kept in what is referred to as 'standard housing' conditions. Standard housing can vary between laboratories, and are often poorly described in literature. In general, standard cages are one level, relatively small (~ 30cm x 20cm x 15cm), and usually include sparse bedding material, and in some cases small plastic shelter boxes, with free access to water and food pellets (Nithianantharajah & Hannan, 2006). These conditions restrict rodents from natural exploratory behaviours, and could have detrimental effects and interfere with treatment effects, especially when a neurodegenerative disease model is investigated. Mice housed in cages containing wheels run between 4-10km per day (Ransome & Hannan, 2013), illustrating the potential impact of a simple running wheel were it to be added to a standard cage. Animals in standard housing are usually held in groups of two to five per cage, but can on some occasions find themselves as the last and single animal in the cage during experimental studies. This leads to other issues, such as social isolation, which have been shown to be detrimental to normal development and behaviour (Liu et al., 2012; Makinodan et al., 2012; Makinodan et al., 2016; Potter et al., 2010). As a result, housing of animals in 'standard' cages was previously suggested to be equivalent to 'deprived' housing, whereas the 'enriched' housing is closer to natural environments (Mo, Renoir, & Hannan, 2015b). However, others argue that standard housing can be considered a form of mild enrichment, since it can promote exercise, play and social interactions (Crofton, Zhang, & Green, 2015).

1.3.2. How to create an enriched environment for laboratory rodents

Enrichment in animal studies has been defined by several components such as: (1) larger than standard housing conditions, often built on several levels;

(2) enhanced housing conditions, by introduction of objects of different shapes, and materials; (3) appropriate sheltering and complex bedding material; (4) increased social housing; and (5) exercise stimulating objects such as running wheels, platforms or stairs (Olsson & Dahlborn, 2002; Nithianantharajah & Hannan, 2006; Singhal et al., 2014). Additionally, cognitive or physical training were also included in some study designs (Keiner et al., 2017; Pang et al., 2008; Van Dellen et al., 2008). Unless investigating aging or late progressive neurodegeneration, most rodents have been allocated to enriched housing immediately post-weaning, and were maintained in such from 1 day to several months, depending on the interest of the researcher. Benefits were shown to usually be augmented with more complex EE interventions, such as those that combine sensory, cognitive, physical and social stimulation, and eliminate stress (Hannan, 2014; Mo, Hannan, & Renoir, 2015a; Mo, Renoir, & Hannan, 2015b). The strength of such effects are also dependent on the duration of the enrichment paradigm, the animal's age at intervention onset, the genetic background, and the sex of the animals (Hannan, 2014; Leger et al., 2015; Pang & Hannan, 2012; Singhal et al., 2014; Tomlinson, Leiton, & Colognato, 2016a). Enrichment protocols vary greatly between laboratories, and there is no standardised paradigm used. Thus, the enrichment components described above used either individually, or combination, and to different complexities, have sometimes yielded inconsistent or conflicting results.

1.3.3. Beneficial effects of enrichment in rodents

Long-lasting effects of animals weaned in enriched environments, as well as enrichment of middle-aged, old or diseased animals, were shown to have beneficial effects on behavioural performance by multiple studies (Nithianantharajah & Hannan, 2006). Early studies pioneering environmental manipulation research demonstrated the susceptibility of the adult brain to enrichment or deprivation. Rats allocated to enriched housing had greater cognitive abilities, thicker cortical layers and a more complex dendritic arborisation compared to isolated rats (Diamond, Krech, & Rosenzweig, 1964; Renner & Rosenzweig, 1987). Another early study showed that spatial

memory was enhanced concomitantly with increased neurogenesis in the dentate gyrus of the hippocamus as an effect of enrichment (Kempermann, Kuhn, & Gage, 1997), an effect subsequently confirmed by later studies (Doulames et al., 2015; Lazic et al., 2006; Novkovic, Mittmann, & Manahan-Vaughan, 2015; Okuda et al., 2009). A more recent study demonstrated that young rats held in enriched cages for 10 weeks post-weaning showed long-lasting improvements in several behavioural tests, indicating better stress-coping strategies, increased motor activity and improved information processing and vigilance (Mosaferi et al., 2015). Performance of middle-aged rats was improved in the Morris Water Maze Task after 4 months of enriched housing (Zhao et al., 2011). In addition, EE was used as rehabilitation therapy following brain injury in rodents, and was demonstrated to positively influence motor, cognitive and psychiatric recovery. For example, enriched rats following experimental stroke exhibited improved functional recovery (Komitova et al., 2006), attenuated cognitive deficits (Hicks et al., 2007), and reversed learning impairment (Dahlqvist et al., 2004), compared to standard housing animals. Both enriched housing and reaching training improved sensorimotor capabilities in the impaired forelimb of rats with induced stroke (Keiner et al., 2008). Furthermore, enhanced performance in learning and memory tasks was observed in enriched middle-aged and aged rats (Zhao et al., 2012), and Alzheimer Disease (AD) mouse models (Arendash et al., 2004; Herring et al., 2010; Jankowsky et al., 2005; Mirochnic et al., 2009; Valero et al., 2011). Motor function recovery also improved in enriched mouse models of Parkinson Disease (PD) (Faherty et al., 2005; Jadavji, Kolb, & Metz, 2006; Tajiri et al., 2010; Tillerson et al., 2003). Exploratory behaviour improved in young and old PD mice after 3 weeks of exposure to EE (Goldberg, Haack, & Meshul, 2010). Therefore, enrichment effects have been explored as a possible preventive, non-drug based therapy, or in other cases, as an ameliorative therapy during disease progression.

1.3.4. Enrichment effects on myelin plasticity and oligodendroglial population dynamics in humans and rodents

There is evidence to suggest that the majority of axons in the cortex and corpus callosum remain unmyelinated into adulthood, indicating that such axons can be myelinated during later stages in life (Sturrock, 1980; Tomassy et al., 2014; Waly et al., 2014). The plastic properties of myelination, and its sensitivity to behavioural and environmental experience, have been observed in humans through use of magnetic resonance imaging (MRI). For example, DTI MRI revealed microstructural white matter (WM) changes following balance training in both healthy young adults (Taubert et al., 2011), and young adults with traumatic brain injury (Drijkoningen et al., 2015). Other imaging studies demonstrated plasticity of myelination through increased fractional anisotropy (FA) as a result of juggling (Scholz et al., 2009), abacus training (Hu et al., 2011), extensive piano practice (Bengtsson et al., 2005; Han et al., 2009), long-life musical training (Schmithorst & Wilke, 2002), working memory training (Takeuchi et al., 2010), reasoning training (Mackey, 2012), and meditation training (Tang et al., 2012). However, to be noted, that decreased FA has been observed in balancing skills training (Taubert et al., 2011).

Recent work using animal models has revealed promising effects of behavioural experience, enriched housing and voluntary exercising on adaptive myelination and oligodendroglial population dynamics in several regions of the brain (Tomlinson, Leiton, & Colognato, 2016a). Oligodendrocyte precursor cells (OPCs), such as NG2-positive cells, were also shown to respond to environmental manipulation. In a recent study, (Keiner et al., 2017) assigned 10-12 weeks old male rats to 3 experimental conditions (standard housing, enriched housing, and standard housing with daily skilled reaching training of the dominant forelimb) for either 10 or 42 days. Injections of the proliferation marker, BrdU, were given to all animals from days 2-6 of the experimental condition. Interestingly, young rats

exhibited a shift in the distribution of oligodendroglial population in sensorimotor cortex, but not in the CC, between short- and long-term enrichment. Compared to standard housing, short-term enriched rats showed differentiation of OPCs into mature oligodendrocytes; however, after long-term enrichment, OPCs and mature GST-pi positive oligodendrocyte populations appeared comparable to the standard housing condition. Additionally, the number of myelinating CNP-positive cells increased in the motor cortex after short-, as well as, long-term enrichment (Keiner et al., 2017). These findings suggest regional differences in myelin and oligodendroglial population exposed to enrichment. Effects of enrichment have also been observed in older rats. Four months of enrichment of middle-aged and old-aged male and female rats led to increased axon volume, myelin sheath volume and the length of myelinated fibres, although no changes were observed in mean axonal diameter or myelin sheath thickness in white matter tracts (Yang et al., 2013). The authors ascribed the increase in myelinated fibres as a result of enrichment to ongoing remyelination (Yang et al., 2013). Consistently, no differences were observed after 1-2 months of enrichment in the numbers of myelinated axons of the CC in 4 months old rats (Markham et al., 2009). A 10% increase in the splenium of the CC was observed after enrichment, but this was attributed to increase in the number of astrocytes branching rather than thicker myelin sheaths (Markham et al., 2009). Increased total corpus callosum (CC) volume, increased myelinated fibre and myelin sheath volume, as well as increased total length of myelinated fibres, were observed specifically in the CC of enriched aged rats (Zhao et al., 2012). Oligodendroglial population related changes were also observed in middle-aged enriched rats, such as an increased number of myelinating CNP-positive oligodendrocytes in the CC (Zhao et al., 2011). The same period of enrichment in middle-aged rats was also shown to increase the total volume of myelinated fibres in sub-cortical, grey matter areas, such as the hippocampus, which was significantly correlated with improvements in spatial learning (Qiu et al., 2012).

In contrast, few studies have provided support for oligodendrogenesis in many cortical regions, or the amygdala, although evidence for increased

numbers of OPCs have been reported (Ehninger & Kempermann, 2003; Ehninger et al., 2011; Makinodan et al., 2012). In adult mice enriched for 40 days, increased number of proliferative OPCs, but no differences in CNPase+ labelled cells (i.e. myelinating oligodendrocytes), were observed in the amygdala compared to control mice (Ehninger et al., 2011). Similarly, no changes in oligodendrocyte density or morphology, nor myelin transcript levels, were found in the prefrontal cortex (PFC) of juvenile male mice which expressed green fluorescent protein (GFP) under the proteolipid protein promoter (PLP) and were enriched for 1.5 months (Makinodan et al., 2012). Besides the effects observed under physiological conditions, EE was also demonstrated to drive post-insult oligodendroglial differentiation (Keiner et al., 2008; Klaissle et al., 2012; Komitova et al., 2006; Simon, Götz, & Dimou, 2011; Steiner et al., 2006). For example, following induction of local cortical infarcts, rats placed for ten days in EE showed a small transient increase in immature oligodendrocytes proliferation; however, no differences were observed in MBP positive cells within the perilesional region (Keiner et al., 2008).

1.3.5. Enrichment effects in HD animal models

Environmental enrichment was first demonstrated to have a positive influence in delaying motor symptoms in a genetic mouse model of HD (van Dellen et al., 2000). Enrichment for 18 weeks in post-weaning R6/1 mice increased novel object exploration, delayed motor coordination impairments, suppressed seizures, and increased striatal and cortical volume by 22 weeks of age, compared to R6/1 mice allocated to standard housing (van Dellen et al., 2000). Since this pioneering study, physiological and cognitive improvements as a result of environmental enrichment have been also demonstrated in several others HD mouse models, including the R6/2 and N171-82Q lines (Hockly et al., 2002; Schilling et al., 2004; Wood et al., 2010). For example, R6/1 mice were associated with ameliorated motor symptoms and rescue of decreased body weight, specific brain-derived neurotrophic factors (BDNF) in the striatum and hippocampus, and the dopamine signaling cortical regulator, DARP-32, after four months of

enrichment (Spires, 2004). The same period of enrichment also showed improved levels of the presynaptic marker synaptophysin, in frontal cortex and hippocampus, and elevated levels of the postsynaptic glutamatergic signaling protein density 95 (PSD-95) in the hippocampus of the R6/1 mouse (Nithianantharajah et al., 2008). Longer life expectancy, along with improved hippocampal neurogenesis and longer neurites in newly born neurons, were observed in the 25 weeks-old enriched R6/1 group compared to control (Lazic et al., 2006). Behavioural and cognitive enrichment-driven improvements in the R6/1 HD model also included reduced spatial memory deficits and delayed cognitive deficits (Nithianantharajah et al., 2008), and amelioration of depressive- (Du et al., 2012a) and emotion- related phenotypes (Renoir et al., 2012). Although complex enrichment provides enhanced benefits, minimal improvements in housing conditions have also been shown to have some positive effects in other models. Indeed, addition of nesting materials and tunneling areas (Hockly et al., 2002), and improving access to food (Carter, Hunt, & Morton, 2000), has also been demonstrated to be beneficial for juvenile R6/2 mice models of HD.

Interestingly, negative outcomes of enrichment have also been reported in a handful of studies. Post-symptomatic 8-week-old R6/2 male mice exposed to a playground overnight, while spending daytime hours in standard cages, had a lower rate of survival than control animals (Skillings, Wood, & Morton, 2014; Wood, Glynn, & Morton, 2011). This could be related to the accelerated HD mouse model employed in these studies. On the other hand, the stress caused by daily transfer from home to playground may also be a potential confound, a point acknowledged by both the authors and others (Mo, Renoir, & Hannan, 2015b).

1.3.6. Enrichment inspired therapies in HD patients

Although animal studies have shown positive and exciting results in terms of the beneficial effect of enrichment and exercise, it is important to note that these animal models do not fully recapitulate the human disease phenotype. In addition, humans already live in what can be considered an ‘enriched environment’, making the extrapolation and translation from cage to the clinic

a difficult task. Nevertheless, multi-disciplinary long-term interventions have highlighted the positive returns of rehabilitation and occupational therapies in neurodegenerative disease (Quinn et al., 2017; Reetz, Werner, & Schiefer, 2015). Several studies have now demonstrated that combining active lifestyle, including physical, social and cognitive stimulation factors could protect against dementia and Alzheimer Disease (Baker et al., 2010a; Baker et al., 2010b; Fratiglioni, Paillard-Borg, & Winblad, 2004). Furthermore, both short- and long-term multidisciplinary rehabilitation may benefit patients suffering of multiple sclerosis (Asano & Finlayson, 2014; Khan et al., 1996; Khan, Amatya, & Turner-Stokes, 2011), Parkinson Disease (Frazzitta et al., 2015; van der Marck & Bloem, 2014; van der Marck et al., 2013), and Huntington Disease (Cruickshank et al., 2015; Piira et al., 2013; Thompson et al., 2013; Zinzi et al., 2007).

To date, reports of multi-disciplinary rehabilitation interventions to slow and improve symptoms in HD patients have been sparse and mostly exploratory, many of them lacking a control group altogether. In addition, most, if not all, interventions have targeted early- to mid-stage HD patients, with little known of the impact at pre-symptomatic and late-stages of the disease. The first evaluation of multi-disciplinary rehabilitation in HD patients was carried out only ten years ago, and examined the effects of a two-year high-intensity program at an early- to mid-stage of the disease, and involved three sessions per year, each including six in-patient days (Zinzi et al., 2007). Despite the high dropout rate (approximately 1/3rd of patients), the intervention improved both physical function, such as gait, balance, and swallowing, as well as social function, such as better mood and social relations (Zinzi et al., 2007). The few studies of this type that followed also looked at the therapeutic potential of long-term interventions in early- to mid-stage HD patients. A nine-month program in a small cohort showed HD intervention patients to exhibit reduced motor and posture deficits, as well as increased fat-free mass and strength, relative to controls (Thompson et al., 2013). In addition, minor improvements in cognition, depression and quality of life were also observed (Thompson et al., 2013). A second, more extensive and carefully designed program, consisted of a one year

intervention, including three admissions of three weeks each, and focused on a combination of physical exercise, teaching sessions and social activities (Piira et al., 2013). The study revealed improved motor function, related to gait and balance, as well as improved general physical quality of life, and Body Mass Index (BMI) (Piira et al., 2013). Additionally, these patients showed decreased anxiety and depressive symptoms. However, a significant decline was identified in the Symbol Digit Modalities Test (SDMT; Smith, 1982), which measures patient attention, concentration and speed of information processing (Piira et al., 2013). These findings highlight the importance of targeted cognition related tests when applying these types of interventions, and raise the possibility that certain types of processing-related deficits may be improved by non-pharmacological methods alone. A further exploratory long-term rehabilitation intervention, consisting of supervised clinical exercise (aerobic and strength exercises), home-based exercise (fine motor training and strength exercise) and occupational therapy sessions, in patients with manifest HD, revealed increased grey matter volume in the dorsolateral PFC and right caudate through MR imaging, which was accompanied by improvements in memory and verbal learning (Cruickshank et al., 2015). Finally, 18 months of individualised outpatient multidisciplinary intervention, prescribed after consultation with a team of specialists, was well-tolerated and found to be feasible and beneficial by HD patients and their carers (Veenhuizen et al., 2011). Therefore, this study indicates that, besides the efficacy of such interventions, HD patients are likely to engage and be highly appreciative of such multi-disciplinary programs.

1.3.7. How to create a socially deprived environment for laboratory animals

Social deprivation in the laboratory involves housing animals individually in standard cages with minimal or no enrichment (Heidbreder et al., 2000). Once isolated, minimal contact or handling is made, with the exception of when bedding requires changing. Although studies have examined the effects of isolation in adult and aged rodents, isolation has more prominent

and long-term effects during the critical period of brain development, in adolescence (Fone & Porkess, 2008).

1.3.8. Social isolation effects on rodent models of health and disease

Rodents are social creatures, similar to humans, such that post-weaning social isolation leads to significant behavioural, cognitive and neurochemical abnormalities. Behavioural and cognitive effects of social isolation in rodents include increased depressive-like behaviour (Brenes, Rodríguez, & Fornaguera, 2008a), aggressive-like behaviour (Matsumoto et al., 2005), anxiety-like behaviour (Ieraci, Mallei, & Popoli, 2016), irritability and hyperactivity (Ieraci et al., 2016), impaired spatial attention and long-term memory (Okada et al., 2015; Ouchi et al., 2013), and reduced social affiliation and conditioned fear (Okada et al., 2015). Detrimental effects of isolation on the central nervous system (Fone & Porkess, 2008) include shrinkage of hippocampal volume (Pereda-Pérez et al., 2013), decreased neurogenesis (Stranahan, Khalil, & Gould, 2006), altered synaptic plasticity (Djordjevic et al. , 2009), and down-regulation of transcription factors related to synaptic plasticity, such as Egr-1, c-Fos and Arc (Ieraci et al., 2016; Matsumoto et al., 2012; Okada et al., 2015). Furthermore, social isolation was also associated with decreased PFC and hippocampal BDNF levels (Ieraci et al., 2016; Scaccianoce et al., 2006), reduced levels of norepinephrine in the ventral striatum (Brenes, Rodríguez, & Fornaguera, 2008a), abnormal GABAergic and glutamatergic activity (Harte et al., 2007; Ieraci et al., 2016; Levine et al., 2007; Matsumoto et al., 2003; Melendez et al., 2004), alteration of the dopaminergic and cholinergic system (Okada et al., 2015), and altered electrophysiological properties of neuronal activity (Peters & O'Donnell, 2005; Roberts & Greene, 2003).

Negative effects of social isolation have also demonstrated in animal models of neurodegenerative disease although the literature is sparser. For example, in the aged APP/PS1 Alzheimer Disease (AD) mouse model, three months of isolated housing enhanced cognitive deficits, and promoted Aβ plaque

accumulation in the hippocampus (Huang et al., 2015b). In turn, social isolation of young adult mice led to early onset of the disease-like phenotype (Hsiao, Chen, Chen, & Gean, 2011; Hsiao, Kuo, Chen, & Gean, 2012). Similarly, in the N17182Q transgenic mouse model, of HD which presents with motor deficits from 11 weeks of age, showed early disease onset, impairments in motor behaviour, and a reduction in striatal volume when housed individually in standard cages with a running wheel from pre-symptomatic age (Potter et al., 2010). On the other hand, past studies demonstrated that the combination of physical stress and corticosterone administration can accelerate onset of specific deficits in HD mice (Mo et al., 2014a; Mo, Renoir, & Hannan, 2014b; 2014c; Mo, Renoir, Pang, & Hannan, 2013). Therefore in the Potter et al. (2010) study, because of the manipulation of two factors, exercise and isolation, which can both impact disease progression, it is unclear which one of the two, or whether the combination of both, contributed to the effects reported.

1.3.9. Social isolation effects on myelin plasticity and oligodendroglial population

One of the earliest studies linking white matter abnormalities with behavioural experience demonstrated that male rhesus monkeys, raised individually from 2-12 months of age, had significantly decreased corpus callosum (CC) sizes compared to monkeys raised in groups, as shown by MRI (Sánchez, Hearn, Do, Rilling, & Herndon, 1998). This decrease was most evident in the posterior CC, and was significantly correlated with the several cognitive deficits observed in these animals. The CC reduction persisted 6 months after animals were socially reintegrated, whereas no differences were identified in the anterior comissure, cerebellum or hippocampus (Sánchez, Hearn, Do, Rilling, & Herndon, 1998). In healthy rodents, social isolation was demonstrated to induce alterations in oligodendroglial population development and maturation, as well as in myelin sheaths characteristics, with many studies focusing on the known inherent plasticity of the prefrontal cortex (PFC) with respect to environmental manipulation (Forbes & Gallo, 2017; Liu et al., 2012; Liu et al., 2016;

Makinodan et al., 2012; Makinodan et al., 2016; Mount & Monje, 2017). Interestingly, a critical window for oligodendrocyte maturation and capacity for myelination was identified as a result of social isolation studies. These demonstrated that atypical oligodendroglial morphology and myelination deficits, along with long-term abnormal mPFC-mediated behaviour, occurred in healthy mice exposed to social isolation from pn21, for only two weeks, after which they were returned to standard housing until pn65 (Makinodan et al., 2012). The same effect was observed in mice kept in isolation from pn21 for four weeks, but not in mice where isolation was initiated after pn35. Furthermore, the complexity of oligodendrocytes morphology was shown to be mediated by neuregulin through ErbB3 receptors on oligodendrocytes (Makinodan et al., 2012). These findings highlight the importance of social interaction during juvenile periods when oligodendrocytes undergo maturation and further axonal myelination (Makinodan et al., 2012).

Reduction of myelin sheath thickness in the PFC of healthy juvenile mice was observed following two, four or eight weeks of post-weaning isolation (Cao et al., 2017; Liu et al., 2012; Makinodan et al., 2012).Two weeks of social deprivation was sufficient to cause thinning of myelin sheaths, and was paralleled by decreased expression of myelin basic protein (MBP) and myelin-associated glycoprotein (MAG), but not alterations of axonal diameters, in the medial PFC (mPFC); in contrast, no myelin related differences were identified in the motor cortex of juvenile mice (Makinodan et al., 2012). Additionally, isolation led to alteration of oligodendrocytes morphology, including shorter processes, fewer branches and fewer internodes per cell (Makinodan et al., 2012). Moreover, isolation-induced changes in myelin were observed in sub-cortical areas of juvenile male CD1 mice reared in isolation for 8 weeks post-weaning, such as thinner myelin sheaths in the hippocampus, as well as decreased heterochromatin formation and reduced levels of MBP expression (Cao et al., 2017).

Adaptive myelination was suggested to be highly sensitive to environmental manipulation particularly during infancy and adolescent periods, with several studies finding no changes in myelin sheath thickness of adult mice. Nine-

week old mice exhibited no alterations in myelin thickness within layer V of the mPFC after 4 weeks of isolation (Makinodan et al., 2016), while 24-week old mice also showed no differences in myelin sheaths of the anterior commissure, the nucleus accumbens, or the cerebellum, after 2 or 8 weeks of isolation, when compared to standard housing controls (Liu et al., 2012). However, following 8 weeks of isolation, 24 week old adult mice exhibited hypomyelination, paralleled by decreased myelin related gene transcripts in the PFC, and reduction in the expression of some oligodendrocyte specific paranodal genes, while nodal length was not affected (Liu et al., 2012). In addition, oligodendrocytes in isolated mice were associated with immature nuclear chromatin and decreased nuclear heterochromatin, associated with decreased transcripts for enzymes regulating histone acetylation and repressive histone methylation (Liu et al., 2012). This was ascribed to reduced oligodendrocyte differentiation in socially isolated mice (Wang & Young, 2014). In contrast, a shorter period of 2 weeks of social deprivation had mild effects on myelin sheath thinning in this region of the brain, but a notable decrease in the proportion of heterochromatin in oligodendrocytes (Liu et al., 2012). Interestingly, social reintegration reversed the negative effects observed as a result of social deprivation when isolation took place in adulthood (Liu et al., 2012), but not in juvenile mice (Makinodan et al., 2012). Detrimental effects were also partially reversed, in selective regions of the brain, such as the hippocampus, but not the PFC, of juvenile isolated animals concurrently exposed to an enriched housing (Cao et al., 2017).

1.3.10. Detrimental effects of social isolation in humans

The translational value of investigating social isolation in preclinical models lies in the fact that social interaction in humans is a critical factor for development of normal social and cognitive function, while childhood social isolation or neglect can cause long-term alterations in normal adult behavior, cognition and neurophysiology (Bos et al., 2011; Chugani et al., 2001; Egeland, Sroufe, & Erickson, 1983; Polak & Saini, 2015). Notably, neglect, social isolation or rejection in children and adolescents can lead to long-term alterations in myelination of prefrontal cortex (PFC) (Chugani et al., 2001;

Egeland et al., 1983; Eluvathingal et al., 2006), and reduced corpus callosum area (Mehta et al., 2009; Teicher et al., 2004). Furthermore, individuals experiencing isolation, or loneliness, are more susceptible to cognitive decline (Badcock et al., 2015; Cacioppo & Hawkley, 2009), depression (Cacioppo et al., 2006), stroke (Avendano et al., 2006), faster progression and greater risk of late-life Alzheimer disease (AD) or other forms of dementia (Dong & Csernansky, 2009; Holwerda et al., 2014; Wilson et al., 2007), and faster onset of schizophrenia (Jiang et al., 2013). In PD, for example, progressive symptoms were shown to impact quality of life, which in turn had an effect on social interaction, leading to social isolation from society (Pell, Cheang, & Leonard, 2006; Schrag, Jahanshahi, & Quinn, 2001). In individuals with diagnosed mild AD, social isolation and loneliness experiences were significantly correlated with increased hallucinations experiences, and were more prevalent compared to elderly, healthy controls (Haj et al., 2016). These studies show how social isolation can not only hasten disease onset, but also be a by-product and catalyst of the disease progression itself, and emphasize the importance of investigating social isolation in controlled animal models of neurodegenerative disease. Interestingly, the effect of social isolation in individuals with Huntington disease (HD), as in animal models, remains unclear, and may be significant given that isolation was previously reported as being one of the features that arise with the diagnosis of the disease, along with avoidance, anxiety and depression (Silva, Lindau, & Giacheti, 2015).

1.4. Microbiota manipulation and the gut-brain axis

The human diet has changed drastically over the last several decades due to rise in global urbanization (Drewnowski & Popkin, 1997; Popkin, 2001). Developed, as well as developing countries, have changed the way they eat, drink and produce their food (Kearney, 2010; Popkin, Adair, & Ng, 2012). Urbanization has brought changes in the living environment, and large swathes of the population are not exposed to the same microbes as they

were in the past (Round & Mazmanian, 2009). Changes in diet and environment have had a direct negative influence on our health, including increased preponderance of diabetes (Aune, Ursin, & Veierød, 2009; Hu, 2011), obesity (Bäckhed et al., 2007; Popkin et al., 2012), risk of developing allergies (Kim & Sampson, 2012; Penders et al., 2007), chronic disease (Nishida et al., 2004), chronic fatigue syndrome (Lakhan & Kirchgessner, 2010), and anxiety (Ohland et al., 2013). Furthermore, emerging evidence has begun to elucidate the impact of environmental and dietary factors on neurodevelopmental, neuropsychiatric and neurodegenerative disorders (Lauer, 2010). Although the interaction between the central nervous system (CNS) and the gastrointestinal (GI) tract has been explored and discussed since the mid-1800s (Aziz & Thompson, 1998), research on these two systems have been mostly conducted independently of each other. However, an intriguing bi-directional communication between both systems was recently revealed and has become a topic of intense research (Cryan & O'Mahony, 2011; Mayer, Tillisch, & Gupta, 2015; McLean et al., 2012; Stilling, Dinan, & Cryan, 2013). Interestingly, recent findings have suggested that dietary and environmental interventions in combination with pharmacological treatments can significantly ameliorate and even prevent aging related disorders (Fontana & Partridge, 2015; Ghosh, Sinha, & Raghunath, 2016; Holzer et al., 2015).

1.4.1. The microbiome and microbiota

The mammalian GI tract is home to between 10-100 trillion microbes (Whitman, Coleman, & Wiebe, 1998). These microbial communities, known collectively as the *gut microbiota* (Frank & Pace, 2008; Turnbaugh et al., 2007) predominantly include bacteria, but also viruses, (eukaryotic, bacterial (bacteriophages), and archaeal viruses), fungi and other eukaryotic organisms (Frank & Pace, 2008; Minot et al., 2011; Qin et al., 2010). Microbiota form several types of relationships with their host, including symbiosis, parasitism, mutualism or commensal (Gevers et al., 2012; Lloyd-Price, Abu-Ali, & Huttenhower, 2016; Round & Mazmanian, 2009; Stilling et al., 2013). There are over 1,800 genera and about 40,000 species of gut

bacteria (Forsythe & Kunze, 2012; Frank & Pace, 2008). The main bacterial phyla in the human gut are *Bacteroidetes* and *Firmicutes*; whereas less dominant phyla include *Cyanobacteria*, *Proteobacteria* and *Actinobacteria* (Qin et al., 2010). Approximately 25-33% of microbiota phylotypes are believed to be shared between individuals, although estimations vary between studies due to technical and biological variability (Qin et al., 2010; Salonen et al., 2012).

The population of genes associated with the gut microbiota is known as the *microbiome*, and thought to number about 3.3 million genes (Zhu, Wang, & Li, 2010); over 100 to 150 times more genes than the human genome (Bäckhed et al., 2005; Ley, Peterson, & Gordon, 2006; Qin et al., 2010). The gut microbiota contributes to pathogen defense (Artis, 2008; Chow & Mazmanian, 2010; Rakoff-Nahoum et al., 2004), synthesis of vitamins (Hooper, Midtvedt, & Gordon, 2002), breakdown and absorption of nutrients (Besten et al., 2013), fortification of intestinal epithelial barriers (Banati et al., 2013; Hooper et al., 2001; Maes et al., 2012; Severance et al., 2013), and intestinal permeability (Camilleri, Lasch, & Zhou, 2012; Matricon et al., 2012), and motility (Cani, Everard, & Duparc, 2013). In addition, they play an important role in host physiology (Forsythe & Kunze, 2012; Marchesi & Shanahan, 2007; Sudo et al., 2004) and immune system development (Hughes et al., 2014; Mazmanian et al., 2005; Ringel & Maharshak, 2013; Round & Mazmanian, 2009).

Initial research suggested that first contact with microbiota occurs at birth, during which the digestive tract of the newborn is colonised by microorganisms from within the birth canal and the environment where the birth takes place (Hooper et al., 2001; Vallès et al., 2014). More recent work (Lauder et al., 2016) has, however, provided evidence supporting prenatal microbiota contact via placental and/or amniotic fluid (Aagaard et al., 2014; DiGiulio, 2012; Gomez de Agüero et al., 2016; Kuperman & Koren, 2016; Vallès et al., 2012; Zheng et al., 2017). *Bifidobacteria* is the most preponderant microbiota phyla within healthy individuals during early life (Bäckhed et al., 2015), although microbiota make-up undergoes significant

and more complex changes throughout life and can swell to between 1100 to 3100 phylotypes (Claesson et al., 2011). Various internal and external factors (Moya & Ferrer, 2016), such as host genetics (Goodrich et al., 2016), diet (David et al., 2014), hygiene (Wang & Kasper, 2014), antibiotics (Bercik, Collins, & Verdu, 2012; Gacias et al., 2016; Minter et al., 2017), infections and disease, as well as age (Claesson et al., 2011; Salazar et al., 2014), all play an important role on GI microbiota variability, stability and health.

1.4.2. Bi-directional microbiota-gut–brain communication

Communication and influence between the microbiota, the GI tract and the CNS is bidirectional and reciprocal, and several systems, as well as direct and indirect pathways, have been revealed (reviewed in Wang and Kasper, 2014). The interaction takes place between the CNS, the hypothalamic-pituitary axis (HPA) axis, the autonomic nervous system (ANS), including the sympathetic and parasympathetic divisions, the enteric nervous system (ENS), and the immune system. The CNS exerts its influence on the gut and its microbial community through the sympathetic and parasympathetic pathway via efferent neurons, through the endocrine pathway via the HPA axis, and through satiation signaling peptides. Indirect control is also obtained through activation of the immune pathway. The reverse communication, from microbiota and gut to the CNS, also involves several pathways: neural, metabolic, endocrine and immune. The neural pathway works through activation of vagal afferent nerves (de Lartigue, La Serre, & Raybould, 2011; Perez-Burgos et al., 2013) and neurons of the ENS, which in turn, are stimulated by microbially associated molecular patterns (MAMPs), and cytokines. The metabolic pathway involves synthesis by gut microbes of neuro-active molecules (such as GABA, tryptophan metabolites etc.) (Holmes et al., 2011). MAMPs, such as lipopolysaccharides (LPS), short-chain fatty acids (SCFA), and bacterial lipoprotein (BLP) also contribute to the metabolic pathway. Endocrine influence is gained, in part, via enteroendocrine cells (EEC), present in the gut epithelium, which secrete signaling peptides and neurotransmitters. The immune pathway is mediated

by the effect of microbes, and MAMPS on the auto-reactivity of peripheral immune cells to the CNS, and by systemic circulation.

The gut microbiota produces a diverse range of metabolites, neurotransmitters and neuromodulators, which act on the gut-brain axis via the metabolic pathway. Among them, generated short-chain fatty acids (SCFAs) are metabolites produced in large amounts by *Bacteroidetes* through microbial fermentation of non-digestible carbohydrates. SCFAs include acetate, butyrate and propionate and make up between 90-95% of the total population. The remaining population consists of branch-chained SCFAs produced by proteins that are not absorbed in the small intestine. SCFAs are involved in multiple functions related to the immune system (reviewed by (Corrêa-Oliveira et al., 2016), which include provision of energetic substrates for epithelial cells in the gut (Donohoe & Bultman, 2012), regulation of epithelial cell signaling (Iraporda et al., 2015), alteration of neutrophil differentiation, recruitment and survival (Rodrigues et al., 2016), modulation of T lymphocytes (Arpaia et al., 2013; Gurav et al., 2015), dendritic cells (Millard et al., 2002; Singh et al., 2010) and macrophages (Cox et al., 2009; Vinolo et al., 2011), and contribution to epithelium homeostasis (Kelly et al., 2015). In addition, gut-brain communication is influenced by SCFAs via several mechanisms, including altered catecholamine (Nankova et al., 2014), dopamine, serotonin and GABA levels (Bravo et al., 2011; El-Ansary, Ben Bacha, & Kotb, 2012), and regulation of microglia maturation and function (Erny et al., 2015; Sampson et al., 2016), glial homeostasis (Huuskonen et al., 2004), and tyrosine hydroxylase gene expression (DeCastro et al., 2005; Parul Shah et al., 2006).

Among neuroactive substances produced by gut microbes, GABA is synthesized by specific strains of *Bifidobacterium* and *Lactobacillus* (Hiraga et al., 2008; Komatsuzaki et al., 2008). Other neuroactive products include catecholamines (such as dopamine (Asano et al., 2012) and noradrenaline), histamine, serotonin (Desbonnet et al., 2014), melatonin, and acetylcholine. GI bacteria can also synthesize tryptophan metabolites (such as kynurenine, 5-hydroxytreptamine (5-HT), indole and tryptamine) and precursors, as well

as cytokines released during the immune response (Bailey et al., 2011; Lyte, 2013). These microbiota-derived substances can signal either via cells and receptors in the gut lumen, or via neurocrine or endocrine pathways and mechanisms. Release of endocrine factors, such as 5-HT, and peptides, including leptin, gastrin, orexin and galanin, which modulate the endocrine pathway, have been suggested to play a key role in stress, depression, addiction, anxiety, arousal and circadian rhythms, and act at the border of the blood brain barrier (BBB) in the area postrema (reviewed in Wang & Kasper, 2014).

1.4.3. Experimental approaches to investigate the influence of the microbiota on the brain

Antibiotic treatment

Treatments using a combination of antibiotics can partially decrease the microbial population in the gut (Reikvam et al., 2011), and alter microbiota make-up and diversity (Bercik et al., 2011; Puhl et al., 2012). The time-scale of the effect of antibiotic treatment on microbiota appears to be dependent on the age of the subject, and produces transient effects on adult mice, but long-term effects on neo-natal mice (Cho et al., 2012; Cox et al., 2014). Recent studies have revealed complex effects of antibiotic treatments on metabolism (Cox et al., 2014), as well on behavioural changes in diabetic mice (Gacias et al., 2016), neuro-inflammation and amyloidosis in an AD mouse model (Minter et al., 2017), and susceptibility to experimental autoimmune encephalomyelitis (Yokote et al., 2010).

Germ-free animal model

Germ-free environments provide a method to deplete gut microbiota to a greater degree than antibiotic treatments. Although the concept of germ-free animals was first proposed and debated in the late 1880's, by Louis Pasteur and Marceli Nencki, it was not until the 1950s that the tools required for laboratory investigations were made commercially available (Luckey, 1963). Several approaches are available to interrogate host-microbe interactions in animal models, including germ-free (GF), ex-germ free (exGF), gnotobiotic,

specific pathogen free (SPF), or conventional (CON) environments. Germ-free animals are born and live in aseptic isolated units, where food water and air are sterilised, such that these animals are free of all 'detectable' microbes and microorganisms (Luckey, 1963; Wostmann, 1981; Yi & Li, 2012). Ex-germ-free animals are born, and live in GF conditions for a limited time, after which they are 'conventionalised' by being introduced to microbe-populated environments. Gnotobiotic animals, in turn, are GF animals colonised with one or more known strains of bacteria (Fritz et al., 2013; Smith, McCoy, & Macpherson, 2007). Similarly, SPF animals are those colonised with a mixture of eight bacterial strains, known as Schaedler flora (Dewhirst et al., 1999). Finally, conventional animals are those born and housed under normal, or conventional, laboratory conditions (Norin & Midtvedt, 2010). Importantly, the effects observed as a result of an absence of microbiota are partially reversed through targeted pathogen recolonization of the microbiota (Braniste et al., 2014; Sudo et al., 2004).

1.4.4. Microbiota modulation of CNS plasticity

Both physical and psychological stress induces changes in normal gut function (Porter & Rettger, 1940), and alters microbiota composition (Bailey & Coe, 1999). Conversely, commensal microbiota is involved in the development of the HPA axis through its interaction with the serotonergic system. The HPA axis, part of the limbic system, regulates anxiety and stress responses to environmental stimuli (Tsigos & Chrousos, 2002). The link between brain plasticity and microbiota was first demonstrated in a seminal study where GF animals had different HPA responses to stress compared to SPF animals, whereas re-colonization of the gut with microbes partially reversed the effects (Sudo et al., 2004). Subsequent studies confirmed and extended this finding, by demonstrating an increased HPA axis response and reduced anxiety related behaviours in GF animals (Clarke et al., 2013; Gareau et al., 2011; Neufeld et al., 2011). Furthermore, anxiety-related behaviours induced by *Lactobacillus rhamnosus were* reduced in vagotomised mice, revealing a key role for the vagal pathway in mediating the effect of microbiota on stress (Bravo et al., 2011).

Other behavioural effects of a germ-free environment include modulation of risk-taking (Clarke et al., 2013), social (Desbonnet et al., 2014), hyperactivity (Heijtz et al., 2011), depressive-like, and anxiety-like, behaviours (Bercik et al., 2011; Bravo et al., 2011; Clarke et al., 2012; Heijtz et al., 2011; Neufeld et al., 2011; Savignac et al., 2014). Reduced memory, as measured using a novel object test, has also been ascribed to GF relative to SPF animals (Gareau et al., 2011).

In terms of brain neurochemistry, GF mice exhibit changes in neurotrophic factors (such as BDNF) (Bercik et al., 2011; Heijtz et al., 2011; Sudo et al., 2004), $GABA_A$ and $GABA_B$ receptor subunits (Bravo et al., 2011), NMDA receptor subunits, and serotonin (Neufeld et al., 2011) and tryptophan, the precursor of serotonin (Clarke et al., 2013).

The contribution of a healthy BBB is essential for normal brain development. However, a recent study revealed increased BBB permeability in GF animals that manifested in intrauterine life and persisted throughout their lives. This was associated with reduced levels of endothelial tight junction proteins, occludin and claudin-5, in the frontal cortex, striatum and hippocampus of GF mice compared to SPF (Braniste et al., 2014). Interestingly, when GF animals were colonised with *Clostridium tyrobutyricum* or *B. thetaiotaomicron* (SPF microbiota) BBB permeability properties were restored to SPF levels and occludin and claudin-5 levels were upregulated. This study suggests that early dysbiosis in the gut could lead to neurodegeneration, through extravasation of neuro-inflammatory substances as a result of increased BBB permeability.

1.4.5. Microbiota effects on myelination

Genome-wide transcriptome profiling of the prefrontal cortex showed upregulation of genes linked to myelination and myelin plasticity, as well as upregulation of genes related to neural activity induced-pathways in germ free animals compared to SPF control (Hoban et al., 2016b). In addition, increased mRNA levels of several myelin related gene transcripts and regulatory factors (MBP, Mobp, MAG, MOG, PLP1) were reported in the

PFC, but not in the frontal cortex, hippocampus, cerebellum, amygdala or striatum of GF mice compared to SPF (Hoban et al., 2016b). Increased expression levels of myelin related genes (MAG, MOG, MBP, PLP1, and MOBP) were also reported in the medial PFC in antibiotic treated compared to vehicle treated non-obese diabetic mice. However, this increase was not observed in healthy controls following antibiotic treatment (Gacias et al., 2016). Interestingly, only oral administration of antibiotics showed this effect, whereas subcutaneous administration failed to induce changes in microbiota composition or myelin differences related to it (Gacias et al., 2016).

Transcriptional changes in myelin related genes were confirmed by hypermyelination of prefrontal cortex axons in GF animals compared to conventional animals (Hoban et al., 2016b). Increased myelin thickness was also seen in the mPFC of healthy mice recipients of the microbiota of diabetic mice treated with antibiotics, as opposed to recipients of the microbiota of non-treated diabetic mice (Gacias et al., 2006).

1.4.6. Microbiota in neurodegenerative disease

Emerging evidence suggests that neurodegenerative, psychiatric, or autoimmune brain disorders can be directly influenced by the microbiota-gut-brain axis. Levels of probiotic bacteria, such as *Fecalibacterium* and *Butyricoccus*, associated with the SCFA butyrate production and inflammation inhibition, were found to be lower in a group of cognitively impaired elderly subjects (Bajaj et al., 2016). In addition, levels of *Lactobacillales* (comprising of *Streptoccaceae*, *Carnobacteriaceae* and *Lactobacillaceae*) were correlated with better performance on memory tests in elderly patients (Bajaj et al., 2016). The Alzheimer Disease (AD) mouse model of Aβ amyloidosis showed alteration in the composition of microbiota during long-term antibiotic treatment, which coincided with a reduction in amyloid plaque deposition and increased levels of soluble Aβ (Minter et al., 2016). Analysis of the fecal microbiome showed that the 5xFAD aggressive AD mouse model exhibited 10-15% lower levels of *Firmicutes,* and 2-15% greater levels of *Bacteroidetes* when compared to healthy controls

(Brandscheid et al., 2016). Motility abnormalities associated with bacterial overgrowth have also been observed in Parkinson disease (PD) patients (Fasano et al., 2015; Gabrielli et al., 2010).

Several studies have recently found altered microbiota in the gut of individuals suffering from multiple sclerosis (MS), one of the most prevalent human demyelinating inflammatory disorders (Cantarel et al., 2015; Chen et al., 2016; Jangi et al., 2016). Interestingly, outside of the gut, microbiota composition in white matter of MS patients was found to exhibit reduced diversity of the most preponderant phylum, *Proteobacteria* (Branton et al., 2016). MS was suggested to be caused by the interaction between complex environmental and genetic factors, and often follows a relapsing-remitting pattern. The relapsing–remitting (RR) mouse model of spontaneously developing Experimental Autoimmune Encephalomyelitis (EAE), recapitulates the main characteristic of this disorder (Baxter, 2007; Constantinescu et al., 2012; Pöllinger et al., 2009). The SPF RR-EAE mouse model is known to develop EAE within 3 to 8 months, but mice bred in a germ free environment were protected from the disease throughout their lives, although ex-GF RR animals developed EAE immediately after they were re-colonised with microbiota (Berer et al., 2011). Moreover, GF animals mono-colonised with the gut microbe, *Segmented Filamentous Bacterium* (SFB), showed increased severity of EAE (Ivanov et al., 2009; Lee et al., 2011), and a cocktail of the probiotic *Lactobacillus* strains given to C57BL/6 mice prevented and delayed EAE (Lavasani et al., 2010).

Epsilon toxin (ε-toxin) is secreted in the intestinal lumen by *Clostridium perfringens,* and thought to play a key role in MS. 10% of MS diagnosed patients were found to harbour ε-toxin in their CSF as opposed to 1% of control individuals (Rumah et al., 2013). This toxin targets oligodendrocytes in the CNS, causing selective death of these cells, while sparing other cell types, such as neurons, glia or astrocytes, and inducing demyelination in a dose and time dependent manner (Linden et al., 2015). Raised levels of hormones of the gut-brain-axis, such as leptin, have been observed in CNS lesions (Sanna et al., 2003) and CSF (Matarese, Moschos, & Mantzoros,

2005) of MS patients, and leptin deficient mice did not go develop EAE (Matarese et al., 2001).

Notably, despite the compelling evidence supporting a key role for microbiota in debilitating neurodegenerative diseases, including myelination-related disorders such as MS, research into the role of microbiota in Huntington disease is sparse. The work presented herein will endeavor to address this research gap.

1.5. Thesis aim, structure and summary of findings

There is growing evidence for white matter (WM) deterioration early in Huntington disease (HD) that is correlated to disease progression. However, little is known about the mechanisms and dynamics of WM changes and their precise role in HD pathogenesis. Elucidating these unanswered questions can provide novel insights into the pathophysiology and clinical manifestation of the disease, and help identify possible treatment strategies. This thesis describes three studies whose aims were to employ environmental and microbiota manipulations to perturb and interrogate white matter plasticity, and examine behavioural changes, in the YAC128 and BACHD mouse models of Huntington disease, and wild-type (WT) controls. These aims were accomplished through use of a battery of behavioural tests, and a range of techniques to examine white matter changes in structure and function, including transmission electron microscopy, immuno-histochemistry, and immunoblotting.

Chapter 2 provides details of the methodologies employed in the studies described in this thesis. Chapters 3 and 4 describe the effects of environmental enrichment and deprivation, respectively, on behaviour and motor performance, and white matter structure and function in the posterior corpus callosum (CC) of the YAC128 mouse model of HD, and WT controls. In turn, Chapter 5 reports our findings with respect to the most novel aspect of this thesis, namely, the effects of microbiota manipulation on white matter

structure and function in the prefrontal cortex (PFC) and CC of the BACHD mouse model of HD, and WT controls. Finally, Chapter 6 endeavours to provide a detailed discussion and overarching interpretation of all results, with reference to available, and occasionally limited, literature, before concluding with an overview of possible future work.

Of note, environmental enrichment was associated with slight improvements in behaviour and motor performance across WT and HD mice, while environmental deprivation elicited minor deficits. Interestingly, a reduction in myelin thickness was observed in WT mice independently exposed to both forms of environmental manipulation, while in YAC128 animals this effect was only seen in response to environmental enrichment. Environmental enrichment was associated with a higher number of small and mid-range diameter axons across genotypes, while environmental deprivation was associated with higher number of large diameter axons in WT animals, but a decrease in YAC128 mice. Both forms of environmental manipulation had no effect on mature oligodendrocyte numbers across genotypes. Germ-free (GF) BACHD mice exhibited an increase in number of regular-shaped myelinated axons, a decrease in irregular shaped myelinated axons, and an overall increase in myelin sheath thickness, relative to BACHD mice raised under control specific pathogen free (SPF) conditions. Myelin basic protein (MBP) expression levels were also associated with a significant decrease in the prefrontal cortex (PFC) of wild-type (WT) GF mice, with a similar, albeit non-significant, effect in BACHD mice. In turn, a reduction in number of mature myelinating oligodendrocyte cells in PFC and CC of WT GF mice was also observed, compared to WT SPF mice. Furthermore, a reduction in mature myelinating oligodendrocyte cells was also seen in the PFC only of BACHD GF animals compared to BACHD SPF controls. Intriguingly, we found that both germ-free WT and BACHD mice exhibited a significant decrease in overall brain weight compared to their SPF housed counterparts. These findings, and others, suggest that environmental and microbiota manipulation induce complex effects on white matter structure, function and development in wild-type and HD mice, which provide novel insights into white matter plasticity and white matter abnormalities in HD.

1.6. Scholarly outputs during the course of PhD study

Poster presentations:

Radulescu C, Vautrelle N, Redgrave P, Bracci E. How do nitric oxide interneurons regulate corticostriatal communication? (2015). Sheffield Psychology Post-Graduate Conference, Sheffield, UK. *(Awarded prize for best 2nd Year PhD poster)*

Radulescu CI, Sidik H, Garcia-Miralles M, Bardile CF, Low H, Chern A, Pouladi MA (2017). The effects of environmental manipulation on myelination in the YAC128 mouse model of Huntington disease. Society for Neuroscience conference, San Diego, USA.

Radulescu CI, Shevin E, Garcia-Miralles M, Bardile CF, Yusof NA, Chern A, Pouladi MA (2017). The effects of a germ free environment on myelination and oligodendroglia in the BACHD mouse model of Huntington disease. International Society for Neurochemistry conference, Paris, France.

Peer-reviewed publications:

Xu X, Tay Y, Sim B, Yoon S, Huang Y, Ooi J, Utami KH, Ziaei A, Ng B, **Radulescu** C, Low D, Ng AYJ, Marie Loh M, Venkatesh B, Ginhoux F, Augustine GJ, Pouladi MA (2017). Reversal of Phenotypic Abnormalities by CRISPR/Cas9-Mediated Gene Correction in Huntington Disease Patient-Derived Induced Pluripotent Stem Cells. *Stem cell reports*, 8(3), 619-633.

Xu X, **Radulescu** CI, Utami KH, Pouladi MA (2017). Multi-electrode Array Recordings from Human Induced Pluripotent Stem Cells - Derived Neurons. *BioProtocol*, (Accepted) doi: 10.21769

Chapter 2. Materials and methods

2.1. Environmental manipulation studies

2.1.1. Experimental groups

All animals were bred and housed in the Biological Resource Centre, at the Biomedical Science Institute, A*STAR, Singapore. All experimental procedures were approved by and conducted in accordance with the ethical guidelines of the animal care committee at our institution.

A total of 67 YAC128 transgenic (HD model) and wild-type (WT, control) mice were used in this study (Table 2.1). Both males and females were included in all experimental groups, unless stated otherwise. Sexing and genotyping of animals were carried out at 3 weeks of age. Mice were weighed on a bi-weekly basis. Animals were sacrificed and their brains harvested at 18 weeks of age.

Table 2.1 Total number of animals used for the environmental manipulation studies

Number of animals per experimental group categorised per sex (WT=Wild Type, YAC128-HD transgenic model, F=female, M=male, EH=enriched housing, SH=standard housing, DH=deprived housing).

	WT			YAC128		
Sex	F	M	Total	F	M	Total
EH	5	5	10	5	5	10
SH	7	6	13	5	6	11
DH	5	6	11	4	8	12

2.1.2. Housing manipulation details

Mice were housed under standard conditions with food ad libitum, in an inverted light-dark cycle until 4 weeks of age. Subsequently, they were placed into their allocated caging conditions, consisting of enriched environment housing (EH), standard housing (SH) or deprived housing (DH). Animals were kept in their allocated condition for a total of 14 weeks (Figure 2.1).

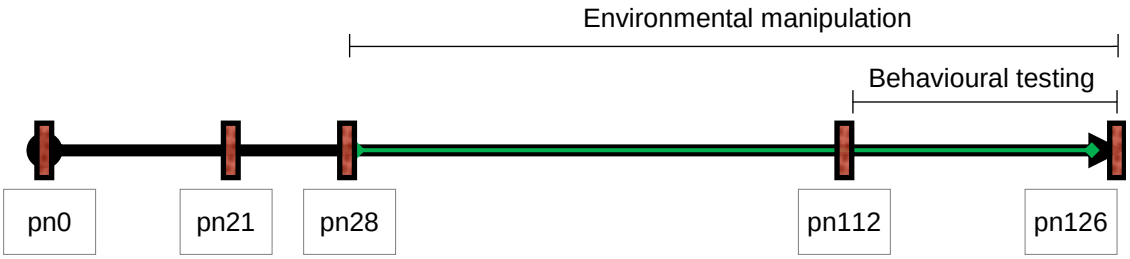

Figure 2.1 Experimental timeline for environmental manipulation studies

Animals were sexed and genotyped at post-natal day (pn) 21, and allocated to experimental conditions at pn day 28. Behavioural testing was started after 12 weeks in their allocated housing conditions, when animals were 112 days old. Tests were carried out for 2 weeks, after which tissue was harvested. Animals were 126 days (i.e. 18 weeks) old when sacrificed.

2.1.3. Behavioural tests description

Behavioural tests were carried for the environmental manipulation (environmental enrichment and deprivation) studies. Mice were subjected to a battery of behavioural tests following 12 weeks of housing according to their experimental condition. All behavioural tests were started at least one hour after the start of a new dark cycle. All animals were moved to the testing room and left to acclimatize for one hour before the start of the experiment. All testing was conducted under dim white-light illumination (about 150 lux) in a sound attenuated room. All behavioural tests run over the course of this study are described below and listed in Table 2.2.

Table 2.2 List of behavioural tests and their interpretation

Behavioural test:	Analysis of:
Spontaneous activity	Motor function and habituation
Open field activity	Anxiety and habituation
Elevated plus maze	Anxiety
Climbing test	Neuromuscular function
Rotarod training **Rotarod test**	Motor function / learning / cognitive

Spontaneous activity (SA)

The spontaneous activity (SA) test was used to measure both gross and fine locomotive movements in mice (Figure 2.2A). Four animals were tested simultaneously in a Mouse Open Field Arena (Med Associates, USA) with the 48 Channel IR Controller for Open Field Activity. The arena dimensions were 27.3cm L x 27.3cm W x 20.3cm H, and consisted of four separated arenas. One mouse at a time was placed in the centre of one of the four arenas, which was automatically activated, and activity started being monitored. Each arena was activated independently of each other. Animals were allowed to explore their allocated arena during this test for 30 minutes. The Activity Monitor software (Med Associates, USA) was used to record horizontal activity (distance travelled, ambulatory counts, ambulatory episodes, velocity), vertical activity (rearing, jumping) and stereotypy in activity.

Open field (OF) activity

The open field (OF) test was used to measure each animal's habituation to a new environment, as well as levels of anxiety, and consisted of measuring the time spent by animals in the centre versus outer area of an arena (Figure 2.2B). An in-house built open field arena, measuring 50cm L x 50cm W x 50cm H, was used. Four animals were tested simultaneously in the arena and their activity was recorded using EthoVision (Noldus, Singapore) video tracking software. Animals were allowed to explore the arena for 10 minutes during which the time spent in the centre of the arena relative to the time spent in the periphery was noted and recorded.

Elevated plus maze (EPM)

The EPM is a well-established test of anxiety (Figure 2.2C). The testing arena is shaped like a "+", with two open arms and two arms having tall enclosing walls. One animal was tested per trial and allowed 5 minutes in the EPM. Recordings were again made using the EthoVision video tracking software. The number of entries into, and time spent, in the open and

enclosed arms, as well as the total number of arm entries, for each animal were noted and recorded.

Climbing test

The climbing test was used to assess motor impairment in mice (Figure 2.2D). Four mesh cylinders were placed on a table and separated by a plastic board so animals were not visible to each other. One animal was placed in each cylinder sequentially. Each trial was video recorded using Sony HDR-CX130 camera for 6 minutes, with the first minute excluded from subsequent analysis The number of times each animal attempted to climb (defined as having placed all four paws onto the mesh) was noted and recorded, as was the latency to the first climbing attempt, and each attempt's climbing time (until any paw was rested back onto the table-top). An animal was excluded from the test if it remained stationary on the table-top during the duration of test, whereas if the animal was mobile but did not attempt to climb, the latency to climb was scored as the maximum duration of the test (i.e. 300s), and climbing time was set to null (i.e. 0s).

Rotarod test (RR)

The rotarod (RR) test was used to assess motor co-ordination and balance in mice, by testing their ability to remain on a rotating rod (Figure 2.2E). The test consisted of 3 days constant-speed rotarod training and one day of testing on an accelerating rotarod. For training, mice were placed on the rotarod in the direction of motion whilst the rotarod turned at 18 revolutions per minute (rpm). Each rotarod contained four lanes that enabled four animals to be trained simultaneously (i.e. one per lane). Animals were returned to the rotarod after each fall during the 300s training period, and every animal underwent two training trials for the first day, and three training trails for the subsequent two days, separated by 2hour intervals. The latency for each mouse to first fall off the rotarod, and the number of falls during training, was noted and recorded. For testing, animals were placed in their respective lanes and allowed to walk on the rotarod (rotating at 5rpm) for a

few seconds in order to gain stability. The rotarod then increased in speed from 5-40rpm over the course of the 300s test duration.

The latency for each mouse to the first fall off the accelerating rotarod was noted and recorded, and the mouse returned back to its home cage after its first fall. Each mouse underwent three test trials on the same day with a two-hour rest-time in between each. Overall performance in the accelerating rotarod test was calculated as the mean of the latency to first fall across the three test trials.

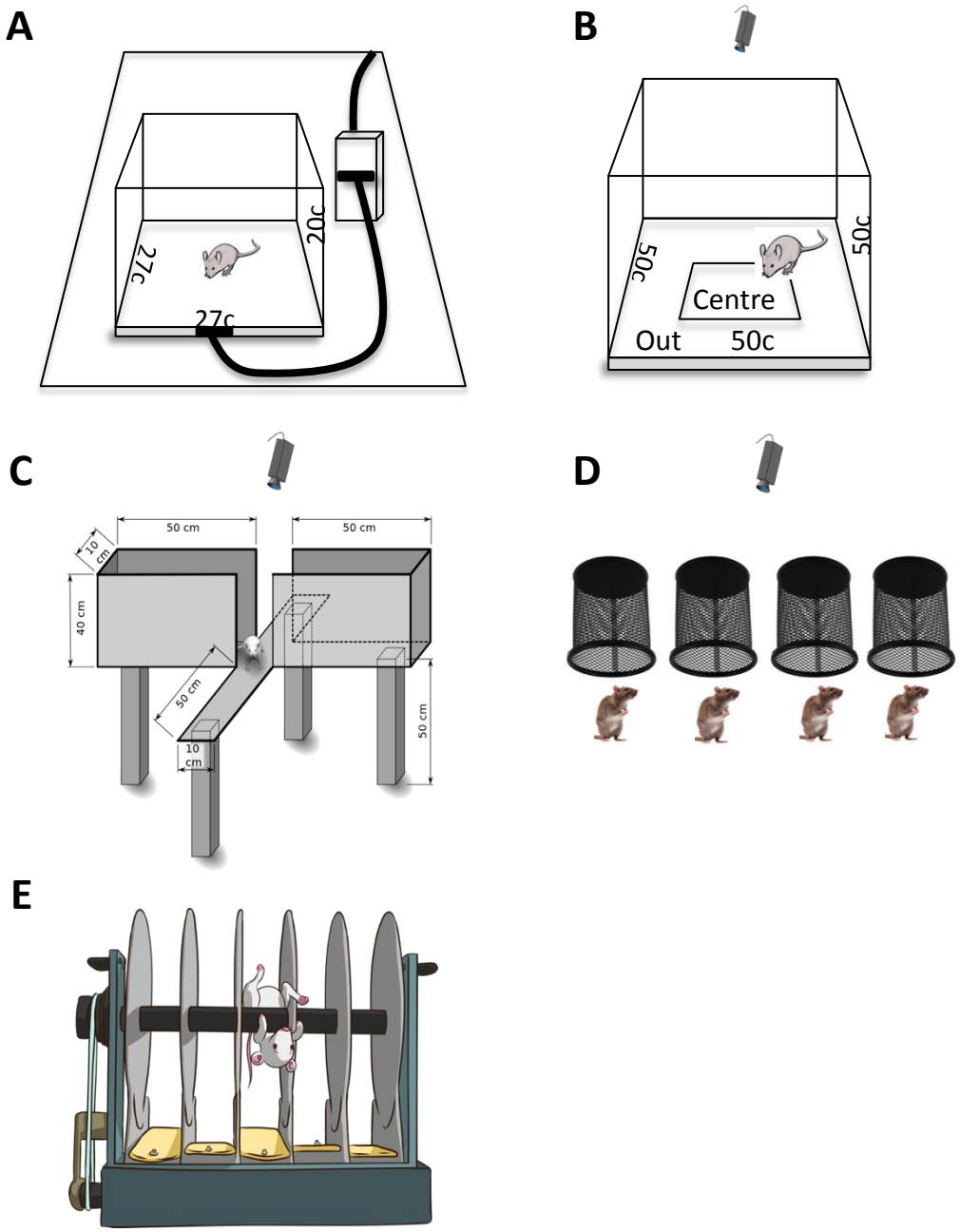

Figure 2.2 Illustrations of behavioural tests

(A) Spontaneous activity (SA); (B) Open field activity (OF); (C) Elevated plus maze (EPM); (D) Climbing test; (E) Rotarod test (RR).

2.2. Microbiome manipulation study

2.2.1. Experimental groups

All mice were bred and housed in the animal facility of the Singapore General Hospital Unit (SGH), Singapore. All experimental procedures were approved by, and conducted in accordance with the ethical guidelines of the animal care committee at our institution. Mice were housed under standard laboratory housing conditions with food ad libitum, in an inverted light-dark cycle.

Wild-type (WT) and BACHD transgenic mouse models of HD were raised under specific pathogen free (SPF) and germ-free (GF) laboratory conditions (Figure 5.1). Each experimental group (N=4) included between 10-13 animals per condition per sex (**Table 2.3**).

Table 2.3 Total number of animals used for the microbiome study

Number of animals per experimental group categorised per sex (WT=wild type, BACHD=transgenic model of HD, GF=germ free, SPF=specific pathogen free, F=female, M=male).

	WT			**BACHD**		
Sex	F	M	**Total**	F	M	**Total**
GF	11	12	**23**	10	14	**24**
SPF	11	13	**24**	10	13	**23**

Animals were genotyped at 3 weeks of age. All animals were weighed at 3 months of age, prior to being sacrificed. Brains were harvested, and weighed comparisons were carried out for both males and females, however, due to cost and time constraints, only males were included in subsequent investigation for the study described in this thesis.

2.3. Tissue harvesting and processing

For all three studies, all brains were segmented through the mid-sagittal plane, and the left hemisphere used for immunohistochemical procedures, while the right hemisphere was microdissected into cortex, prefrontal cortex, striatum, hippocampus, cerebellum and olfactory bulb, and placed in cryo-tubes on dry ice to be used for immunoblotting procedures.

In addition to the brains harvested for immunostaining and immunoblotting, three to four animals in each experimental condition were perfused and harvested, to investigate axonal and myelin related characteristics (i.e. axonal shape and size, and myelin thickness) using transmission electron microscopy (TEM) (Section 2.4).

2.4. Transmission electron microscopy (TEM)

2.4.1. Tissue extraction fixation and storage

Mice were anesthetized with Ketamine (150mg /Kg) and Xylazine (10 mg/Kg), and then transcardially perfused via a catheter inserted through the left ventricle and connected to a pump set to 0.1ml /min. Perfusion was performed with 25ml of ice cold phosphate buffer solution (PBS, made in-house, Table 2.8), followed by transmission electron microscopy (TEM) fixative solution comprising of 25ml of ice cold 2.5% paraformaldehyde (PFA, Sigma-Aldrich, USA, see Appendix A) and 2.5% glutaraldehyde (GlutAH). Following perfusion, all brains were segmented through the mid-sagittal plane, and the right hemisphere placed in 5ml of TEM fixative solution in preparation for TEM. The tissue was stored at 4^{o}C overnight. The following day, brains were washed 3 times in 1xPBS (5-10min per wash; Table 2.8) and stored in 5ml sucrose (5% sucrose, 1^{st} Base, Singapore, & 0.1% sodium azide (NaN_3, Merck, Germany) at 4^{o}C.

2.4.2. Pre-processing and microdissection

The corpus callosum (CC) was microdissected one day before sample preparation for TEM. The mid-sagittal sectioned brain was placed in a mouse-specific stainless steel matrix *(*Roboz Surgical Instrument Company, Inc. Gaithersburg, MD*)*, and the intersection between the CC and fornix used to determine the region where a 1mm coronal section would be segmented using a commercial blade. For the environmental manipulation studies, the posterior CC (splenium) was microdissected (~Bregma -1.82 to -2.70mm, the equivalent of region 5 as described by Barazany et al. (2009) (Figure 3.11 and Figure 4.9); whereas, for the microbiome study, the anterior mid-body region of the CC was microdissected (~Bregma -0.8 to 0 mm) (Figure 5.2). The microdissection was carried out in a petri dish filled with 1xPBS (Table 2.8), and visualised under a dissecting microscope (Figure 2.3). The samples were cut in the shape of a rectangular cuboid in order to determine the direction of the fibres for TEM. Tissue samples were washed in 1xPBS and left overnight at 4^{o}C before sample preparation the next day.

A

B

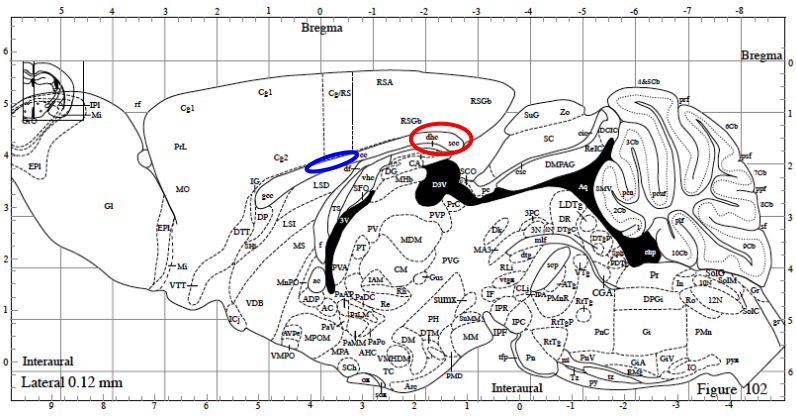

Figure 2.3 Corpus callosum microdissection for TEM

(A) Microdissection of the posterior (splenium) CC viewed under the microscope.
(B) Sagittal map (adapted from Paxinos and Franklin, 2012) indicating (red circle) splenium, and (blue circle) anterior mid-body of the CC.

2.4.3. Sample processing and embedding

On the first day, samples were post fixed in 1% osmium tetroxide (OsO_4, 1g of osmium in 100ml PBS (Table 2.8), pH 7.4) for 1 hour at room temperature under a fume hood, and then washed twice in deionised water for 5-10min. The next process was dehydration through an ascending ethanol series, at room temperature:

a) 25% ethanol (Merck, Germany)– 5 minutes;
b) 50% ethanol – 10 minutes;
c) 75% ethanol – 10 minutes;
d) 95% ethanol – 10 minutes;

e) 100% ethanol – 10 minutes;
f) 100% acetone – 10 minutes – 2 changes.

The final process on day 1 was infiltration, using acetone and resin. Resin was prepared from Araldite (90g), DDSA (80g) and DMP-30 (2.4g) (all purchased from Sigma Aldrich, Singapore). The following two steps were followed:

a) 100% acetone:resin (1:1) for 30 minutes at room temperature;
b) 100% acetone:resin (1:6) overnight at room temperature;

On the second day, three incubation sessions with resin were used:

a) First change of fresh resin – for 20 minutes at room temperature;
b) Transfer to oven (40 ^{O}C – 50 ^{O}C) for 30 minutes;
c) Two changes of fresh resin for 1 hour each (45 ^{O}C and 50 ^{O}C respectively);
d) Finally, samples were aligned and placed in a cavity embedding mould (1 or 2 samples per block, Zivic Instruments, USA), and embedded in fresh resin to polymerise at 60^{O} C for 24 hours.

2.4.4. Ultramicrotome trimming and sectioning

Cavity embedding mould was removed from the oven after 24 hours and samples were taken for sectioning.

Each sample was isolated from the resin by trimming prior to ultra-thin cutting. The samples were visualised through the resin due to their black colour as a result of osmication. Samples were revealed by trimming the resin manually using a commercial razor blade and subsequently aligned and positioned in the ultra-microtome (Reichert-Jung ultracut E) block holder for further trimming using an in-home built glass knife. Glass knives were obtained by cutting glass strips under a Leica EM KMR2 microscope. Cutting speed was set to 1.5 mm/sec and cutting thickness was set to 0.5µm. Semi-thin sectioning was performed and several sections stained with toluidine

blue dye so as to visualise tissue network under the microscope, and confirm target region and viability of the sample.

Following confirmation of the target region, ultra-thin sectioning was performed using a diamond knife with a boat (Diatome, Ultra45, 3mm length, USA). Cutting speed was set to 1.5 mm/sec and cutting thickness was set to 90nm. At this thickness the samples, which form a ribbon, are seen as a gold colour when visualised under the microscope. The golden colour indicates an appropriate thickness (see figure of colour band – ultra-microtome). After securing the ribbon on a 200-mesh grid (Ellipsiz DSS Pte Ltd, Singapore), it was left to dry and placed in a plastic capsule.

2.4.5. Axonal (fibre) staining

When enough grids were collected (5-6 per animal), fibres were stained at room temperature using lead citrate (Reynolds lead citrate, composed of lead nitrate and sodium citrate, 3%) for 8 minutes, followed by thorough washing in deionised water. The grids were dried with filter paper, placed on a different filter paper and left to dry for several minutes before being returned to the plastic capsules housing.

2.4.6. TEM viewing, image capturing, and analysis

Samples were viewed using a Tecnai G^2 Spirit Twin/ Biotwin model (FEI, USA) trasnimission electron microscope. Representative micrograph of callosal axons is illustrated below, in Figure 2.5A. Two grids were chosen based on the quality of the ribbons and 10-12 images were taken from each grid. A total of 12 images per animal were chosen to be analysed using ImageJ software (version 2.0.0, National Institutes of Health, USA). An unbiased frame was randomly selected using the rectangular tool and superimposed on each image. Conversion of image magnification was performed using the line tool in ImageJ. Axonal myelin thickness was calculated using g-ratio analysis, in which the inner and outer diameter of regular shaped axons were measured using the line tool in ImageJ, and the ratio between both values calculated (Friede, 1972; Figure 2.4). Between 25-

40 axons per image, giving a total of 300 to 480 values per animal, were measured. The results were exported to Matlab (Matlab, USA), where the g-ratios were calculated.

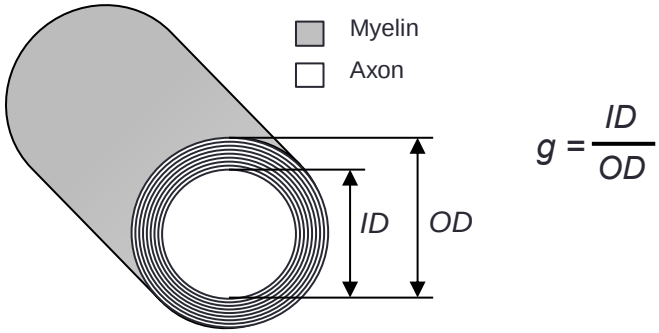

Figure 2.4 Calculation of g-ratio diagram

The g-ratio, used as measure of myelin thickness, was calculated as the inner diameter over the outer diameter (i.e. higher g-ratios are associated with reduced myelin thickness).

For axonal counting, all unmyelinated axons within the selected unbiased frame were counted. In addition, myelinated axons were classified as ‘regular’ or ‘irregular’ shaped axons based on their circular properties. Thus, axons with quasi-, circular or elliptical shapes were counted as ‘regular’ axons, whereas remaining axons were categorised as ‘irregular’ shaped (Figure 2.5B).

A

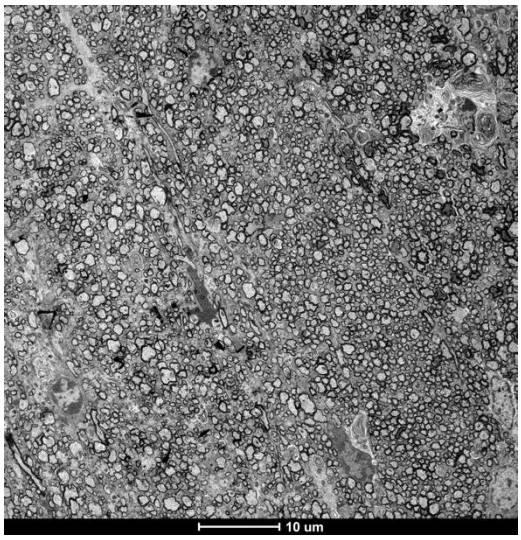

B

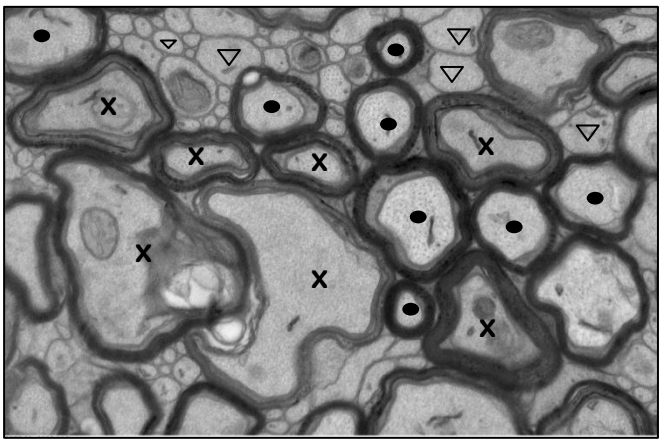

Figure 2.5 Representative micrographs of myelinated and unmyelinated axons in the posterior corpus callosum of the mouse brain

(A) Representative micrograph of callosal axons as viewed using transmission electron microscopy (Tecnai G^2 Spirit Twin microscope). Scale bar at 10µm.
(B) Myelinated axons were classified as regular (filled circles) and irregular (black crosses). Unmyelinated axons are denoted by triangles.

2.5. Immunohistochemistry and immunofluorescence

2.5.1. Tissue extraction, fixation and storage

Mice were placed in a CO_2 gas chamber for 5 minutes after which they were euthanized by cervical dislocation. Brains were carefully extracted, segmented through the mid-sagittal plane, and the left hemisphere placed in 5ml of 4% PFA solution (4g in 100ml 1xPBS; see Appendix for PFA recipe)

at 4^{o}C overnight. The next day, brains were washed 3 times in 1xPBS (5-10min per wash) and stored in 5ml sucrose (30% sucrose & 0.1% NaN3 in 1xPBS) at 4^{o} C until further processing.

2.5.2. Cyrosectioning

Left hemispheres were removed from the sucrose solution and dried on filter paper. Prior to cryosectioning, brains were cryopreserved in dry ice and isopentane (2-methylbutane) to preserve structurally intact cells and tissues. The cryopreserved brains were embedded onto chucks using optimum cutting temperature (OCT) compound (VWR, USA). Coronal slices were sectioned at a thickness of 25µm, at -20^{o} C using a cryostat (Thermo Scientific, USA). Collection began when the forceps minor of the corpus callosum (fmiCC) became visible during sectioning. Following sectioning, brain slices were placed in 1xPBS and 0.1% NaN3 solution in a 24 well plate. The slice corresponding to the location where the fmiCC from each hemisphere meet to form the genu (gCC) of the corpus callosum (~ Interaural 4.98-4.90 mm and ~Bregma 1.18-1.10 mm) was visually identified. A mark was made on the well where this section was placed.

2.5.3. Immunohistochemistry staining

The well to be stained was chosen based on the mark of the gCC on the well plate. All sections (4-5 per well) were removed from each of the selected wells and placed into 12-well plate in NetWell inserts (one well per animal and one well for as a negative control for each condition) and placed in 1xPBS. Brain sections were then:

1) Incubated in 2ml/well phenylhydrazine solution (Sigma-Aldrich, USA, 10µl phenylhydrazine / 1ml 1xPBS) and left for 45 minutes at room temperature (RT) on a rocker to block endogenous expression of peroxidase. This was followed by 3 washes in 1xPBS for 10 minutes per wash.

2) Incubated in blocking solution (1xPBS: 5% Normal Goat Serum - NGS, Sigma-Aldrich, USA; 5% BSA, GE Lifesciences, USA; 0.1% Triton, OmniPur, USA) for 30 minutes at RT on a rocker.
3) Immersed in the primary antibody and incubated with 5% NGS and 0.2% Triton, in 1xPBS overnight at 4ºC.
4) The following day, sections were washed 3 times in 1xPBS for 10 minutes per wash. This was followed by incubation in biotinylated secondary antibody for 1.5 hours at RT. Secondary Antibody Solution was prepared in 1xPBS: 1% NGS, 0.2% Triton and 1:200 ABC Vectastain Kit solution (rabbit kit, Vector Laboratories, USA). Post-incubation, sections were washed 3 more times in 1xPBS for 10 minutes per wash.
5) Incubated in ABC solution for 2 hours at RT on the rocker. ABC reagent was prepared in 1xPBS: 1:100 of solution A and 1:100 of solution B. Post-incubation, sections were washed 3 times in 1xPBS for 10 minutes per wash.
6) Finally, sections were stained using DAB (1:40, chromogen:buffer; Vector Laboratories, USA,). After staining, sections were returned to 1XPBS, mounted on a glass slide (Biomedia, Singapore) and allowed to dry. Once dry, a coverslip with DPx Mountant (Sigma-Aldrich, USA) was placed over the brain section.

2.5.4. Immunofluorescence staining

Immunofluorescence (IF) staining was performed using platelet-derived growth factor receptor alpha (PDGFRα) antibodies. The well to be stained was chosen based on the mark of the gCC on the well plate. All sections (4-5) were removed from each of the selected wells and placed into 12-well plates in NetWell inserts (one well per animal and one well as a negative control for each condition) and placed in 1xPBS. Sections were first pre-treated in hydrochloric acid (HCl) based solution (stock of 1N and 2N was prepared from 37% HCl solution), an antigen retrieval reagent, to break protein cross-links formed by formalin fixation and uncover hidden antigenic

sites, was conducted. Sections were subsequently incubated in the following manner whilst being agitated using an orbital shaker:

1) 10 min on ice in 1N HCl in pre-cooled wells
2) 10 min at RT in 2N HCl
3) 20 min at 37^{o} C in 2N HCl in pre-warmed wells
4) 10 min at RT in 0.1M borate buffer solution, (pH 9)

A standard staining protocol was then followed where sections were sequentially:

5) Washed 3 times in 1xPBS for 10min per wash.
6) Incubated for 90-120 min in blocking solution (5% normal donkey serum - NDS, Sigma-Aldrich, USA; 0.2% Triton; in PBS)
7) Incubated in primary antibody solution (1% NDS, 0.2% Triton, in PBS) overnight at room temperature.
8) Washed 3 times in 1xPBS for 10min per wash the following day
9) Incubated in secondary antibody 1:500 in PBS (0.2% Triton in PBS) for 2 hours, and well plates covered with aluminium foil to prevent fluorochrome bleaching.
10) Washed 3 times in 1xPBS for 10min per wash.
11) Finally mounted on a glass slide and allowed to dry.

2.5.5. Stereology

Cell counting was blind to the experimental conditions, as new IDs were randomly assigned to all animals prior to the start of staining. An upright microscope (Olympus, Japan) was used to view the stained brain sections and Stereo Investigator software (MBF Bioscience, USA) was used for imaging and analysis. Section cut thickness was set to 25 µm, whereas the section evaluation interval was 12 (since each section was 12 wells apart from the next). The coronal navigation of the mouse brain atlas (Paxinos and Franklin, 2001) was used as reference to draw contours for the regions of interest: prefrontal cortex (PFC, Bregma 1.18 to -0.94 mm), corpus callosum (CC, Bregma 1.18 to 0.86 mm). The grid size was set to 100 for the PFC,

and 50 for the CC. A total of 15 counting frame sites were selected for counting cells in both regions. Areas that contained no cell bodies or were outside the contour were omitted. After counting from all the selected sites for each specific region, a results file containing several variables was generated by the software. The Gundersen and Schmizh-Hof coefficient of errors were used to decide whether enough sites were counted for each section.

The estimated cell population was exported to excel and each animal was re-assigned to its corresponding experimental group. Statistical analysis was performed in Prism (see Section 2.7).

2.6. Western blot processing

2.6.1. Tissue extraction, fixation and storage

The right hemisphere of each brain was microdissected into cortex, prefrontal cortex, striatum, hippocampus, cerebellum and olfactory bulb, and placed in cryo-tubes on dry ice. The cryo-tubes were stored at -80^{o}C to be later used for immunoblotting procedures.

2.6.2. Tissue lysis

Microdissected cortex tissue was removed from -80° C and placed on dry ice. The first step of the protocol involved preparing the lysis buffer on ice (see Table 2.4).

Table 2.4 Lysis buffer recipe for western blot

Solutions	Stock	Final	Vol to add to 1ml	Company
RIPA	NA	NA	944	Sigma-Aldrich
PMSF	100mM	1mM	10	Sigma-Aldrich
PI cocktail	25x	1x	40	Roche
Z-VAD	5mM	5µm	1	Promega
NaVan	700mM	1mM	5	Sigma

The steps below were followed for the tissue lysis process:

1) Tissue was lysed in the prepared buffer using a tissue homogenizer glass.
2) Tissue lysates were incubated on ice for 20 minutes.
3) After incubation, tissue lysates was spun in a 4°C pre-cooled centrifuge at 15,000rpm, for 20 minutes, to remove cell debris.
4) Supernatant was transferred into newly labeled 1.7mL tubes and kept on ice.

2.6.3. Bradford and protein quantification

Bradford Standards was prepared using bovine serum albumin (BSA) (Table 2.5). BSA stock was prepared by dissolving BSA Fraction V powder in sterile PBS to a final concentration of 2mg/mL (Table 2.8) and syringe filter (0.2µm).

Table 2.5 Bradford standards for western blot

	PBS (µL)	BSA standard (µL)	Final concen-tration µg/ml	Final volume (µL)
A	400	-	0	400
B	325	325 of C	125	325
C	375	375 of D	250	375
D	325	325 of F	500	325
E	175	175 of G	750	350
F	325	325	1000	325
G	125	375	1500	325
H	0	300	2000	300

In addition, 1xBradford dye (Bio-Rad, USA) was prepared in deionised water from stock (Table 2.7A) and stored on ice.

The following steps were then followed:

1) Samples were diluted in strip tubes up to 10-fold in RIPA buffer (9µL of RIPA buffer: 1µL of protein sample) and vortexed.

1µL of Bradford standards and 1µL of diluted protein samples were aliquoted in triplicate into 96-well clear flat bottom plates (Table 2.6).

Table 2.6 Plate reader format for the Microplate Reader

	1	2	3	4	5	6	7	8	9	10	11	12
A	0 µg/mL			Sample 1			Sample 9			Sample 17		
B	125 µg/mL			Sample 2			Sample 10			Sample 18		
C	250 µg/mL			Sample 3			Sample 11			Sample 19		
D	500 µg/mL			Sample 4			Sample 12			Sample 20		
E	750 µg/mL			Sample 5			Sample 13			Sample 21		
F	1000 µg/mL			Sample 6			Sample 14			Sample 22		
G	1500 µg/mL			Sample 7			Sample 15			Sample 23		
H	2000 µg/mL			Sample 8			Sample 16			Sample 24		

2) 1x Bradford dye was added into the reagent reservoir. 200µL of 1x Bradford dye was added to each well using a multichannel pipet.
3) The plates were incubated in the dark for 15 minutes and agitated using a rotary shaker.
4) The plates were then placed in the Microplate Reader (BMG Labtech, Germany)
5) Omega MARS (BMG Labtech, Germany) software was used to measure absorbance of the samples.
6) The obtained results were then exported to excel where the protein concentration was calculated. See Table 2.7B for protein calculation formulas.
7) An amount of desired protein was chosen – between 30µg and 20µg. A final volume of 20µL of sample was chosen.
8) The following items were calculated for the gel sample preparation:
    a. The volume of protein (Vp) sample to be loaded (Table 2.7C).
    b. The Loading Dye (NuPAGE LDS Sample Buffer, Novex, USA) and reducing buffer (NuPAGE Sample Reducing Agent, Novex, USA) volume (Table 2.8).
    c. Volume of lysis buffer (Vlb) to be added (Table 2.7D).

Table 2.7 Western blot calculations

	Calculations	Abbreviations and notes
A) Bradford dye	$Vbd = (st + sp)\ x\ 3\ x\ 200\mu L$	*Vbd* = volume Bradford dye; *st* = no. of Bradford standards; *sp* = no. samples; *3* = triplicates.
B) Protein concentration	$y = m \times x + c \ \rightarrow\ x = (y - c) \div m$; Final $C = x * 10$	*y* = absorbance measurement, *m* = gradient of curve; *x* = concentration; *c* = the y-intercept; 10 is the dilation factor.
C) Volume protein sample to be loaded	$Vp = Sp \div C$	*Vp* = volume protein; *Sp* = amount of desired protein; *C* = concentration of protein sample.
D) Final volume of lysis buffer	$Vlb\ = Vs - LDS\ SB - \mathrm{SRA} - \mathrm{Vp}$	*Vlb* = volume lysis buffer; *Vs* = volume sample, LDS SB = LDS sample buffer; SRA = sample reducing agent; *Vp* = volume protein.

2.6.4. Sample preparation and gel running

The final volume per sample was 20µL and included protein samples, NuPAGE LDS Sample Buffer, NuPAGE Sample Reducing Agent and lysis buffer. This was aliquoted into strip tubes according to the Bradford Sheet calculations. The strip tubes were vortexed and spun, followed by 10 minutes boiling at 70°C.

While samples were boiling, the Precision Plus Protein All Blue Standards ladder (Bio-Rad, USA) was thawed at room temperature and a 20X MES Running Buffer (Novex, USA) was prepared. A 10 well, 12% Bis-Tris protein gel (Novex, USA) was used. The protein gel tank (Novex, USA) was configured and the gel comb carefully removed without disrupting the wells. MES Running Buffer was poured into the tank.

10µL of protein ladder was first loaded in the first well, and 5µL added to the tenth well. Once boiled, samples were vortexed and spun and then loaded into the gel (20µL per well). Finally, the gel tank was plugged into PowerPac and the gel was run for 3-4 hours at 100V.

2.6.5. Western transfer

1X Western Transfer Buffer (1L) was prepared using 10X Transfer Buffer (100mL), 100% Methanol (200mL, Merck, Germany) and deionised water (700mL), and cooled at 4°C before use.

Transfer tank was set up using the following steps:

1) Transfer buffer was poured into the assembly tray.
2) 1x gel holder cassette, two foam pads and four filter papers were soaked in the transfer buffer.
3) Transfer membrane was then activated. Nitrocellulose (Bio-Rad, USA) – Transfer Buffer; PVDF – 100% Methanol.
4) The gel holder cassette was placed in the assembly tray with the black side facing down and the transparent side against the slope of the assembly tray.
5) A pre-soaked foam pad was placed on the black side of the gel holder cassette and the roller used to remove any bubbles.
6) Two pre-soaked filter papers were placed on top of the foam pad and removed of any bubbles.
7) The protein gel cassette was opened to release gel.
8) The end of the gel was trimmed off.
9) The gel was placed on top of filter paper from step 6.
10) Transfer membrane was soaked in transfer buffer before placing over the gel.
11) Two pieces of pre-soaked filter paper were placed on top of transfer membrane and any bubbles gently rolled out using the roller.
12) Another foam pad was placed on top of the filter papers in step 11 and any bubbles gently rolled out using the roller.
13) The clamp on the transparent side of the gel holder cassette was locked to secure all components.
14) The gel holder cassette was placed into trans-blot central core.
15) Trans-blot central core was placed into mini trans-blot cell.
16) A frozen ice-pack was placed in the trans-blot cell.
17) The gel was run at 120V for 1.5hours.

Table 2.8 Agents concentrations

Agent	Stock concentration	Final concentration	Company
BSA		2 mg / ml	
Bradford Dye	5X	1X	Bio-Rad
NuPAGE LDS Sample Buffer	4X	1X	Novex
NuPAGE Sample Reducing Agent	10X	1X	Novex
NuPAGE MES SDS Running Buffer	20X	1X	Novex
Tris-Glycine Transfer Buffer	10X	1X	Made in-house
PBS	10X	1X	
Tween (PBS-T)	100%	0.1%	In-house

2.6.6. Western blot – LiCor System

1X PBS-T was prepared from 10X in-house made PBS in deionised water and adding 100% Tween-20 (OmniPur, USA) for a final concentration of 0.1%. Endogenous control used for primary antibodies were rabbit anti-Calnexin (90kDa) or mouse anti-β-actin (42kDa). Primary antibodies included MBP (Millipore, USA), MAG (Millipore, USA), PLP (Abcam, USA) and Ermin (Merck, Germany) (Table 2.x).

Secondary antibodies were diluted at a concentration of 1:10,000, and included: Alexa-Fluor goat anti-rabbit 680 (Life Technologies, USA) Alexa-Fluor goat anti-mouse 800 (Life Technologies, USA) and Alexa-Fluor goat anti-rat 800 (Life Technologies, USA).

The following steps were involved:

1) Approximately 10mL of LiCor Blocking Buffer (LiCor, USA) were added to containers labelled with their corresponding ID.
2) Membrane from transfer cassette was placed into the container with Blocking Buffer and incubated for 1 hour shaking at RT.
3) Blocking buffer was removed and primary antibody was added to the container containing the membrane. This was placed at 4°C on the shaker overnight.

4) The next day the membrane was washed 1x30 minutes, 1x15minutes, 1x10min and 1x5min at room temperature.
5) All subsequent steps were conducted in the dark to prevent the fluorophore from degrading. The membrane was incubated in secondary antibody for 1 hour at RT.
6) The membrane was then washed 1x15minutes and 3x5minutes in PBS-T.
7) A LiCor Imaging System (LiCor, USA) was used to scan and visualize the blots.

2.6.7. Membrane imaging

The membrane was imaged using the LiCor Imaging System and Odyssey V3.0 software (LiCor, USA). LiCor system can only detect 700 and 800 wavelengths. The intensity was adjusted for the 700 and 800 channels individually. The image curves were adjusted after the membrane was scanned. The image was then saved and exported as TIF files.

2.6.8. Western blot analysis

Scanned images of the blots were imported to Image Studio Lite (ver 5.2). The image intensity was adjusted using the software adjust tool. Relevant channels were selected based on the secondary antibodies used. A rectangle was drawn over the largest band representing one of the samples tested, and the same rectangle was copied and pasted over the other bands for each of the samples. Thus, the area of interest for each sample was equal within one gel. This was followed by drawing a rectangle over the control bands (i.e. Calnexin). The background average was selected overlying, or adjacent to, the bands, or both. Each band was then labeled with its corresponding condition name. Signal intensity and background values for each band was then automatically calculated and exported to Excel (Microsoft, USA). Here, the total signal of the protein of interest (i.e. MBP) was normalised to the corresponding total signal of the control protein (i.e. Calnexin) for each sample. The resulting values were then normalised to the average of all the values of the control condition for that comparison. For

example, in the case where SPF animals were compared to GF animals, the SPF group was used as control, and GF data normalised to that of SPF. Results were then exported to Prism (GraphPad, USA) for statistical analysis.

Table 2.9 Primary antibodies details

Antibodies	Isotope	MW (kda)	Application	Dilution	DAB (min)	Source
GST-π	rabbit		IHC	1:3000	2.5	Scientific Hub Services
Olig2	rabbit		IHC	1:300	6.5	Merck Milipore
Olig2	rabbit		IF	1:750	-	Merck Milipore
MBP	rat	18-20	WB	1:1000	-	Milipore
PLP	rabbit	26.3	WB	1:1000	-	Abcam

2.7. Statistical analysis

All statistical analysis was run using GraphPad Prism (version 6.07). Student's t-test, two-way ANOVA with Sidak's correction for multiple comparisons, and repeated measures ANOVA with Tukey's correction for multiple comparisons were used to observe whether differences between the groups were statistically significant. Any p-values above 0.05 were not considered statistically significant. Variables are reported as mean ± SEM unless otherwise stated.

Chapter 3. The effects of environmental enrichment on myelination and mature oligodendrocytes in the YAC128 mouse model of Huntington disease and wild-type control

3.1. Summary

Enriched laboratory environments (EE) have been shown to improve, or delay, motor and cognitive deficits in several neurodegenerative animal models. It is becoming increasingly apparent that environmental conditions are closely linked to myelination and oligodendrogenesis. White matter abnormalities have been revealed to be dysfunctional starting from early stages of Huntington disease (HD). Therefore, in the current study we investigated the extent to which the status of the environment could modulate myelination in the posterior corpus callosum (CC) of the early manifest YAC128 mouse model of HD. Animals of mixed genotype were allocated to either enriched housing (EH) or standard housing (SH) conditions from 4 to 18 weeks of age. Results revealed an overall reduction in myelin thickness, and a larger number of small diameter axons in both EH groups, regardless of genotype, compared to their corresponding SH controls. As previously reported, no changes in the number of mature oligodendrocytes were observed in the CC. We propose that environmental enrichment could conceivably prolong the 'window of myelination', and thinner myelin sheaths could be explained by an increase in number of newly myelinated axons, a previously suggested possible property of adult myelination. Furthermore, on a battery of behavioural tests, we observed, first, that animals housed in enriched conditions, regardless of genotype, exhibited decreased overall locomotor activity. Second, our findings suggest a marginal effect of an enriched environment on motor learning and motor performance in the WT group, and minor beneficial effects on motor learning, but not motor performance in the YAC128 mouse. And third, we observed an evident effect of enrichment on female body weight in the YAC129 mouse model, and a minor effect on the body-weight of WT females and males. Our findings indicated a lack of profound effects of enrichement on behavioural performance in this HD model, possibly due to the mild disease phenotype associated with the YAC128, which may have not progressed significantly over the course of this study.

3.2. Introduction

Recent studies have demonstrated the beneficial effects of enriched environments (EE) on both healthy and disease animal models. These pre-clinical insights have been partially translated to the clinic in patients suffering from psychiatric or neurodegenerative disorders. While Huntington disease (HD) is an autosomal-dominant genetic disorder, other highly prevalent human neurodegenerative disorders arise from the complex interaction between environmental and genetic factors. Thus, animal models of HD have become important tools to investigate the interplay between progressive physical, cognitive and psychiatric decline, and environmental components (Mo, Hannan, & Renoir, 2015a).

Environmental enriching was first found to have a positive influence in delaying motor symptoms in a genetic mouse model of HD (van Dellen et al., 2000). Since then, physiological and cognitive improvements with environmental enrichment have been demonstrated in several HD models, including the R6/1, R6/2 and N171-82Q (Hockly et al., 2002; Schilling et al., 2004; Wood et al., 2010). These improvements have included reduced brain atrophy (Spires, 2004), improved spatial memory deficits (Nithianantharajah & Hannan, 2006), improved hippocampal neurogenesis (Lazic et al., 2006), delayed cognitive deficits (Nithianantharajah et al., 2008), and amelioration of depressive- (Du et al., 2012b) and emotion-related phenotypes (Renoir et al., 2012).

Additionally, myelination has been demonstrated to be a plastic process and to undergo remodeling throughout adult life (Waly et al., 2014), with several animal studies demonstrating the effects of behavioural experience, enriched housing and voluntary exercising on adaptive myelination and oligodendroglial population dynamics in a variety of brain regions (Forbes & Gallo, 2017; Mount & Monje, 2017; Tomlinson, Leiton, & Colognato, 2016a). After four months of enrichment, middle-aged and old-aged rats showed increased axon and myelin sheath volume (Yang et al., 2013), while middle-aged rats had an increased number of myelinating CNPase+ oligodendrocytes in the corpus callosum (CC) (Zhao et al., 2011).

Interestingly, young rats exhibited a shift in the distribution of oligodendroglial population in sensorimotor cortex between a short-term (10 days) and long-term (42 days) period of enrichment (Keiner et al., 2017). Specifically, compared to standard housing, rats showed a decreased number of oligodendrocyte precursor cells (OPCs; labeled BrdU+NG2+) and an increase in the number of mature oligodendrocytes (labeled BrdU+NG2+GST-pi+) cells after 10 days of enrichment reflecting differentiation of OPCs into mature oligodendrocytes (Keiner et al., 2017). However, after 42 days of enrichment, OPCs and mature oligodendrocyte populations appeared comparable to the standard housing condition. Additionally, the number of newly differentiated myelinating oligodendrocytes, as labeled by BrdU+CNPase+, was increased after 10 days, and remained increased following 42 days of enriched housing, relative to the standard housing condition (Keiner et al., 2017). However, other studies have provided little support for oligodendrogenesis in some cortical regions, or the amygdala, although evidence for increases in OPC populations was found (Ehninger et al., 2011; Ehninger & Kempermann, 2003; Makinodan et al., 2012). In adult mice enriched for 40 days, increased number of proliferative OPCs (BrdU+NG2+S100b- labeled) were observed in the amygdala, but no differences were seen in CNPase+ labelled cells (i.e. myelinating oligodendrocytes) in this region compared to control mice (Ehninger et al., 2011). Similarly, no changes in oligodendrocyte density or morphology, or myelin transcript levels were found in prefrontal cortex (PFC), of young mice housed for 1.5 months in an EE setup (Makinodan et al., 2012).

In this study we aimed to investigate the effects of environmental enrichment on myelin plasticity and mature oligodendrocytes in the white matter tracts of the posterior corpus callosum of the early manifest YAC128 HD mouse model, and healthy littermates (as control). We also evaluated motor function and habituation, as well as anxiety- and depressive-like behaviour using a battery of behavioural tests. In addition, body weight over time, and brain weight were compared between groups.

3.3. Methods

3.3.1. Experimental groups and housing conditions

A total of 67 YAC128 transgenic (HD model) and wild-type (WT, control) mice were used in this study. Both males and females were included in all experimental groups. Sexing and genotyping of animals were carried out at 3 weeks of age. Mice were housed under standard conditions with food ad libitum, in an inverted light-dark cycle until 4 weeks of age. Subsequently, they were placed into their allocated caging conditions under the same inverted light-dark cycle: enriched housing (EH), or standard housing (SH). Animals were housed in their allocated condition for a total of 14 weeks. At 18 weeks (4.5 months) of age, animals were sacrificed, and their brains were harvested. Animals were weighed on a bi-weekly basis.

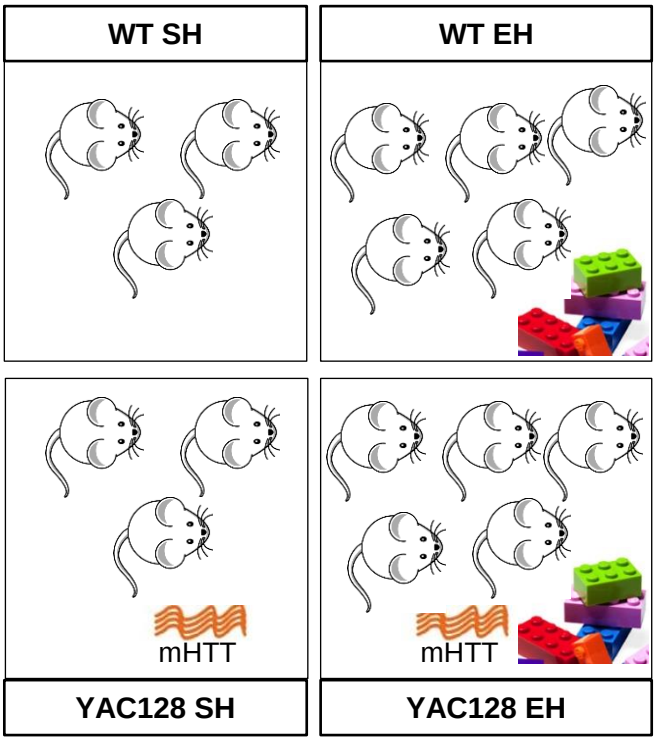

Figure 3.1 Experimental groups for standard and enriched condition

Four groups were used for these experiments: wild type (WT) groups – standard housing (SH) and enriched housing (EH), and YAC128 groups – also SH and EH.

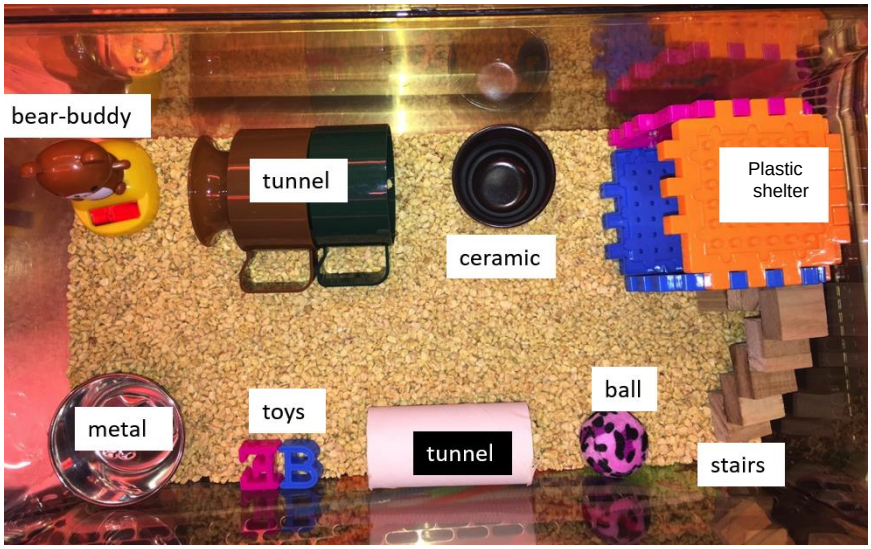

Figure 3.2 Typical enriched housing

Enriched cages contained objects, which offered various tactile and visual stimuli in terms of material, texture and shape. Objects included a small plastic box (‘my lego house’) filled with shredded paper, plastic and carton tunnels, wooden stairs, metal and ceramic bowls, cotton play balls, wooden stairs, and plastic toys (‘bear-buddy’ and plastic letters).

Several factors were taken into consideration in the design of a suitable enriched housing environment (Figure 3.3). Animals allocated to the EH group were housed in larger than standard cages (48 × 26 × 21 cm). Five animals were housed in a single cage in order to stimulate social interaction. Additionally, novelty items that varied in shape, size, and texture were placed in the cage (Figure 3.2). This allowed for sensory, cognitive and motor stimulation through interaction with the environment. Three mice per cage were allocated to the SH condition and were housed in standard mouse cages (39 x 19 x 16 cm; Techniplast, Greenline, sealsafe plus mouse, GM500). To note that these animals were used as control SH for the deprivation study (Chapter 4).

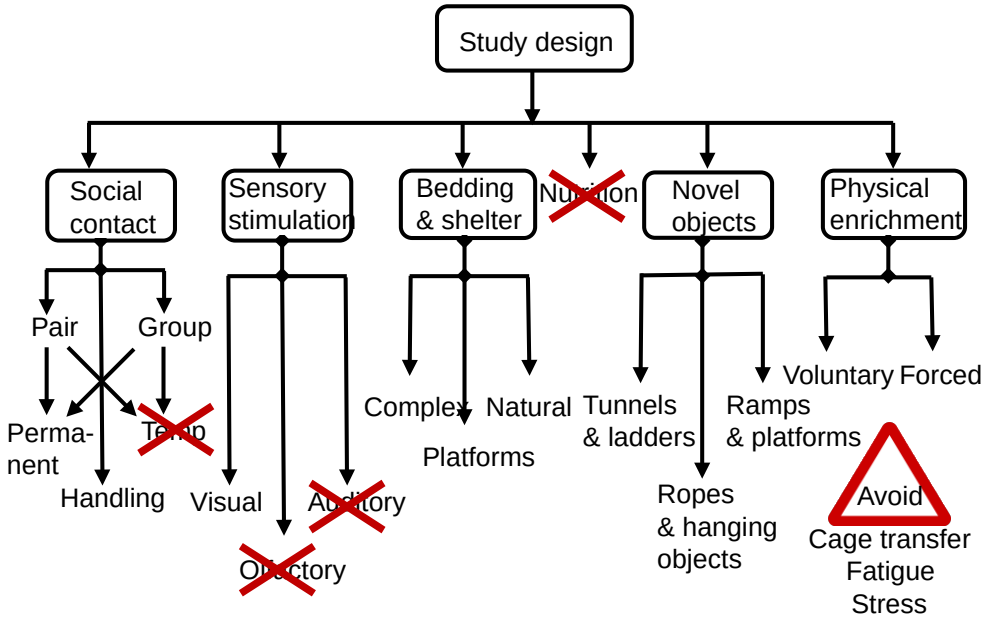

Figure 3.3 Study design for an enriched housing conditions in laboratory animals

Several factors were considered for the design of an ideal enriched housing condition (adapted from Singhal et al., 2014). Red crosses indicate environmental enrichment factors not implemented in the study.

3.3.2. Overview of behavioural tests

After 12 weeks of housing in their experimental conditions, several behavioural tests (Table 2.2) were carried out. This included evaluation of motor function and habituation (spontaneous activity test (SA)); anxiety and habituation (open field test (OFT)); anxiety (elevated plus maze (EPM)); motor function (climbing test); motor function and motor learning (rotarod test (RR)). Details of the behavioural tests are described in Chapter 2 - Materials and Methods (Section 2.1.3).

3.3.3. Tissue harvesting and processing

All brains were segmented through the mid-sagittal plane, and the left hemisphere was used for immunohistochemical procedures (Section 2.5). Sections were immunostained for the mature oligodendrocyte marker, Glutathione S-transferase (GST)-pi (Table 2.9). Stereo Investigator software was used for cell counting in the corpus callosum (Section 2.5.5).

Prior to cryosectioning for IHC procedures, the left hemisphere, of both males and females, was weighed. Brain weights were recorded and compared between the experimental groups.

In addition to the brains harvested for immunostaining, three to four animals in each experimental condition were perfused and their brains harvested, for investigation of myelin ultrastructural analysis (i.e. axonal shape and size, and myelin thickness). For this study, posterior region (splenium) of the CC (~Bregma -1.82 to -2.70, according to the Mouse Brain Atlas, Paxinos and Franklin, 2001) was microdissected (Figure 2.3A) to be processed and imaged for TEM (Section 2.4).

3.3.4. Statistical analysis

The 2x2 factorial design (genotype x housing condition) of the study was statistically analysed using two-way independent ANOVA with Sidak's correction for multiple comparisons, and repeated measures ANOVA statistical tests with Tukey's correction for multiple comparisons. P-values equal to or greater than 0.05 were not considered statistically significant. P values and n values were indicated in the associated figure legends for each figure, while mean values are stated in the results section. Variables are reported as mean ± SEM unless otherwise stated.

3.4. Results

3.4.1. Behavioural tests results

3.4.1.1. Spontaneous activity results

Over the 30 minutes duration of the SA test, comparisons in the distance travelled using two-way ANOVA revealed no significant interaction between genotype and housing condition ($F(1, 40) = 0.11$, $p > 0.05$), significant main effect of housing condition ($F(1, 40) = 12.81$, $p < 0.001$), but no effect of genotype ($F(1, 40) = 2.5$, $p > 0.05$). Sidak's correction for multiple

comparisons post-hoc tests revealed that wild-type enriched-housed (WT EH) animals (6240±522.9 cm) travelled less than wild-type standard-housed (WT SH) (10377±1793 cm, $p < 0.05$; Figure 3.4A). YAC128 EH (4926±207.4 cm) mice also showed a trend towards decreased activity levels compared to their SH controls (8344±502.2 cm). Additionally, over the 10 minutes duration of the OF test, total distance travelled was compared using two-way ANOVA showing no significant interaction between genotype and housing condition ($F (1, 40) = 3.97$, $p > 0.05$), however, a significant main effect of housing condition ($F (1, 40) = 6.46$, $p < 0.001$), but no effect of genotype ($F (1, 40) = 0.35$, $p > 0.05$). Sidak's correction for multiple comparisons post-hoc tests revealed reduced distance travelled in WT EH animals (5995±721.8 cm) compared to SH controls (10509±1586 cm, $p < 0.05$; Figure 3.4F). Other measures of activity levels taken during the SA test included resting time, vertical (rearing) and jump counts, and average velocity. For all these measures, two-way ANOVA revealed no significant interaction between genotype and housing condition, a significant main effect of housing condition, but no effect of genotype. Sidak's correction for multiple comparisons post-hoc tests revealed that EH mice of both genotypes showed increased levels of mean resting time (WT: 1010±28.24 s; YAC128: 1066±17.51 s) when compared to their SH control group (WT: 846.6±48.96 s; $p < 0.01$; YAC128: 880.6±24.57 s; $p < 0.001$; Figure 3.4B). Additionally, averaged vertical counts (Figure 3.4C), jump counts (Figure 3.4D), and velocity (Figure 3.4E) were significantly decreased in the YAC128 EH group compared to its SH control (vertical counts: EH 461.5±20.44, SH 659.2±37.76, $p < 0.01$; jump counts: EH 499±48.42, SH 754.3±82.1, $p \leq 0.05$; average velocity: EH 34.16±0.75, SH 37.94±0.98, $p \leq 0.05$).

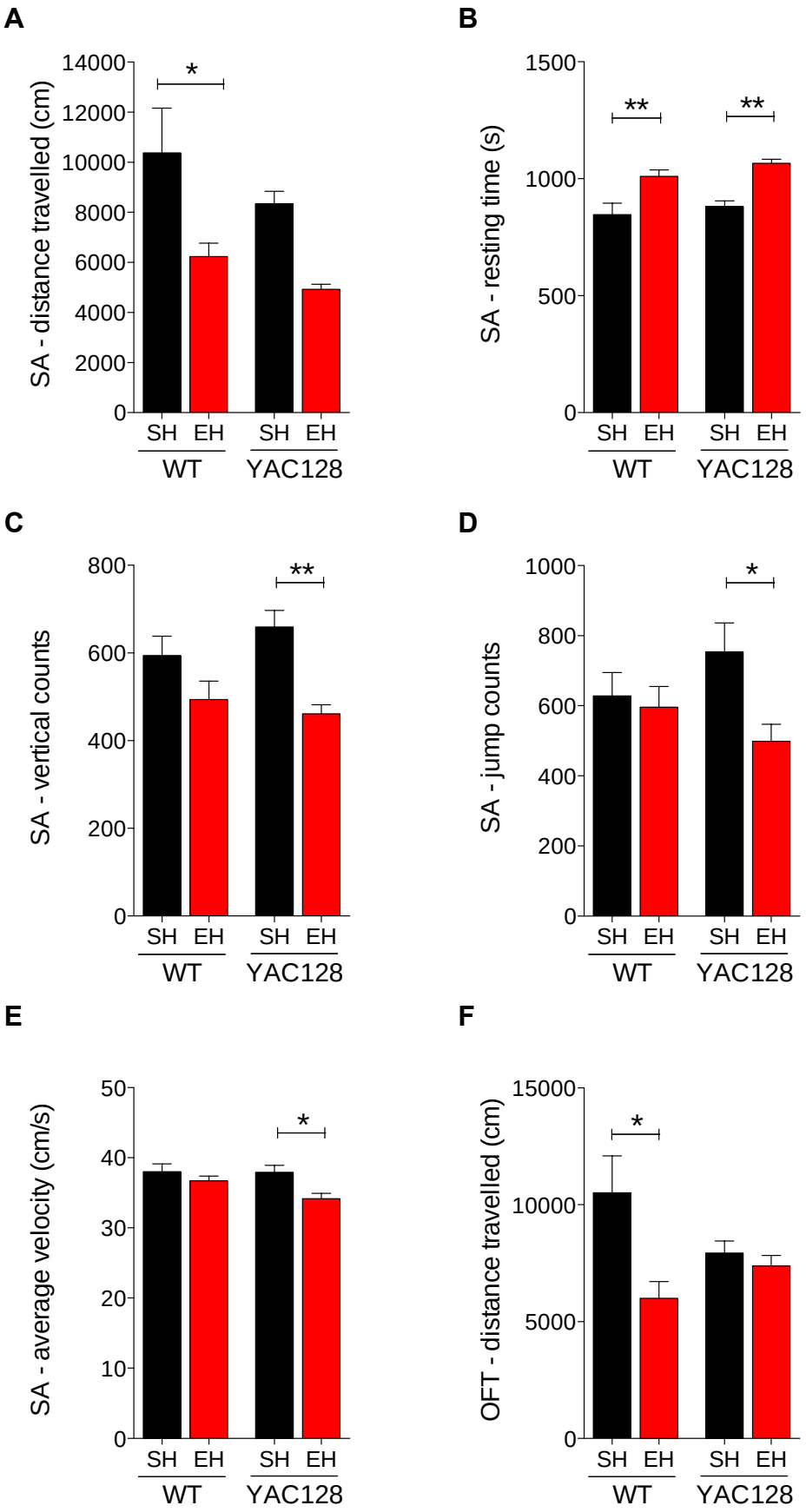
A
SA - distance travelled (cm)
14000
12000
10000
8000
6000
4000
2000
0
*
SH EH SH EH
WT YAC128
B
SA - resting time (s)
1500
1000
500
0
**
**
SH EH SH EH
WT YAC128
C
SA - vertical counts
800
600
400
200
0
**
SH EH SH EH
WT YAC128
D
SA - jump counts
1000
800
600
400
200
0
*
SH EH SH EH
WT YAC128
E
SA - average velocity (cm/s)
50
40
30
20
10
0
*
SH EH SH EH
WT YAC128
F
OFT - distance travelled (cm)
15000
10000
5000
0
*
SH EH SH EH
WT YAC128

Figure 3.4 Comparison of spontaneous activity measures in YAC128 and WT mice under standard and enriched housing conditions

(C) Total distance travelled during the SA test was lower in EH groups compared to SH groups, regardless of genotype.
(D) Resting time was significantly higher in the EH groups compared to their SH controls, regardless of genotype.
(E) Vertical counts were significantly lower in the YAC EH group compared to YAC SH controls, and a similar non-significant trend was observed in the WT groups' comparison.
(F) Number of jumps were also significantly lower in the YAC EH group compared to YAC SH control, but no significant differences were seen in WT SH/EH comparisons.
(G) Average velocity was significantly lower in YAC EH group compared to YAC SH control.
(H) Distance travelled during the OFT test was significantly lower in the YAC EH compared to YAC SH control, but no significant differences were seen in the WT EH compared to WT SH.

The SA test was run over 30 minutes, while OFT was run for 10 minutes. All readouts were obtained from the video tracking software associated with each test. n = 10-12 animals of mixed sex per condition; bar graphs represent mean ± SEM. Two-way ANOVA, with Sidak's correction for multiple comparisons. *p < 0.05; **p < 0.01. Abbreviations: SA, spontaneous activity; OF, open field test.

3.4.1.2. Anxiety-like behaviour results

When comparing the total time spent in the centre of the arena during the 10 minutes OF test of anxiety, two-way ANOVA revealed no significant interaction between genotype and housing condition ($F(1, 39) = 0.09$, $p > 0.05$), no significant main effect of housing condition ($F(1, 39) = 0.14$, $p > 0.05$), and no effect of genotype ($F(1, 39) = 0$, $p > 0.05$) between experimental groups (Figure 3.5A). Additionally, no significant differences were seen between any of the groups of interest in the total time spent in the open arms of the maze during 5 minutes of the EPM test of anxiety (two-way ANOVA, interaction ($F(1, 36) = 3.2$, $p > 0.05$); housing condition ($F(1, 36) = 0.16$, $p > 0.05$); genotype ($F(1, 36) = 0.4$, $p > 0.05$); Figure 3.5B).

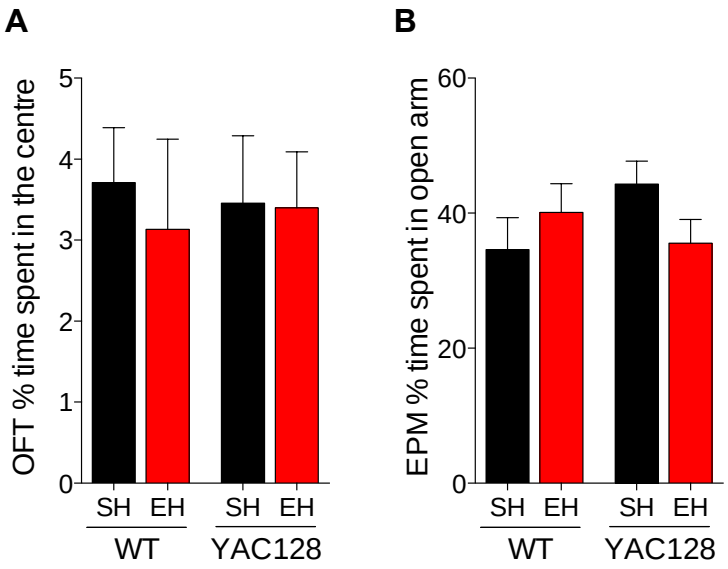

Figure 3.5 Comparison of anxiety-like behaviour in YAC128 and WT mice housed under standard and enriched conditions

(A) No significant differences were observed between groups in percentage time spent in the centre of the arena in the OFT.
(B) No significant differences were observed between groups in percentage time spent in the open arms during the EPM test.

The OFT had a duration of 10 minutes, the EPM test was run for 5 minutes. Readouts for the OFT and EPM were obtained from the EthoVision, video tracking software. Percentage (%) of total time was calculated for each condition. n = 10-12 animals of mixed sex per condition; bar graphs represent mean±SEM. Two-way ANOVA. Abbreviations: OFT, open field test; EPM, elevated plus maze.

3.4.1.3. Motor function results

When comparing the latency to climb two-way ANOVA revealed no significant interaction between genotype and housing condition ($F(1, 40) = 0.95$, $p > 0.05$), no significant main effect of housing condition ($F(1, 40) = 1.05$, $p > 0.05$), and no effect of genotype ($F(1, 40) = 0.01$, $p > 0.05$) (Figure 3.6A) across experimental conditions. For time spent climbing, two-way ANOVA revealed no significant interaction between genotype and housing condition ($F(1, 40) = 0.31$, $p > 0.05$), however a significant main effect of housing condition ($F(1, 40) = 9.05$, $p < 0.05$), but no effect of genotype ($F(1, 40) = 0.4$, $p > 0.05$). Sidak's correction for multiple comparisons post-hoc test revealed a significant difference in time spent climbing between YAC128 SH

and EH groups ($p < 0.05$), and a similar non-significant trend was observed between WT SH and EH ($p > 0.05$; Figure 3.6B). For number of climbing attempts, two-way ANOVA revealed no significant interaction between genotype and housing condition ($F (1, 40) = 0.005$, $p > 0.05$), however a significant main effect of housing condition ($F (1, 40) = 11.62$, $p < 0.01$), but no effect of genotype ($F (1, 40) = 3.4$, $p > 0.05$). Sidak's correction for multiple comparisons post-hoc test revealed differences in the number of climbing attempts between WT EH (8.8±2.08) and WT SH controls (15.33±2.05; $p < 0.05$), and between YAC128 EH (5±1.01) and YAC128 SH controls (11.83±2.19, $p < 0.05$). Both WT and YAC128 animals in the EH condition were associated with a lower number of climbing attempts than their corresponding SH controls (Figure 3.6C).

3.4.1.4. Motor function and motor learning evaluation

The latency to first fall (Figure 3.7) and the number of falls (Figure 3.8) were recorded as measures of motor learning performance on the fixed speed rotarod training over three days, with three trials per day, except the first day when only two trials were recorded. For the latency to fall, repeated measures ANOVA revealed a significant main effects of time ($F (7,280) = 2.557$, $p < 0.05$), but no effect of genotype and housing condition ($F (3, 40) = 1.533$, $p > 0.05$), and no effect of the interaction between the two ($F (21,280) = 0.673$, $p > 0.05$). No significant differences in latency to fall were found between experimental groups when corrected for multiple comparisons ($p >0.05$). However, YAC128 EH mice were able to remain on the rotarod for longer (increased latency to fall) compared to YAC128 SH mice, during trials 2-6, although this difference was not significant (Figure 3.7C). When averaged over training days, WT EH mice showed a trend towards a slightly longer latency to fall compared to the other groups on the first two training days, however this also was not significant (two-way ANOVA for each training day; $p > 0.05$, Figure 3.9A). The number of falls, and latency to fall was similar across all animal groups and plateaued by trial 6-7 ($p > 0.05$; (Figure 3.7C).

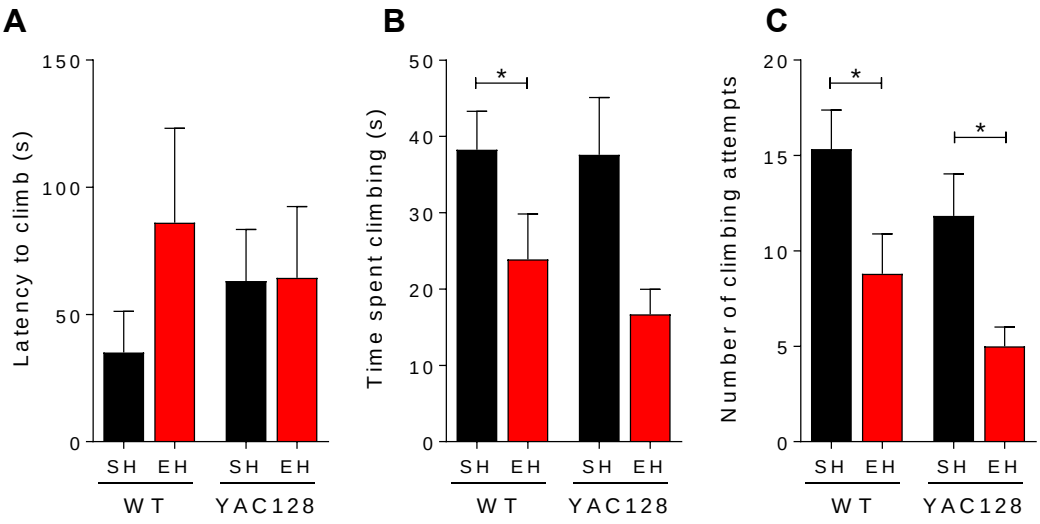

Figure 3.6 Comparison of climbing characteristics of YAC128 and WT controls housed under standard and enriched conditions

(A) No significant differences were observed between the latency for the first climbing attempt, although there was a trend for WT EH to take longer before attempting climbing compared to its SH control.
(B) No significant differences were observed between the total time spent climbing, although there was a trend for both the WT EH and YAC EH to spend less time climbing compared to their SH controls.
(C) Both WT EH and YAC EH performed less climbing attempts compared to their corresponding SH controls.

The climbing test had a total duration of 6 minutes, and videos were examined manually. n = 10-12 animals of mixed sex per condition; bar graphs represent mean±SEM. Two-way ANOVA, with Sidak's correction for multiple comparisons; *$p < 0.05$.

In terms of number of falls, repeated measures ANOVA revealed significant main effects of time ($F(7,280) = 3.66$, $p < 0.001$), but no effect of the genotype and housing condition ($F(3, 40) = 1.952$, $p > 0.05$), and no effect of the interaction between the two ($F(21,280) = 1.095$, $p > 0.05$). On the first trial of training, WT EH mice showed a trend towards falling less (0.1±0.1) than YAC128 EH (1±0.39) animals, and WT SH mice also fell less (0.33±0.14) than YAC128 SH animals (1.16±0.6). Although, no statistical differences were seen between the groups in the number of falls, WT EH animals exhibited the smallest number of falls over all training trials (red squares), followed by WT SH (black squares) and YAC EH mice (red triangles; Figure 3.8A, B, and C). In addition, from trial 1 to 5, the YAC128

EH group showed a slightly smaller, non-significant, number of falls compared to YAC128 SH controls ($p > 0.05$; Figure 3.8C).

The proportion of mice in each experimental group that fell off the rotarod in each session was calculated, and averaged over trials for each training day (Figure 3.9B). Although not statistically significant, the WT EH group showed a trend towards smaller proportion of mice falling off the rotarod compared to all the other groups. During the first day of training (2 trials) 10% (±0%) of WT EH mice consistently fell off the rotarod compared to 20.83% (±12.50%) of WT SH mice, 40% (±20%) of YAC128 EH mice, and 37.5% (±4.17%) of YAC128 SH mice. On the second training day (3 trials), as little as 3.33% (±3.33%) WT EH mice had fallen off the rotarod, 13.89% (±5.5%) WT SH, and 16.67% (±3.33%) YAC128 EH and 27.78% (±2.78%) YAC128 SH mice fell off the rotarod. Finally, on the third training day, only 6.67% (±3.33%) WT EH mice fell off the rotarod, compared to 13.89% (±2.78%) of WT SH mice, 23.33% (±3.33%) of YAC128 EH, and 16.67% (±4.81%) of YAC128 SH.

After three days of training, on the fourth day, the rotarod test was run over three trials, at an accelerated speed, and the latency to first fall was taken as a measure of motor performance. Repeated measures ANOVA revealed no significant main effects of time ($F(2,80) = 0.56$, $p > 0.05$), but a main effect of genotype and housing condition ($F(3,40) = 2.87$, $p < 0.05$), and no effect of the interaction between the two ($F(6,80) = 0.54$, $p > 0.05$). Tukey's correction for multiple comparisons post-hoc test revealed on the first trial, the WT EH group showed longer latency to fall (286.7±8.02 s) compared to all the other groups, but significantly different only to YAC128 EH (194.2±30.13 s, $p < 0.05$; Figure 3.10B). When averaged over all three testing trials, two-way ANOVA revealed a significant interaction between genotype and housing condition ($F(1, 40) = 4.19$, $p > 0.05$), no significant main effect of housing condition ($F(1, 40) = 0.35$, $p > 0.05$), and significant effect of genotype ($F(1, 40) = 4.83$, $p > 0.05$) between experimental groups. WT EH (276.7±10.33 s) animals took significantly longer to fall compared to YAC128 EH (215.9±14.72 s, $p < 0.05$) mice, and a non-significant trend towards a higher latency to fall relative to WT SH was also notable (238.9±16.02 s, $p > 0.05$; Figure 3.10A).

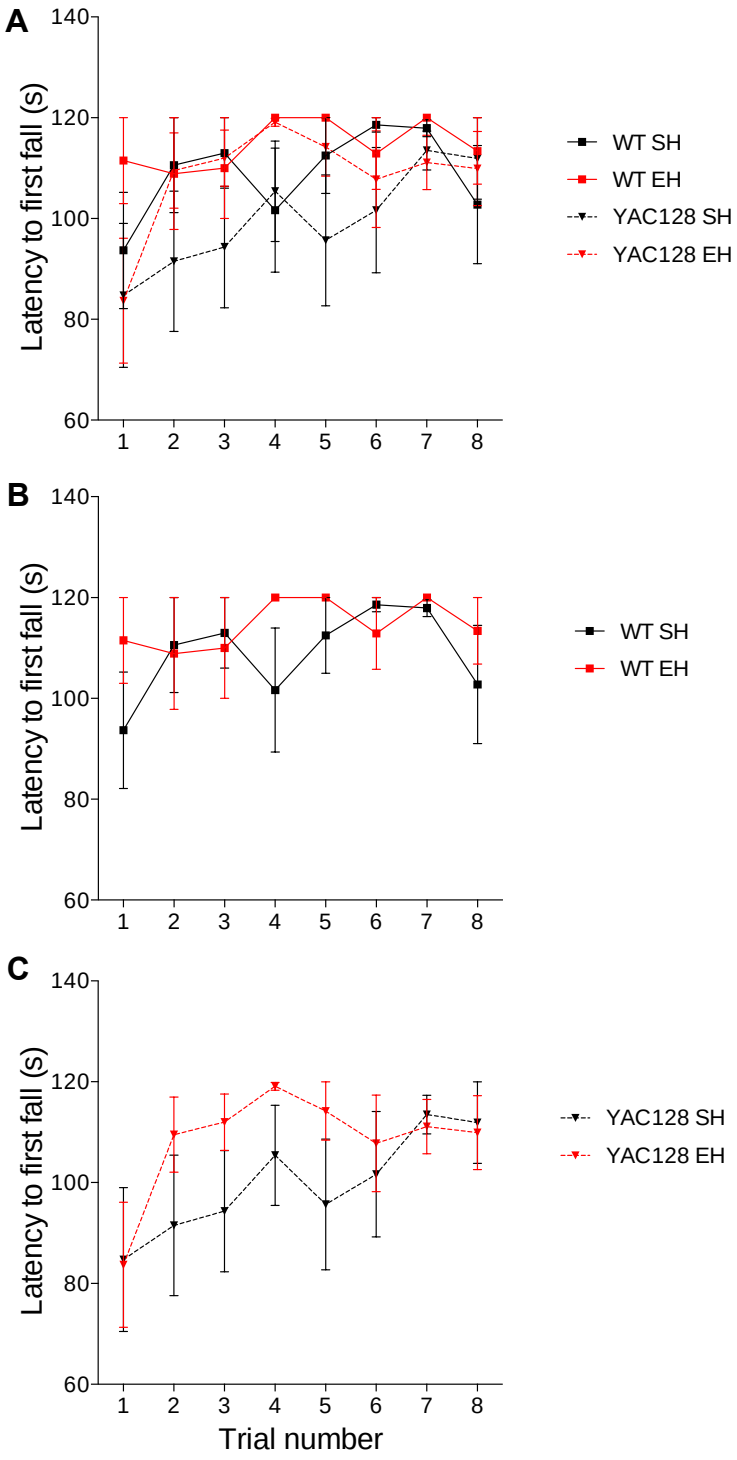

Figure 3.7 Comparison of latency to fall during fixed speed rotarod training for YAC128 and WT mice in SH and EH conditions

(A) Latency to fall over 8 trials of training in all groups.
(B) Slightly better performance in WT EH compared to WT SH for several sessions.
(C) Faster motor learning performance in YAC128 EH mice compared to SH control.
Latency to fall illustrated in seconds (s). Training was run over 3 days with 2-3 trial sessions per day. n = 10-12 animals of mixed sex per condition; error bars represent mean±SEM. Repeated measures ANOVA.

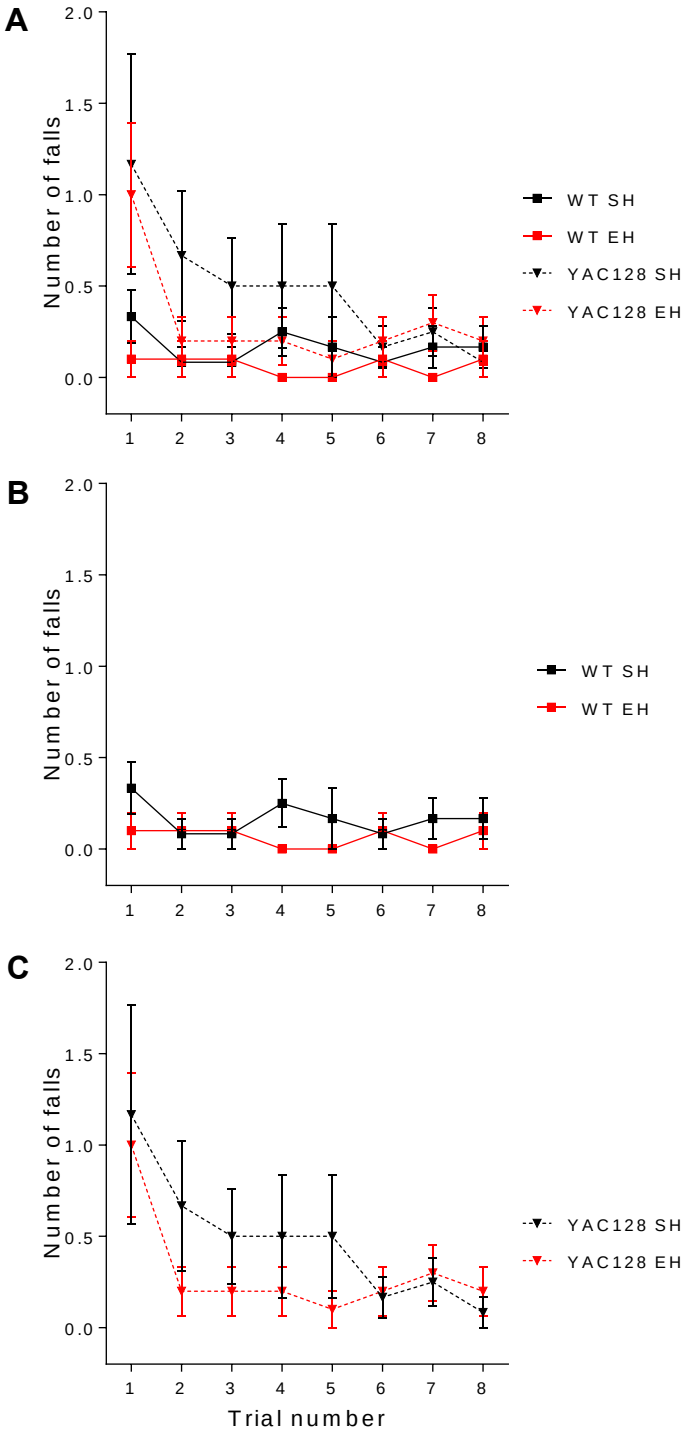

Figure 3.8 Comparison of number of falls of YAC128 and WT mice housed under standard and enriched conditions during fixed speed rotarod training

(A) Number of falls over the 8 trials of training for all groups.
(B) WT EH had similar number of falls to WT SH with the exception of several trials.
(C) YAC128 EH mice had less number of falls over 4 trials compared to SH control.
Error bars represent mean±SEM. Repeated measures ANOVA.

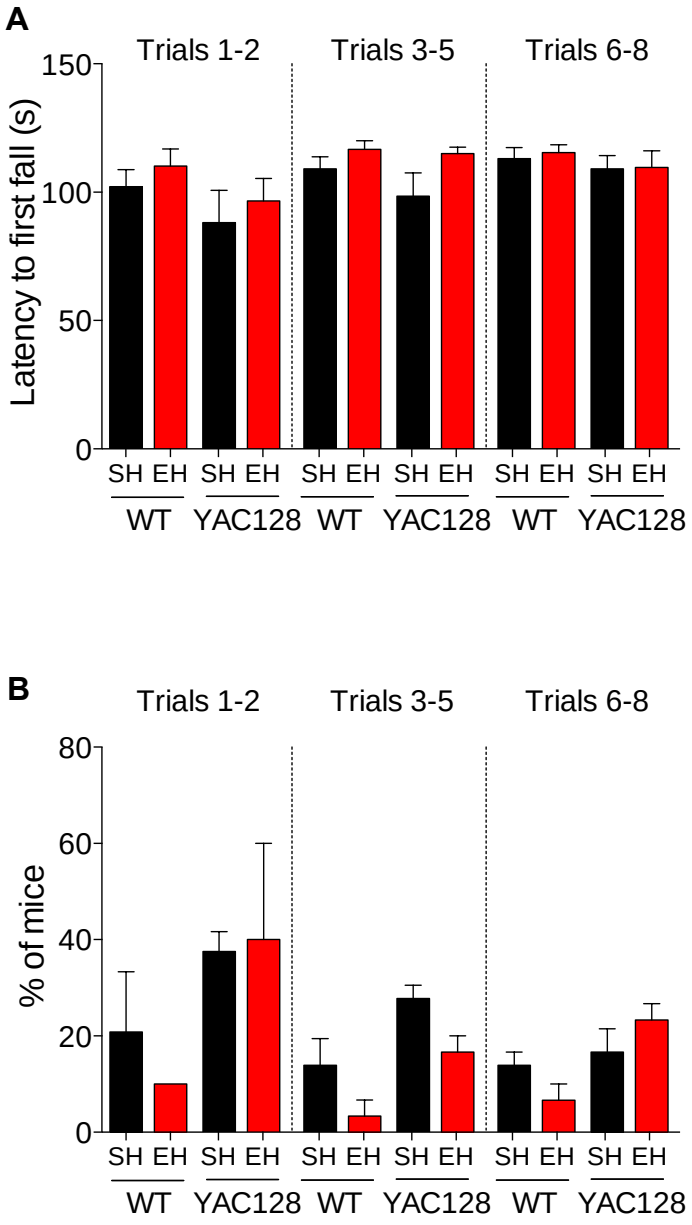

Figure 3.9 Session averages of latency to fall and percentage of mice fallen for YAC128 and WT mice housed under standard and enriched conditions

(A) Average latency to fall for each day of training shows some trends towards EH groups performing slightly better, although no significant differences were found.
(B) Percentage of mice that fell off the rotarod was (non-statistically significant) smaller in the WT EH group compared to the other groups.

Testing was run over 2-3 trials within the same day. n = 10-12 animals of mixed sex per condition; bar graphs represent the mean±SEM. Two-way ANOVA, with Sidak's correction for multiple comparisons. Latency to fall illustrated in seconds (s) (A). Proportion of mice that fell off the rotarod averaged over trials for each training day (B).

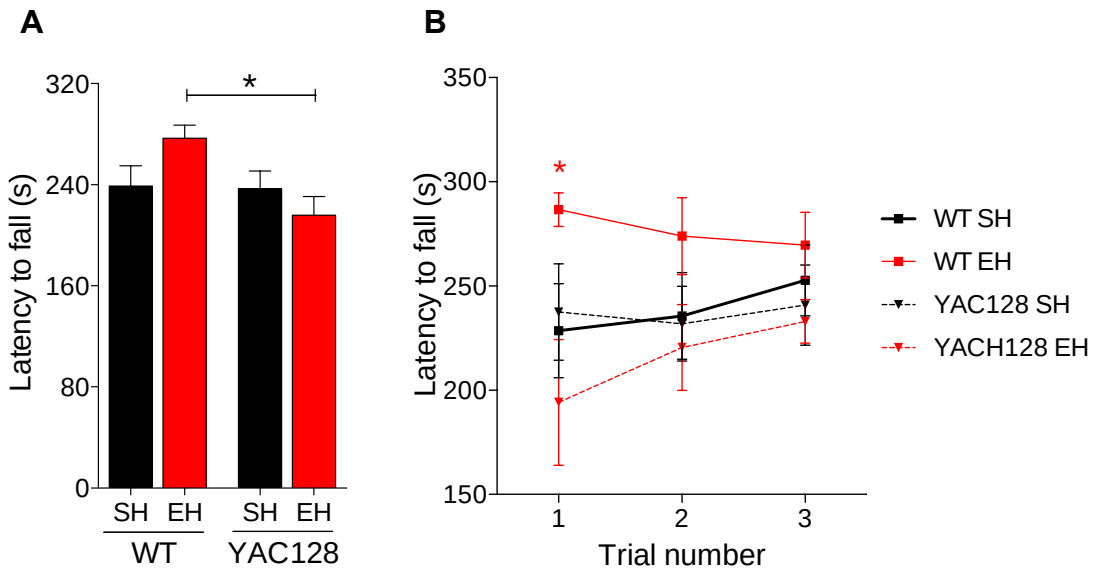

Figure 3.10 Comparison of latency to fall in YAC128 and WT mice housed under standard and enriched conditions during accelerated rotarod test

(A) WT EH mice outperformed all groups over 3 trials of accelerated rotarod testing session.
(B) Latency to fall was significantly higher in the WT EH group compared to YAC EH, and (non-statistically significant) higher than all the other groups over all 3 trials.

Latency to fall illustrated in seconds (s). Testing was run over 3 trials within the same day. n = 10-12 animals of mixed sex per condition; bar graphs represent mean±SEM (A); and, error bars represent ±SEM (B). Two-way ANOVA, with Sidak's multiple comparisons test (A), and repeated measures ANOVA, with Tukey's multiple comparisons test (B). *p < 0.05. Comparison symbols: * WT EH vs YAC128 EH.

3.4.2. Ultrastructural analysis of myelin

The inner (axoplasm) and outer (axoplasm and myelin sheath) diameters of regular-shaped axons in the posterior part (splenium) of the CC were measured (Figure 2.3). Representative micrographs of callosal axons for each experimental group are illustrated below, in Figure 3.11. G-ratios were calculated as the inner diameter divided by the outer diameter, and used as a measure of myelin thickness (Figure 2.4).

G-ratios were first evaluated against inner diameter for each axon to examine the variability of myelin thickness at different ranges of axonal diameters. WT EH mice exhibited qualitatively higher g-ratios, suggestive of thinner myelin sheath, at small axonal diameters (ID < 500nm), and smaller g-ratios, suggestive of thicker myelin sheath, at large axonal diameter (ID ≥ 1000nm) compared to WT SH animals (Figure 3.12A). Cumulative frequency analysis confirmed a shift towards overall larger g-ratios, in WT EH animals compared to WT SH mice (Figure 3.12B). Similarly, YAC128 EH animals showed a trend towards overall larger g-ratios relative to YAC128 SH, although not to the same extent as that seen in WT groups (Figure 3.12C and D).

When the g-ratio was averaged over all axonal diameters, two-way ANOVA revealed no significant interaction between genotype and housing condition ($F(1, 2635) = 1.54$, $p > 0.05$), significant main effect of housing condition ($F(1, 2635) = 37.21$, $p < 0.0001$), and no main effect of genotype ($F(1, 2635) = 2.51$, $p > 0.05$). Both WT and YAC128 EH groups showed higher g-ratios, suggestive of thinner myelin sheaths, compared to their respective SH controls (Figure 3.13A). Specifically, Sidak's correction for multiple comparisons post-hoc test revealed WT EH (0.798±0.002) animals possessed a significantly greater mean g-ratio compared to WT SH (0.779±0.003, $p < 0.0001$), and YAC128 EH (0.798±0.002) showed significantly higher g-ratios compared to YAC128 SH (0.786±0.002, $p < 0.0001$).

In addition, g-ratio values were classified, averaged and compared according to three inner diameter ranges: small diameter axons (ID < 500nm), mid-range diameter axons (500 ≤ ID < 1000nm), and large diameter axons (ID ≥ 1000nm) (Figure 3.13B). At small diameter ranges, two-way ANOVA revealed significant interaction between genotype and housing condition ($F(1, 939) = 18.6$, $p < 0.0001$), significant main effect of housing condition ($F(1, 939) = 24.45$, $p < 0.0001$), but no main effect of genotype ($F(1, 939) = 0.24$, $p > 0.05$). Sidak's correction for multiple comparisons post-hoc test revealed WT EH (0.765±0.003) showed a significantly higher mean g-ratio,

suggestive of thinner myelin sheath, compared to both WT SH (0.727±0.004, $p < 0.0001$), and YAC128 EH animals (0.749±0.004, $p < 0.01$). In addition, YAC128 SH (0.747±0.004) also showed a significantly larger mean g-ratio, suggestive of thinner myelin sheath, compared to WT SH ($p < 0.01$). At mid-range axonal diameters, two-way ANOVA revealed no significant interaction between genotype and housing condition ($F (1, 1420) = 0.54$, $p > 0.05$), significant main effect of housing condition ($F (1, 1420) = 57.05$, $p < 0.0001$), and no main effect of genotype ($F (1, 1420) = 1.21$, $p > 0.05$). Sidak's correction for multiple comparisons post-hoc test revealed g-ratio of WT EH (0.814±0.002) and YAC128 EH (0.819±0.003) animals were significantly larger than that of WT SH (0.793±0.003, $p < 0.0001$), and YAC128 SH (0.794±0.002, $p < 0.0001$) mice, respectively. No differences were observed at the mid-diameter range between WT and YAC128, regardless of housing condition ($p > 0.05$). Finally, at large axonal diameters, two-way ANOVA revealed significant interaction between genotype and housing condition ($F (1, 271) = 13.38$, $p < 0.001$), significant main effect of housing condition ($F (1, 271) = 11.34$, $p < 0.001$), but no main effect of genotype ($F (1, 271) = 0.48$, $p > 0.05$). Sidak's correction for multiple comparisons post-hoc test revealed YAC128 EH (0.883±0.004) showed a significantly higher average g-ratio compared to both YAC128 SH (0.844±0.005, $p < 0.0001$), and WT EH (0.859±0.005, $p < 0.05$). However, no significant differences were seen between WT SH (0.860±0.005) and WT EH ($p > 0.05$) at this range.

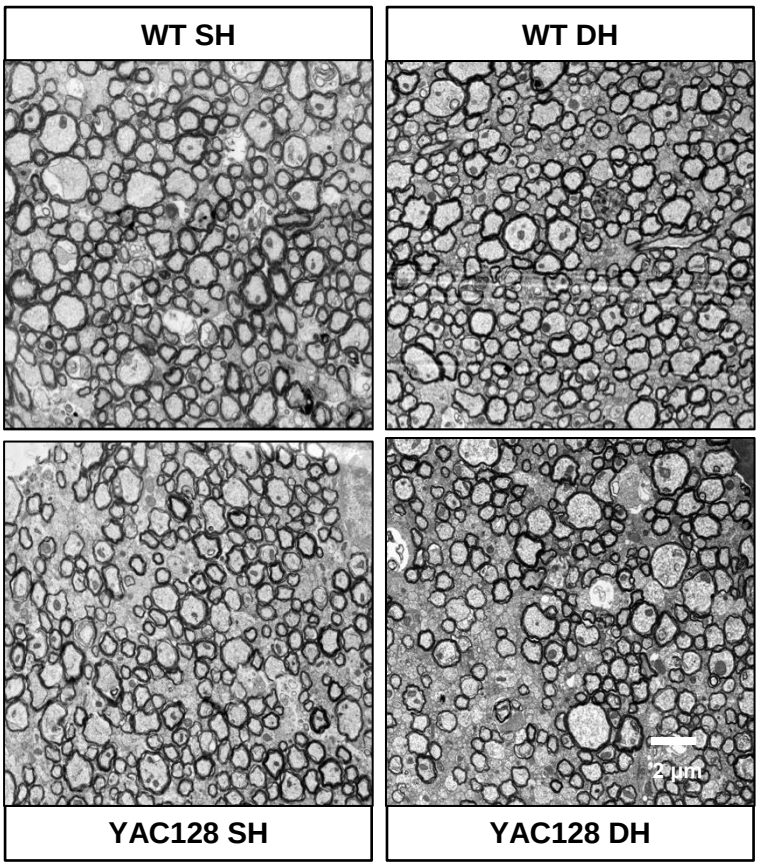

Figure 3.11 Representative TEM images of callosal axons in YAC128 and WT mice housed under standard and enriched conditions

Representative micrographs of axons from the posterior (splenium) region of the corpus callosum for each experimental group. Scale bar at 2µm.

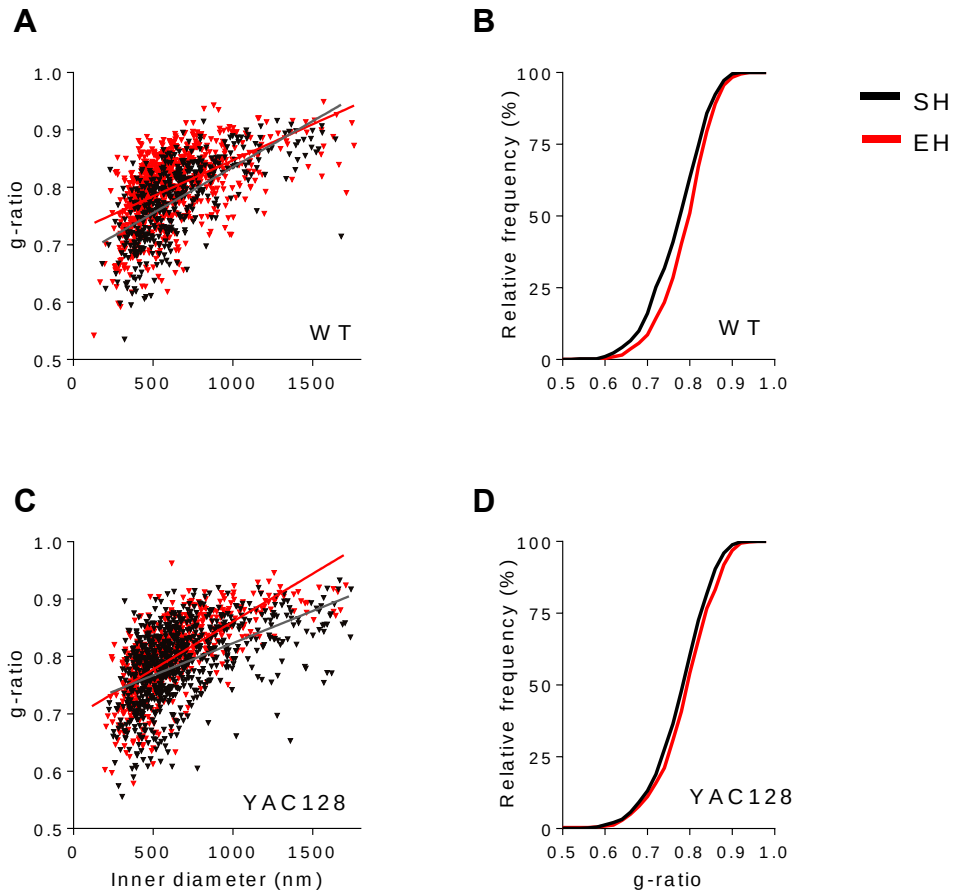

Figure 3.12 G-ratios and axonal diameters of YAC128 and WT mice housed under standard and enriched conditions

(A) Scatter plot of g-ratio values against inner axonal diameter showed higher g-ratios at small ID (ID < 500nm), and smaller g-ratio at mid-range and large ID (ID ≥ 500) for the WT EH (red) compared to SH group (black).
(B) Cumulative frequency plot of g-ratios showed an overall shift towards larger g-ratios for WT EH mice compared to WT SH.
(C) Scatter plot indicating lower g-ratio values at smaller to mid-range axonal diameters (ID < 700 nm), and higher values for mid-range to large axonsal diameters (ID > 700nm) for YAC128 EH (red) compared to SH (black).
(D) Cumulative frequency of g-ratio showed a close overlap of the two curves representative of the YAC128 groups, although a small overall shift towards larger g-ratios can be observed.

n = 474 - 916 axons per condition (WT SH, n = 474 axons; WT EH, n = 843 axons; YAC128 SH, n = 782 axons; YAC128 EH, n = 556 axons). 2-4 animals per condition.

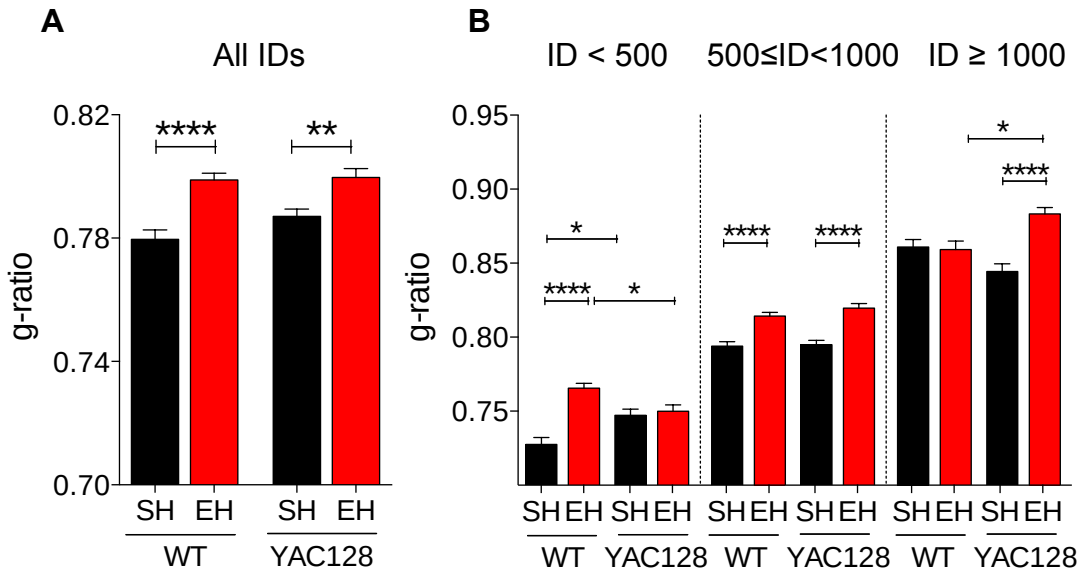

Figure 3.13 Average g-ratio for YAC128 and WT mice housed under standard and enriched conditions

(A) The EH groups showed significantly smaller g-ratio values for both the WT and the YAC128 groups, when compared to their respective SH controls.
(B) G-ratio values were classified and compared based on their corresponding inner diameter ranges (small diameter axons, ID < 500nm; mid-range diameter axons, 500 ≤ ID< 1000nm; large diameter axons, ID ≥ 1000nm). Note the overall increase in g-ratio with increasing axonal diameter, as well as increased g-ratios of EH mice compared to SH mice, for both WT and YAC128 groups, at small and medium diameter ranges (IDs).

Bar graphs represent mean±SEM. SEM comes from axonal variance. n = 474 - 916 axons per condition (WT SH, n = 474 axons; WT EH, n = 843 axons; YAC128 SH, n = 782 axons; YAC128 EH, n = 556 axons); 2-4 animals per condition. Two-way ANOVA, with Tukey's multiple comparisons test. *p < 0.05; **p < 0.01; ****p < 0.0001. Inner diameter shown in nanometres (nm). Abbreviations: ID, inner diameter, SH, standard housing, EH, enriched housing, WT, wild type.

3.4.3. Differences in axonal characteristics

WT EH animals exhibited a higher number of axons with small axonal diameters (300 ≤ ID ≤ 600nm), and a smaller or similar number of axons with large axonal diameters (ID ≥ 700nm), compared to WT SH controls (Figure 3.14A). Cumulative frequency plot of inner diameters showed a close overlap of the two curves representative of the EH and SH WT groups, with a small

shift towards smaller g-ratios, driven by the aforementioned larger number of smaller axonal diameters, for the WT EH group (Figure 3.14B). In addition, when the means of the axonal diameters were compared, WT EH animals (614.6±8.7) showed significantly higher number of axons with smaller inner diameters compared to their WT SH control (652.5±12.6, $p < 0.05$, (Figure 3.14C). A higher number of axons with small diameters (100 to 500nm), and a smaller number of axons at mid-range axonal diameters (600 to 700nm) were observed in the YAC128 EH animals compared to SH controls (Figure 3.15A). The YAC128 EH cumulative frequency curve also showed a shift towards the left, driven by a larger number of small-to mid-range axonal diameters, compared to the SH group (Figure 3.15B). In addition, the mean axonal diameter of YAC128 EH mice (626.7±11.8) was significantly smaller than that of YAC128 SH animals (672.7±10.7, $p < 0.01$, Figure 3.15C).

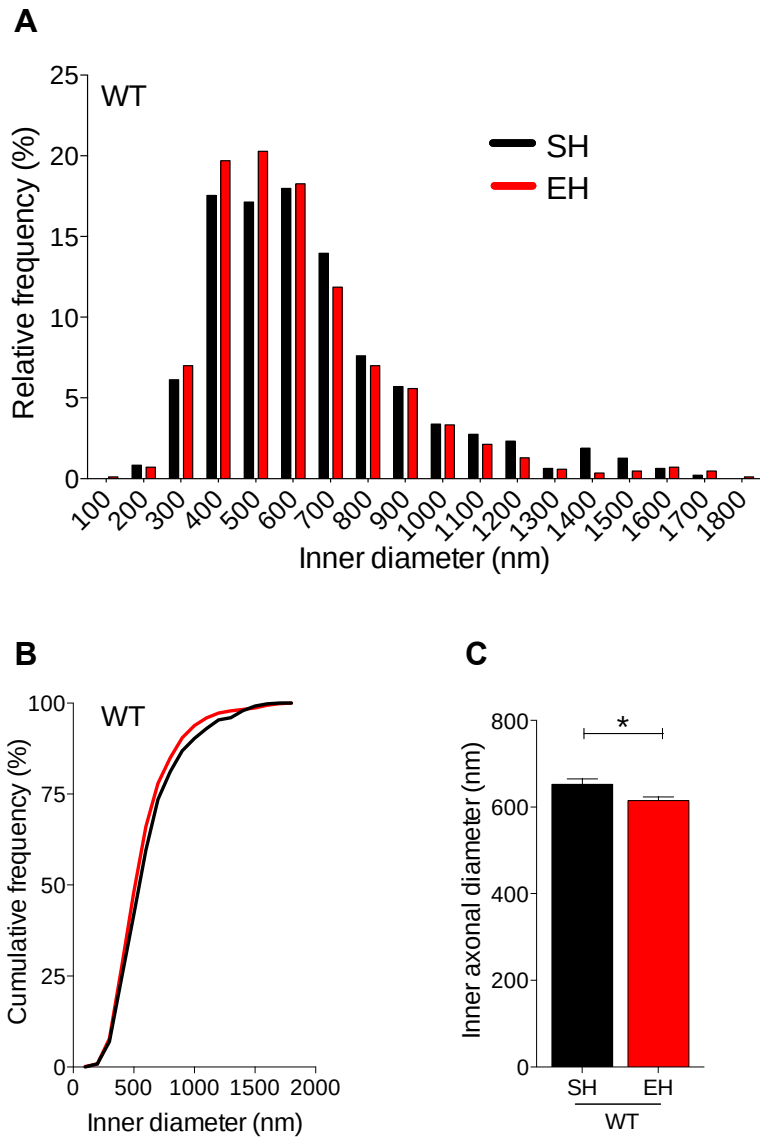

Figure 3.14 Axonal diameters of WT mice house under standard and enriched conditions

(A) Higher number of axons with a small diameter (300 to 600nm), and a smaller or similar number of axons with a large diameters (≥700nm), in WT EH animals compared to their WT SH controls.
(B) Cumulative frequency of axonal diameters showed a small shift towards smaller diameters in WT EH mice (red) compared to WT SH (black).
(C) WT EH animals showed smaller average axonal diameter myelinated axons compared to WT SH.

n = 474 - 916 axons per condition (WT SH, n = 474 axons; WT EH, n = 843 axons; YAC128 SH, n = 782 axons; YAC128 EH, n = 556 axons); 2-4 animals per condition. Relative frequency histogram (A) and cumulative frequency (B), bin width = 100nm (A). Unpaired, two-tailed t-test, 95% confidence intervals, *p < 0.05; bar graphs represent mean ± SEM (C). Abbreviations: ID, inner diameter.

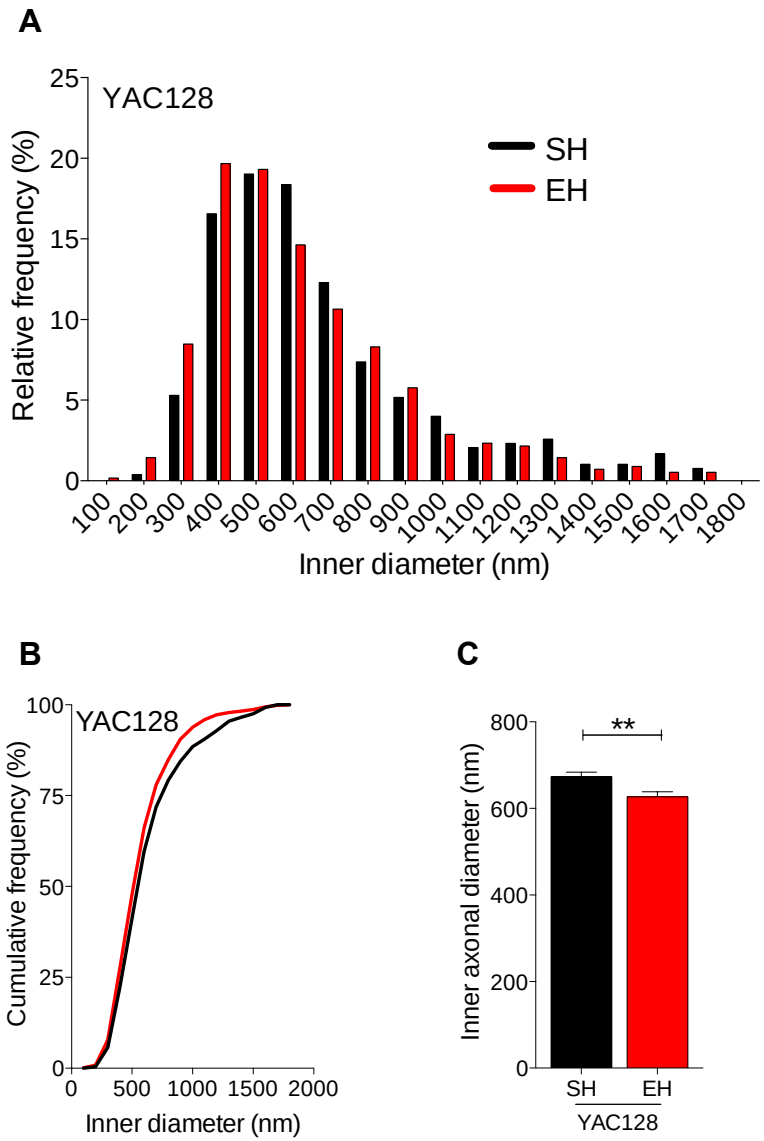

Figure 3.15 Axonal diameters of YAC128 mice housed under standard and enriched conditions

(A) Higher number of axons with a small diameter (100 to 500nm), and a smaller number of mid-range diameter axons (600 to 700nm), in YAC128 EH animals compared to their YAC128 SH controls.
(B) Cumulative frequency of axonal diameters exhibiting a small shift towards smaller diameters for YAC128 EH mice (red) compared to YAC128 SH (black).
(C) Myelinated axons of YAC128 EH animals possessed a smaller average diameter compared to YAC128 SH.

n = 474 - 916 axons per condition (WT SH, n = 474 axons; WT EH, n = 843 axons; YAC128 SH, n = 782 axons; YAC128 EH, n = 556 axons); 2-4 animals per condition. Relative frequency histogram (A) and cumulative frequency (B), bin width = 100nm (A). Unpaired, two-tailed t-test, 95% confidence intervals, **p ≤ 0.01; bar graphs represent mean±SEM (C). Abbreviations: ID, inner diameter.

3.4.4. Mature oligodendrocyte numbers

Mature oligodendrocytes, as identified by GST-pi staining, were counted in all regions of the corpus callosum. No differences were seen between any of the four groups (two-way ANOVA, $p > 0.05$, Figure 3.16).

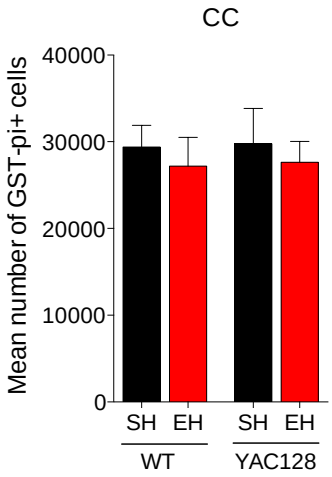

Figure 3.16 Number of GST-pi positive cells in the CC of YAC128 and WT mice housed under standard and enriched conditions

No significant differences were seen in callosal GST-pi positive cell population between the four experimental groups.

Bar graphs represent the average of a total of 7-10 animals per condition; bar graphs represent mean±SEM. Two-way ANOVA. Abbreviations: CC, corpus callosum; Glutathione S-transferase (GST)-pi.

3.4.5. Brain weight for standard and enriched WT and YAC128 animals

Left hemisphere of the brain was weighed for each animal prior to tissue processing. No significant differences were found at 4.5 months between any of the groups when comparing the brain weights of mixed sex (Figure 3.17A), female (Figure 3.17B), or male (Figure 3.17C) mice (two-way ANOVA).

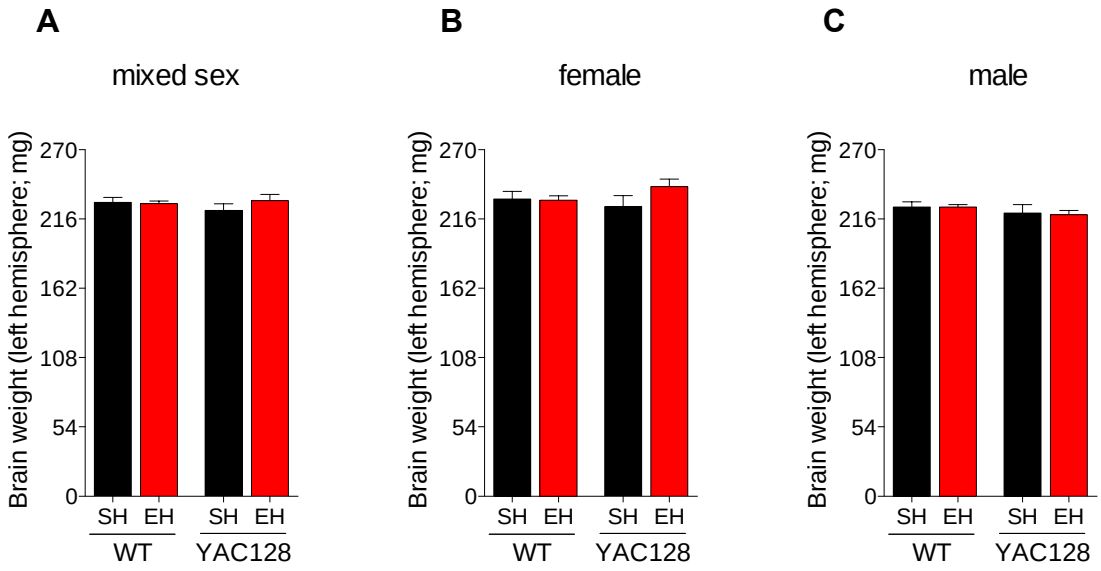

Figure 3.17 Brain weight comparison in YAC128 and WT mice housed under standard and enriched conditions

(A) Mixed sex animals showed similar brain weights regardless of experimental condition.
(B) Female mice had similar brain weights across experimental conditions.
(C) Male mice also showed similar brain weights across experimental conditions.

Animals' brains were weighed at 18 weeks (4.5 months) of age. Left hemisphere weight shown in milligrams (mg). n = 5-7 males per condition, and 5-7 females per condition; bar graphs represent mean±SEM. Two-way ANOVA.

3.4.6. Body weight comparison over time for standard and enriched WT and YAC128 animals

Animals were weighed fortnightly starting from pn50 (~7 weeks) until being sacrificed on pn126 (18 weeks). Weight comparisons were evaluated and compared separately for females and males.

In the female groups (Figure 3.18A), repeated measures ANOVA revealed significant main effects of age ($F(5,90) = 64$, $p < 0.0001$), and experimental group (genotype and housing condition) ($F(3,18) = 12.62$, $p < 0.0001$), as well as a significant effect of the interaction between the two ($F(15,90) = 6.283$, $p < 0.0001$). Female YAC128 EH body weights exceeded those of all

other experimental groups between pn50-126. Female YAC128 EH body weights (24.72±0.45) at pn64 were significantly larger ($p < 0.05$) than those of WT EH females (21.34±0.46g), and remained so until the day of sacrifice ($p < 0.0001$) (Tukey's correction for multiple comparisons). The difference in YAC128 EH and WT EH body weight increased over time (pn78: WT EH 22.8±0.72g, YAC128 EH 26.58±0.75g, $p < 0.01$; pn92: WT EH 22.24±0.79g, YAC128 EH 28.80±1.32g, $p < 0.0001$; pn106: WT EH 22.32±0.83g, YAC128 EH 27.48±10.4g, $p < 0.0001$; pn126: WT EH 24.06±0.67g, YAC128 EH 28.48±0.82g, $p < 0.001$). Additionally, YAC128 EH (26.58±0.75g) females showed increased body weights compared to YAC128 SH (23.16±1.16g) at pn78 ($p < 0.05$), and pn106 (YAC128 EH: 27.48±1.04g; YAC128 SH: 24.46±1.03g; $p < 0.05$); whereas YAC128 SH (23.16±1.16g) females showed increased body weights when compared to WT SH (20.21±0.54g) at pn78 ($p \leq 0.05$), and pn92 (YAC128 SH: 23.46±1.32g; WT SH: 20.57±0.4g; $p < 0.05$).

When comparing male body weights (Figure 3.18B), repeated measures ANOVA also revealed significant main effects of time ($F(5,90) = 129$, $p < 0.0001$), and experimental group (genotype and housing condition) ($F(3,18) = 3.52$, $p < 0.05$), as well as an effect of the interaction between the two ($F(15,90) = 2.846$, $p < 0.05$). YAC128 SH (29.71±0.8g) males had increased body weights compared to WT SH (26.92±1.03g) males at pn92 ($p < 0.05$), and 106 (YAC128 SH: 30.93±0.9g; WT SH: 27.2±1.08g; $p < 0.05$). Additionally, YAC128 EH (32.14±0.65g) males showed increased body weight compared to WT EH (29±0.7g) males at pn126 ($p < 0.05$).

At the final time point, 18 weeks of age, when weight was taken prior to sacrifice, for female mice, two-way ANOVA revealed a significant interaction between genotype and housing ($F(1, 18) = 5.6$, $p < 0.05$), a main effect of housing condition ($F(1, 18) = 19.12$, $p < 0.001$), and a main effect of genotype ($F(1, 18) = 13.42$, $p < 0.01$). Female YAC128 EH mice showed significantly increased body weights compared to both WT EH, and YAC128 SH (with Sidak's correction for multiple comparisons, $p < 0.01$; Figure 3.19). For male mice, two-way ANOVA revealed no significant interaction between genotype and housing ($F(1, 18) = 0.6$, $p > 0.05$), no main effect of housing

condition ($F(1, 18) = 0$, $p > 0.05$), but a main effect of genotype ($F(1, 18) = 8.04$, $p < 0.05$). Sidak's correction for multiple comparisons revealed that YAC128 EH male mice (29±0.69g) showed a trend towards increased body weight compared to WT EH mice (32.14±0.65g; $p < 0.05$).

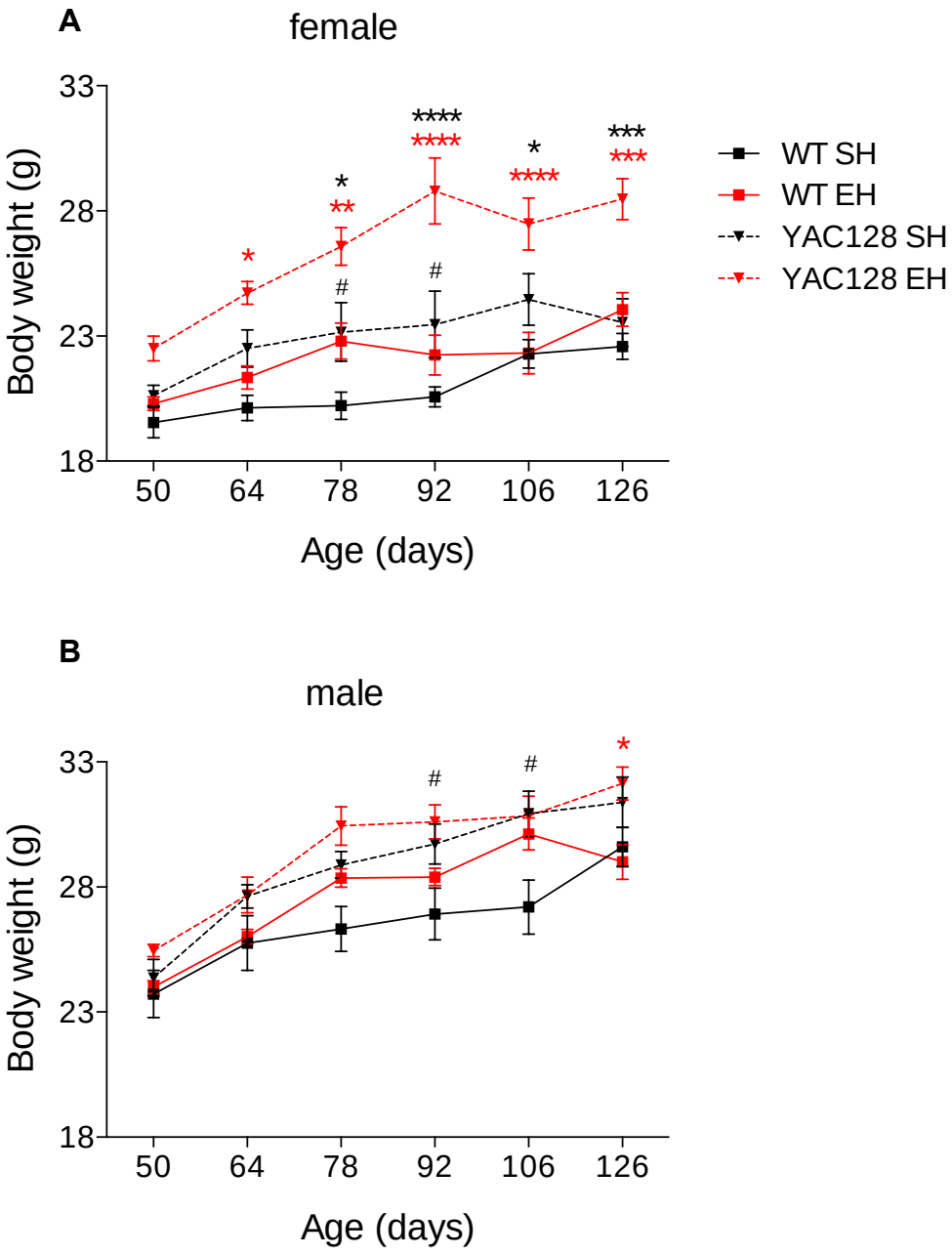

Figure 3.18 Body weight over time for female and male YAC128 and WT mice housed under standard and enriched conditions

(A) YAC128 EH female mice showed increased body weights compared to the other groups throughout all time points.
(B) Male body weights were similar between groups with the exception of later time points (>pn92).

Animals were weighed fortnightly: pn 50 (~7weeks) to 126 (18weeks). Body weight in grams (g). n = 5-7 mice per sex per condition; error bars as mean±SEM. Repeated measures ANOVA, with Tukey's corrections for multiple comparisons. *p < 0.05; **p< 0.01; ***p < 0.001; ****p < 0.0001. Symbols: # WT SH vs WT EH; * WT EH vs YAC128 EH; #WT SH vs YAC128 SH; * YAC128 SH vs YAC128 EH.

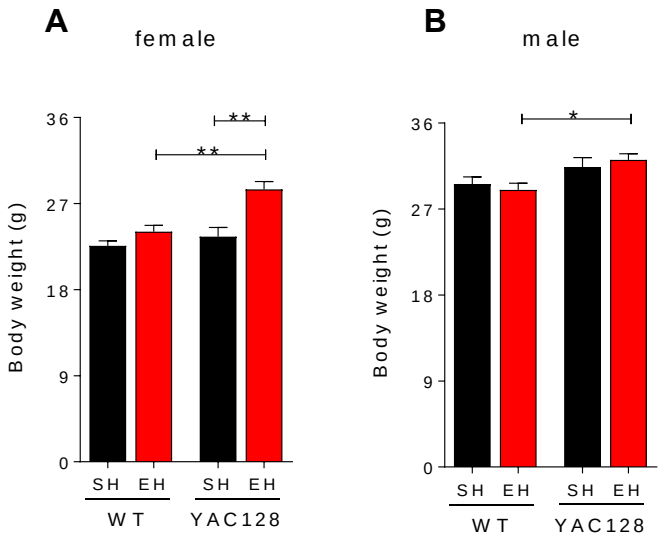

Figure 3.19 Final body weight of female and male YAC128 and WT mice housed under standard and enriched conditions

(A) Female YAC128 mice in the EH condition showed increased body weight compared to all the other groups.
(B) Male body weights were similar across conditions although slightly larger in the YAC128 SH/EH groups compared to WT.

Average body weight on sacrifice day, pn 126 (18 weeks). Body weight shown in grams (g). n = 5-7 animals of each sex per condition; bar graphs represent mean±SEM. Two-way ANOVA, with Sidak's multiple comparisons test. *p < 0.05; **p < 0.01.

3.5. Discussion

Enrichment effects on behavioural performance and motor function

Locomotor activity in enriched mice was decreased across WT and YAC128 animals, and relative activity levels between both genotypes were broadly comparable. These observations are in keeping with previous reports that enriched rodents were less likely to exhibit exploratory behaviours (Brenes, Rodríguez, & Fornaguera, 2008a; Hellemans, Benge, & Olmstead, 2004; Leger et al., 2015; Makinodan et al., 2012; Mosaferi et al., 2015), and that early manifest YAC128 mice locomote similarly to WT counterparts (Van Raamsdonk et al., 2005). No effect of enrichment on anxiety-like behaviour

was observed across genotypes, somewhat consistent with earlier WT rodent studies (Brenes, Rodríguez, & Fornaguera, 2008a; Peña et al., 2006; Peña et al., 2009), but at variance with others (Galani et al., 2007; Hellemans et al., 2004). Increased anxiety-like behaviour was previously seen in 7 months' old YAC128 mice (Southwell et al., 2009), raising the possibility that our younger YAC128 animals (4.5 months) could have been yet to manifest this phenotype. Similarly, climbing characteristics were found to be approximately equivalent across genotypes and housing conditions, roughly in keeping with a previous report of no changes in climbing performance in standard housed YAC128 FVB mice compared to WT controls, across most age groups (Menalled et al., 2009). Finally, YAC128 animals housed under standard conditions were associated with the weakest rotarod training performance, consistent with previous studies reporting motor learning deficits in YAC128 SH mice (Franciosi et al., 2012; Lawhorn, Smith, & Brown, 2008; Slow et al., 2003; Van Raamsdonk et al., 2005). Furthermore, a non-significant improvement in rotarod performance was seen, to a small extent, during training and testing in enriched WT mice compared to other experimental groups, and, to a greater degree, during rotarod training in enriched YAC128 animals, compared to their SH counterparts. These results suggest that enrichment marginally improved motor learning in both genotypes, and motor function in WT animals. Interestingly, enrichment was previously reported to improve rotarod test (i.e. motor) performance in the early onset and aggressive R6/2 mouse model of HD (Hockly et al., 2002). This disparity in results, as well as the mild effects of enrichment on behaviour we observed, may be due to the late onset phenotype associated with our YAC128 model, as well as the early stage of disease manifestation at which these tests were conducted.

Enrichment effects on myelination and mature oligodendrocytes

We observed an overall reduction in average myelin thickness across all axons in enriched versus standard-housed animals, across both genotypes. Furthermore, enriched mice of both genotypes were associated with an increased number of small diameter axons relative to standard-housed

counterparts. Environmental enrichment was associated with a decrease in average axonal diameter across genotypes. These observations are consistent with a previous study reporting an increase in number of small-diameter axons in enriched aged rats, and that these were associated with a decreased myelin thickness (Yang et al., 2013). Since large diameter axons are the first axons to become myelinated (Almeida et al., 2011; Hahn et al., 1987; Matthews & Duncan, 1971), we speculate that myelination may have been ongoing (Karttunen, 2017; Powers et al., 2013), such that at the time of our analysis smaller diameter axons were still undergoing myelination, with these freshly myelinated axons being associated with an intrinsically thinner myelin sheath.

A further notable observation was that of a significantly thinner myelin sheath in small diameter axons in YAC128 animals housed under standard conditions relative to WT controls. However, while a trend towards thinner myelin in YAC128 SH animals, relative to WT SH, was observed across all diameter axons, this was not found to be significant. Previous work by our laboratory has demonstrated that thinner myelin sheaths in the same brain region (i.e. posterior CC) in standard housed YAC128 mice only becomes evident after 6 months of age (Teo et al., 2016). Furthermore, our group has also previously shown thinner myelin sheaths in the anterior mid-body of the CC in the standard housed YAC128 mouse from 1.5 months of age (Teo et al., 2016). This suggests that development of myelin-related pathology in the posterior region of the CC may be more protracted than in the anterior to mid-region, and that our observation at 4.5 months of age took place prior to this becoming severe and significant.

Enrichment was not found to influence the number of GST-pi positive cells (i.e. mature myelinating oligodendrocytes) in posterior CC. This observation is in keeping a previous report of unchanged oligodendrocyte density or morphology, nor in myelin transcript levels, in the PFC of enriched young mice (Makinodan et al., 2012). A further study showed that a decrease in OPC number, and increase in mature oligodendrocyte number, observed after ten days in sensorimotor cortex of enriched rats became absent after 42

days (Keiner et al., 2017). Therefore, it is possible that the differentiation of OPCs into mature oligodendrocytes, driven by enrichment and behavioural experience, could take place within the first week of manipulation, and would not be detected at later points (such as those used in our study).

Enrichment effects on brain and body weight

Brain weights were comparable in animals across genotypes and housing conditions, which may be due to the early recording time point since a previous study has demonstrated a 5-10% decrease in the brain weight of 9 and 12 months old YAC128 mice (Slow et al., 2003). Interestingly, we found enriched females of both genotypes to weigh more than their standard housed counterparts, an effect which was not as evident in males, although reports into the effects of enrichment on body weight are notoriously inconsistent, and are sensitive to a variety of factors such as sex, strain and enrichment protocol (Tsai et al., 2016).

Chapter 4. The effects of environmental deprivation and social isolation on myelination and mature oligodendrocytes in the YAC128 model of Huntington disease and wild-type control

4.1. Summary

Social isolation has been revealed to contribute to cognitive decline, and have negative effects on development and aging. Furthermore, emerging evidence supports an association between social isolation and myelination-related abnormalities. White matter abnormalities have also been recently observed during the early stages of Huntington disease (HD) in patients and animal models. This suggests that social deprivation could exacerbate these pathological features, which could have important implications for the design of experimental protocols using animal models of HD, as well as inform on factors that could contribute to the clinical progression of the disease. We therefore investigated the impact of 14 weeks of social deprivation on myelination and mature oligodendrocytes population in the corpus callosum of the early manifest YAC128 mouse model of HD. Animals were allocated post-weaning to either standard housing (SH) or socially deprived housing (DH). Ultrastructural characterization of myelin sheaths and axonal diameter, using electron microscopy, revealed thinner myelin sheaths in the deprived wild-type (WT) mice compared to their standard housing control; however, no change in myelin sheath thickness was observed in YAC128 deprived relative to animals reared in standard conditions. No significant differences in mature oligodendrocyte numbers, habituation, general locomotor activity or anxiety-like behaviour were observed as a result of isolation, regardless of genotype. Modest signs of depressive-like behaviour were detected in deprived animals compared to their SH controls for both genotypes. Deprivation had a minor impact on motor learning and motor performance on the early manifest YAC128 mouse at 18 weeks of age. These findings, supported by past studies, suggest that isolation alters myelination in healthy mice. However, YAC128 mice fail to respond to environmental deprivation in the same way as WT animals, pointing to possible dominant effects of the disease.

4.2. Introduction

Environmental manipulation in Huntington disease (HD) patients and animal models, as described in the previous chapter, has primarily focused on the impact of enrichment (Mo et al., 2015b). In contrast, there appears to be little research, investigating the effects of environmental and social deprivation on the pathological progression of HD. HD patients and animals models exhibit myelination related abnormalities that in of themselves can be induced by deprivation and isolation. Indeed, emerging evidence indicates that myelination is adaptive to environmental and behaviorally-driven experiences (Forbes & Gallo, 2017; McKenzie et al., 2014; Mount & Monje, 2017; Tomlinson, Leiton, & Colognato, 2016a; Xiao et al., 2016). This suggests that environmental or social deprivation could exacerbate HD-driven myelination deficits (Mo, Hannan, & Renoir, 2015a; Potter et al., 2010), which could hasten the clinical progression of the disease, and be an important consideration when employing animal models of HD.

Social isolation of healthy mice has been shown to induce alterations in oligodendroglial population development and maturation, and capacity to myelinate axons, particularly in the prefrontal cortex (PFC) (Forbes & Gallo, 2017; Liu et al., 2012; Liu et al., 2016; Makinodan et al., 2012; Makinodan et al., 2016; Mount & Monje, 2017). Two weeks of social isolation was sufficient to cause thinning of myelin sheaths and alteration of oligodendrocyte morphology, paralleled by decreased expression of myelin basic protein (MBP), in the medial PFC (mPFC), but not in the motor cortex, of socially deprived juvenile mice (Makinodan et al. 2012). Additionally, decreased myelin sheath thickness and MBP expression was also observed in sub-cortical regions of juvenile mice subjected to 8 weeks of social deprivation (Cao et al., 2017). Delayed oligodendrocytes precursor cell (OPC) differentiation and abnormal chromatin structure in oligodendrocytes were shown to precede disturbances in behavior (Cao et al., 2017; Liu et al., 2012). Isolated housing was also demonstrated to affect myelination in adult mice. Following 8 weeks of isolation, 24 weeks old adult mice exhibited hypomyelination, paralleled by decreased myelin related gene transcripts in

the PFC; whereas a shorter period of only 2 weeks of social deprivation had mild effects on myelin sheath thinning (Liu et al., 2012). However, others found no alterations in myelin thickness in the mPFC (Makinodan et al., 2016), the white matter tracts of the anterior commissure, the nucleus accumbens, or the cerebellum of adult mice placed kept in 2-8 weeks isolation (Liu et al., 2012).

Similarly, reduction in myelin sheaths thickness, and lower levels of expression of myelin related genes and transcripts have been reported in several animal models of HD, reared in standard housing conditions (Garcia-Miralles et al., 2016; Gatto et al., 2015; Jin et al., 2015; Teo et al., 2016; Xiang et al., 2011). Surprisingly, these alterations were reported prior to motor deficit onset or neuronal loss in the anterior region of CC of juvenile YAC128 mouse (Teo et al., 2016). Additionally, mice expressing mutant huntingtin (htt) selectively in oligodendrocytes exhibited locomotor deficits, along with progressive demyelination and decreased expression of myelin related proteins (Huang et al., 2015a). Such reports of early myelination abnormalities in pre-symptomatic HD mouse models underscore the importance of understanding how behavioural experience modulates the influence of mutant HTT on oligodendrocytes myelination.

The main focus of the current study was to understand the effects of a deprived environment on axonal myelination in the posterior corpus callosum of the young, early manifest, YAC128 mouse model of HD, as well as healthy controls. In addition, we investigated behavioural alteration and physiological effects of deprivation in these animals.

4.3. Methods

4.3.1. Experimental groups

The YAC128 transgenic mouse model of HD and wild-type (WT) control littermates were used in this study. Both males and females were included in all experimental groups. Sexing and genotyping of animals were carried out

at 3 weeks of age. Mice were weighed on a bi-weekly basis. Mice were housed under standard conditions with food ad libitum, in an inverted light-dark cycle until 4 weeks of age. Subsequently, they were placed into their allocated caging conditions, under the same inverted light-dark cycle: standard housing (SH) or deprived housing (DH). Animals were kept in their allocated condition for 14 weeks in total. At 18 weeks of age, animals were sacrificed and their brains harvested.

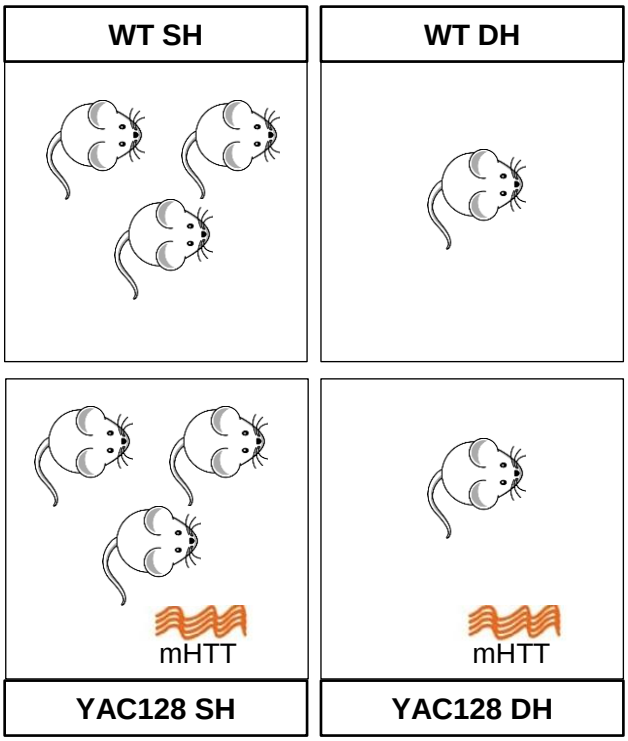

Figure 4.1 Experimental groups for standard and deprived housing conditions

Four groups were used for these experiments: wild type (WT) groups – standard housing (SH) and deprived housing (DH), and YAC128 groups – also SH and DH.

Four groups were used for these experiments: wild type (WT) groups – standard housing (SH) and deprived housing (DH), and YAC128 groups – also SH and DH (Figure 4.1). Mice allocated to the SH condition were housed in standard mouse cages (39 x 19 x 16 cm; Techniplast, Greenline, sealsafe plus mouse, GM500) with 3 mice per cage. These animals were used as SH controls in the enrichment study presented earlier in this thesis (Chapter 3). DH condition mice were single housed housed in the same type of cage as animals in standard housing. No novelty items were added for

either of these groups; however, cages included bedding material (i.e. shredded paper).

4.3.2. Overview of behavioural testing

After 12 weeks of housing in their experimental conditions, several behavioural tests were carried out: the spontaneous activity test (SA), a motor function and habituation test; the open field activity (OF), an anxiety test; the elevated plus maze (EPM), also an anxiety test; the climbing test, a motor function test; the rotarod (RR) test, a motor function, learning and cognition test. Details of behavioural tests were described in Chapter 2 - Materials and Methods (Section 2.1.3).

4.3.3. Tissue harvesting and processing

Three to four animals in each experimental condition were perfused and their brains harvested, to investigate axonal and myelin related characteristics (i.e. axonal shape and size, and myelin thickness). For this study, splenium of the CC (~Bregma -1.82 to -2.70, Mouse Brain Atlas, Paxinos and Franklin, 2001) was microdissected (Figure 2.3A) to be processed and imaged for transmission electron microscopy (TEM). Details of TEM processing were described in Chapter 2 - Materials and Methods (Section 2.4).

All brains were segmented through the mid-sagittal plane, and the left hemisphere used for immunohistochemical (IHC) procedures. Sections were immunostained for the Glutathione S-transferase (GST)-pi Stereo Investigator software was used for cell counting in the corpus callosum. Details of IHC processing and analysis were described in Chapter 2 - Materials and Methods (Section 2.5). Prior to cryosectioning for IHC procedures, the left hemisphere of the brain was weighed. Brain weights were recorded and compared between the experimental groups.

4.3.4. Statistical analysis

The 2x2 factorial design (genotype x housing condition) of the study was statistically analysed using two-way independent ANOVA with Sidak’s

correction for multiple comparisons, and repeated measures ANOVA statistical tests with Tukey's correction for multiple comparisons. P-values equal to or greater than 0.05 were not considered statistically significant. P values and n values were indicated in the associated figure legends for each figure, while mean values are stated in the results section. Variables are reported as mean ± SEM unless otherwise stated.

4.4. Results

4.4.1. Behavioural tests

4.4.1.1. Spontaneous activity results

No housing condition x genotype interaction effect ($p > 0.05$), housing condition effect ($p > 0.05$), or genotype effect ($p > 0.05$) was found during the spontaneous activity (SA) test or open field (OF) tests (two-way ANOVA, Sidak's correction for multiple comparisons; Figure 4.2). In the SA test, WT groups (SH: 10377±1793 cm; DH: 10335±1826 cm) showed a non-significant trend towards increased distance travelled compared to YAC128 groups (SH: 8344±502 cm; DH: 8652±622 cm; Figure 4.2A). No significant differences were observed in the mean resting time (Figure 4.2B), mean vertical counts (Figure 4.2C), mean jump counts (Figure 4.2D), or average velocity ($p > 0.05$; Figure 4.2E). In the OFT, no significant differences in mean distance travelled were observed between the groups (Figure 4.2F).

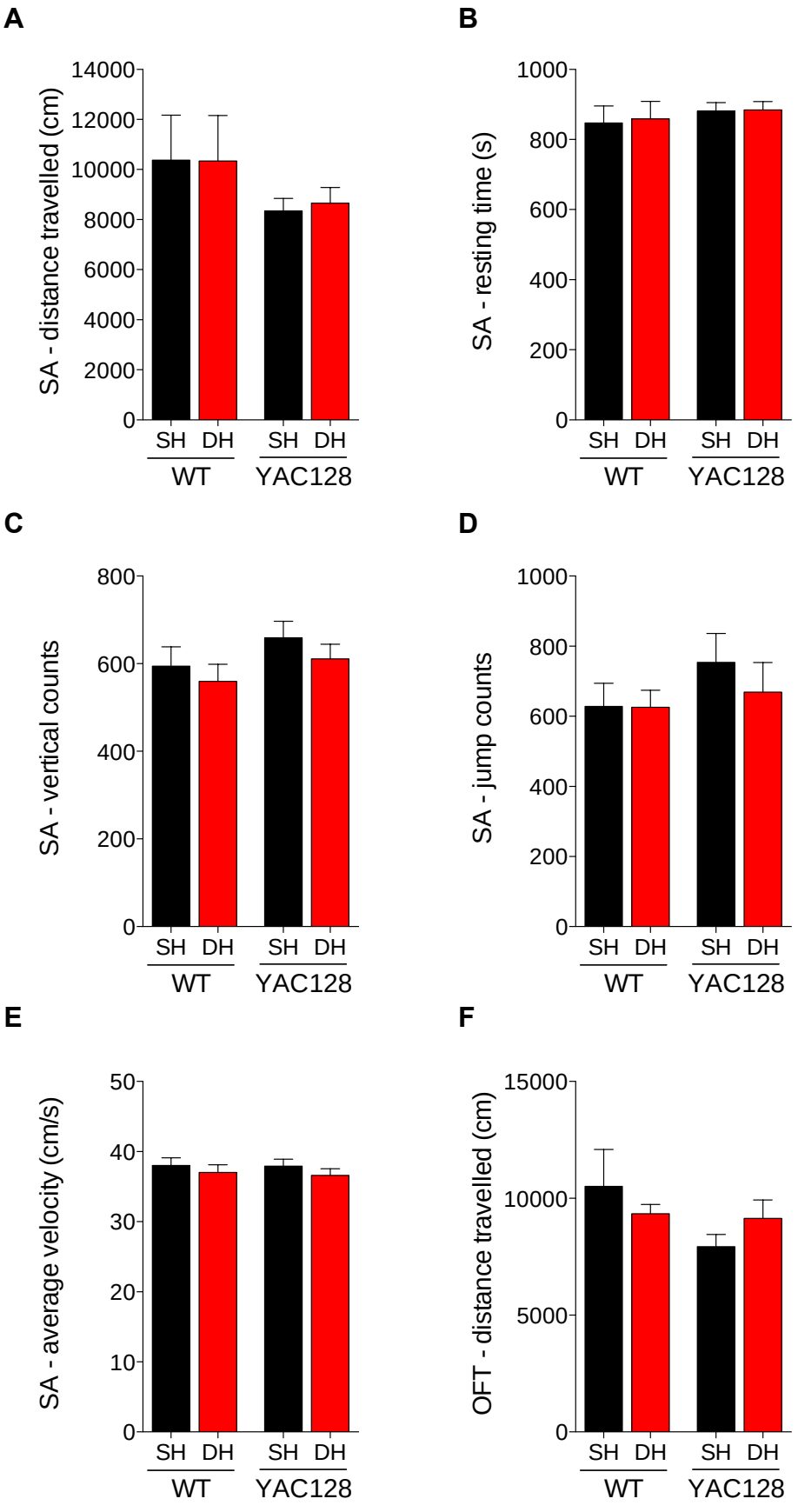
A
SA - distance travelled (cm)
14000
12000
10000
8000
6000
4000
2000
0
SH DH SH DH
WT YAC128
B
SA - resting time (s)
1000
800
600
400
200
0
SH DH SH DH
WT YAC128
C
SA - vertical counts
800
600
400
200
0
SH DH SH DH
WT YAC128
D
SA - jump counts
1000
800
600
400
200
0
SH DH SH DH
WT YAC128
E
SA - average velocity (cm/s)
50
40
30
20
10
0
SH DH SH DH
WT YAC128
F
OFT - distance travelled (cm)
15000
10000
5000
0
SH DH SH DH
WT YAC128

Figure 4.2 Comparison of spontaneous activity measures in YAC128 and WT mice under standard and deprived housing

(A) Total distance travelled over the duration of the SA test was similar between the groups, but a non-significant higher travel distance was observed in the WT groups.
(B) No significant differences were found in resting time between groups.
(C) Mean vertical counts were similar between all groups compared.
(D) Mean number of jumps was also similar between all the groups.
(E) Average velocity was comparable between all groups.
(F) No significant differences were found in distance travelled in the OF test across groups.

The SA test was run over 30 minutes, while OFT was run for 10 minutes. All readouts were obtained from the video tracking software associated with each test. n = 10-12 animals of mixed sex per condition; bar plots and error bars represent the mean±SEM. Two-way ANOVA. Abbreviations: SA, spontaneous activity; OFT, open field test.

4.4.1.2. Anxiety-like behaviour results

There were no significant differences between experimental groups in the total time spent in the centre of the arena during the 10 minutes OF test of anxiety (two-way ANOVA; $p > 0.05$; Figure 4.3A). However, there was a non-significant trend towards decreased proportion of the time spent in the centre of the OF arena for WT DH mice (2.56±0.37%) compared to WT SH controls (3.709±0.67%). This trend was not seen in the YAC128 groups. Additionally, no significant differences were seen in the total time spent in the open arms of the maze during 5 minutes of the EPM test of anxiety (two-way ANOVA; $p > 0.05$; Figure 4.3B). WT SH mice spent a decreased proportion of time in the open arm of the EPM maze (34.59±4.76%) compared to WT DH animals (43.11±4.75%).

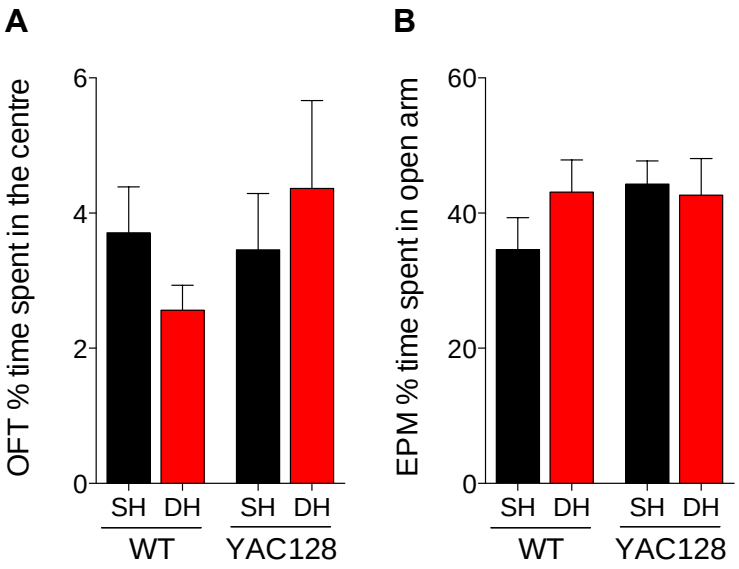

Figure 4.3 Comparison of anxiety-like behaviour in YAC128 and WT mice housed under standard and deprived housing

(A) No significant differences were observed between the groups in the time spent in the centre of the arena of the OFT.
(B) No significant differences were observed between the groups in the time spent in the open arm of the EPM test.

The OFT had a duration of 10 minutes, the EPM test was run for 5 minutes. Readouts for the OFT and EPM were obtained using EthoVision video tracking software. Percentage (%) of total time was calculated for each condition. n = 10-12 animals of mixed sex per condition; bar graphs represent mean±SEM. Two-way ANOVA. Abbreviations: OFT, open field test; EPM, elevated plus maze.

4.4.1.3. Motor function results

When comparing latency to climb, time spent climbing and number of climbing attempts two-way ANOVA revealed no significant interaction between genotype and housing condition ($p > 0.05$), however a significant main effect of housing condition (latency to climb: $F(1, 42) = 7.11$, $p < 0.05$; time spent climbing: $F(1, 42) = 5.75$, $p < 0.05$; number of climbing attempts: $F(1, 42) = 4.45$, $p < 0.05$), but no effect of genotype ($p > 0.05$). Sidak's correction for multiple comparisons post-hoc for the housing effects revealed no significant differences in climbing characteristics during the climbing test, although both DH groups (WT and YAC128) were associated with an increased latency to climb, reduced climbing time, and lower number of

climbing attempts compared to their corresponding SH controls ($p > 0.05$; Figure 4.4). Specifically, both WT (96.5±27.9s) and YAC128 (117.3±22.3s) animals in the DH group exhibited a higher mean latency to climb than their respective SH controls (WT SH: 35.0±16.1s; YAC128 SH: 63.1±20.3s; Figure 4.4A). Both DH groups (WT DH: 25.1±3.4s; YAC128 SH: 24.6±4.1 s) spent, on average, less time climbing compared to SH controls (WT SH: 38.2±5.0s; YAC128SH: 37.5±7.5s; Figure 4.4B), regardless of genotype. And finally, both DH groups (WT DH: 9.6±1.2; YAC128 DH: 9.3±1.9) had a lower mean number of climbing attempts than SH controls (WT SH: 15.3±2.0; YAC128 SH: 11.8±2.1; Figure 4.4C).

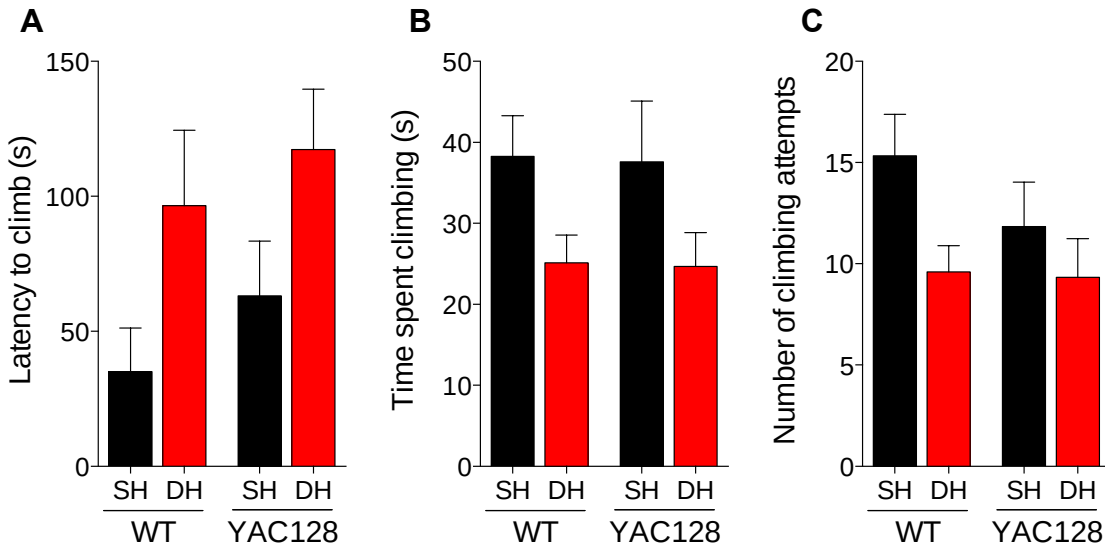

Figure 4.4 Comparison of climbing characteristics of YAC128 and WT controls housed under standard and deprived housing

(A) No significant differences were observed between the latency for the first climbing attempt, although there was a trend for both WT DH and YAC DH to take longer before attempting to climb compared to their SH controls.
(B) No significant differences were observed between the total time spent climbing, although there was a trend for both DH groups to spend less time climbing compared to their SH controls.
(C) Consistently, both WT DH and YAC128 DH groups attempted climbing to a lesser extent than their corresponding SH controls.

The climbing test had a total duration of 6 minutes, and videos were scored manually. n = 10-12 animals of mixed sex per condition; bar graphs represent mean±SEM. Two-way ANOVA, with Sidak's correction for multiple comparisons post-hoc.

4.4.1.4. Motor function and motor learning evaluation

The latency to first fall (Figure 4.5) and the number of falls (Figure 4.6) were recorded as measures of performance on the fixed speed rotarod training over three days, with three trials per day, except the first day when only two trials were recorded. For the latency to fall, repeated measures ANOVA revealed significant main effects of time ($F(7,301) = 4.751$, $p < 0.0001$), but no effect of the group (genotype and housing condition) ($F(3,43) = 1.629$, $p > 0.05$), and no effect of the interaction between the two ($F(21,301) = 0.975$, $p > 0.05$). The significant effect of time reflects improved rotarod performance with increased training (Figure 4.5A). Nevertheless, several non-significant trends were observed. Firstly, YAC128 DH mice (trial 1: 65.25±14.77s; trial 2: 68.33±12.16s) remained on the rotarod for the least time compared to all the other groups (trial 1: WT DH: 88.81±13.18s; YAC128 SH: 84.75±14.26s; WT SH: 93.66±11.54s; trial 2: WT DH: 100.45±10.4s; YAC128 SH: 91.5±13.92s; WT SH: 110.58±9.41s) during the first two training sessions on the first day of the training (Figure 4.5A). Secondly, when averaged together over training trials for each day, YAC DH mice spent less time on the rotarod on the first and final day of training (day 1 (trials 1-2): 71.25±13.03; day 3 (trials 6-8): 99.33±8.48) compared to the other groups (day 1 (trials 1-2): WT DH: 94.64±10.89; YAC128 SH: 88.13±12.67; WT SH: 102.1±6.64; day 3 (trials 6-8): WT DH: 115.6±2.41; YAC128 SH: 109±5.23; WT SH: 113.1±4.29), although this difference did not reach significance (two-way ANOVA, $p > 0.05$, Figure 4.7A). Thirdly, WT DH animals also spent marginally less time on the rotarod compared to WT SH animals during most training trials (with the exception of trials 4 and 8).

In terms of the average number of falls, repeated measures ANOVA revealed significant main effects of time ($F(7,301) = 3.57$, $p < 0.001$), but no effect of group (genotype and housing condition) ($F(3,43) = 1.514$, $p > 0.05$), and no effect of the interaction between the two ($F(21,301) = 0.768$, $p > 0.05$). The significant effect of time again reflects the effect of more training on increased performance (Figure 4.6A). Several non-significant trends were observed: firstly, WT SH mice fell the least number of times over most

training trials compared to all the other groups, while YAC128 SH mice were associated with the most number of falls, compared to all the other groups, over the majority of trials (Figure 4.6).

The proportion of mice in each experimental group that fell off the rotarod was calculated and averaged over trials for each training day (Figure 4.7B). Two-way ANOVA calculated for each of the training days to identify any group differences revealed no significant effect of interaction for day 1 and 3 (day 1: $F(1,4) = 0.36$, $p > 0.05$; day 2: $F(1,8) = 6$, $p < 0.05$; day 3: $F(1,8) = 1.36$, $p > 0.05$), no effect of the housing condition (day 1: $F(1,4) = 3.83$, $p > 0.05$; day 2: $F(1,8) = 2.66$, $p > 0.05$; day 3: $F(1,8) = 0.71$, $p > 0.05$) and no effect of genotype (day 1: $F(1,4) = 7.07$, $p > 0.05$; day 2: $F(1,8) = 2.66$, $p > 0.05$; day 3: $F(1,8) = 2.79$, $p > 0.05$). Interestingly, although not statistically significant, YAC128 DH animals fell more often than other groups during the first and last day of training. During the first day of training (2 trials), 58.33±8.33% of YAC128 DH mice fell off the rotarod compared to 37.5±4.16% of YAC128 SH mice, 31.82±4.54% of WT DH mice, and 20.83%±12.5% of WT SH mice. On the second day of training, only 25% of YAC128 DH mice fell of the rotarod, compared to 27.78%±2.77% of YAC128 SH mice, and the same proportion of WT DH mice. WT SH mice fell less often off the rotarod (13.89±5.56%). Finally, on the last day of training, YAC128 DH mice had the highest number of falls (27.78±7.34%) compared to YAC128 SH (16.67±4.81%) of mice, WT DH (12.12%±6.06%) and WT SH mice (13.89%±2.77%).

The accelerated rotarod test was performed after three days of training on the fixed speed rotarod, and the latency to first fall was recorded as a measure of motor performance (Figure 4.8). No significant differences were observed between the groups ($p > 0.05$; two-way ANOVA). However, YAC128 DH mice (216.6±21.24 s) showed a trend towards a shorter latency to fall compared to other groups, when averaged over all test trials (YAC128 SH: 236.8±14.19s; WT DH: 242.3±17.63s; WT SH: 238.9±16.02s), although variability in this group was relatively high (Figure 4.8A). Latency to fall was lowest in YAC128 DH mice during each of the three test trials (Figure 4.8B).

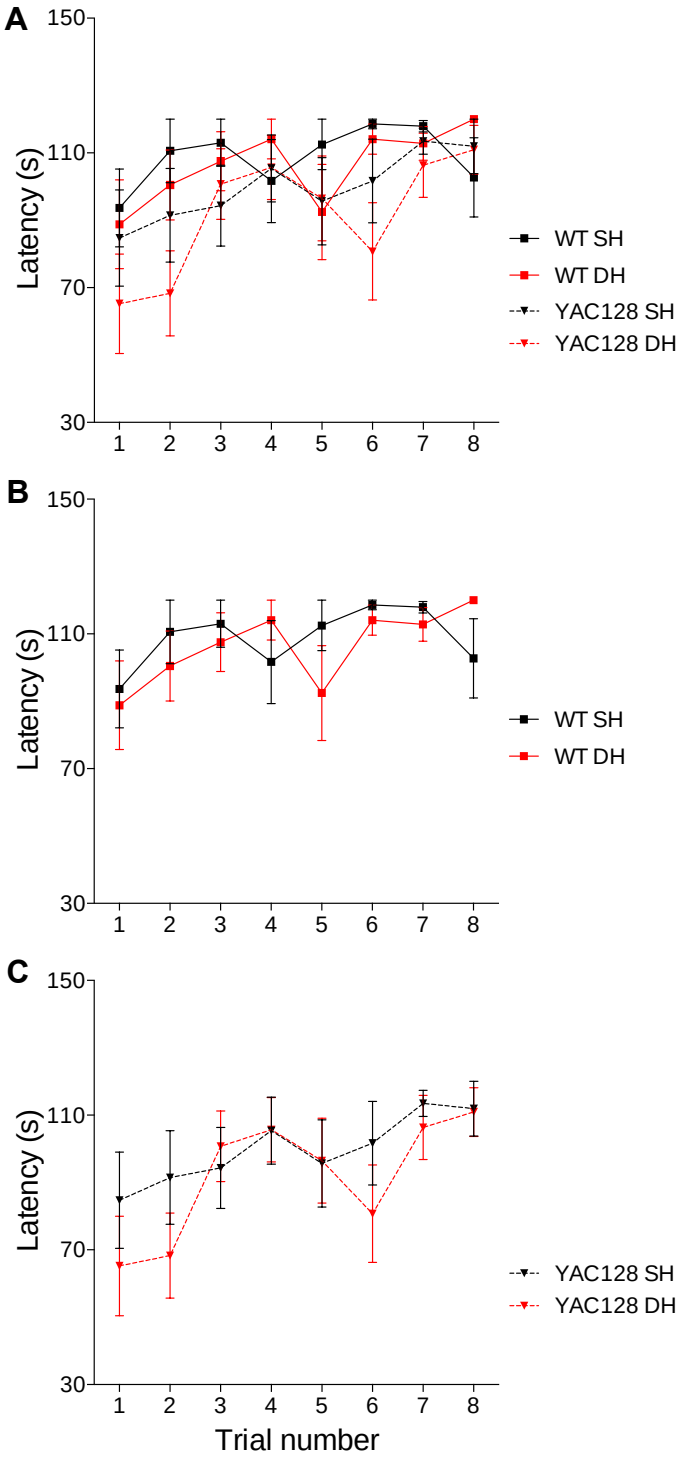

Figure 4.5 Comparison of latency to fall during fixed speed rotarod training for YAC128 and WT mice housed under SH and DH

(A) Latency to fall over 8 trials of training in all groups.
(B) WT DH mice performed poorly compared to WT SH animals on most trials.
(C) YAC128 DH mice performed poorly or comparably to YAC128 SH animals.
Latency to fall illustrated in seconds (s). Training was run over 3 days with 2 trials on first day and 3 trial sessions on last two days. n = 10-12 animals of mixed sex per condition; error bars are ±SEM. Repeated measures ANOVA.

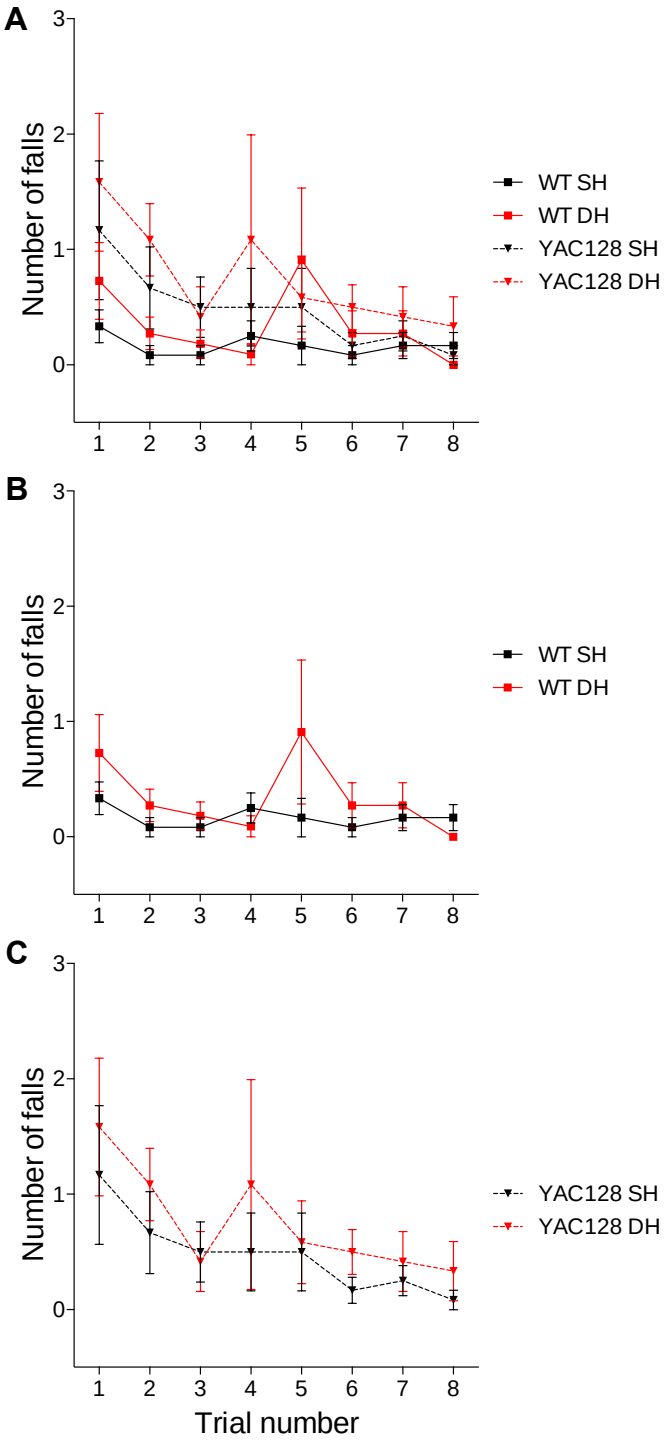

Figure 4.6 Comparison of number of falls of YAC128 and WT mice from SH and DH conditions during fixed speed rotarod training

(A) Number of falls over the 8 training for all groups.
(B) WT DH had increased number of falls compared to WT SH during most trials.
(C) YAC128 DH showed slight increased number of falls compared to YAC128 SH.
Training was run over 3 days, with 2 trials on first day and 3 trials on second and third days.
n = 10-12 animals per condition; Error bars represent ±SEM. Repeated measures ANOVA.

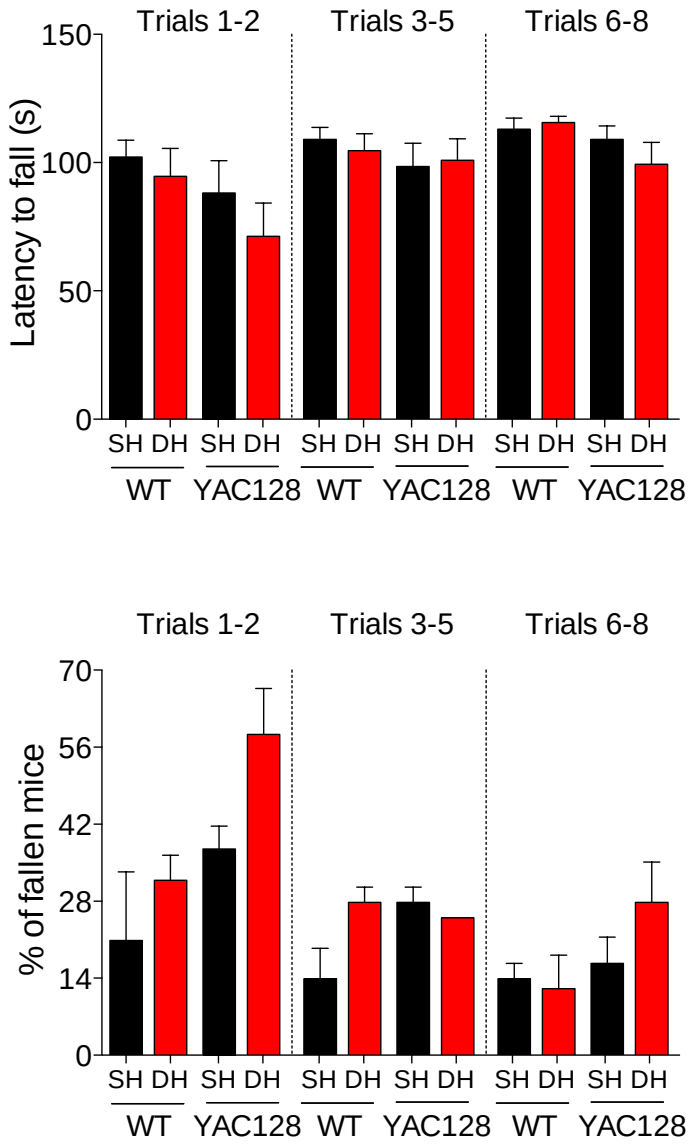

Figure 4.7 Session averages of latency to fall and percentage of mice fallen for YAC128 and WT mice housed under standard and deprived conditions

(A) Average latency to fall for each day of training showed a trend towards decreased performance by the YAC128 DH group, although no significant differences were found.

(B) YAC128 DH mice were more likely to fall off the rotarod compared to any of the other groups on the first and last day of training.

Testing was run over 2-3 trials within the same day. n = 10-12 animals of mixed sex per condition; Bars graphs represent mean±SEM. Two-way ANOVA, with Sidak's multiple comparisons test. Latency to fall illustrated in seconds (s) (A). Proportion of mice that fell of the rotarod averaged over trials for each training day (B).

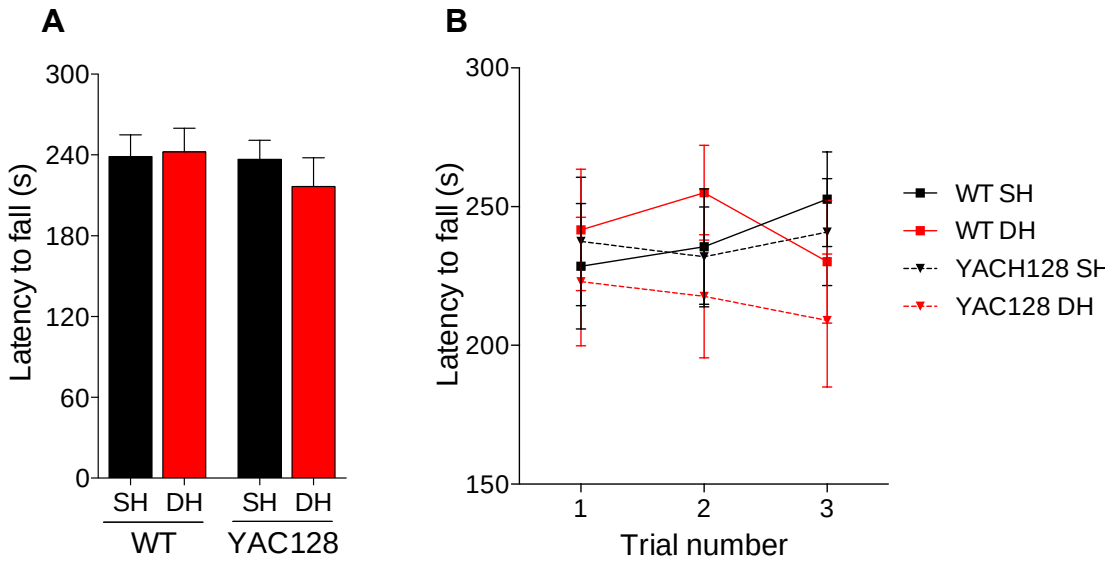

Figure 4.8 Comparison of latency to fall in YAC128 and WT mice housed under standard and deprived conditions during accelerated rotarod test

(A) All groups had a similar mean latency to fall over the 3 trials of the testing session, although YAC128 DH mice were associated with a shorter time spent on the accelerated rotarod compared to other groups.
(B) No significant differences in latency to fall were found between groups across the 3 testing trials, although WT DH animals consistently spent less time on the rotarod during each of the testing trials compared to other groups.

Mean latency to fall illustrated in seconds (s). Testing was run over 3 trials within the same day. n = 10-12 animals of mixed sex per condition; bar graphs represent mean±SEM (A); error bars represent ±SEM (B). Two-way ANOVA, with Sidak's multiple comparisons test (A), and repeated measures ANOVA (B).

4.4.2. Ultrastructural analysis of myelin

The inner (axoplasm) and outer (axoplasm and myelin sheath) diameters of regular-shaped axons in the posterior (splenium) of the corpus callosum (CC) were measured (Figure 2.3). G-ratios were calculated as the inner diameter divided by the outer diameter, and used as a measure of myelin thickness (Friede, 1972; Figure 2.4). Representative micrographs of callosal axons for each experimental group are illustrated below, in Figure 4.9.

WT DH mice exhibited qualitatively larger g-ratios at small axonal diameters (ID < 500nm), and smaller g-ratios at large axonal diameter (ID > 1000nm), compared to WT SH animals (Figure 4.10A). Cumulative frequency analysis confirmed a shift towards overall larger g-ratios for WT DH mice compared to WT SH mice (Figure 4.10B). In contrast, YAC128 DH animals showed qualitatively smaller g-ratios at small and mid-range diameter (ID < 1000nm) compared to SH controls, while no differences were seen at large diameters (Figure 4.10C). Cumulative frequency analysis showed a closer overlap of the two curves representative of the YAC128 groups (Figure 4.10D).

G-ratios were averaged over all axonal diameters for quantitative comparison between groups (Figure 4.11A). Two-way ANOVA revealed significant interaction between genotype and housing condition ($F(1, 2995) = 63.91$, $p < 0.0001$), significant main effect of housing condition ($F(1, 2995) = 29.65$, $p < 0.0001$), and significant main effect of genotype ($F(1, 2995) = 28.4$, $p < 0.0001$). Sidak's correction for multiple comparisons post-hoc tests revealed WT DH animals (0.814±0.002) exhibited a significantly larger mean g-ratio compared to all the other groups (WT SH: 0.779±0.003; YAC128 SH: 0.786±0.002). In contrast, the mean g-ratio in YAC128 DH mice (0.779±0.002) was comparable to that of YAC128 SH controls.

Finally, g-ratios were classified according to their respective inner axonal diameter: small diameter axons (ID < 500nm), mid-range diameter axons (500 ≤ ID < 1000nm), and large diameter axons (ID ≥ 1000nm) (Figure 4.11B). There was an overall increase in g-ratio with increasing axonal diameter. At small axonal diameters, two-way ANOVA revealed significant interaction between genotype and housing condition ($F(1, 1007) = 27.98$, $p < 0.0001$), significant main effect of housing condition ($F(1, 1007) = 13.57$, $p < 0.001$), but no significant main effect of genotype ($F(1, 1007) = 0.377$, $p > 0.05$). Sidak's correction for multiple comparisons post-hoc tests revealed WT DH mice possessed larger g-ratio (0.765±0.004) relative to both WT SH (0.727±0.004; $p < 0.0001$) and YAC128 DH (0.740±0.003, $p > 0.05$) animals. Additionally, YAC128 SH mice showed slightly higher g-ratios (0.747±0.004; $p > 0.05$) compared to that of WT SH control. At mid-range inner diameters,

two-way ANOVA revealed significant interaction between genotype and housing condition ($F (1, 1592) = 22.66$, $p < 0.0001$), significant main effect of housing condition ($F (1, 1592) = 25.06$, $p < 0.0001$), and significant main effect of genotype ($F (1, 1592) = 19.14$, $p < 0.0001$). Sidak's correction for multiple comparisons post-hoc tests revealed WT DH mice also exhibited larger g-ratios (0.821±0.002) than both WT SH (0.793±0.003; $p < 0.0001$) and YAC128 DH (0.795±0.002; $p < 0.0001$) animals. In contrast, YAC128 DH and SH (0.794±0.002) mice had comparable g-ratios. Finally, at large axonal diameters, two-way ANOVA revealed no significant interaction between genotype and housing condition ($F (1, 386) = 1.7$, $p > 0.05$), a significant main effect of housing condition ($F (1, 386) = 13.52$, $p < 0.001$), and no significant main effect of genotype ($F (1, 386) = 3.58$, $p > 0.05$). Sidak's correction for multiple comparisons post-hoc tests for housing effect revealed both WT and YAC128 DH groups showed an increased mean g-ratio compared to corresponding SH groups, regardless of genotype. However, only the mean g-ratio of YAC128 DH animals (0.869±0.004) was significantly larger than that of YAC128 SH animals (0.844±0.005; $p < 0.001$), whereas the mean g-ratio of WT DH mice (0.872±0.004) was not significantly greater than that of WT SH mice (0.860±0.005).

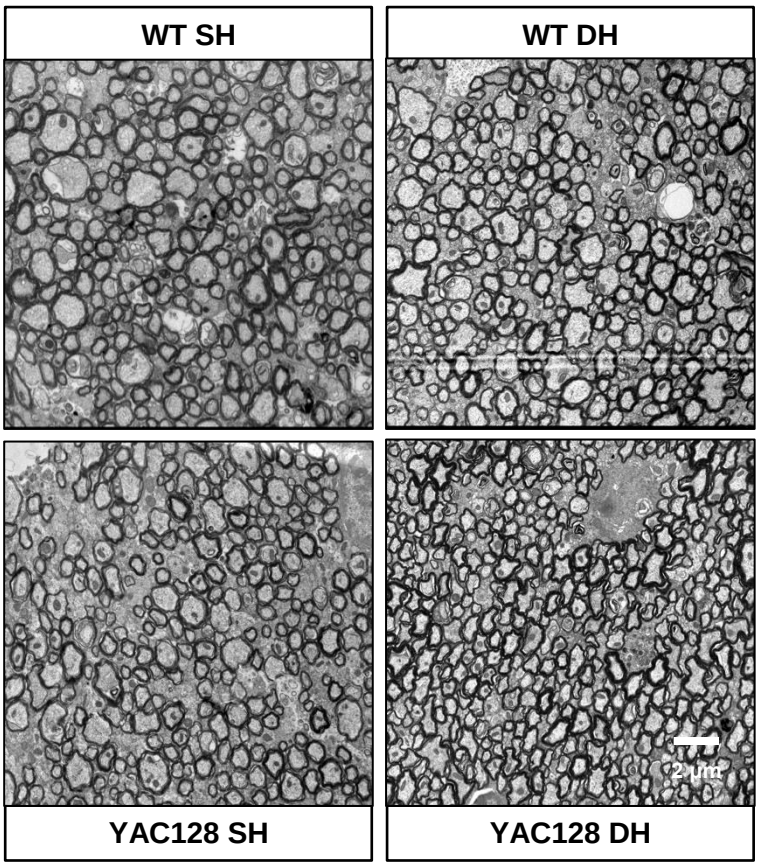

Figure 4.9 Representative TEM images of callosal axons in YAC128 and WT mice housed under standard and enriched conditions

Representative micrographs of axons from the posterior (splenium) region of the corpus callosum for each experimental group. Scale bar at 2µm.

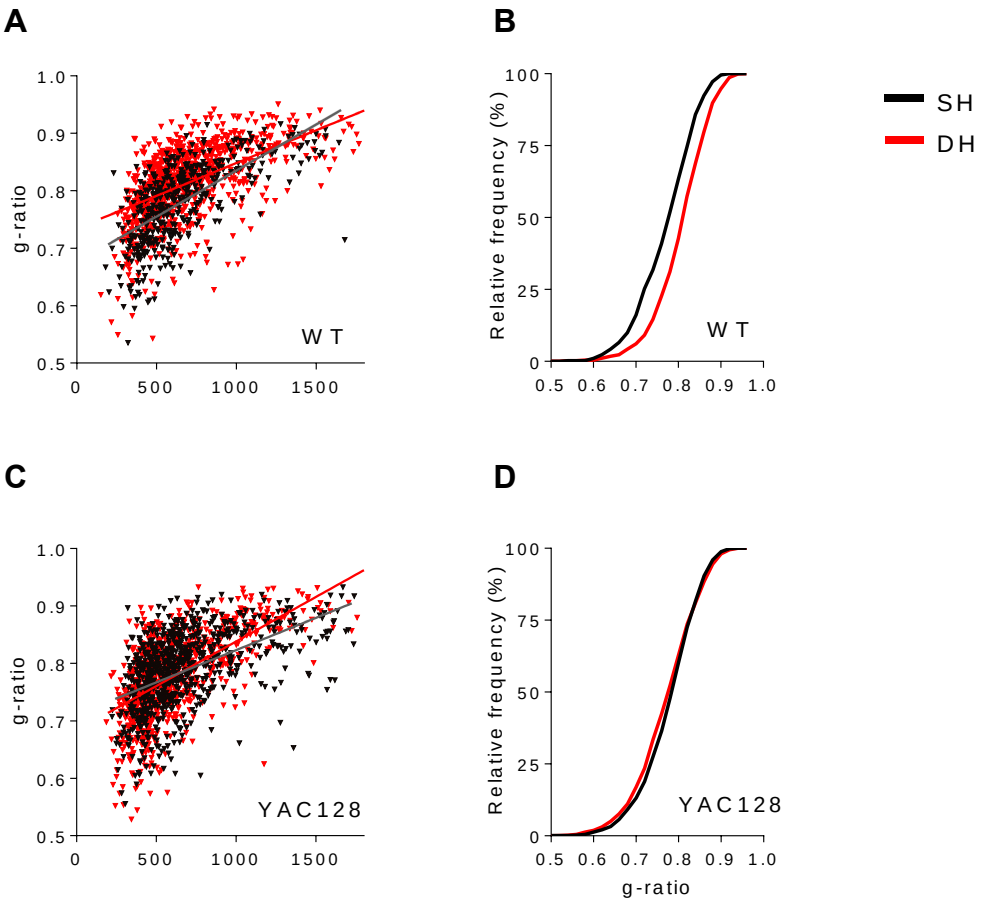

Figure 4.10 G-ratios and axonal diameters of YAC128 and WT mice housed under standard and deprived housing

(A) Scatter plot of g-ratio values against inner axonal diameter (ID) showed higher g-ratios at small IDs (< 500nm), and smaller g-ratios at large IDs (> 1000nm) for WT DH (red) animals relative to WT SH (black).
(B) Cumulative frequency plot of g-ratios showed an evident shift towards larger g-ratios in the WT DH condition compared to WT SH.
(C) Scatter plot showing lower g-ratio values at small and mid-range axonal diameters (IDs < 1000 nm), and higher g-ratios at large axonal diameters (ID > 1000nm) for YAC128 DH animals (red) compared to YAC128 SH mice (black).
(D) Cumulative frequency plot of g-ratios showed a close overlap of the two curves representative of both YAC128 SH and DH groups.

n = 474 - 916 axons per condition (WT SH, n = 474 axons; WT DH, n = 916 axons; YAC128 SH, n = 782 axons; YAC128 DH, n = 841 axons); 2-4 animals per condition.

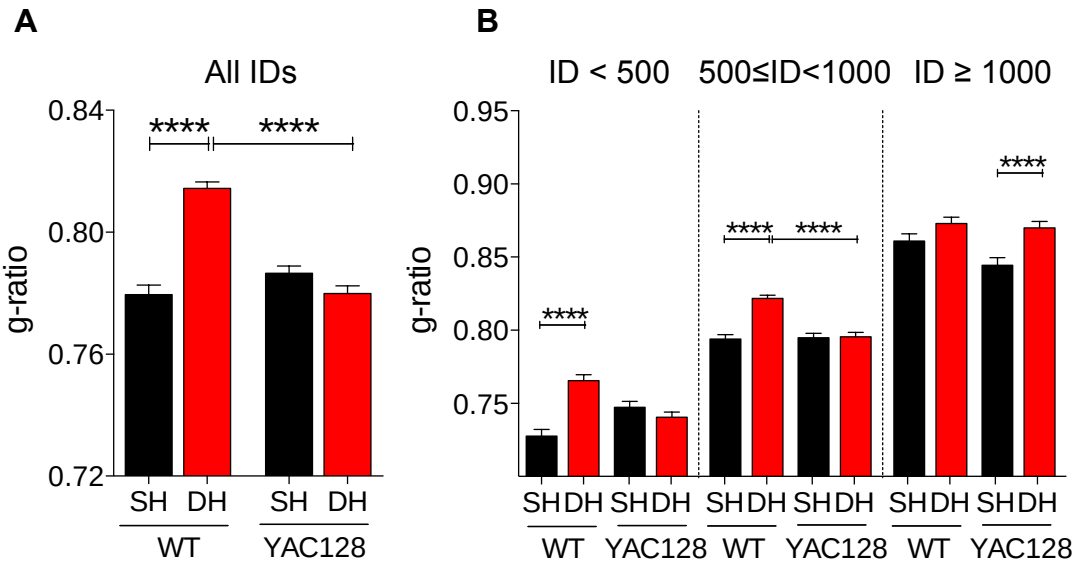

Figure 4.11 Average g-ratio for YAC128 and WT mice housed under standard and deprived housing

(A) The WT DH group showed a significantly higher mean g-ratio compared to YAC128 DH animals and WT SH controls.

(B) G-ratio values were classified according to their corresponding inner axonal diameter (ID, small diameter axons, ID≤500nm; mid-range diameter axons, 500<ID≤1000nm; large diameter axons, ID≥1000nm). Overall, there was an increase in g-ratio with increasing axonal diameter, as well as an increased g-ratio in DH mice compared to SH mice, for WT groups, but not YAC128 groups at small and medium axonal diameter ranges. A larger mean g-ratio value was observed at large diameters in YAC128 DH animals compared to YAC128 SH controls.

Bar graphs represent mean±SEM. SEM comes from axonal variance. n = 474 - 916 axons per condition (WT SH, n = 474 axons; WT DH, n = 916 axons; YAC128 SH, n = 782 axons; YAC128 DH, n = 841 axons); 2-4 animals per condition. Two-way ANOVA, with Sidak's multiple comparisons test. *p < 0.05; ****p < 0.0001. Inner diameter shown in nanometres (nm). Abbreviations: ID, inner diameter.

4.4.3. Differences in axonal characteristics

Analysis of axonal diameter revealed a lower number of small diameter axons (200 to 400nm), and a comparable or higher number of medium and large diameter axons (500 to 1300nm) in WT DH animals compared to WT SH controls (Figure 4.12A). Cumulative frequency plots of inner diameters showed a close overlap of the two curves representative of both WT groups, with a small shift towards larger g-ratios driven by the increased number of

large axonal diameters in the WT DH group (Figure 4.12B). Additionally, the mean inner axonal diameter was significantly greater in WT DH animals (685.6±9.39nm) compared to WT SH (652.5±12.67nm; $p < 0.05$). On the other hand, YAC128 DH animals possessed a larger number of small diameter axons (200-500nm), and a similar or smaller number of mid-range diameter axons (600-1000nm), compared to YAC128 SH mice ($p < 0.001$). Cumulative frequency analysis of inner diameters revealed a close overlap of the two curves representative of both YAC128 SH and DH groups. Additionally, the mean axonal diameter of YAC128 DH mice (618.2±9.66nm) was significantly smaller than that of YAC128 SH animals (672.7±10.76nm).

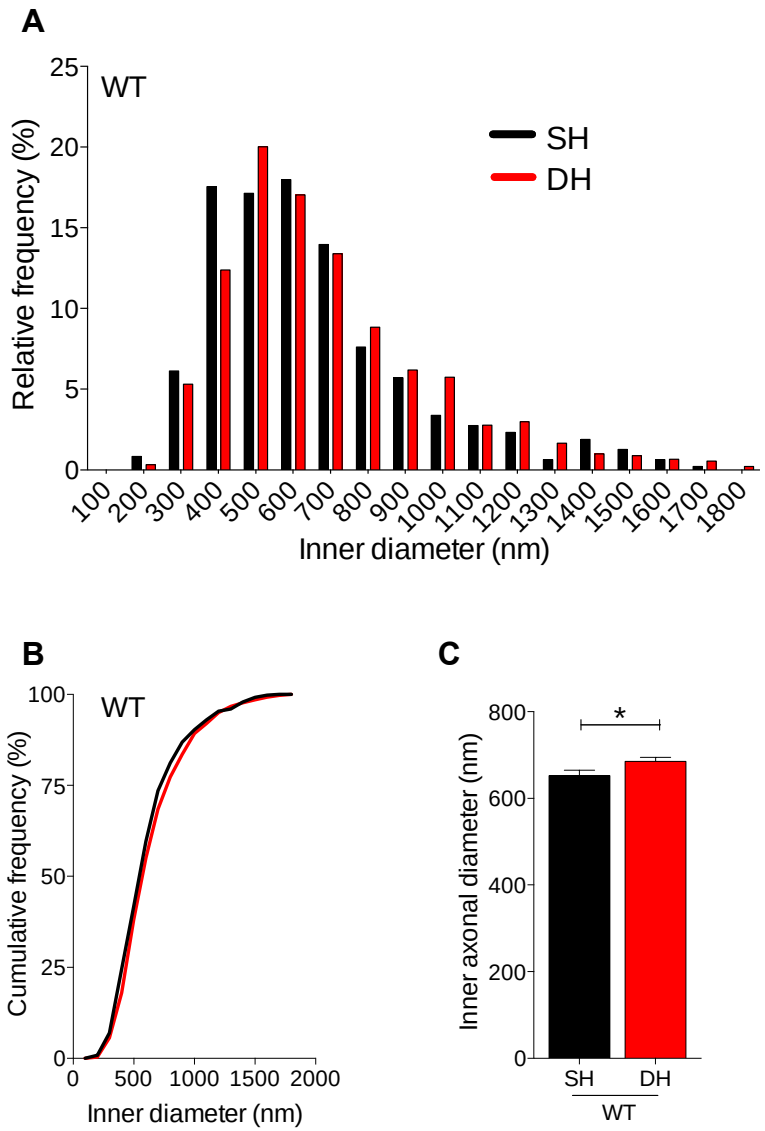

Figure 4.12 Axonal diameters of WT mice housed under standard and deprived conditions

(A) Smaller number of axons with a small diameter (200-400nm), and a higher or similar number of axons with a large diameter (500-1300nm) in WT DH animals compared to WT SH controls.
(B) Cumulative frequency of IDs showed a close overlap of the two curves representative of both WT groups.
(C) WT DH animals were associated with a significantly larger mean axonal diameter in myelinated axons compared to WT SH mice.

Average of 2-4 animals per condition; n = 474 - 916 axons per condition (WT SH, n = 474 axons; WT DH, n = 916 axons; YAC128 SH, n = 782 axons; YAC128 DH, n = 841 axons). Relative frequency histogram (A) and cumulative frequency (B), bin width = 100nm (A). Unpaired, two-tailed t-test, 95% confidence intervals, *p < 0.05; Bars graphs represent mean±SEM (C). Abbreviations: ID, inner diameter

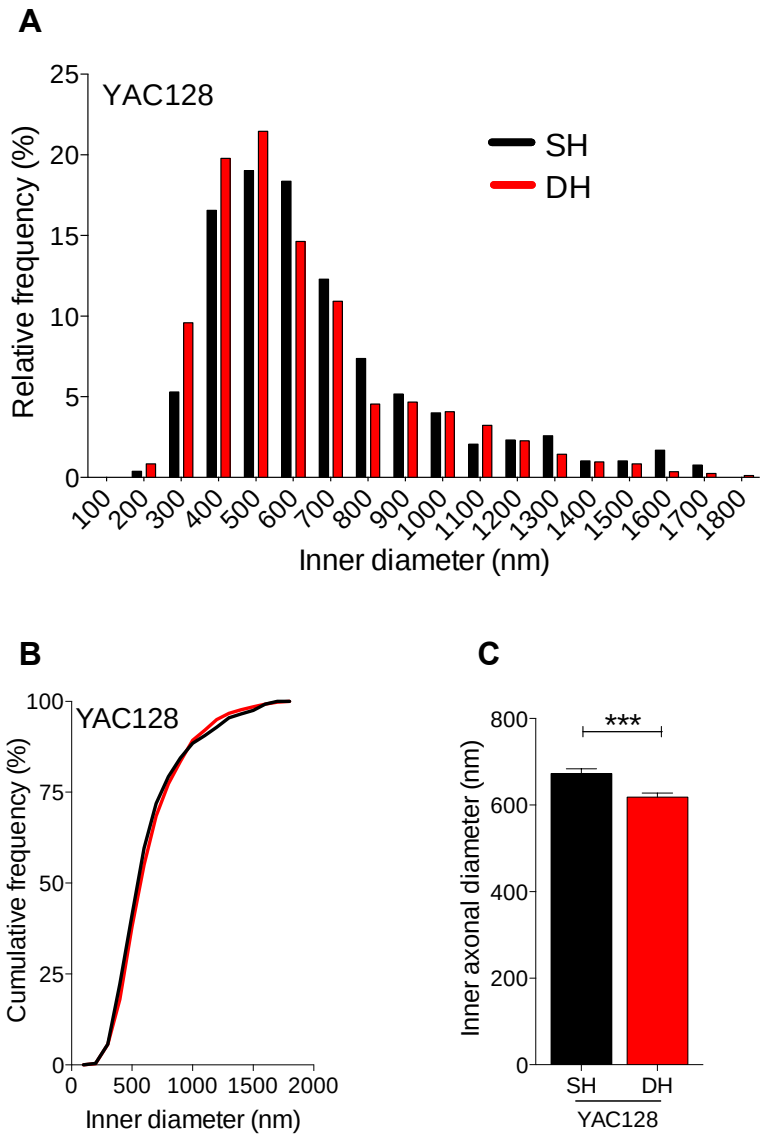

Figure 4.13 Axonal diameters of YAC128 mice housed under standard and deprived conditions

(A) Higher number of axons with small diameters (200-500nm), and a smaller or similar number of axons at mid-range axonal diameters (600 to 1000nm) in the YAC128 DH animals compared to YAC128 SH controls.
(B) Cumulative frequency of IDs showed a close overlap of the two curves representative of the YAC128 groups.
(C) YAC128 DH animals showed significantly smaller diameter average for myelinated axons compared to SH control.

Average of 2-4 animals per condition; n = 474 - 916 axons per condition (WT SH, n = 474 axons; WT DH, n = 916 axons; YAC128 SH, n = 782 axons; YAC128 DH, n = 841 axons). Relative frequency histogram (A) and cumulative frequency (B), bin width = 100nm (A). Unpaired, two-tailed t-test, 95% confidence intervals, ***p < 0.001; bar graphs represent mean±SEM (C). Abbreviations: ID, inner diameter.

4.4.4. Quantification of mature oligodendrocytes

Mature oligodendrocytes, as identified by GST-pi staining, were counted in the corpus callosum. No significant differences in number of GST-pi positive cells were seen between any of the four groups (two-way ANOVA, $p > 0.05$, Figure 4.14). However, a trend towards an increased number of GST-pi positive cells was observed in WT DH (35,726±4,265) mice compared to WT SH (29,406±2,498), and YAC128 DH (32,692±2,420) compared to YAC128 SH (29,766±4,065), mice.

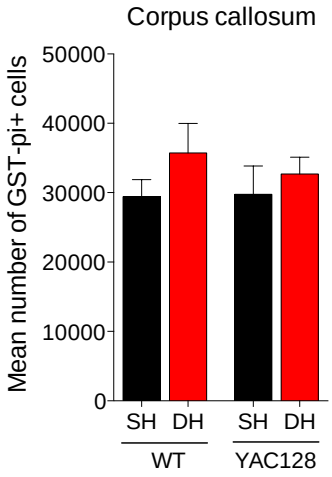

Figure 4.14 Number of GST-pi positive cells in the posterior corpus callosum of YAC128 and WT mice housed under standard and deprived conditions

No significant differences in number of GST-pi cells were seen between any of the four experimental groups. Bar graphs represent the average of a total of 8-10 animals per condition, 6-8 sections per animals; bar graphs represent mean±SEM. Abbreviations: CC, corpus callosum; Glutathione S-transferase (GST)-pi.

4.4.5. Brain weights for standard and deprived WT and YAC128 animals

The left cerebral hemisphere of each animal was weighed prior to tissue processing. No significant differences were found at 4.5 months between any of the groups when comparing the brain weights of mixed sex (Figure 4.15.A), females (Figure 4.15.B), or males (Figure 4.15C) mice (two-way

ANOVA, $p > 0.05$). However, left hemisphere brain weights for WT and YAC128 animals in the DH condition were consistently larger than their SH counterparts, regardless of sex (Figure 4.13A-C).

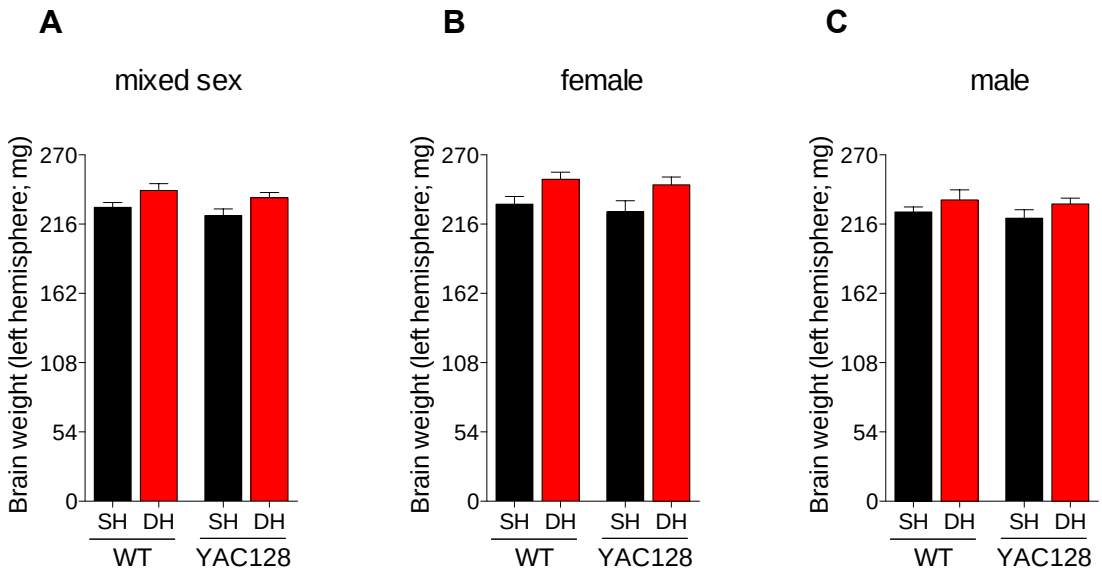

Figure 4.15 Brain weight (left hemisphere) in YAC128 and WT mice housed under standard and deprived conditions

(A) No significant differences were seen in the brain weights of mixed sex groups across conditions.
(B) No significant differences were seen in the brain weights of female mice across conditions.
(C) No significant differences were seen in the brain weights of male mice across conditions.

Animals' left cerebral hemisphere were weighed at 18 weeks (4.5 months) of age. Left hemisphere weight shown in milligrams (mg). n = 5-8 males per condition, and 5-7 females per condition; Bar graphs represent mean±SEM. Two-way ANOVA.

4.4.6. Body weight comparison over time for standard and deprived WT and YAC128 animals

Animals were weighed fortnightly starting from pn50 (~7 weeks) until sacrifice, on pn126 (18 weeks). Body weights were evaluated and compared separately for females and males. In the female groups (Figure 4.16A), repeated measures ANOVA revealed significant main effects of time ($F(5,85) = 37.33$, $p < 0.0001$), but not of animal group (genotype and housing

condition) ($F(3,17) = 1.567$, $p > 0.05$), although a significant effect of the interaction between the two was observed ($F(15,85) = 2.87$, $p < 0.01$). WT SH female mice consistently possessed the lowest mean body weight at all time-points, followed by WT DH mice, although no significant differences were observed between both groups. In turn, YAC128 SH female mice were, on average, generally heavier than other groups at most time-points; however this only reached statistical significance when compared to WT SH at pn78 (YAC128 SH: 23.16±1.165g; WT SH: 20.21±0.54g; $p < 0.05$). When compared at the last time point, no significant differences were observed between groups (two-way ANOVA), although a trend towards lower body weights for WT SH (22.59±0.52g) compared to all the other groups was observed (WT DH: 23.86±0.52g; YAC128 SH: 23.54±0.95g; YAC128 DH: 24.23±1.09g; Figure 4.17A). On the other hand, in the male comparisons (Figure 4.16B), repeated measures ANOVA revealed significant main effects of time ($F(5,110) = 77.39$, $p < 0.0001$), of animal group (genotype and housing condition) ($F(3,22) = 4.952$, $p < 0.01$), and a significant effect of the interaction between the two ($F(15,110) = 2.006$, $p < 0.05$). Significantly increased body weights at most time-points were observed in YAC128 DH male mice (pn50: 26.21±0.84g; pn78: 28.65±1.03g; pn92: 29.62±1.09g; pn106: 30.23±1.18g; pn126: 30.71±1.04g) compared to WT DH male animals (pn50: 22.76±0.5g; pn78: 24.78±0.7g; pn92: 25.63±0.86g; pn106: 25.81±0.74g; pn126: 27.21±0.52g). A further significant difference was seen between YAC128 SH (30.92±0.9g) and WT SH (27.2±1.08g) males at pn106. Overall, WT DH male mice had the lowest body weights at all time-points recorded, followed by WT SH mice. The body weights of YAC128 DH and SH groups were approximately similar at all-time points. At the final time-point, two-way ANOVA revealed no significant interaction between genotype and housing ($F(1, 22) = 0.8$, $p > 0.05$), no main effect of housing condition ($F(1, 22) = 2.61$, $p < 0.05$), but a main effect of genotype ($F(1, 22) = 7.79$, $p > 0.05$). WT DH male mice (27.22±0.53g) were associated with the lowest body weight of all the groups at the final time-point, but this was only statistically different to YAC DH mice (30.71±1.04g; Sidak's multiple comparisons, $p < 0.05$; Figure 4.17B).

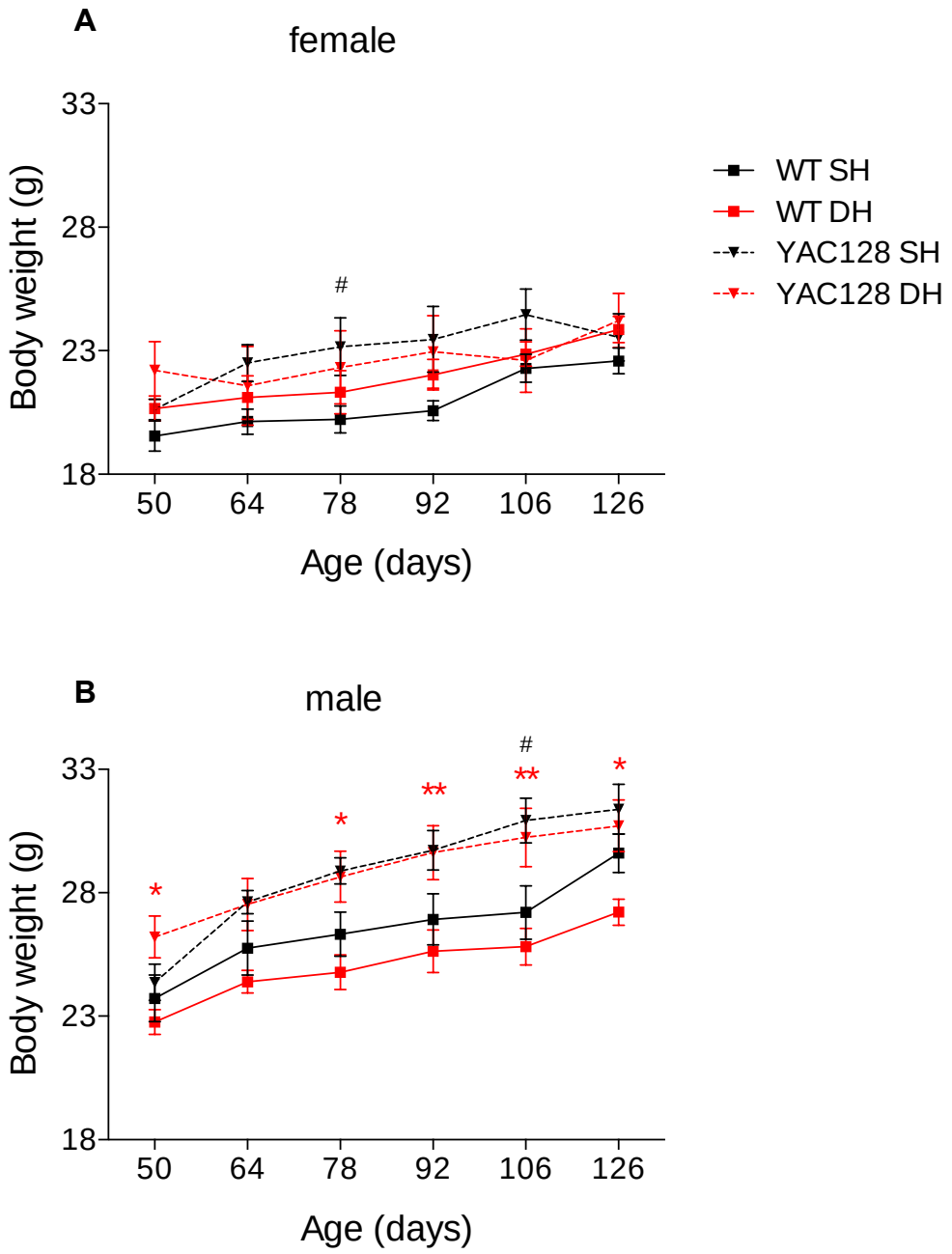

Figure 4.16 Body weight over time for female and male YAC128 and WT mice housed under standard and deprived conditions

(A) WT SH females had generally lower mean body weights compared to all other groups, while YAC128 SH females showed the opposite at most time-points.
(B) WT DH males had overall lower mean body weights compared to all other groups, whereas YAC128 groups were comparable.

Animals were weighed fortnightly starting from pn50 (~7 weeks) until sacrificed at pn126 (18 weeks). Body weight shown in grams (g). n = 5-8 animals of each sex per condition; Error bars represent ±SEM. Two-way ANOVA, with Tukey correction. *p < 0.05; **p<0.01. Comparison symbols: * WT DH vs YAC128 DH; #WT SH vs YAC128 SH.

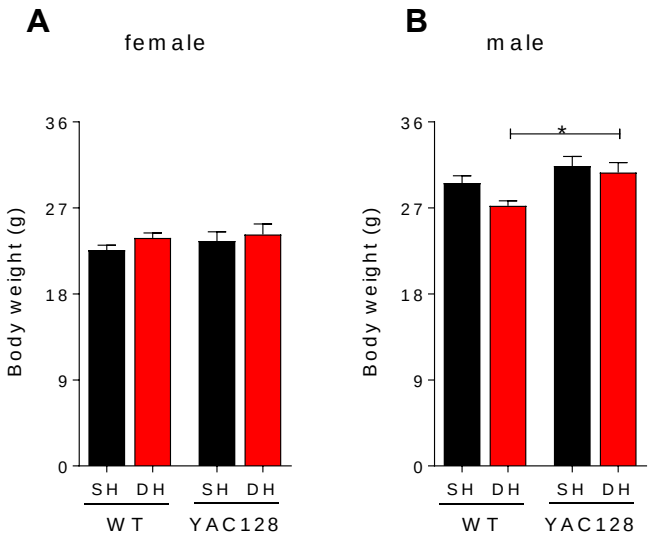

Figure 4.17 Final body weight of female and male YAC128 and WT mice housed under standard and deprived housing

(A) No significant differences were observed in female body weights between conditions when weighed at the final time point.
(B) No significant differences were seen in male body weights at the final time point.

Average body weight on sacrifice day, pn126 (18 weeks). Body weight shown in grams (g). n = 5-8 animals of each sex per condition; bar graphs represent mean±SEM. Two-way ANOVA, with Sidak's multiple comparisons test.

4.5. Discussion

Social isolation effects on behavioural performance and motor function

Social isolation was not found to affect locomotor activity of either WT or YAC128 mice, consistent with previous work examining social isolation in juvenile and adult mice (Makinodan et al., 2012; Liu et al., 2012). Furthermore, and similarly to environmental enrichment, no clear effect of social isolation was observed on anxiety-like behaviour. This is at variance with other reports of increased anxiety-like behaviour in socially isolated adolescent and adult mice (Cao et al., 2017; Lander, Linder-Shacham, & Gaisler-Salomon, 2017), and may be due to differing technical approaches to induce social isolation. The climbing performance of socially isolated animals of both genotypes was poor relative to their standard-house counterparts,

although this was not found to be significant. Socially isolated YAC128 mice were associated with the weakest rotarod performance during training and testing across groups, and deprived WT animals were slightly more predisposed to falls during the initial stages of rotarod training. These observations indicate that environmental deprivation and social isolation had a mild negative influence on motor learning and function in both WT and YAC128 mice. While our results provide support for the notion that environmental deprivation likely confers negative effects on, at least some, behaviours in WT rodents, it is challenging to contextualise this with respect to HD models, since the associated research is limited.

Social isolation effects on myelination and mature oligodendrocytes

Socially isolated WT mice were associated with significantly thinner myelin sheaths in the posterior corpus callosum (CC) relative to all other groups, and this effect persisted across all axonal diameters when compared to standard-housed WT mice. Additionally, environmental deprivation was associated with an increase in axonal diameter in WT animals, but a decrease in YAC128 mice. This finding is in keeping with an early study demonstrating white matter abnormalities in the posterior CC of socially isolated male rhesus monkeys (Sánchez et al., 1998). It is also consistent with other reports of thinner myelin sheaths in the medial prefrontal cortex of juvenile (Cao et al., 2017; Liu et al., 2012; Makinodan et al. 2012), and adult mice subjected to social isolation (Liu et al., 2012), and which was lessened with shorter periods of isolation. Axonal diameters of WT deprived mice were, on average, significantly larger than standard housed WT mice. In contrast, social isolation was not seen to have an effect on axonal diameter in the medial prefrontal cortex (mPFC) of juvenile mice (Makinodan et al., 2012), suggesting that the effect of isolation on myelination may be brain region and/or age dependent. Interestingly, no differences in myelin sheath thickness were observed between socially isolated and standard housed YAC128 mice, which suggest a dominant effect of this disease phenotype. Finally, we found no significant differences in mature oligodendrocyte population in both genotypes as a result of social isolation, in keeping with

other work reporting the same in the mPC of juvenile mice (Makinodan et al., 2012).

Social isolation effects on brain and body weight

Brain weights across animals were comparable across genotypes and housing condition, as observed during environmental enrichment. Furthermore, while social isolation did not significantly affect body weight across experimental groups, socially isolated female mice were associated with a mild increase in body weight relative to their standard house counterparts, with males exhibiting the reverse trend. These observations are supported by other studies showing socially isolated female rats to weigh approximately 10% more than standard-housed females (Hermes et al., 2011), and socially isolated male mice to have a decreased body weight relative to their standard controls (Lander et al., 2017). However, these trends were not observed in YAC128 mice, which is suggestive of an over-riding effect of the disease phenotype.

Chapter 5. The effects of microbiota manipulation on myelination and oligodendroglial population in the BACHD model of Huntington disease and wild-type control

5.1. Summary

Structural and molecular myelination deficits occur in the early stages of Huntington disease (HD). Recent evidence from germ-free (GF) and antibiotic-treated animal models has suggested that gut microbiota influences brain development and function. Specifically, microbiota-gut-brain bidirectional communication has been shown to be involved in the regulation of oligodendrocyte differentiation and myelination. However, little is known about the effect of microbiota on white matter in HD. In this study, therefore, we aimed to investigate the impact of microbiota on myelination plasticity and oligodendroglial populations in the early manifest stage of the BACHD mouse model of HD. Three months old specific-pathogen-free (SPF) and GF male mice of mixed genotype of each genotype (wild type and BACHD) were used here. Ultrastructural analysis of myelin in the anterior mid-body region of the corpus callosum indicated contrasting alterations in myelin thickness at different axonal diameters in the WT GF group compared to SPF control, whereas alterations of myelin thickness particularly at small and mid-range axonal diameter were evident in the BACHD GF group. In addition, WT animals placed in a germ-free environment exhibited reduction of premyelinating and myelinating, cortical and callosal, oligodendrocytes, and decreased levels of mature myelin related proteins in the prefrontal cortex. Further reductions were observed in cortical myelinating oligodendrocytes and callosal oligodendrocytes precursor cells (OPCs) in the BACHD GF animals compared to their SPF control. Finally, in a germ-free environment, the characteristic body weight gain of BACHD animals is normalised to the body weight of WT animals, whereas both genotypes showed decreased overall brain weight. Therefore, our results indicate complex effects of microbiota on myelin-related characteristics, revealing, further, the adaptive properties of myelination in both the BACHD and wild-type animal.

5.2. Introduction

White matter (WM) atrophy has been widely identified as an early feature of Huntington disease (HD) in both patients and animal models (Bartzokis et al., 2007; Ciarmiello et al., 2006; Fennema-Notestine et al., 2004; Novak et al., 2014; Rosas et al., 2003; Tabrizi et al., 2009; Xiang et al., 2011). Previous work in our laboratory explored the molecular and ultrastructural features of WM abnormalities in HD mouse and rat models (Garcia-Miralles et al., 2016; Teo et al., 2016). Diffusion tensor imaging (DTI) imaging revealed WM microstructural abnormalities prior to neuronal loss in the CC of the YAC128 mouse model and the BACHD rat model (Teo et al., 2016). In addition, thinner myelin sheath and lower levels of myelin-related gene transcripts were seen in these animals compared to wild-type controls (Teo et al., 2016). Others also reported microstructural abnormalities and reduction in myelin sheath thickness, as well as decreased expression of myelin related genes in the BACHD, HdhQ250 and R6/2 mouse models (Gatto et al., 2015; Jin et al., 2015; Wade, Jacobs, & Morton, 2008; Xiang et al., 2011). In addition, transgenic mice that expressed mHTT selectively in oligodendrocytes showed impaired myelination with thinner myelin thickness in the striatum, reduction of myelin basic protein gene expression, along with progressive motor impairments, metabolic deficits and reduced survival (Huang et al., 2015).

Emerging evidence suggests the microbiota-gut-brain axis to be involved in modulation of adaptive myelination, and myelin-related characteristics, in the rodent brain. An upregulation of genes linked to myelination and myelin plasticity was described in the wild-type GF mouse (Hoban et al., 2016b). Increased mRNA levels of myelin related genes and transcript factors were identified, specifically in the prefrontal cortex (PFC), of wild-type animals (Hoban et al., 2016b), as well as in antibiotic treated non-obese diabetic mice (Gacias et al., 2016). These transcriptional changes were consistent with hypermyelination of PFC axons in GF animals, compared to animals raised in conventional laboratory conditions (Hoban et al., 2016b).

The PFC and the CC are highly enriched in myelinated fibres, and both regions were shown to be affected by environmental manipulation and behavioural experience (Hoban et al., 2016b; Liu et al., 2012; Makinodan et al., 2012; Sánchez et al., 1998; Tomlinson, Leiton, & Colognato, 2016a). On the other hand, the PFC and CC are two of the most affected regions by disease pathology in HD patients and animal models (Gatto et al., 2015), and several studies reported white matter alterations in the PFC and CC of pre-symptomatic and symptomatic HD gene carriers (Bourbon-Teles et al., 2017; Di Paola et al., 2012; Dumas et al., 2011; Matsui et al., 2013; Phillips et al., 2014; Poudel et al., 2015; Rosas et al., 2006; Tomassy et al., 2014).

The findings described above indicate the need for further investigation into possible modulating environmental factors of plastic and adaptive myelination in HD, particularly with respect to white matter-related abnormalities. Therefore, the purpose of our study was to use microbiome manipulation as an assay to understand myelination plasticity and oligodendroglial population changes in the BACHD mouse model and WT controls. Using transmission electron microcopy (TEM), we investigated ultrastructural characteristics of myelin in the anterior mid-body region of the CC. Cortical myelin-related proteins, such as MBP and PLP, were also compared between experimental groups, and oligodendroglial populations in the CC and PFC were examined at different stages of maturity in their development.

5.3. Methods

5.3.1. Experimental groups

Wild-type (WT) and BACHD transgenic mice on the FVB background were raised either under normal laboratory conditions (SPF) or in a germ-free environment (GF) (Figure 5.1). Every experimental group included between 10 to 13 animals per condition per sex.

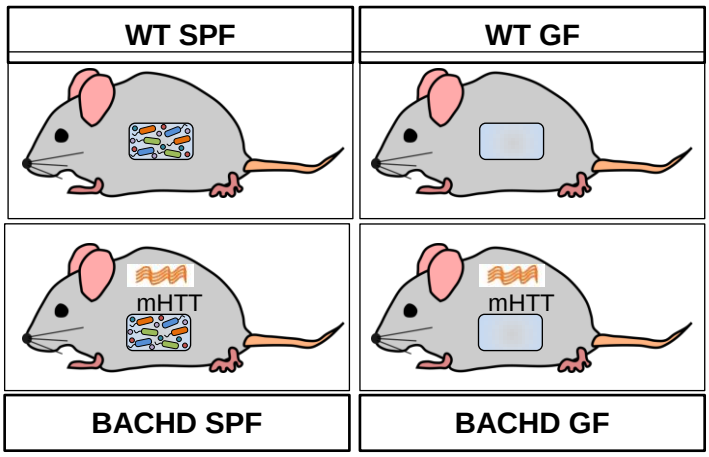

Figure 5.1 Experimental groups used for microbiota manipulation study

Four groups were used for these experiments: wild type (WT) groups – specific pathogen free (SPF) and germ free (GF), and BACHD groups – also SPF and GF.

GF animals were born through caesarean section in aseptic conditions, where all incoming air, water and food were sterilised. These animals were, therefore, free of all 'detectable' microbes and microorganisms. GF pups were housed in gnotobiotic isolators with the same strain GF adoptive mothers. SPFs were conventional laboratory animals, whose strains of bacteria were allowed to acquire microbiota naturally, and were known to this specific animal unit.

Animals were genotyped at 3 weeks of age. All animals were weighed at 3 months of age, prior to being sacrificed. Brains were harvested from both males and females, however, due to time and cost constraints, only males brains were included for investigation in the current study.

5.3.2. Tissue processing

All brains were segmented through the mid-sagittal plane, and the left hemisphere placed in 4% PFA solution to be used for immunohistochemical procedures (Section 2.5). Sections were immunostained for the oligodendroglia precursor marker, platelet derived growth factor receptor alpha (PDGFR), the oligodendroglial lineage marker, Olig2, and the mature oligodendrocyte marker, Glutathione S-transferase (GST)-pi (Table 2.9).

Stereo Investigator software was used for PFC, CC and striatum cell counting and area estimation (Section 2.5.5).

The right hemisphere was microdissected, and protein extracted from PFC tissue and processed for western blot. The samples were probed for myelin basic protein (MBP), myelin proteolipid protein (PLP), and Ermin. The blots obtained were quantified using Image Studio Lite, and values obtained were normalised in Excel (Chapter 2. Materials and methods. Section 2.6). Concentration of protein of interest (i.e. MBP) was first normalised to control (i.e. Calnexin), and then expressed relative to its experimental control condition. The SPF group was taken as the control condition for all comparisons between GF and SPF and described in the results section below. Each blot included comparisons between two of the four experimental conditions, and contained 8 samples (one per animal) in total (Figure 5.11A, Figure 5.12A). Box and whiskers plots represent quantification of samples from 4 animals per condition (Figure 5.11 and Figure 5.12).

In addition to the brains harvested for immunostaining and immunoblotting, three to four animals in each experimental condition were perfused and harvested, to investigate axonal and myelin related characteristics (i.e. axonal shape and size, and myelin thickness) using TEM. For this study, anterior mid-body of the CC (~Bregma -0.80 to 0 mm, according to the Mouse Brain Atlas, Paxinos and Franklin, 2001; Figure 2.3) was microdissected (Figure 5.2A) to be processed and imaged for TEM (Chapter 2. Materials and methods. Section 2.4).

Prior to cryosectioning for IHC procedures, the left hemisphere, of both males and females, was weighed. The brains were weighed again following removal of the olfactory bulb (OB) and cerebellum. For the purpose of simplicity, the remaining brain is henceforth referred to in the text as ‘forebrain’ (Figure 5.13D-F). Brain weights were recorded and compared between the experimental groups (Figure 5.13).

5.3.3. Statistical analysis

Pairwise comparisons were generated using Student's two-tailed t tests. Two-way ANOVA with Sidak's correction for multiple comparisons was used for the 2x2 study design (genotype x microbiota presence) to observe whether differences between the groups were statistically significant, as appropriate. P-values equal to or greater than 0.05 were considered not statistically significant. P-values and n-values were indicated in the associated figure legends for each figure, while mean values were stated in the results section. Bar graphs were built based on mean ± SEM unless otherwise stated.

5.4. Results

5.4.1. Ultrastructural analysis of myelin

Representative micrographs of callosal axons for each experimental group are illustrated below, in Figure 5.2. G-ratio values were plotted against inner diameter, for each axon, using scatter plots to exhibit variability of myelin thickness at different ranges of axonal diameters. Comparison of WT groups showed similar g-ratios over all diameter ranges for SPF and GF animals (Figure 5.3A). In addition, the cumulative g-ratio frequency plot of both WT groups showed a close overlap (Figure 5.3B). In contrast, small axons (ID < 500 nm) displaying lower g-ratios, and large axons (ID > 1000nm) displaying higher g-ratios, were observed in BACHD GF animals compared to BACHD SPF animals (Figure 5.3C). Cumulative frequency analysis of g-ratios showed an evident shift towards smaller values for BACHD GF compared to BACHD SPF (Figure 5.3D).

G-ratio values were subsequently classified, averaged and compared according to three inner diameter ranges: small diameter axons (ID < 500nm), mid-range diameter axons (500 ≤ ID < 1000nm), and large diameter axons (ID ≥ 1000nm) (Figure 5.4B). For small diameter ranges two-way ANOVA revealed significant interaction between genotype and microbiota

presence ($F (1, 1869) = 105.1$, $p < 0.0001$), significant main effect of microbiota presence ($F (1, 1869) = 6.96$, $p < 0.01$), as well as of genotype ($F (1, 1869) = 62.15$, $p < 0.0001$). For mid-range diameter axons, two-way ANOVA revealed significant interaction between genotype and microbiota presence ($F (1, 2601) = 17.56$, $p < 0.0001$), significant main effect of microbiota presence ($F (1, 2601) = 13.36$, $p < 0.001$), as well as of genotype ($F (1, 2601) = 45.22$, $p < 0.0001$). Whereas, for large diameter axons, two-way ANOVA revealed no significant interaction between genotype and microbiota presence ($F (1, 402) = 0.77$, $p > 0.05$), significant main effect of microbiota presence ($F (1, 402) = 14.52$, $p < 0.001$), as well as of genotype ($F (1, 402) = 45.22$, $p < 0.01$). Sidak's correction for multiple comparisons post-hoc tests revealed at small diameter ranges WT GF (0.805±0.002) animals showed higher mean g-ratio, suggestive of thinner myelin, compared to WT SPF (0.782±0.002; $p < 0.001$), whereas at mid-range diameter no significant differences were seen ($p > 0.05$). On the other hand, when comparing between the BACHD groups, the same difference persisted at both small (BACHD GF: 0.752±0.003; BACHD SPF: 0.789±0.002) and mid-range diameters (BACHD GF: 0.824±0.002; BACHD SPF: 0.841±0.001), with a smaller mean g-ratio, suggestive of thicker myelin sheath, observed in BACHD GF animals compared to BACHD SPF ($p < 0.001$), which diminished at large diameter values, although the same trend was still observed ($p > 0.05$). Additional differences in mean g-ratio were seen between WT GF and BACHD GF animal at both small (WT GF: 0.805±0.002; BACHD GF: 0.752±0.003) and mid-range (WT GF: 0.847±0.002; BACHD GF: 0.825±0.002) axonal diameters, with a smaller mean g-ratio values for BACHD GF ($p < 0.001$). At large diameter ranges, no significant interaction between genotype and microbiota presence was observed, however, WT GF animals (0.875±0.005) showed a trend towards smaller mean g-ratio, suggestive of thicker myelin, compared to WT SPF (0.895±0.002), whereas BACHD SPF animals (0.878±0.003) showed a trend towards reduced g-ratio compared to WT SPF (0.895±0.002) ($p < 0.001$).

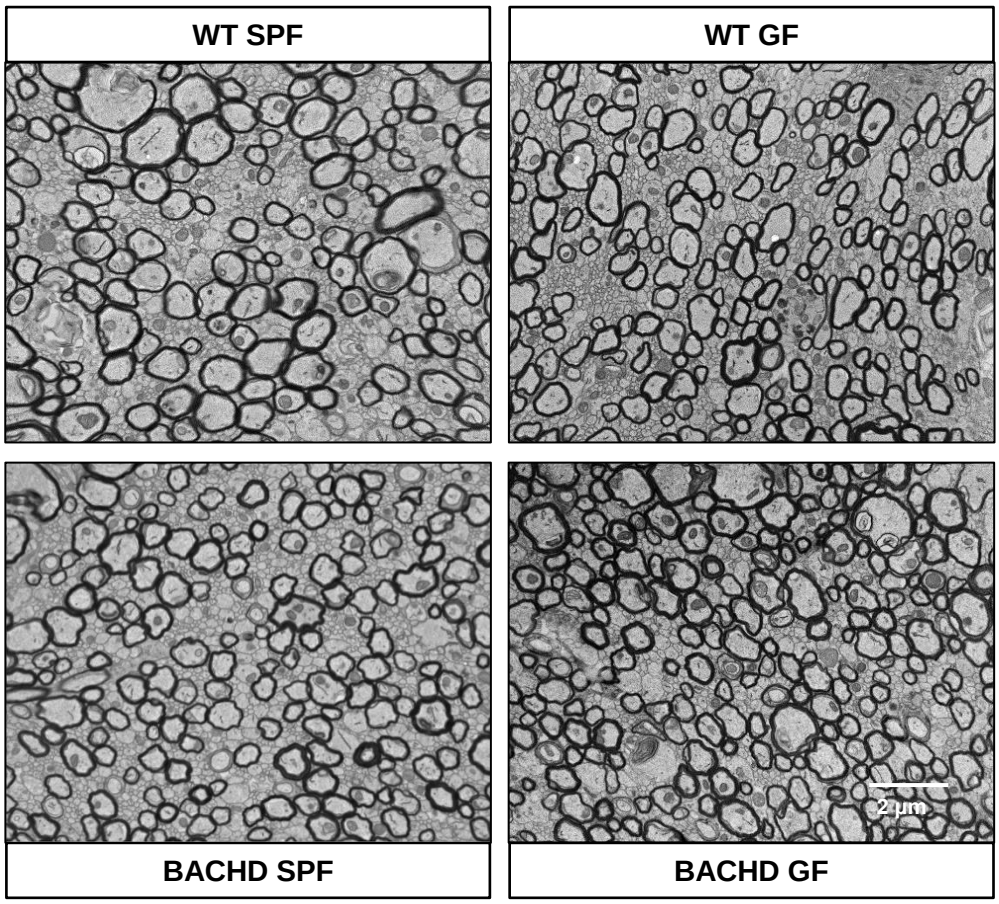

Figure 5.2 Representative TEM images of callosal axons in BACHD and WT mice housed under SPF and GF conditions

Representative micrographs of axons from the anterior mid-body region of the CC for each experimental group. Scale bar at 2µm.

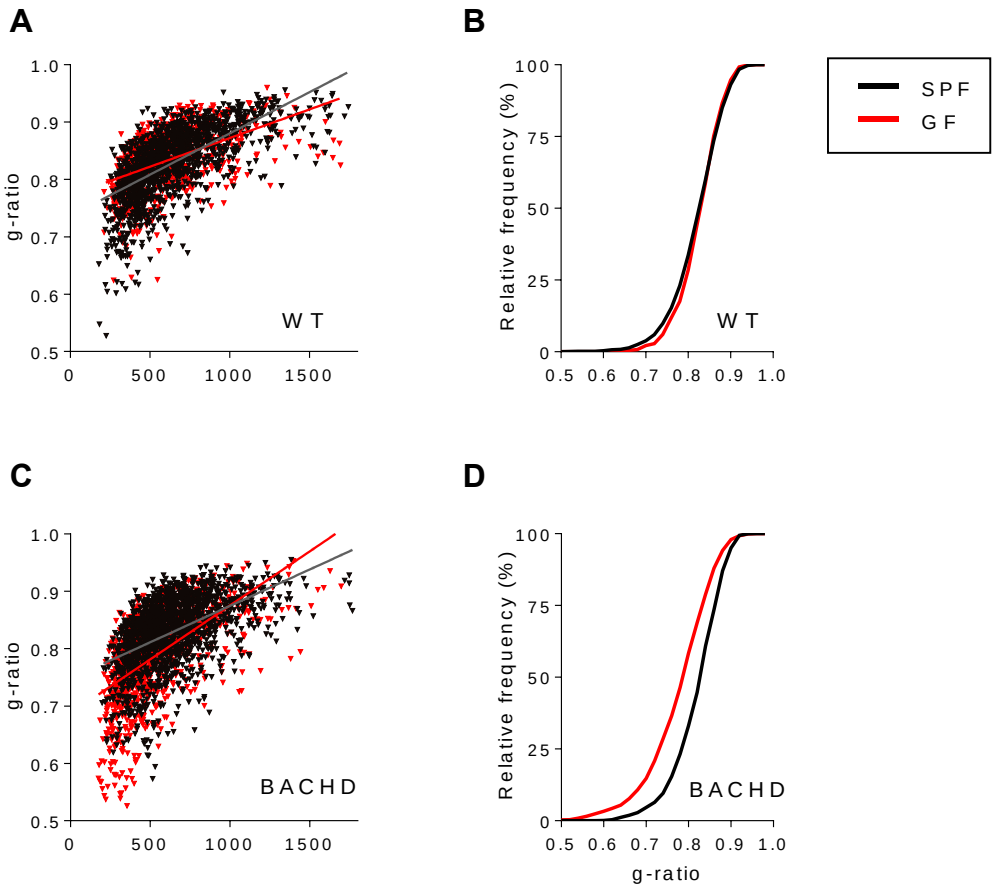

Figure 5.3 Axonal g-ratios in BACHD and WT mice housed under SPF and GF conditions

(A) Scatter plot of g-ratio values against inner axonal diameter showed similar g-ratios at all diameter ranges for WT SPF and GF.
(B) Cumulative frequency plot of g-ratios showed a close overlap of the two curves representative of the WT groups.
(C) Scatter plot indicating lower g-ratio values at small axonal diameters (ID < 500 nm), and higher values for large axonal diameters (ID > 1000nm), in BACHD GF animals (red) compared to BACHD SPF (black).
(D) Cumulative frequency analysis of g-ratios showed a robust shift towards smaller g-rations in the case BACHD GF (red) relative to BACHD SPF (black).

n = 775 - 1440 axons per condition (WT SPF, n = 1440 axons; WT GF, n = 775; BACHD SPF, n = 1133; BACHD GF, n = 1028); 3-4 animals per condition.

When averaged over all axons, two-way ANOVA revealed significant interaction between genotype and microbiota presence ($F(1, 4374) = 121.7$, $p < 0.0001$), significant main effect of microbiota presence ($F(1, 4374) = 72.3$, $p < 0.0001$), as well as of genotype ($F(1, 4374) = 175.8$, $p < 0.0001$). Sidak's correction for multiple comparisons post-hoc tests revealed WT

groups presented with a similar g-ratio ($p > 0.05$), while the mean g-ratio in BACHD GF animals (0.786±0.002) was significantly reduced compared to both WT GF (0.834±0.001; $p < 0.0001$), as well as, when compared to BACHD SPF (0.824±0.001; $p \leq 0.0001$; Figure 5.4A).

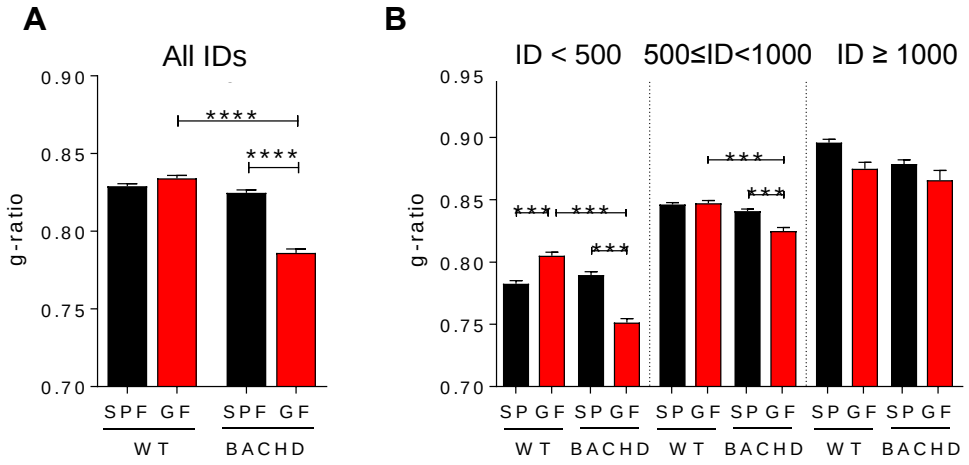

Figure 5.4 Mean g-ratio across all axons and different axonal diameters in BACHD and WT animals housed under SPF and GF conditions

(A) BACHD GF animals were associated with a significantly smaller mean g-ratio compared to both WT GF, and to BACHD SPF. WT groups had similar mean g-ratios ($p>0.05$).
(B) G-ratios were classified according to inner axonal diameter (small diameter axons, ID<500nm; mid-range diameter axons, 500≤ID<1000nm; large diameter axons, ID≥1000nm).

Bar graphs represent mean±SEM. Error bars represent SEM from axonal variance. n = 775 - 1440 axons per condition (WT SPF, n = 1440 axons; WT GF, n = 775; BACHD SPF, n = 1133; BACHD GF, n = 1028); 3-4 animals per condition. Two-way ANOVA, with Sidak's correction for multiple comparisons. ***$p < 0.001$; ****$p < 0.0001$. Inner diameter shown in nanometres (nm). Abbreviations: ID, inner diameter.

5.4.2. Differences in axonal characteristics

Axons in the anterior mid-body region of the CC for each animal were examined using TEM (Figure 5.2B). Regular and irregular myelinated axons were visually categorised based on their shape. Circular or elliptical myelinated axons were classified as 'regular shaped axons', whereas those that deviated from this were classified as 'irregular shaped axons' (Figure

2.5B). On the other hand, unmyelinated axons were not classified based on shape, and are simply referred to as ‘unmyelinated axons’.

The total number of myelinated axons was similar across conditions (WT SPF: 86.38±3.12; WT GF: 82.26±3.02; BACHD SPF: 81.86±4.84; BACHD GF: 88.38±1.78; Figure 5.5A). Two-way ANOVA revealed no significant interaction between genotype and microbiota presence ($F(1, 129) = 2.62$, $p > 0.05$), no main effect of microbiota presence ($F(1, 129) = 0.13$, $p > 0.05$), and no main effect of genotype ($F(1, 129) = 0.05$, $p > 0.05$). However, further investigation revealed differences in axonal shapes between groups. When comparing the number of regular myelinated axons two-way ANOVA showed significant interaction between genotype and microbiota presence ($F(1, 129) = 14.84$, $p < 0.001$), significant main effect of microbiota presence ($F(1, 129) = 6.04$, $p < 0.05$), but no main effect of genotype ($F(1, 129) = 0.76$, $p > 0.05$). Sidak’s correction for multiple comparisons post-hoc test revealed the number of regular myelinated axons was reduced in the BACHD SPF (32.62±2.71) compared to WT SPF (44.18±2.49; $p < 0.01$). However, no significant differences were observed between GF groups, although BACHD GF animals were associated with a marginally higher number of axons (48.06±1.82) than WT GF controls (40.77±2.62; $p > 0.05$). No main effect of genotype was found however, BACHD GF showed a trend towards a higher number of regular myelinated axons compared to BACHD SPF (Figure 5.5B). When comparing irregular myelinated axons, two-way ANOVA showed significant interaction between genotype and microbiota presence ($F(1, 128) = 4.66$, $p < 0.05$), significant main effect of microbiota presence ($F(1, 128) = 6.27$, $p < 0.05$), but no main effect of genotype ($F(1, 128) = 1.36$, $p > 0.05$). Sidak’s correction for multiple comparisons post-hoc test revealed that WT groups showed similar numbers (SPF, 42.21±1.77; GF 41.48±1.62). In contrast, the BACHD SPF group (49.24±3.45) was associated with higher numbers of irregular myelinated axons compared to all the other groups, but this difference was only significant when compared to BACHD GF (39.39±1.33; $p < 0.01$; Figure 5.5C). Interestingly, unmyelinated axon number was comparable across all groups (Figure 5.5D).

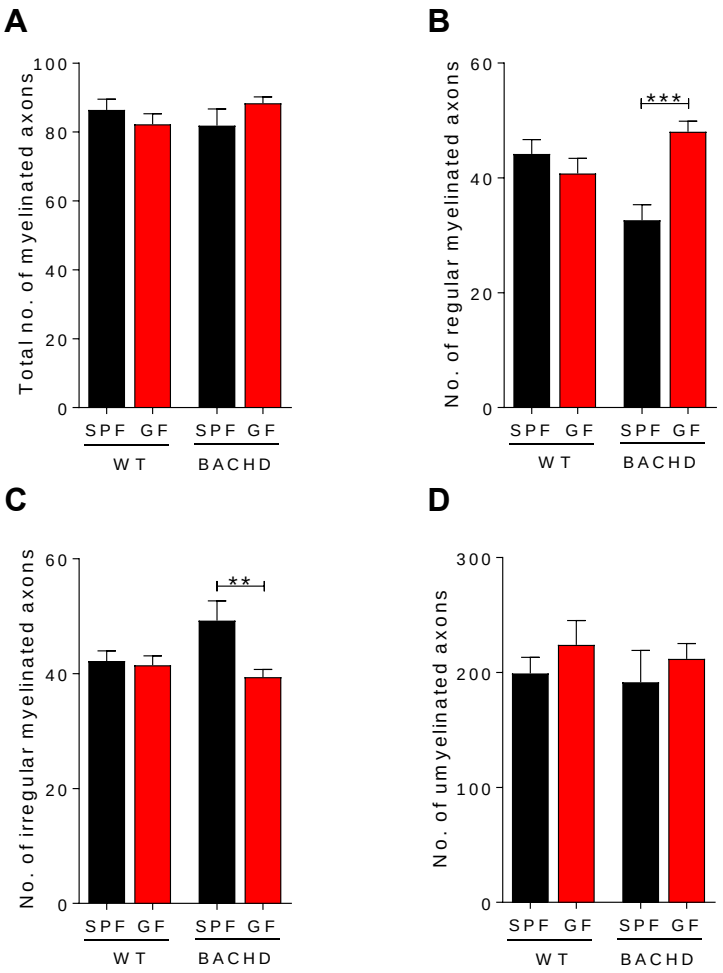

Figure 5.5 Average number of unmyelinated and myelinated axons per selected area in BACHD and WT mice under SPF and GF conditions

(A) Total number of myelinated axons was similar across all groups.
(B) Number of regular myelinated axons in the BACHD SPF was smaller compared to WT SPF, whereas the BACHD GF group was associated with a larger number relative to BACHD SPF.
(C) Number of irregular myelinated axons was comparable between WT groups. The BACHD SPF group possessed a greater number compared to all the other groups, but was only significant in comparison to BACHD GF.
(D) Unmyelinated axon number was similar between all the groups, although GF animals were associated with a larger number compared to SPF counterparts, regardless of genotype.

Selected area for axonal counting was equivalent to 7.35×10^7 nm^2. Bar graphs represent the average of a total of 6-12 images per animal, from 3-4 animals per condition; n = 21-39 images per condition; Bar graphs represent mean±SEM. Error bars represent. Two-way ANOVA, with Sidak's correction for multiple comparisons. *$p < 0.05$; **$p < 0.01$; ***$p < 0.001$.

Inner axonal diameter was measured for regular shaped axons using ImageJ software (line tool). Relative frequency, cumulative frequency, and bar graphs, were plotted to illustrate the differences between inner axonal diameters in the four groups. When comparing between WT groups, relative frequency distribution showed similar number of axons at all diameter ranges (Figure 5.6A). Cumulative frequency plot of inner diameters showed a close overlap of the two curves representative of the WT groups (Figure 5.6B). In addition, no significant difference was found between WT groups when averaging over all inner axonal diameters ($p > 0.05$; Figure 5.6C). The BACHD comparisons, however, showed differences in the relative frequency distribution graph. Higher number of axons with small diameter (200 to 400nm), and smaller number of axons with large diameter (700 to 1000nm), was observed in the BACHD GF animals compared to its SPF control (Figure 5.7A). Cumulative frequency plot of inner diameters showed an evident shift towards smaller diameters in BACHD GF compared to BACHD SPF (Figure 5.7B). Additionally, when all diameter ranges were pooled and averaged for each group, BACHD GF animals were associated with a smaller mean axonal diameter (525.1nm±7.33) compared to both BACHD SPF (647.7nm±7.11; $p < 0.0001$; Figure 5.7C), and WT GF (619nm±8.9; $p < 0.0001$; data not shown).

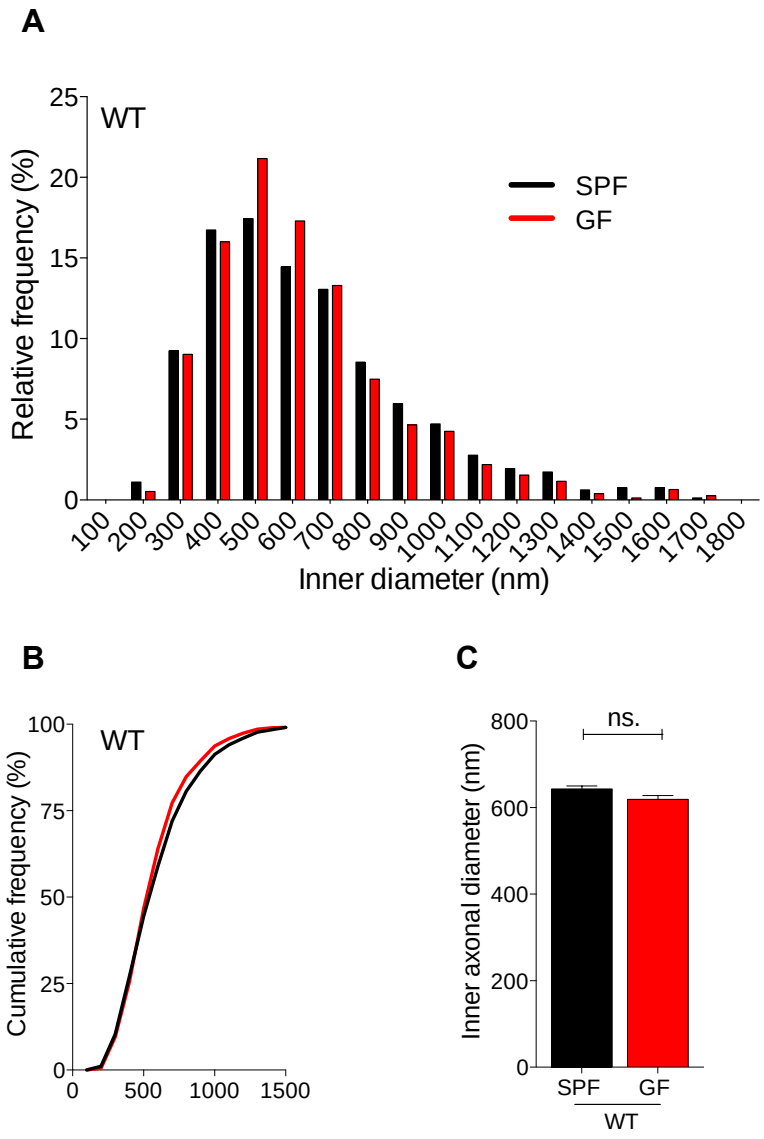

Figure 5.6 Inner axonal diameter in SPF and GF WT animals

(A) Distribution of inner axonal diameters was similar in WT SPF and GF animals.
(B) Cumulative frequency plot of inner diameters showed a close overlap of the two curves representative of the WT groups.
(C) No significant difference in mean axonal diameter between WT SPF and WT GF groups ($p>0.05$).

Inner diameter shown in nanometres (nm). n = 775 - 1440 axons per condition (WT SPF, n = 1440 axons, WT GF, n = 775); 3-4 animals per condition. Relative frequency histogram (A) and cumulative frequency (B), bin width = 100 (A). Unpaired two-tailed t-test, 95% confidence intervals; Bar graphs represent mean±SEM (C). Abbreviations: ID, inner diameter.

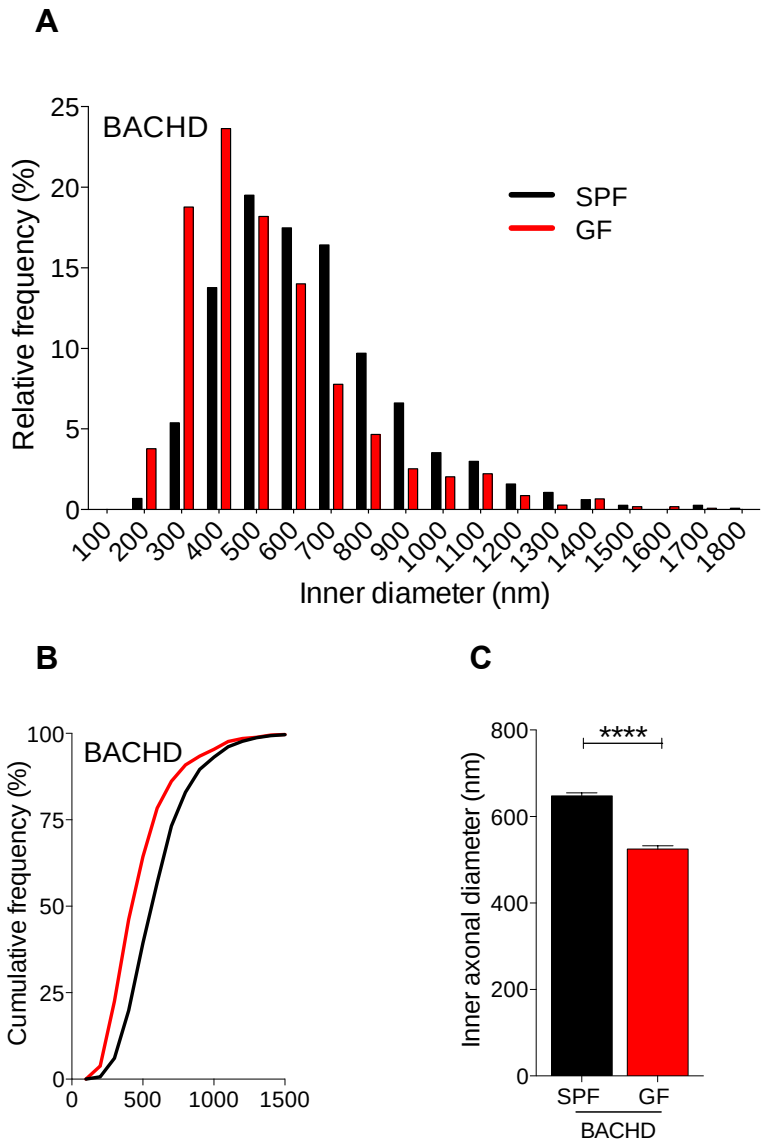

Figure 5.7 Inner axonal diameter in SPF and GF BACHD animals

(A) Greater number of axons with a small diameter (200 to 400nm), and a smaller number of axons with a large diameter (700 to 1000nm), in BACHD GF animals compared to BACHD SPF.
(B) Cumulative frequency analysis of IDs showed a robust shift towards smaller diameters in BACHD GF (red) animals compared to BACHD SPF (black).
(C) BACHD GF animals possessed a significantly smaller mean axonal diameter compared to BACHD SPF.

Inner diameter shown in nanometres (nm). n = 1028 - 1133 axons per condition (BACHD SPF, n = 1133; BACHD GF, n = 1028); 3-4 animals per condition. Relative frequency histogram (A) and cumulative frequency plot (B), bin width = 100 (A). Unpaired, two-tailed t-test, 95% confidence intervals, ****p < 0.0001; bar graphs represent mean±SEM (C). Abbreviations: ID, inner diameter.

5.4.3. Oligodendroglial cell differences in the prefrontal cortex and corpus callosum

No significant differences were observed as a result of microbiota manipulation in the number of cortical oligodendrocytes precursor cells (OPCs), as labeled by the platelet-derived growth factor receptor α (PDGFRα). When comparing groups in the corpus callosum region, two-way ANOVA showed no significant interaction between genotype and microbiota presence ($F(1, 40) = 1.79$, $p > 0.05$), significant main effect of microbiota presence ($F(1, 40) = 4.15$, $p < 0.05$), but no main effect of genotype ($F(1, 40) = 0.47$, $p > 0.05$). Additionally, when comparing groups in the PFC region, two-way ANOVA showed no significant interaction between genotype and microbiota presence ($F(1, 40) = 0.33$, $p > 0.05$), no significant main effect of microbiota presence ($F(1, 40) = 1.62$, $p > 0.05$), and no main effect of genotype ($F(1, 40) = 0.36$, $p > 0.05$). A non-significant trend towards increased number of cells was seen in the PFC of WT GF (1,647±248) compared to the other experimental groups (WT SPF: 1,283±194; BACHD GF: 1,414±177; $p > 0.05$; Figure 5.8C). In contrast, BACHD SPF (1,133±113) showed a non-significant increased number of OPCs in the CC compared to the other groups, which was normalised to wild-type levels in the BACHD animals held in GF conditions (BACHD GF: 818±64; WT SPF: 941±110; Figure 5.8D).

The number of oligodendrocytes, as labeled by the oligodendroglial lineage marker, Olig2, in the PFC and CC region showed no significant differences between the groups. When comparing groups in the corpus callosum region, two-way ANOVA showed significant interaction between genotype and microbiota presence ($F(1, 41) = 10.67$, $p < 0.01$), no significant main effect of microbiota presence ($F(1, 41) = 0.84$, $p > 0.05$), and no main effect of genotype ($F(1, 41) = 0.58$, $p > 0.05$). Additionally, when comparing groups in the PFC region, two-way ANOVA also showed significant interaction between genotype and microbiota presence ($F(1, 42) = 4.31$, $p < 0.05$), but no significant main effect of microbiota presence ($F(1, 42) = 0.62$, $p > 0.05$), and no main effect of genotype ($F(1, 42) = 1.38$, $p > 0.05$). Olig2 population

showed a trend towards reduced population in WT GF animals compared to SPF controls (WT GF: 8,228±805.9, WT SPF: 8,228±805.9). In addition, WT GF also showed a decreased number of Olig2-positive cells compared to BACHD GF (13,575±2,283; Figure 5.9B). A similar non-statistically significant trend to that in the PFC was observed when comparing the Olig2 population in the CC of WT GF and SPF animals. The number of Olig2-positive cells was slightly decreased in WT GF compared to WT SPF controls (WT GF, 23,263±2,261; WT SPF, 38,460±4,630; Figure 5.9C). In addition, BACHD SPF (23,812±2,632) exhibited a reduced number of Olig2-positive cells compared to WT SPF. As in the PFC, BACHD GF and SPF animals showed a similar number of Olig2-positive cells in the CC.

When comparing GST-pi positive cells in the corpus callosum region, two-way ANOVA showed no significant interaction between genotype and microbiota presence ($F (1, 38) = 3.64$, $p > 0.05$), no significant main effect of microbiota presence ($F (1, 38) = 0.03$, $p > 0.05$), and no main effect of genotype ($F (1, 38) = 0.47$, $p > 0.05$). A trend for a decreased GST-pi positive cell population was seen in the WT GF compared to its SPF control (WT GF, 21,027±2,570, WT SPF, 31,360±5,445; Figure 5.10C). When comparing groups in the PFC region, two-way ANOVA also showed no significant interaction between genotype and microbiota presence ($F (1, 35) = 0.68$, $p > 0.05$), but a significant main effect of microbiota presence ($F (1, 35) = 24.46$, $p < 0.0001$), however no main effect of genotype ($F (1, 35) = 0.15$, $p > 0.05$). The GST-pi-positive population was decreased in the PFC of both GF groups compared to SPF controls (Figure 5.10B). Sidak's correction for multiple comparisons post-hoc tests for microbiota main effect revealed WT GF had significantly less GST-pi positive cells compared to WT SPF (WT GF, 3,318±412; WT SPF, 8574±1291; $p < 0.001$), while BACHD GF GST-pi-positive population was reduced relative to BACHD SPF (BACHD GF, 4,430±352; BACHD SPF, 8,180±720; $p < 0.05$). When comparing within the same genotype and between microbiota conditions, both the WT and BACHD groups were similar in terms of GST-pi cell numbers ($p > 0.05$; Figure 5.10B).

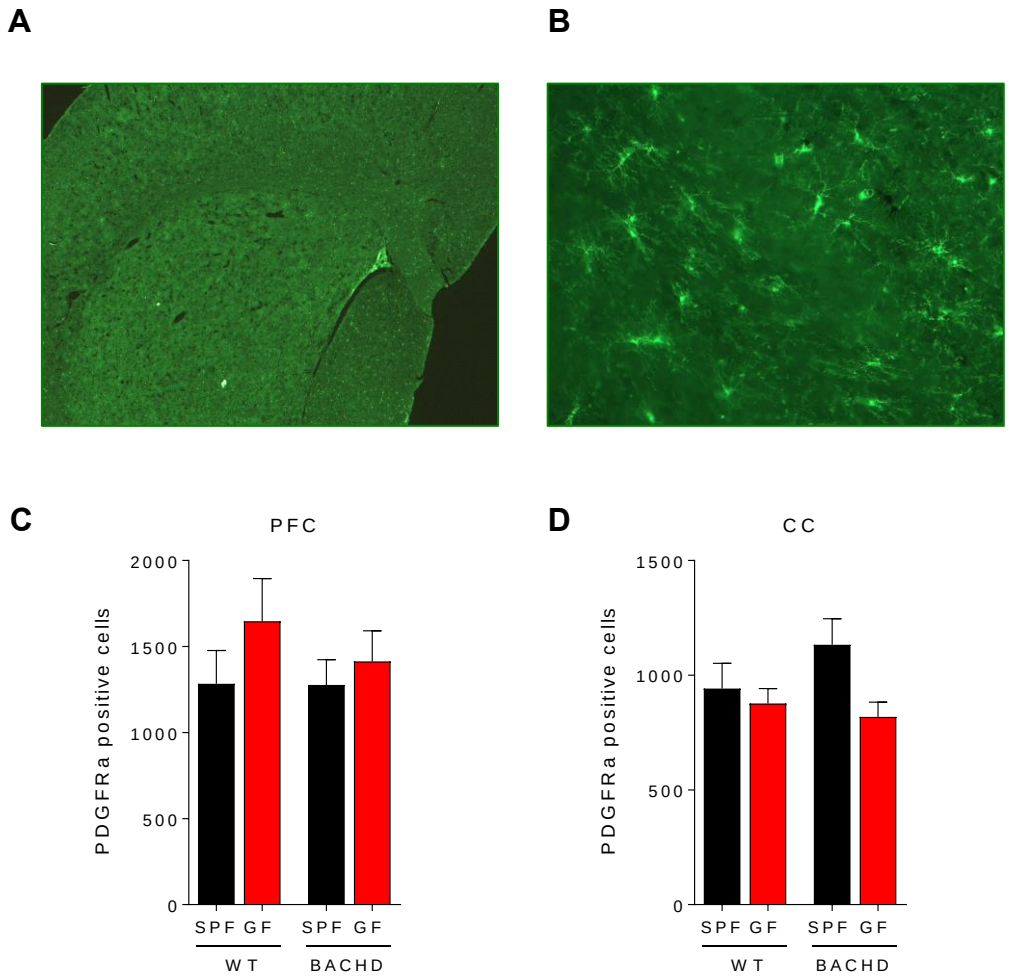

Figure 5.8 PDGFRα positive cell populations in the PFC and CC of BACHD and WT mice housed under SPF and GF conditions

(A) 2.5x magnification of representative image of coronal section labelled for PDGFRα.
(B) 20x magnification of representative image of coronal section of PFC and CC labelled for PDGFRα.
(C) Minor non-significant increase in number of PDGFRα positive cells in the PFC of WT GF group compared to the other groups.
(D) Number of PDGFRα positive cells was significantly decreased in the CC of BACHD GF compared to its SPF control.

Bar graphs represent the average of a total of 9-12 animals per condition, and 8-12 sections per animal; bar graphs represent mean±SEM. Two-way ANOVA. Abbreviations: CC, corpus callosum; PFC, prefrontal cortex. PDGFRα, platelet derived growth factor receptor alpha.

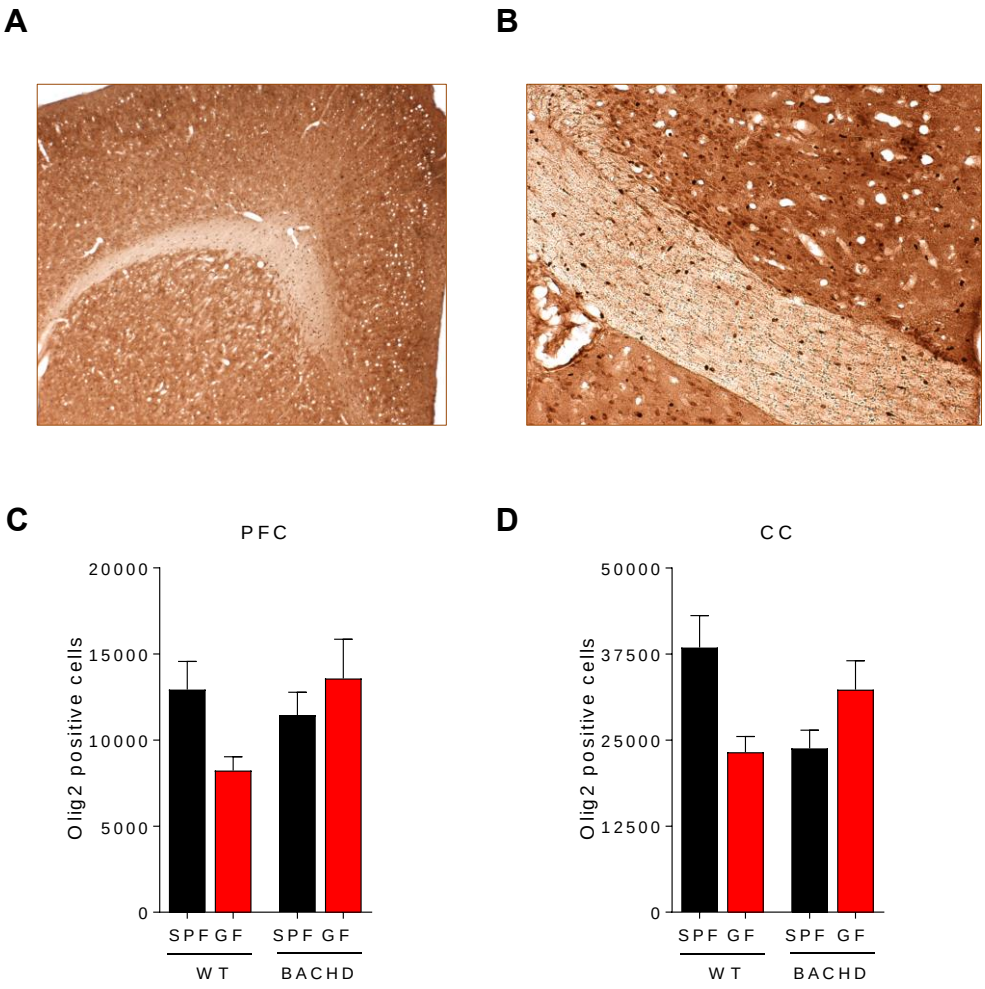

Figure 5.9 Olig2 positive cell populations in the PFC and CC of BACHD and WT mice housed under SPF and GF conditions

(A) 2.5x magnification of representative image of coronal section labelled for Olig2.
(B) 20x magnification of representative image of coronal section of PFC and CC labelled for Olig2.
(C) Decreased number of Olig2 positive cells in the PFC of WT GF group compared to the other groups.
(D) Number of Olig2 positive cells was also decreased in the CC of WT GF compared to its SPF control. BACHD SPF also showed smaller number of Olig2-positive cells compared to WT SPF.

Bar graphs represent the average of a total of 9-12 animals per condition, and 8-12 sections per animal; bar graphs represent mean±SEM. Two-way ANOVA. Abbreviations: CC, corpus callosum; PFC, prefrontal cortex.

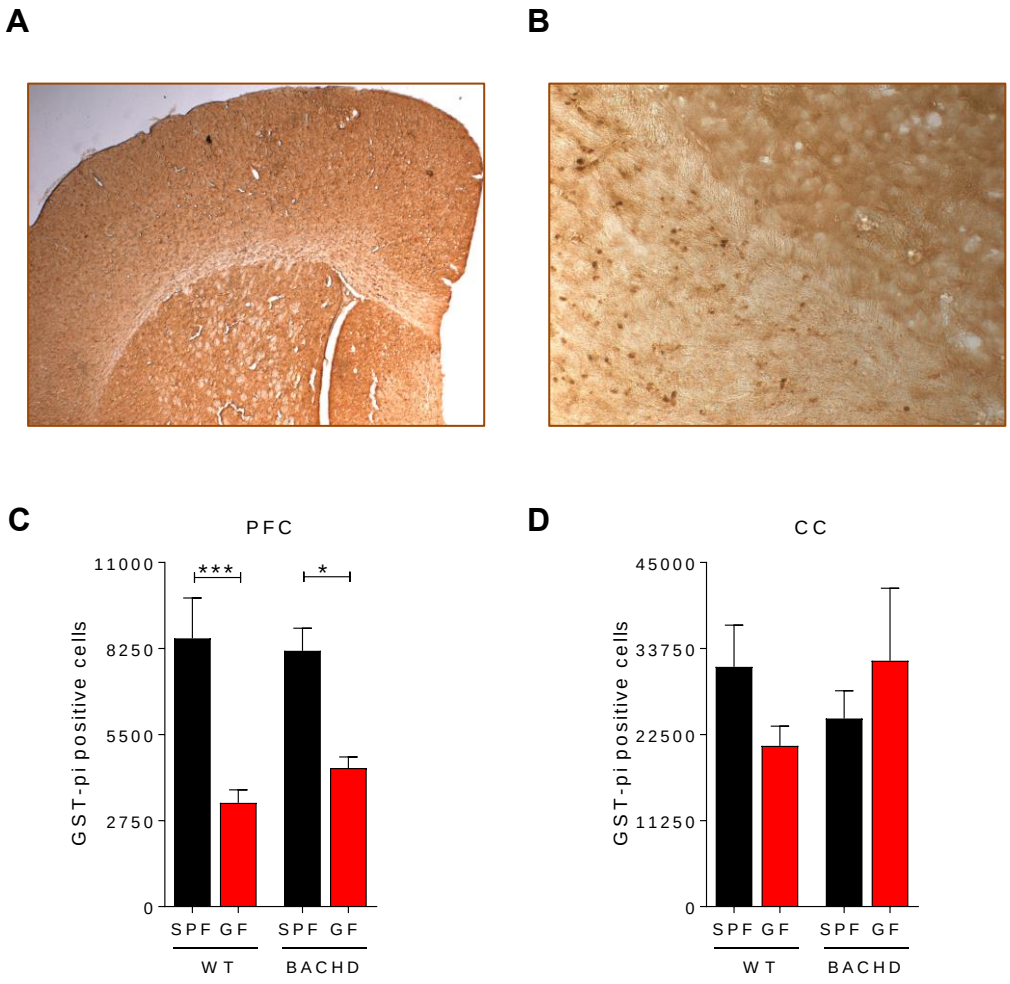

Figure 5.10 GST-pi positive cells in PFC and CC of BACHD and WT mice housed under SPF and GF conditions

(A) 2.5x magnification of image of coronal section labelled for GST-pi.
(B) 20x magnification of representative image of coronal section of PFC and CC labelled for GST-pi.
(C) Decreased number of GST-pi positive cells in the PFC of both WT and BACHD GF groups compared to their SPF controls.
(D) No significant differences in GST-pi positive cells observed in the CC.

Bar graphs represent the average of a total of 9-12 animals per condition, and 8-12 sections per animal; bar graphs represent mean±SEM. Two-way ANOVA, with Sidak's correction for multiple comparisons. *p < 0.05. Abbreviations: GST-pi, Glutathione S-transferase; CC, corpus callosum; PFC, prefrontal cortex.

5.4.4. Expression of myelin related proteins

Myelin basic protein (MBP) expression levels were decreased in the PFC of WT GF (0.547±0.068) compared to WT SPF animals (1±0.132; $p < 0.05$; Figure 5.11B). A similar trend was found in BACHD GF animals (0.716±0.149) when compared to SPF controls (1±0.261), however, this did not reach statistical significance ($p > 0.05$; Figure 5.11C).

Lower levels of PLP expression in the PFC of WT GF animals (0.738±0.050) compared to SPF controls (1±0.193) did not reach significance ($p > 0.05$; Figure 5.12B). A similar trend, and absence of significance, was also observed between the BACHD groups (SPF: 1±0.382; GF: 0.790±0.213, $p > 0.05$; Figure 5.12C).

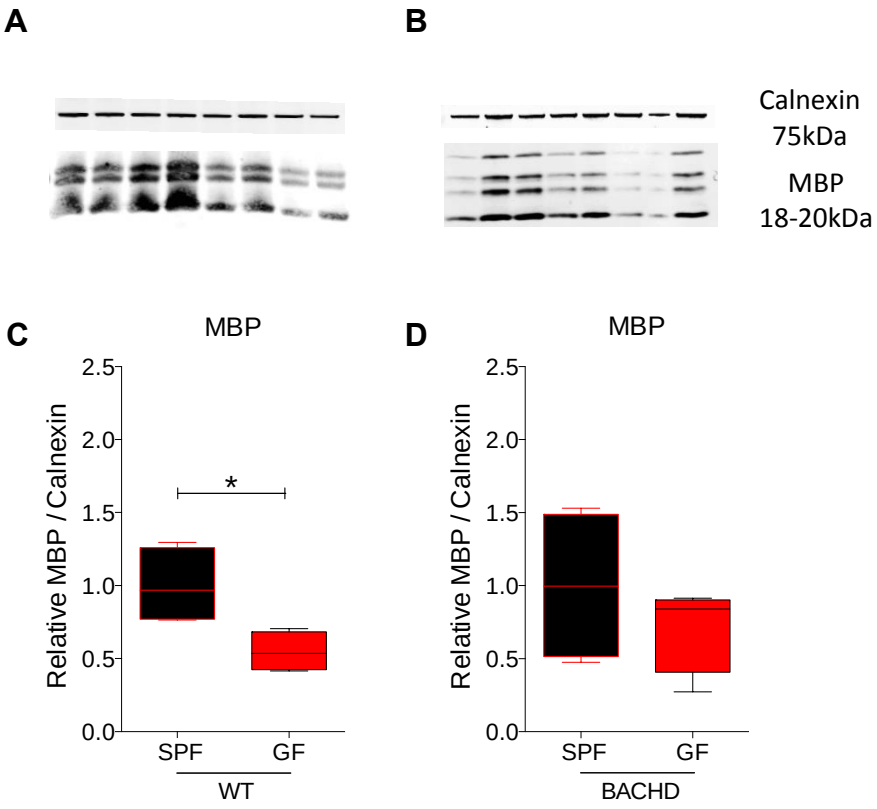

Figure 5.11 MBP levels in the PFC of BACHD and WT mice housed under SPF and GF conditions

(A) Representative western blots of PFC homogenates, immunostained with MBP (and Calnexin) in WT groups.
(B) Representative western blots of PFC homogenates, immunostained with MBP (and Calnexin) in BACHD groups.
(C) MBP levels decreased significantly in the PFC of WT GF compared to SPF controls.
(D) MBP levels decreased in the PFC of BACHD GF compared to SPF controls, but was not statistically significant.

Quantification of MBP protein (18-20kDa) concentration was normalised to Calnexin (75kDa), and expressed relative to control; SPF was taken as control for each blot. Box and whiskers represent quantification of samples from 4 animals per condition; n = 4; whiskers represent min to max. Unpaired two-tailed t-test, 95% confidence intervals; *p < 0.05. Abbreviations: MBP, myelin basic protein.

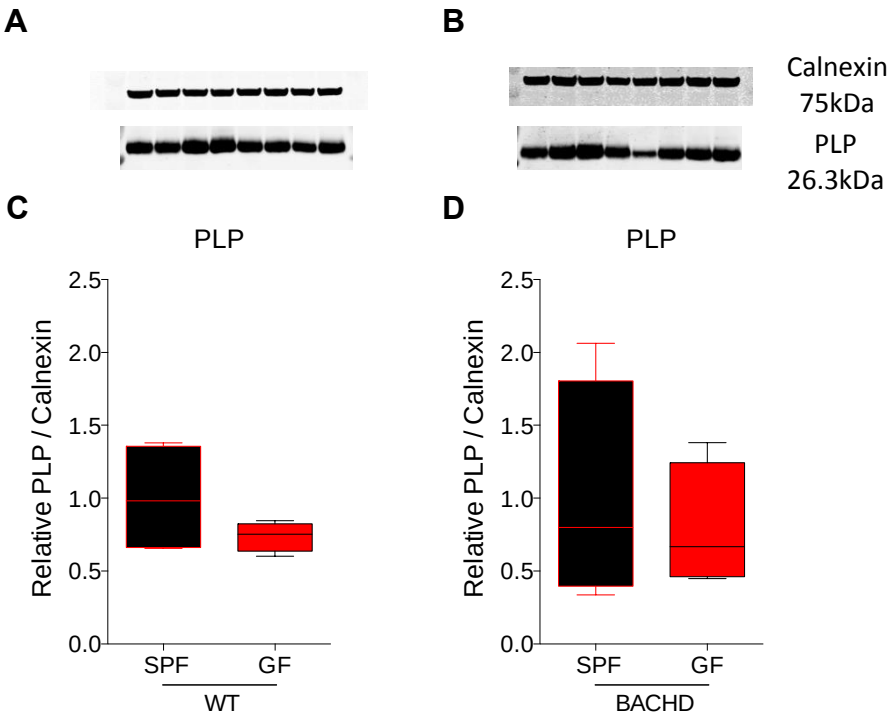

Figure 5.12 PLP levels in the PFC of BACHD and WT mice housed under SPF and GF conditions

(A) Representative western blots of PFC homogenates, immunostained with PLP (and Calnexin) in WT groups.
(B) Representative western blots of PFC homogenates, immunostained with PLP (and Calnexin) in BACHD groups.
(C) Non-significant lower levels of PLP in the PFC of GF WT compared to SPF WT.
(D) Non-significant difference between the BACHD groups, but similar trend to the WT groups.

Quantification of PLP protein (26.3kDa) concentration was normalised to Calnexin (75kDa), and expressed relative to control; SPF was taken as control for each blot. Box and whiskers represent quantification of samples from 4 animals per condition; n = 4; whiskers represent min to max. Unpaired two-tailed t-test, 95% confidence intervals. Abbreviations: PFC, prefrontal cortex; PLP, (myelin) proteolipid protein.

5.4.5. Brain weight differences in GF animals

Two-way ANOVA showed no significant interaction between genotype and microbiota presence ($F(1, 64) = 0.14$, $p > 0.05$), but a significant main effect of microbiota presence ($F(1, 64) = 42.91$, $p < 0.0001$), however no main effect of genotype ($F(1, 64) = 0.14$, $p > 0.05$). Sidak's correction for multiple comparisons post-hoc tests revealed both WT (216.9±3.72mg) and BACHD

(212.7±3.08 mg) GF mice showed significantly smaller brain weight when compared to SPF controls (WT SPF, 243.6±4.14 mg; BACHD SPF, 236.5±4.47 mg; $p < 0.0001$; Figure 5.13A). When grouped by sex, two-way ANOVA showed no significant interaction between genotype and microbiota presence ($F (1, 16) = 0.68$, $p > 0.05$), no significant main effect of microbiota presence ($F (1, 16) = 4.39$, > 0.05), and no main effect of genotype ($F (1, 16) = 0.38$, $p > 0.05$). Female BACHD GF mice showed a trend towards smaller brain weights (222.4±5.57 mg) compared to SPF controls (246.1±9.39 mg; $p < 0.05$), whereas WT groups looked fairly similar in terms of brain weight (Figure 5.13B). When comparing males, two-way ANOVA showed no significant interaction between genotype and microbiota presence ($F (1, 44) = 1.02$, $p > 0.05$), but a significant main effect of microbiota presence ($F (1, 44) = 48.69$, $p < 0.0001$), and a main effect of genotype ($F (1, 44) = 6.32$, $p < 0.05$). Sidak's correction for multiple comparisons post-hoc tests revealed the same trends of significance were seen as when comparing mixed sex groups (Figure 5.13C), in which WT GF (214±4.18 mg) animals had significantly smaller brains than WT SPF animals (246.4±4.27 mg; $p < 0.0001$), and BACHD GF (207.9±2.91 mg) brain weights were significantly smaller than those of BACHD SPF (232.1±4.63 mg; $p < 0.001$). In addition, BACHD SPF showed smaller brain weight compared to WT SPF animals ($p < 0.05$).

For forebrain weight, two-way ANOVA showed no significant interaction between genotype and microbiota presence ($F (1, 64) = 0.04$, $p > 0.05$), but a significant main effect of microbiota presence ($F (1, 64) = 21.62$, $p < 0.0001$), however no main effect of genotype ($F (1, 64) = 3.87$, $p > 0.05$). Sidak's correction for multiple comparisons post-hoc tests revealed significantly decreased forebrain weight in the mixed sex GF group compared to SPF controls ($p < 0.01$; Figure 5.13D). When comparing male forebrains, two-way ANOVA showed no significant interaction between genotype and microbiota presence ($F (1, 44) = 0.05$, $p > 0.05$), but a significant main effect of microbiota presence ($F (1, 44) = 17.91$, $p < 0.0001$), however no main effect of genotype ($F (1, 44) = 4.4$, $p > 0.05$). Sidak's correction for multiple comparisons post-hoc tests revealed significantly smaller forebrains in male WT GF animals (165.7±3.98 mg) and BACHD GF

animals (159.9±2.36 mg) compared to SPF controls (WT SPF, 179.5±2.72 mg; BACHD SPF, 172.3g±3.08 mg; $p < 0.05$; Figure 5.13F). However, when comparing female forebrains, two-way ANOVA showed no significant interaction between genotype and microbiota presence ($F (1, 16) = 0.08$, $p > 0.05$), no significant main effect of microbiota presence ($F (1, 16) = 3.06$, $p > 0.05$), and no main effect of genotype ($F (1, 16) = 0$, $p > 0.05$; Figure 5.13E).

5.4.6. Lack of microbiota affects body weight of GF BACHD animals

Two-way ANOVA showed significant interaction between genotype and microbiota presence ($F (1, 88) = 36.05$, $p < 0.0001$), significant main effect of microbiota presence ($F (1, 88) = 76.98$, $p < 0.0001$), and significant main effect of genotype ($F (1, 88) = 71.99$, $p < 0.0001$). Sidak's correction for multiple comparisons post-hoc tests revealed BACHD SPF (36.68±0.91g) bodyweights significantly exceeded those of WT SPF (27.16±0.75g) littermates ($p < 0.0001$). A significant difference in bodyweight was also seen between BACHD SPF and BACHD GF (26.97±0.45g, $p < 0.0001$). The BACHD GF body weight was comparable to that of WT groups (Figure 5.14A). Female body weight characteristics across groups were similar to that observed for mixed sex (Figure 5.14B). When comparing the body weight of males, a similar effect of a GF environment on BACHD animals was also observed, with an additional significant effect ($p < 0.05$) of WT GF animals possessing a decreased body weight (25.84±0.46g) compared to WT SPF (29.27±0.80g) (Figure 5.14C).

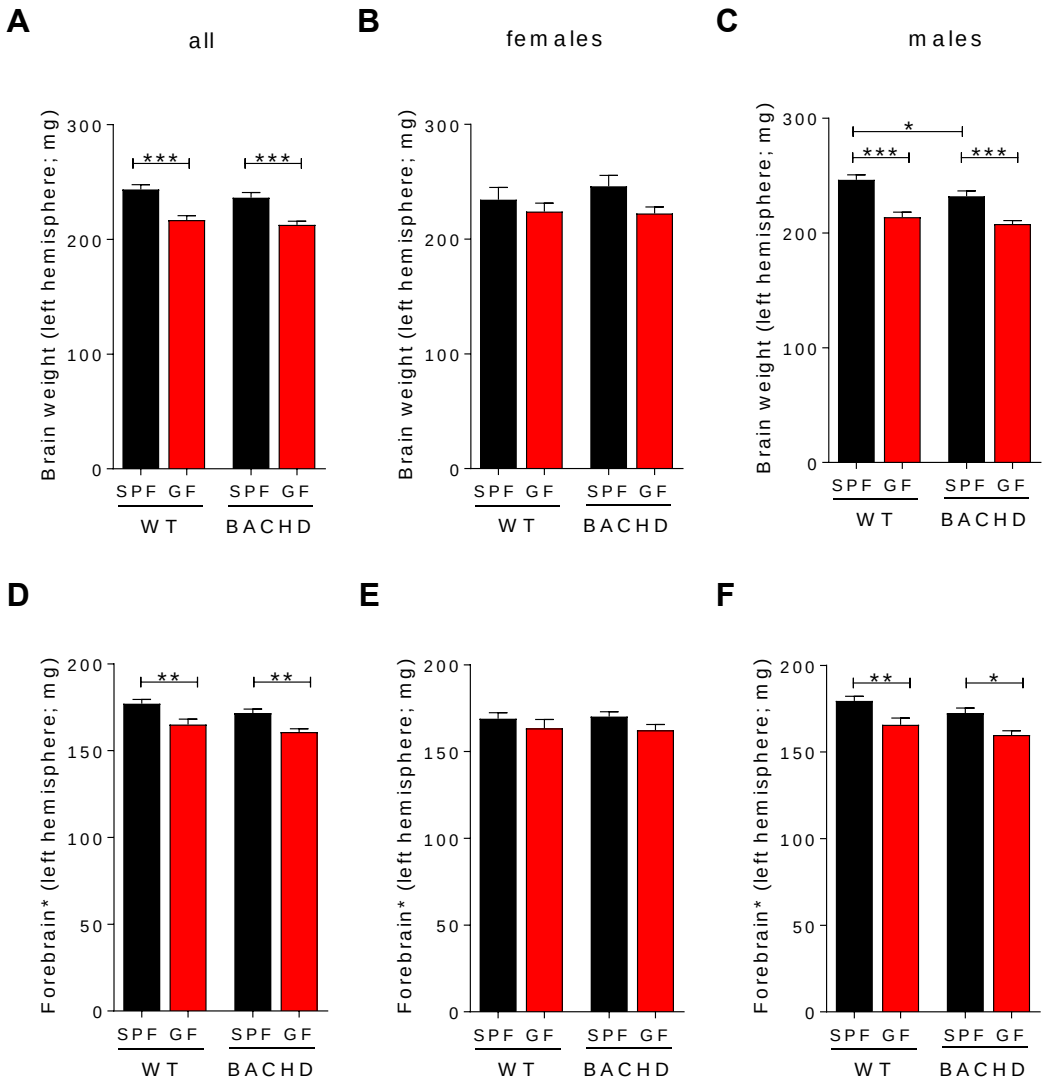

Figure 5.13 Comparison of brain weight (left hemisphere and forebrain) in BACHD and WT mice housed under SPF and GF conditions

(A) Both WT and BACHD GF mice were associated with significantly smaller brain weights compared to their SPF controls.
(B) Female WT and BACHD GF mice were associated with smaller brain weights compared to their SPF controls, although this was only significant in the case of BACHD animals.
(C) When comparing males only, the same trends of significance were seen as when comparing mixed sex groups (Fig. 2A). WT GF showed significantly smaller brain weights than WT SPF, and BACHD GF showed significantly smaller brain weights than BACHD SPF.
(D) Forebrain weight was also significantly reduced in GF groups compared to SPF controls.
(E) No significant differences in forebrain weight was observed when comparing females, although GF animals were associated with smaller forebrain weights compared to SPF animals, regardless of genotype.

(F) Significantly smaller forebrain weights were seen in male WT GF and BACHD GF animals compared to their SPF controls.

Animals' brains were weighed at 3 months of age. Weight shown in milligrams (mg). n = 11-13 males per condition, and 4-6 females per condition; Bars represent mean±SEM. Two-way ANOVA, with Sidak's correction for multiple comparisons. *p < 0.05; **p < 0.01; ***p < 0.001. For figures E, F and G, 'Forebrain*' refers to the left hemisphere, not including the olfactory bulb and cerebellum.

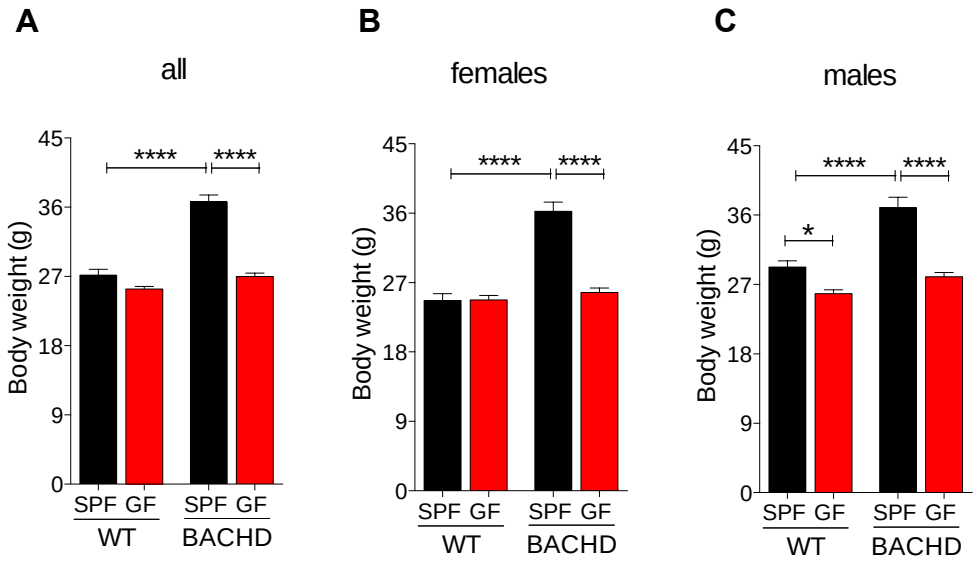

Figure 5.14 Body weight of BACHD and WT mice housed under SPF and GF conditions

(A) Expected significant difference in body weight between WT SPF and BACHD SPF animals. BACHD GF animals' body weight was significantly reduced relative to BACHD SPF animals and similar to both WT groups.
(B) Differences in body weight in females showed the same trend as when comparing mixed sex groups in figure 1(A).
(C) When comparing males only, an additional difference was seen within the WT group, with WT GF animals showing significantly decreased body weight compared to WT SPF.

Animals were weighed at 3 months of age. Body weight shown in grams (g). n = 10-13 animals of each sex; Bar graphs represent mean±SEM. Two-way ANOVA, with Sidak's correction for multiple comparisons. *p < 0.05; ****p < 0.0001. Abbreviations: SPF, specific pathogen free; GF, germ free; WT, wild type; BACHD, bacterial artificial chromosome (BAC) mouse model of Huntington Disease (HD).

5.5. Discussion

Myelination and axonal diameter differences as a result of microbiota manipulation

Contrary to that in wild-type (WT) mice, we found that a germ-free (GF) environment markedly altered axonal and myelination-related characteristics in BACHD mice. This included an increase in population of regular-shaped myelinated axons, and a decrease in number of irregular shaped myelinated axons compared to BACHD animals housed under specific pathogen free (SPF) conditions. Furthermore, we found that germ-free BACHD mice were associated with a larger number of small-to-medium diameter axons, and that these possessed thicker myelin sheaths (i.e. with reduced g-ratio values), than BACHD SPF mice. Our results are at variance with a previous report that reported thicker myelin sheaths, or hypermyelination, in axons of the prefrontal cortex (PFC) of WT GF animals (Hoban et al., 2016b). This disparity may be due to differences in brain region investigated (anterior CC here vs PFC), age of the animals (12 weeks here vs 10 weeks), or the mouse genetic background (FVB/N here vs Swiss Webster).

Myelin-related protein differences

Myelin basic protein (MBP) expression levels were found to be significantly reduced in the PFC of WT GF mice compared to their SPF counterparts, with an analogous, albeit non-significant, decrease in proteolipid protein (PLP) expression also observed in the same animals as a result of germ-free conditions. In turn, BACHD GF animals were associated with a non-significant decrease in MBP and PLP levels in PFC. Our finding in WT animals is in keeping with our observation (described in the next section) of a reduction in mature oligodendrocyte number in the PFC of WT GF animals, but in contrast to a recent study demonstrating increases in MBP levels in the same brain region and animals (Hoban et al., 2016b). This disparity may once again be due to differences in age and genetic background of wild-type mice used in both our and their studies.

Regulation of oligodendroglial population by microbiota

Germ-free conditions were associated with a significant reduction in mature myelinating oligodendrocyte (GST-pi+) cells in the prefrontal cortex (PFC) of animals regardless of genotype. However, in the corpus callosum (CC) region, a small non-significant reduction was observed only for WT GF animals compared to SPF control, but not for BACHD GF compared to SPF control. A minor reduction was also observed in the number of oligodendrocyte lineage (Olig2+) of WT GF mice compared to SPF mice in both brain regions investigated. Olig2+ cell numbers of BACHD mice were comparable across housing conditions and brain regions. In contrast, there were no significant differences in number of oligodendrocyte precursor cells (OPCs / PDGFRα+) cells in either the CC or PFC of WT GF mice relative to WT SPF mice. In summary, these findings suggest that a proportion of OPC cells might lose their capacity to differentiate into mature oligodendrocytes when placed in a germ-free environment, which we found to be consistent in the PFC region of both WT and BACHD animals.

Differences in brain weight

We only found brain weights to differ significantly between WT and BACHD animals when comparing males. Brain and forebrain weights were fairly similar between WT and BACHD animals when males and females were grouped together and compared, or when females only were compared. This may be due to the early age at which measurements were taken (3 months) since a previous study demonstrated decreased forebrain weights at 12, but not at 6 months of age, in BACHD mice relative to WT animals (Gray et al., 2008). Interestingly, we did find that both germ-free WT and BACHD mice exhibited a significant decrease in overall brain weight compared to their SPF housed counterparts. This effect was significant when examining male germ-free mice only, and also discernible in females, although only significant between female BACHD and BACHD SPF mice.

Differences in body weight

BACHD animals housed under SPF conditions were associated with a significant increase in body weight relative to WT counterparts, as previously observed by us, and others (Hult et al., 2011; Pouladi, Morton, & Hayden, 2013a; Slow et al., 2003). Interestingly, this weight gain was absent, and comparable to WT controls, in BACHD animals housed under germ-free conditions. We also found that male WT GF mice displayed a decrease in body weight relative to male WT SPF mice, while female weights remained unchanged. This appears to roughly consistent with early studies which reported germ-free WT animals to weigh either less, or the same, as SPF counterparts despite the former being associated with an increase in food intake (Bäckhed et al., 2004; Wostmann, 1981).

Chapter 6. General discussion and conclusions

6.1. Overview of findings

The research presented in this thesis employed environmental and microbiota manipulations as assays to interrogate white matter and behavioural abnormalities in two mouse models of Huntington disease (YAC128 and BACHD), as well as wild-type control animals. The environmental manipulation studies investigated the posterior (splenium) region of the corpus callosum (CC), whereas the microbiota manipulation study investigated the anterior mid-body region of the CC and the prefrontal cortex (PFC). Overall, the key findings presented here are as following; firstly, environmental enrichment (EE) of YAC128 and wild-type (WT) mice was associated with an increase in the number of small and mid-range diameter axons, which possessed thinner myelin in the posterior (splenium) region of the corpus callosum. Secondly, social deprivation was associated with reduced myelin sheath thickness across all axonal diameters in WT mice, but no clear myelination-related effects in YAC128 animals. Thirdly, in a germ-free environment (GF), BACHD mice were seen to have a larger number of small to mid-range diameter axons, and they possessed thicker myelin sheaths. Increases in the number of myelinated axons, and decreases in the number of unmyelinated axons, were observed in BACHD GF mice, compared to diseased controls housed under specific pathogen free (SPF) conditions. Myelin basic protein (MBP) and proteolipid protein (PLP) levels in WT and BACHD mice were generally reduced under germ-free conditions. We further observed a reduction in mature myelinating oligodendrocytes (GST-pi+) in the PFC and CC of WT germ-free mice, but only a reduction of myelinating oligodendrocytes in the prefrontal cortex of BACHD germ-free animals. Additionally, oligodendrocyte precursor (PDGFRα+) cell numbers were fairly similar across groups in both regions investigated. Therefore, our findings suggested that myelination in the CC region of YAC128 mice was relatively insensitive to social deprivation, but responded to enrichment in a similar manner to wild-type mice. In contrast, manipulation of microbiota had complex effects on myelin-related characteristics, oligodendroglial populations, body and brain weight,

revealing a wide ranging influence of a germ-free environment in both the BACHD mouse model of Huntington disease, as well as wild-type animals.

6.2. Environmental enrichment manipulation effects on the YAC128 mouse and WT control

Enriched housing effects on behavioural performance

Several behavioural tests have been established to assess HD specific phenotypes in the YAC128 mouse model and WT littermates (Brooks & Dunnett, 2009; Slow et al., 2003). These tests assess the habituation and acclimatization to a new environment, anxiety- and depressive-like behaviour, locomotor ability and motor learning.

In the spontaneous activity and open field tests, habituation is measured during exposure to the testing chambers, whereas general locomotor activity is recorded throughout the duration of testing (Zhu et al., 2007). Here, we demonstrate that several measures of activity levels resulting from these behavioural tests indicated decreased overall locomotor activity in animals housed in an enriched environment, regardless of genotype. Specifically, YAC128 and WT animals allocated to an EH condition travelled less, and rested for longer compared to their respective SH controls during the spontaneous activity test. Other measures, such as vertical and jump counts, and average velocity, were also decreased in enriched YAC128 mice compared to healthy controls. On the other hand, in the open field test, WT EH mice travelled less in comparison to WT SH. Our findings are thus consistent with past studies where rats and mice reared in enriched conditions also explored less in spontaneous or open field activity tests compared to control animals reared in standard housing conditions (Brenes, Rodríguez, & Fornaguera, 2008a; Brenes, Padilla, & Fornaguera, 2009; Hellemans et al., 2004; Leger et al., 2015; Makinodan et al., 2012; Mosaferi et al., 2015; Segovia et al., 2008). This could be ascribed to decreased motivation of animals to explore, as enrichment could lead to faster

habituation since animals are exposed to complex stimuli in their home cages, while the open field and spontaneous activity tests lack object novelty. Although grooming time was not recorded in our study, it was also previously demonstrated that enriched rats exhibited prolonged grooming behaviour compared to rats housed in standard conditions (Brenes, Rodríguez, & Fornaguera, 2008a; Mosaferi et al., 2015). Additionally, another study showed that the proportion of area travelled was greater in early-enriched pups, although total distance travelled was comparable to standard housing mice (Simonetti et al., 2009). These two studies, then, could be a contributing factor for the low level of activity observed in our behavioural tests. Finally, we did not observe any difference in overall activity and exploratory behaviour between YAC128 mice and their WT control groups across housing conditions. This finding is consistent with previous studies, which found early manifest YAC128 mice to exhibit the same levels of general locomotion as their WT counterparts (Van Raamsdonk et al., 2005).

The OFT and EPM were used to test for anxiety-like behaviour and reduced time spent in the centre of the open field or the open arm of the EPM suggests increased anxiety-like behaviour in mice (Southwell, Ko, & Patterson, 2009). We found no differences between the four experimental groups in either of the two tests of anxiety. Moreover, animals, regardless of genotype or experimental condition, spent a similar proportion of time in the centre of the OFT arena, and in the open arms of the EPM. Although not commonly reported in studies, anxiety-like behaviour, as inferred by reduced time spent in the centre of the open field arena, was previously detected in the YAC128 mouse at 7 months of age (Southwell et al., 2009). However, we did not observe a similar phenotype manifest in the YAC128 SH group, possibly as a result of age differences between our mice (4.5 months of age) and those of the aforementioned study. In addition, previous reports related to the effect of enrichment on anxiety-like behaviour have been inconsistent. Some studies, like ours, found no effects of enrichment on anxiety-like behaviour (Brenes, Rodríguez, & Fornaguera, 2008a; Peña et al., 2006; 2009). Others, however, reported reduced anxiety as an effect of enrichment

(Galani et al., 2007; Hellemans et al., 2004). Interestingly, in a study investigating the effects of different durations of enrichment (24hrs, 1, 3, 5 and 6 weeks), anxiety-like behaviour in mice was only reduced by a 3-week exposure to enrichment, but not by any of the other enrichment durations (Leger et al., 2015).

The climbing test is often used as a measure of motor ability in HD mouse models (Menalled et al., 2009; Southwell et al., 2009). No differences in any of the climbing measures (latency to fall, time spent climbing or number of climbing attempts) were found between YAC128 and WT at 18 weeks of age, regardless of housing condition. Elsewhere, decreased latency to climb was only observed at 16 weeks of age in the YAC128 FVB (as used here) compared to WT, but not at other preceding or succeeding age groups (Menalled et al., 2009). Decreased climbing time in YAC128 FVB animals compared to WT littermates was also previously reported at 7 months of age (Southwell et al., 2009). In addition, we observed no differences in latency to climb, or time spent climbing, in the climbing test between any of the experimental groups regardless of genotype. Interestingly, both YAC128 and WT mice from the EH groups had fewer number of climbing attempts compared to animals from the SH groups. Enriched cages contained stairs, tunnels and objects offering the possibility for climbing. Therefore, it is possible that enriched animals were less motivated, and habituated faster to the climbing mesh cylinders compared to standard housing animals, leading to reduced climbing activity, similarly to the reduction in exploratory activity observed in the spontaneous activity test. Thus, this test, and that of spontaneous activity, could be susceptible to confounds relating to the animal's motivation to climb and explore.

The rotarod is a commonly used test of motor performance in animal models of HD (Garcia-Miralles et al., 2016; Pouladi et al., 2008; Slow et al., 2003). In our study, the YAC128 SH group remained the least time on the fixed rotarod, and had the highest number of falls and the highest percentage of animals that fell off the rotarod, for the first 6 out of 8 training trials. However, statistically significant differences were only observed between YAC128 SH

and WT SH mice on the first trial of the first training day only. This suggests that YAC128 SH mice exhibit minor motor learning deficits in this behavioural test. Consistent with our findings, motor learning deficits were seen at 2 months of age in the YAC128 HD model housed under standard conditions, as well as minor locomotor deficits from the age of 4 months, which worsened progressively and reached statistical significance after 6 months of age (Franciosi et al., 2012; Lawhorn et al., 2008; Slow et al., 2003; Van Raamsdonk et al., 2005).

In addition, our study revealed that WT animals housed in enriched housing (EH) marginally outperformed other groups on fixed speed rotarod training sessions, as well as the accelerated rotarod test. Although not statistically significant, this group had an overall smaller number of falls compared to the other groups. In addition, WT EH animals also performed better on the accelerated rotarod testing session, showing a higher latency to fall compared to all the other groups. Furthermore, despite the YAC128 EH group starting the first training trial at a similar level to YAC128 SH controls, the YAC128 EH group consistently outperformed the YAC128 SH group over the next four training trials, remaining a greater time on the rotarod until the first fall, and a succumbing to a smaller number of falls. However, these differences in performance did not reach statistical significance. YAC128 EH animals attained the same performance as WT SH and WT EH animals after 2 training trials, while YAC128 SH animals required 6 trials to learn the test and reach similar performance levels. Thus, the YAC128 EH animals learnt the rotarod task more quickly than the YAC128 SH control group. In contrast, no advantages were conferred to YAC128 EH animals compared to YAC128 SH controls in the accelerated rotarod test. Taken together, these findings suggest a marginal effect of an enriched environment on motor learning and motor performance in the healthy WT group, and minor beneficial effects on learning, but not motor performance, on this task in the YAC128 HD mouse model at the tested age of 18 weeks (~4.5 months). In contrast, a previous study reported improvements in rotarod test performance in another HD model as a result of enrichment. Specifically, at 8 weeks of age, the R6/2 mouse, an HD model with accelerated phenotype and impairments beginning

at 5-6 weeks and a life-span of about 12-14 weeks (Mangiarini et al., 1996), showed improvements in the latency to fall during the rotarod test after 4 weeks of enriched housing (Hockly et al., 2002). On the other hand, no effect of post-weaning enrichment was found on the rotarod test at 10 or 25 weeks of age in the R6/1 mouse, an HD model with an aggressive onset and a shortened life-span of about 9 months (Lazic et al., 2006). An important caveat to this report, however, is that the R6/1 mouse performed relatively poorly relative to WT controls, regardless of housing condition (Lazic et al., 2006). However, other studies showed that enrichment did have beneficial effects on the R6/1 mice in the performance on the horizontal rod test (very similar to rotarod test; van Dellen et al., 2000, Nature) and on the rotarod test (Spires, 2004).

Overall, our results are roughly in keeping with the notion that environmental enrichment confers some beneficial effects on laboratory mice. While we did not observe clear and consistent positive effects of enrichment on behaviour and motor function in YAC128 HD mice above and beyond that seen in WT mice – which might be expected due to the background pathology - this may be due to this particular HD model being a late-onset phenotype, and/or the early manifest stage at which tests were conducted. Mouse models of HD with accelerated onset phenotypes, such as those described above, may therefore be more predisposed to displaying more overt behavioural and motor improvements due to environmental enrichment. Notwithstanding, and as described, the available literature examining behaviour and motor function in mouse models of HD has several inconsistencies, and underscores the need for standardization of relevant protocols across laboratories (Ross & Tabrizi, 2011).

Impact of environmental manipulation on myelination and mature oligodendrocytes in the corpus callosum

Myelination in the brain begins during development and continues into adult life (Miller et al., 2012), and it has been recently shown that myelin is adaptive and plastic to environmental and behaviorally driven experiences

(Forbes and Gallo, 2017; McKenzie et al., 2014; Mount and Monje, 2017; Tomlinson et al., 2015). Our study aimed to understand enrichment driven effects on adaptive myelination in the white matter tracts of the posterior region (splenium) of the corpus callosum in WT and YAC128 mice. By examining the variability of myelin thickness at different ranges of axonal diameters, we identified similar trends between the WT and YAC128 animals exposed to enrichment. Firstly, in the WT enriched animals, small and mid-range axons exhibited thinner myelin thickness compared to SH controls, but no differences were seen for large axons. Furthermore, in enriched YAC128 mice, mid-range and large axons had thinner myelin compared to YAC128 SH mice, while no differences were observed in small axons. However, when g-ratios were averaged together across all axonal diameters, both enriched groups, regardless of genotype, showed increased g-ratio values, thus thinner myelin, compared to their corresponding standard housing controls. In addition, by analysing the distribution of myelinated axonal diameters, we revealed that both enriched groups, regardless of genotype, exhibited an overall larger number of small diameter axons, compared to their corresponding standard housing controls. Thus, EH animals in both genotypes were associated with a significantly reduced axonal diameter compared to their SH counterparts, and which was more pronounced in YAC128 animals.

Interestingly, it has been established that the first axons to be myelinated both in the brain and spinal cord are those with the largest diameter within the population (Almeida et al., 2011; Hahn et al., 1987; Matthews & Duncan, 1971). If this occurred in our animals during the time spent in the allocated environment, or prior to environmental manipulation, possibly at the peak of myelination (Matthieu et al., 1973; Wiggins, 1986), small and mid-range axons might still be in the process of being myelinated at the time of our analysis. This would support our observation of comparable g-ratios between WT SH and WT EH in large diameter axons, as well as a greater number of small diameter axons in EH animals relative to SH, regardless of genotype. A previous study has reported an increase in the number of myelinated axons of small and mid-range diameter (ID ≤ 1000) in aged rats after four months of

enriched housing, and showed that these newly myelinated axons had thinner myelin sheath (Yang et al., 2013). The authors suggested that the observed increased axon and myelin sheath volume in these animals was not due to increase in axonal size or increase myelin sheath thickness but, rather, could be explained by an increase in number of newly myelinated axons (Yang et al., 2013). Thus, it is possible that small axons get myelinated later as a result of an enriched environment, and these newly myelinated axons have thinner myelin compared to axons myelinated prior to allocation to experimental condition, resulting in overall thinner myelin sheaths in WT EH animals compared to WT SH, as we observed. Therefore, we speculate that myelination was on going, and had not reached the end point of this process, at the time of our analysis (Karttunen, 2017; Powers et al., 2013).

Myelination in standard housed mice was reported to be achieved in almost all brain regions by p60 (Baumann & Pham-Dinh, 2001). However, others have shown that myelin continues to be synthetized later into adult life (Dimou et al., 2008; Rivers et al., 2008; Waly et al., 2014). In addition, 20% of oligodendrocytes are generated in the mouse CC after 7 weeks of age, whereas mature myelin producing oligodendrocytes continued to be generated until at least 8 months of age (Psachoulia et al., 2009; Rivers et al., 2008). In an interesting study using Cre-Lox fate mapping in mice, it was observed that myelin synthesized in adulthood (after p120) was associated with larger g-ratios (i.e. thinner myelin sheaths) compared to myelin that was synthetized earlier in life (Young et al., 2013). Our mice were placed in their allocated condition from p28 to p126; therefore, it is possible that EE used here could prolong the ‘window of myelination’, and thinner myelin sheaths could be a property of myelination in the adult CNS, as previously suggested (Franklin & Ffrench-Constant, 2008; Franklin & Hinks, 1999; Waly et al., 2014; Young et al., 2013). Unfortunately, due to sparse literature investigating on the effects of enrichment on myelination, and the absence of further myelin-related measurements, such as total number of myelinated and unmyelinated axons, or total myelin sheath or axonal volume, it is difficult for this study to draw a clear conclusion on these findings.

Additionally, YAC128 SH mice had significantly thinner myelin at small axonal diameters, whereas a trend towards a minor decrease in g-ratio, thus thicker myelin, was observed in large diameter axons, compared to WT SH controls. However, since small diameter axons outnumber large ones, when averaged across all axonal diameters, a minor, non-significant, higher g-ratio, suggestive of thinner myelin, was observed in YAC128 SH animals compared to WT SH. Previous work in our laboratory has demonstrated WM microstructural abnormalities in the anterior mid-body region of the CC of the YAC128 mouse from 1.5 months of age, and that these differences were accompanied by thinner myelin sheaths in the same region (Teo et al., 2016). However, differences in the posterior region (splenium) of the CC were only detected from 6 months of age (Teo et al., 2016). Our current study has investigated the posterior region of the CC, thus it is possible that myelin pathology in the posterior region of the YAC128 HD mouse model is less severe compared to the anterior region, and/or or becomes manifest at a later age. Consistent with this possibility, curprizone-induced demyelination in mice induced regional differences in demyelination along the CC (Binder et al., 2008; Steelman, Thompson, & Li, 2012). Taken together, these results provide further evidence into the complex effects of enrichment on axonal and myelin-related characteristics, which may underpin the observed beneficial effects of enrichment on specific behaviours and motor function.

Finally, no significant differences were observed in GST-pi positive cells in the corpus callosum between any of our experimental groups. This finding suggests that 14 weeks of post-weaning enrichment does not have an effect on the number of mature myelinating oligodendrocytes in the corpus callosum. Similarly, others have also found no differences in CNPase+ cells in the amygdala of mice after 40 days of enrichment, although an increase in number of OPCs was observed (Ehninger et al., 2011); while 28 days of enriched housing was linked to higher number of oligodendrocytes in the substantia nigra (Klaissle et al., 2012). However, no changes were found in PFC oligodendrocyte density or morphology, or in myelin transcript levels of young mice that spent 1.5 months in an enriched setting (Makinodan et al., 2012). On the other hand, decreased number of OPCs and increased

number of mature oligodendrocytes were observed after 10 days, but not 42 days (~1.4 months), in sensorimotor cortex, but not the CC, of enriched young rats compared to standard housing (Keiner et al., 2017). Therefore, it is possible that the differentiation of OPCs into mature oligodendrocytes, driven by enrichment and behavioural experience, could take place within the first week of manipulation, and would not be detected at later points (such as those used in our study). A caveat to this observation is that our use of oligodendrocyte counts might be considered a crude measure, and as such it is insensitive to myelin-related changes at the sub-cellular level (internode distance, number of branches, etc.).

Brain and body weight changes as an effect of enriched housing

No differences in brain weight between any of the groups were found at 4.5 months of age, regardless of genotype or housing manipulation. Previous work in YAC128 mice (line 53), demonstrated a 5% and 10% decrease in mean brain weight at 9 and 12 months of age, respectively, compared to WT controls (Slow et al., 2003). In addition, a 10-15% decrease in striatal volume was also previously observed at 9 months of age and persisted at 12 months, whereas a 7-8% decrease in cortical volume was only observed at 12 months of age (Slow et al., 2003; van Oostrom et al., 2007; Van Raamsdonk et al., 2005). No differences in brain weight between YAC128 mice and WT littermates were previously reported before 9 months of age. Interestingly, in terms of the effect of enrichment, global brain volume of adult rats was decreased after 6 weeks of enrichment compared to 1.5 weeks of enrichment (Keiner et al., 2017).

Increased body weight is a known phenotype of the YAC128 mouse due to the influence of full-length mutant huntingtin levels in this HD model (Pouladi et al., 2010; Slow et al., 2003; Van Raamsdonk et al., 2006). Animals in the current study were weighed fortnightly from 7 weeks (50 days) to 18 weeks of age (126 days), and comparisons were made separately for females and males. A significant main effect of time indicated all groups gained weight over the duration of the study. In the standard housing conditions, YAC128

females and males weighed more than WT SH controls at two of the recorded time-points. In addition, comparison between the two enriched groups revealed that YAC128 EH females weighed more than WT EH at all time-points recorded with the exception of the first.

Reports into the effects of enrichment on body weight are inconsistent, and vary with sex, strain or animal model, as well as duration or complexity of enrichment (Tsai et al., 2016; Tsai et al., 2003). With minimal enrichment containing a nest box, a wood bar and nesting material, no differences were found in body weights of three strains of mice: BALB/c, C57BL and A/J, at any recorded time-points between enrichment onset to 10 weeks later (Tsai et al., 2003). In 10 weeks old C3H/eB mice, 6 weeks of enrichment also did not have a significant effect on body weight (Benaroya-Milshtein et al., 2004). In the R6/1 HD mouse model, 4 months of enrichment was shown to partially rescue characteristic weight loss, eliminating the differences between WT and the disease model at 5 months of age (Spires, 2004). However, another study showed no effect of enrichment on body weight in the R6/1 model after 4.5 months in their allocated condition (van Dellen et al., 2002). Interestingly, in our study, both enriched female groups, regardless of genotype, weighed more compared to their standard housing control. Enriched YAC128 female mice weighed significantly more than standard housing YAC128, between 11-18 weeks of age. A non-significant trend was observed for increased body weight in WT EH females compared to WT SH females. In contrast, the effect of enrichment on male body weight was not as clear, although a trend of increased body weight in the WT EH group compared to WT SH was observed at several time points (11-15 weeks). These findings suggest a larger effect of enrichment on female body weight in the HD mouse model, and only a minor effect on the body weight of WT females and males.

6.3. Social deprivation effects on the YAC128 mouse and WT control

Isolation effects on behavioural performance

No significant patterns in measures of activity level were observed during spontaneous activity test in standard housed (SH) and socially isolated WT and YAC128 mice. Animals from all groups showed comparable resting time, mean vertical counts, mean jump counts, as well as average velocity. A trend was, however, observed in the mean distance travelled during this test, with both YAC128 groups travelling less than their WT counterparts, regardless of housing condition. This non-significant trend was replicated in the open field test, but only in the SH group, where YAC128 SH mice travelled less than WT SH mice. These findings indicate that general locomotor activity in WT controls and YAC128 mice was not affected by social isolation. This is consistent with previous studies in wild-type rodents, where four and eight weeks of social isolation in juvenile (Makinodan et al., 2012) and adult (Liu et al., 2012) mice, respectively, did not affect mean distance travelled in the OF test. Likewise, three weeks of social deprivation in adolescent or adult mice did not affect total distance travelled in the OF test (Lander et al., 2017). Being reared in social isolation also does not appear to affect the performance of healthy male rats in the OFT (Brenes, Rodríguez, & Fornaguera, 2008b), although others studies have reported hyperactivity (decreased resting time; Fone & Porkess, 2008).

Furthermore, no clear trends in standard housed and socially isolated WT and YAC128 mice were distinguished in the two tests of anxiety. In contrast, a recent study found that three weeks of social deprivation caused male mice to spend less time in the centre of the open field arena regardless of whether they were allocated to isolation at adolescence or adulthood (Lander et al., 2017). Additionally, male mice of the CD1 strain, after being socially isolated post-weaning for 8 weeks, besides showing decreased heterochromatin formation and MBP expression, also spent less time in the open arm, and entered the open arm less times, than standard controls (Cao et al., 2017),

suggesting that social isolation induced anxiety-like behaviour. However, anxiety-like behaviour in rats was also found to be highly variable, and somewhat dependent on the time spent in isolation (e.g. Butler, Carter, & Weiner, 2014; Mosaferi et al., 2015; Hermes et al., 2011). Therefore, our observation of a lack of an effect of social isolation anxiety-like behaviour may be due to differences in experimental protocol that were unable to unearth significant effects.

Several measures, such as latency to climb, time spent climbing and number of climbing attempts, were recorded during the climbing test to assess motor ability. Although we found no statistically significant differences between groups related to any of these measures, socially deprived groups, regardless of genotype, took longer to attempt their first climb, spent less time climbing, and attempted climbing, on average, less than their respective standard-housing controls. Therefore, our results indicate a modest negative effect of isolation on climbing performance, and possibly motivation to climb, regardless of genotype. Furthermore, deprived housing appeared to have a slight negative effect on YAC128 mice motor learning, as this group performed worse than all the other groups on the first two trials of the fixed speed rotarod training, with a shorter latency to fall, more number of falls and a higher proportion of mice that fell off the rotarod. Subsequent sessions, however, showed comparable rotarod performance between all the groups. The YAC128 deprived animals also showed the lowest latency to first fall on all three trials of the accelerated rotarod testing, however, this was not found to differ statistically from the other groups. In addition, WT deprived animals were more likely to fall off the rotarod during the first two days of training, and these animals showed slightly decreased performance both in terms of latency to fall and number of falls during the first two training trials, compared to standard housing controls. Therefore, the rotarod test revealed that environmental deprivation had a mild impact on motor learning and motor performance on the early manifest YAC128 mouse at 18 weeks of age, and a minimal impact on WT deprived animals with regards to motor learning, but not performance, during testing.

Taken together, our observation of only minor negative behavioural and motor effects as a result of social isolation, across WT and YAC128 animals, is intriguing, since we expected this to be more pronounced, particularly in the YAC128 mouse model of HD. However, it is important to note that the available literature with which to contextualise our results is limited, and that there is lack of standardization between deprivation protocols across studies. A likely explanation is that HD pathology is such a dominant factor that social deprivation does not worsen it sufficiently to detect an effect with the measures used. Additionally, it is possible that the short time window, immediately after weaning (3 weeks of age), when deprivation seems to affect the mice more severely, could have been missed in our study, since mice were weaned and placed in their allocated condition at 4 weeks of age rather than 3 weeks. Nevertheless, we cannot exclude that our environmental deprivation protocol may not have been sufficiently severe to induce significant effects. One way to make deprivation conditions more severe for the current study would involve removing the bedding material altogether.

Isolation effects on myelination and mature oligodendrocytes in the corpus callosum

The current study aimed to understand social deprivation driven effects on adaptive myelination in the white matter tracts of the posterior (splenium) corpus callosum in the early manifest YAC128 mouse model of HD, as well as WT controls. Socially deprived WT animals exhibited significantly higher g-ratios, suggestive of thinner myelin sheaths, compared to all the other groups in our study. Higher g-ratios in socially deprived WT animals, compared to WT SH mice, persisted across all axonal diameter ranges. Consistent with our findings, an early study examining the relationship between white matter abnormalities and behavioural experience demonstrated that male rhesus monkeys raised in isolation from 2 to 12 months of age had significant decreased corpus callosum (CC) size, which was particularly evident in the posterior region, when compared to monkeys raised in social groups (Sánchez et al., 1998)). Thinner myelin sheaths have

also been reported in the medial prefrontal cortex (mPFC) of healthy juvenile mice following 2, 4 or 8 weeks of post-weaning isolation (Cao et al., 2017; Liu et al., 2012; Makinodan et al., 2012). Moreover, juvenile male CD1 mice reared in isolation for 8 weeks post-weaning exhibited thinner myelin sheaths in the hippocampus, as well as decreased heterochromatin formation and MBP expression (Cao et al., 2017). Additionally, adult mice were also seen to exhibit hypomyelination in the PFC following 8 weeks of social deprivation, whereas myelin sheath thinning was milder after only 2 weeks of isolation (Liu et al., 2012). In contrast, other reported no differences in layer V of the mPFC myelin thickness of adult mice placed in social isolation for 4 weeks (Makinodan et al., 2016). Furthermore, no differences in myelin sheath thickness or myelin gene transcripts were found in the white matter tracts of the anterior commissure, the nucleus accumbens or the cerebellum, between isolated and standard house adult mice, placed in their allocated condition at 16 weeks of age, regardless of the period of isolation (2 or 8 weeks) (Liu et al., 2012). These studies confirm that the predominant effect of social isolation is a thinning of myelin sheaths, but that that the variability in observations may be underpinned by brain-region, age dependencies, or duration of isolation paradigm employed.

In terms of axonal diameter, our study revealed that WT deprived mice had fewer smaller diameter, and more mid-range to large diameter, myelinated axons compared to their WT standard housed control. Thus, on average, myelinated axons in deprived WT mice were of a significantly larger diameter compared to WT SH controls. This finding is at variance with a previous report of no differences in axonal diameter in juvenile mice after 4 weeks of deprivation, however, this was observed in a different region of the brain, the mPFC (Makinodan et al., 2012), suggesting that the duration of deprivation, age of the animal, and region of the brain investigated, could be important factors in determining the effect of social isolation on axonal characteristics.

On the other hand, socially deprived YAC128 mice had comparable myelin sheath thickness to YAC128 and WT mice housed under standard conditions. However, at large axonal diameters, YAC128 DH animals

showed increased g-ratios, thus thinner myelin, compared to their standard house YAC128 controls. This difference, although considerable, did not influence the overall g-ratio average, because the population of large diameter axons was much smaller relative to mid-range and small axons, which make up the majority of axons in this region of the CC, as shown by our findings. In addition, socially deprived YAC128 mice were associated with, on average, a smaller axonal diameter compared to their standard housed YAC128 controls. These results indicate that social isolation does not appear to negatively influence myelination in YAC128 mice in the same manner as was observed in WT animals, possibly due to the dominant effect of the disease phenotype. However, mean axonal diameter changes due to social isolation in WT and YAC128 mice were diametrically opposed, which might suggest that the (currently unknown) environmental deprivation mechanism(s) leading to increases in axonal diameter in WT animals is reversed by the YAC128 disease phenotype. Regardless of mechanism, our results indicate that signal conduction velocities in deprived YAC128 mice may be decreased as a result of decreased axonal diameter (Waxman, 1980), which could tentatively suggest that social isolation may exacerbate the development of symptoms in HD models.

Finally, our study revealed no significant differences in mature oligodendrocyte population, labeled by GST-pi positive cells, to 14 weeks of social deprivation in 18-week-old mice. This observation appears in keeping with a previous report of no change in oligodendrocyte density in mPFC after a 2 or 4-week period of social deprivation in juvenile mice, although shorter processes, fewer branches and fewer internodes per cell in oligodendrocytes were also described (Makinodan et al., 2012). Also of note, 8 weeks of social isolation in adult mice (16 weeks old) did not affect nodal length in the PFC, however, the expression of some oligodendrocyte specific paranodal genes were lower compared to standard house control (Liu et al., 2012). Taken together, and in combination with our environmental enrichment study, these findings suggest that environmental manipulation in both directions has little effect on mature oligodendrocyte numbers, at least at the time points studied, and on this mouse background.

Brain and body weight changes as an effect of social deprivation

No significant differences in brain weight between any of the groups were found at the age of 4.5 months regardless of genotype or housing manipulation. All groups gained in body weight over the duration of the study. No significant differences were observed between any of the female groups as a result of social deprivation, although the WT deprived female mice exhibited slightly increased body weights compared to WT females in standard housing conditions. This observation is consistent with a previous study that reported isolated female rats (7 weeks post-weaning) to weigh approximately 10% more than their standard housing counterparts (Hermes et al., 2011). In addition, our study showed no significant effect of deprivation on male groups either, although WT DH males were consistently of a lower body weight compared to WT SH males. A recent study has similarly shown that socially isolated juvenile C57BL/6 male mice (3 weeks of isolation) exhibited a decreased body weight, whereas isolated adult mice exhibited no alterations in body weight (Lander et al., 2017). Conflicting results related to the effect of social deprivation on body weight in animals have been ascribed to a number of factors, including paradigm duration, sex, strain or species of animal (Sakakibara et al., 2012; Sun et al., 2014). As for the reason for gender specific differences in body weight in deprived WT mice, it is possible that this is due to known difference in food intake in different sexes as a result of the potential chronic stress induced by the experimental condition (Sun et al., 2014). On the other hand, the body weights of YAC128 mice closely overlapped, regardless of sex or housing condition, suggesting that while social deprivation has minor effects on the body weights of WT animals, it does not affect YAC128 mice, at least at the time-points studied. This again would be consistent with a dominant effect of the disease as seen for myelin-related characteristics, as described earlier.

6.4. Microbiota manipulation effects on the BACHD mouse and WT control

Myelination and axonal diameter differences as a result of microbiota manipulation

Overall, ultrastructural analyses indicated that a germ free (GF) environment had a greater effect on the number, diameter size, and extent of myelination of axons in the anterior mid-body region of the corpus callosum (CC) in BACHD animals compared to WT controls. More specifically, overall myelination thickness in WT animals showed relatively little response to GF manipulation, and the number of regular and irregular myelinated axons was also not affected in these animals. In contrast, BACHD mice raised and maintained under GF conditions showed a larger number of small to mid-range diameter axons associated with thicker myelin sheaths (lower g-ratios) compared to both BACHD SPF, as well as WT GF controls, and exhibited a higher number of regular shaped myelinated axons, and a lower number of irregular shaped myelinated axons compared to BACHD controls housed in SPF conditions. Thus, based on the literature presented in the introduction chapter, we speculate that a germ-free environment could promote myelination of small diameter axons through one or a combination of mechanisms. This may happen through facilitation of an increase in axonal myelination diameter of previously under-threshold diameter axons to above the required threshold for myelination, such that supra-threshold axons would then become new candidates for possible myelination, as previously observed in cerebellar granule cells (Goebbels et al., 2017). Alternatively, already myelinated axons could receive further ensheathment, and thus, become hypermyelinated, possibly through alterations in intrinsic oligodendrocytes programs (Bechler et al., 2017), or modifications of axonal cues (Brinkmann et al., 2008; Hines et al., 2015). Indeed, axonal signaling has been recently demonstrated to modulate myelin sheath characteristics (Gautier et al., 2015; Gibson et al., 2014; Hines et al., 2015; Wake et al., 2015). Furthermore, increased neuronal activity, induced through optogenetic stimulation, was associated with thicker myelin sheaths in the

projection fibres arising from the premotor cortex and entering the CC (Gibson et al., 2014). Thus, although this remains to be demonstrated by future studies, it is possible that neuronal activity may be increased in BACHD animals raised in a germ-free environment, and lead to hypermyelination in small and medium-sized axons. On the other hand, an interesting follow-up would be to determine whether the hypermyelination observed, using g-ratio calculation, translates into thicker myelin, or whether the observation is rather due to decreased compactness of the myelin sheaths which could make the myelin sheaths appear thicker. Compactness can be easily determined in electron micrographs by calculating the ratio between myelin thickness and number of myelin lamellae.

Hypermyelination was previously reported in wild-type GF animals, where male GF mice presented with thicker myelin sheaths in PFC axons, but no difference in axonal diameter, compared to SPF controls (Hoban et al., 2016b). In contrast, our study indicates overall similar myelin sheath thickness between wild-type GF and SPF animal, although with small variations, such as hypomyelination at small diameter axons, and a trend towards hypermyelination at large diameter axons, while similar myelination was observed at mid-range diameter axons. The overall g-ratio in our findings is reflective of the fact that mid-range axons represent the majority of the axonal population in this anterior region of the CC investigated. Possible reasons for discrepancy in findings between our study and (Hoban et al., 2016b) are the brain region investigated (anterior CC here vs PFC), the age of the animals (12 vs 10 weeks), or the mouse genetic background (FVB/N vs Swiss Webster). It is also possible that the PFC might be particularly susceptible to microbiota-driven changes in a way that the CC is not, since myelination in the PFC was previously speculated to be particularly plastic and susceptible to adaptation due to environmental, as well as social factors (Forbes & Gallo, 2017; Mount & Monje, 2017; Tomlinson, Leiton, & Colognato, 2016b). This possibility is further supported, by observations of no differences in relative myelin-related protein expression in other brain regions, such as the frontal cortex (rather than specifically the prefrontal region of the cortex), amygdala, cerebellum, hippocampus or striatum, as

result of a GF environment, although ultrastructural myelin characteristics in these regions were notably not investigated (Hoban et al., 2016b).

Another method frequently used to deplete animals of gut microbiota, with similar effects of a germ-free environment, is through the use antibiotic treatment (Reikvam et al., 2011). The use of a cocktail of antibiotics, aimed at different bacterial strains, was shown to have transient alteration effects on the diversity and composition of the gut microbiota (Bercik et al., 2011; Minter et al., 2017; Puhl et al., 2012). Alternatively, alteration of microbiota composition can be obtained by transplant of faecal or cecal content from one subject to that of another. A combination of both methods, by first depleting existing host microbiota with antibiotics, followed by faecal / cecal transplant of microbiota from another host, can be used to examine the effects of certain strains of microbiota on the recipient host, and the impact of microbiota from a diseased donor to a healthy donor, or vice-versa. Using this combination of microbiota manipulation methods Gacias et al. (2016) initially depleted wild-type C57BL/6 mice of their own microbiota, followed by transplant of microbiota from diabetic mice, which were either treated with antibiotics or treated with a vehicle. They reported increased myelin thickness, in the medial region of the PFC (mPFC), but not nucleus accumbens, of 13 weeks old wild-type mice recipients of microbiota from antibiotic-treated diabetics, compared to recipients of microbiota from vehicle-treated diabetics (Gacias et al., 2016). This effect was ascribed to exposure of oligodendrocytes to raised levels of the metabolite cresol, the synthesis of which modified by gut microbiota, prevented myelin gene expression and differentiation (Gacias et al., 2016). It is therefore tempting to speculate that the effects of GF conditions on myelination in BACHD mice may also reflect intrinsic changes in HD oligodendroglia and their response to similar microbiota-derived metabolites.

Therefore, our results, and the sparse available literature, suggest that gut microbiota can regulate myelination of cortical and callosal axons, and can exert this influence to different extents in different brain regions, and which could also be modulated, in part, by the health status of the animal.

Additionally, it is possible that the intrinsic pathological characteristics of HD animal models confers these animals with a higher susceptibility to myelination alterations in response to certain environmental manipulations, such as microbiota manipulation, but not others, such as social isolation (see previous chapter).

Myelin-related protein differences

Both MBP and PLP are compact myelin proteins, and among the most abundant specific myelin-related proteins in the CNS (Boggs, 2006). Our findings showed a general decrease in both MBP and PLP expression levels, in WT GF animals compared SPF controls. Notably, MBP expression levels were significantly lower in the PFC of WT GF animals compared to SPF controls, and a similar non-significant trend of lower levels of PLP expression was also identified in WT GF mice compared to SPF controls. This finding is consistent with a reduction of mature oligodendrocytes identified in the PFC of WT GF animals compared to WT SPF, but at variance to a previous study that found increased MBP levels in the PFC of wild-type GF animals (Hoban et al., 2016b). Again, differences in mouse genetic background (FVB/N here vs Swiss Webster), or possibly the age of the animals (12 vs 10 weeks) may underpin differences in findings.

Interestingly, BACHD GF animals also showed a non-significant trend towards lower levels of MBP and PLP in the prefrontal cortex, compared to BACHD SPF animals. However, it is important to note that our findings related to hypermyelination in the BACHD GF mouse described earlier were identified in the anterior corpus callosum, which limits an overarching interpretation of our myelin-related measures. As a result, we cannot exclude that a germ-free environment produced differential myelin-related effects on the CC and PFC of the BACHD mouse.

Regulation of oligodendroglial (OLs) population by microbiota

We further used several markers to identify oligodendrocytes at different stages of development in the CC and PFC of our experimental groups. We used the following markers to identify oligodendrocyte precursor cells

(PDGFRα+), oligodendrocyte lineage population (Olig2+), and mature myelinating oligodendrocytes (GST-pi+).

The comparison between wild-type groups revealed comparable numbers of oligodendrocyte precursor cells (OPCs) in both brain regions investigated, however, a minor reduction in number of oligodendroglial lineage, and a significant reduction of mature oligodendrocytes cells in the PFC of WT mice reared in GF conditions compared to SPF controls was also observed. The comparison between BACHD groups revealed OPC numbers in the PFC region to be comparable, while Olig2+ cell numbers were similar in both the PFC and CC regions. In addition, similarly to WT groups, a reduction in mature oligodendrocytes was identified in the PFC of BACHD GF animals compared to SPF controls. Analysis of microbiota influence on oligodendrocytes populations in the CC region of the WT mouse showed similar, statistically non-significant, trends to that in the PFC, although some variance was observed in BACHD animals. These findings suggest that while OPC numbers may not be affected by a germ-free environment, a proportion of these in the PFC region of both WT and BACHD animals might lose their capacity to differentiate into mature oligodendrocytes when placed in a germ-free environment. Past studies observed that the rate of OPC differentiation into oligodendrocytes was faster in the cortex than other white matter regions (Young et al., 2013), while myelination in this region was previously demonstrated to be highly plastic and malleable, particularly in response to environmental manipulation (Forbes & Gallo, 2017; Mount & Monje, 2017). These findings highlight the possibility that cortical oligodendroglia may be more vulnerable to germ-free environments than populations in other regions of the brain. Thus, gut microbiota may be indirectly involved in the regulation of oligodendroglial development (Nishiyama et al., 2009), particularly the maturation of oligodendrocytes, in a regionally dependent manner in the mouse brain. The mechanisms by which microbiota regulate oligodendroglial differentiation of adult mouse brain remains to be fully elucidated.

Finally, the possible hypermyelination observed in the corpus callosum of BACHD mice under GF conditions was not underpinned by an increase in

the number of mature oligodendrocytes, as we did not observed this increase in the CC region. Possibly other mechanisms, such as axonal-related factors or signaling, as discussed earlier, or an altered capacity for oligodendrocytes to myelinate, were the cause of this possible hypermyelination. This is supported by recent evidence suggesting that the extent of axonal myelination is independent of the number of newly formed and matured oligodendrocytes (Young et al., 2013).

Differences in brain weight

We only found brain weights to differ between WT and BACHD animals when comparing males only. Brain and forebrain weights were fairly similar between WT and BACHD animals when males and females were grouped together and compared, or when females only were compared. Others have previously shown decreased forebrain weights at 12, but not 6 months of age, in BACHD animals compared to WT controls (Gray et al., 2008). Interestingly, in our study, both WT and BACHD showed a reduction in overall brain weight when placed in a germ-free environment. We also found a decrease in total brain weight in both WT and BACHD GF male mice compared to their respective SPF controls, whereas female mice brain weight reductions were only statistically significant in the BACHD GF condition compared to female BACHD SPF, although a similar trend was observed in WT GF animals compared to WT SPF.

GF animals are born through caesarian, and reared by adoptive mothers. As a result, early developmental influence of maternal rearing, which was seen to play a significant effect in brain weight (Henderson, 1973), could potentially lead to the differences we observed between our GF and SPF animals, across both genotypes. However, both environmental and genetic aspects have also been demonstrated to influence brain weight (Kruska, 2005). Thus, while it is difficult to link our finding to a particular factor, our observation does suggest that a lack of microbiota can have significant effects on the rodent brain weight.

Differences in body weight

The findings of our study revealed that BACHD animals had reduced body weights, comparable to that of WT animals, when placed in a germ-free environment. Under normal environmental conditions, BACHD mice have been reported to display significant increases in body weight compared to WT littermates (Hult et al., 2011; Pouladi, Morton, & Hayden, 2013b). Healthy mice also expressed exaggerated metabolic phenotypes of the BACHD model when mutant HTT was selectively expressed in the hypothalamus (Hult et al., 2011). In addition, inactivation of mutant HTT in 1/4th of hypothalamic neurons in the BACHD mouse was sufficient to prevent the metabolic phenotype (Hult et al., 2011). Furthermore, gut microbiota was shown to be involved in the development of the HPA axis (Clarke et al., 2013; Sudo et al., 2004). Gut microbiota was associated with the regulation of HPA via the endocrine pathway, which involves microbiota acting on peptides released by enteroendocrine cells (EEC), present in the gut epithelium, such as orexin, galanin and ghrelin (Merlino et al., 2014; Yi & Tschöp, 2012). Altered orexin receptor levels were shown in BACHD mice (Hult et al., 2013). Therefore, gut microbiota may alter hypothalamus-related mechanisms and pathways, and contribute to the overweight and obesity related phenotype seen in BACHD animals. However, it is important to note that the transcriptional profile of the healthy GF mouse showed almost no differential alteration in hypothalamus gene expression (Heijtz et al., 2011). Hence, it is possible that the presence of mutant HTT is a requirement for metabolism-related effects of gut microbiota.

In addition, our study indicated a decrease in body weight of WT GF male mice, while female mice showed very similar weights to animals reared in SPF conditions. Initial studies looking at body weight in GF animals, reported GF to weigh less, or about the same as SPF despite consuming more food (Bäckhed et al., 2004). However, it was later found that differences in body weight were dependent on the type of dietary interventions (Fleissner, 2010).

6.5. Potential future work

Taking into consideration recent findings on the oligodendroglial population capacity to myelinate during certain windows of time, assigning the animals to several periods of enrichment or deprivation, such as short-term, mid-term and long-term manipulations, could reveal transient changes that might have been missed by our long-term manipulation. Furthermore, and as described earlier, a potential reason for our lack of observation of wide-ranging behavioural changes to environmental manipulation may be due to our choice of a relatively slow onset mouse model of HD (i.e. YAC128), at an early-manifest stage of the disease. Therefore, a potential avenue for further investigation may be to extend the work presented here to more aggressive models of HD, such as the R6/1 and R6/2 mouse lines, or to use the YAC128 model at a later stage in the disease progression. In addition, from a less technical perspective, future work to help standardise environmental manipulation and behavioural test protocols would be invaluable to minimising inconsistencies in findings across studies further down the line.

An immediate follow-up to our own microbiota manipulation study would be to determine the microbiome profiling of BACHD and wild-type animals, and identify any shifts in relative abundance of gut microbial taxa at phylum or genera levels. Identifying certain bacteria strains previously correlated to neurodegeneration, inflammation, or myelin related abnormalities could aid to the understanding of the gut-microbiota-brain communication, and the potential effects of commensal bacteria on the brain.

Furthermore, to examine the interaction between gut microbiota and oligodendroglial population on an HD background, future studies could repeat our experiments in a germ-free setting using recently developed transgenic models that selectively express mutant huntingtin in oligodendrocytes (e.g. PLP-150Q). Another interesting avenue for potential research would be to first deplete existing host microbiota with antibiotics, followed by faecal transplant of microbiota from another host (HD affected mouse or human). These combined methods can be used to examine the

effects of certain strains of microbiota on the recipient host, and the impact of microbiota from a diseased donor to a healthy donor, or vice-versa.

Considering Huntington disease is an autosomal-dominant disorder, it would be of interest to determine whether human carries of the mutant *HTT* gene show any major or minor shifts in gut commensal bacteria at a pre-, early- and late-manifest stage. Correlating bacterial genera to symptoms severity, could aid to the understanding of whether certain populations of bacteria in combination with a diseased carrier could exacerbate symptoms. Moreover, it is now well known that for HD, a greater disease onset variance was associated with lower CAG repeats, potentially due to a greater influence of genetic and environmental modifiers (Langbehn et al., 2004). In addition, treatments using combinations of antibiotics can partially decrease the microbial population in the gut (Reikvam et al., 2011), and alter microbiota make-up and diversity (Bercik et al., 2011; Puhl et al., 2012). Thus, a longitudinal study following mutant *HTT* gene carriers could determine whether the use of antibiotics at different stages of life could also contribute to the variance in disease onset which cannot be explained by the number of CAG repeats. Finally, other techniques to examine the effect of environmental and microbiota manipulations on white matter changes in HD, such as diffusion tensor imaging, might also be valuable, and would have the added benefit of 'bench-to bedside' appeal, given that this technique can be conducted in pre-clinical models and validated in HD patients.

References

Aagaard, K., Ma, J., Antony, K. M., Ganu, R., Petrosino, J., & Versalovic, J. (2014). The placenta harbors a unique microbiome. *Science Translational Medicine*, *6*(237), 237ra65–237ra65. http://doi.org/10.1126/scitranslmed.3008599

Ali, N. J., & Levine, M. S. (2006). Changes in Expression of N-Methyl-D-Aspartate Receptor Subunits Occur Early in the R6/2 Mouse Model of Huntington's Disease. *Developmental Neuroscience*, *28*(3), 230–238. http://doi.org/10.1159/000091921

Almeida, R. G., Czopka, T., ffrench-Constant, C., & Lyons, D. A. (2011). Individual axons regulate the myelinating potential of single oligodendrocytes in vivo. *Development*, *138*(20), 4443–4450. http://doi.org/10.1242/dev.071001

Andrade, M. A., & Bork, P. (1995). HEAT repeats in the Huntington's disease protein. *Nature Genetics*, *11*(2), 115–116. http://doi.org/10.1038/ng1095-115

Andrew, S. E., Goldberg, Y. P., Kremer, B., Telenius, H., Theilmann, J., Adam, S., et al. (1993). The relationship between trinucleotide (CAG) repeat length and clinical features of Huntington's disease. *Nature Genetics*, *4*(4), 398–403. http://doi.org/10.1038/ng0893-398

Arendash, G. W., Garcia, M. F., Costa, D. A., Cracchiolo, J. R., Wefes, I. M., & Potter, H. (2004). Environmental enrichment improves cognition in aged Alzheimer's transgenic mice despite stable beta-amyloid deposition. *Neuroreport*, *15*(11), 1751–1754.

Arpaia, N., Campbell, C., Fan, X., Dikiy, S., van der Veeken, J., deRoos, P., et al. (2013). Metabolites produced by commensal bacteria promote peripheral regulatory T-cell generation. *Nature*, *504*(7480), 451–455. http://doi.org/10.1038/nature12726

Artis, D. (2008). Epithelial-cell recognition of commensal bacteria and maintenance of immune homeostasis in the gut. *Nature Reviews Immunology*, *8*(6), 411–420. http://doi.org/10.1038/nri2316

Asano, M., & Finlayson, M. L. (2014). Meta-analysis of three different types of fatigue management interventions for people with multiple sclerosis: exercise, education, and medication. *Multiple Sclerosis International*, *2014*(3), 798285–12. http://doi.org/10.1155/2014/798285

Asano, Y., Hiramoto, T., Nishino, R., Aiba, Y., Kimura, T., Yoshihara, K., et al. (2012). Critical role of gut microbiota in the production of biologically active, free catecholamines in the gut lumen of mice. *American Journal of Physiology. Gastrointestinal and Liver Physiology*, *303*(11), G1288–95. http://doi.org/10.1152/ajpgi.00341.2012

Aune, D., Ursin, G., & Veierød, M. B. (2009). Meat consumption and the risk of type 2 diabetes: a systematic review and meta-analysis of cohort studies. *Diabetologia*, *52*(11), 2277–2287. http://doi.org/10.1007/s00125-009-1481-x

Avendano, M., Kawachi, I., Van Lenthe, F., Boshuizen, H. C., Mackenbach, J. P., Van den Bos, G. A. M., et al. (2006). Socioeconomic status and stroke incidence in the US elderly: the role of risk factors in the EPESE study. *Stroke*, *37*(6), 1368–1373.

http://doi.org/10.1161/01.STR.0000221702.75002.66
Aziz, Q., & Thompson, D. G. (1998). Brain-gut axis in health and disease. *Gastroenterology*, *114*(3), 559–578.
Badcock, J. C., Shah, S., Mackinnon, A., Stain, H. J., Galletly, C., Jablensky, A., & Morgan, V. A. (2015). Loneliness in psychotic disorders and its association with cognitive function and symptom profile. *Schizophrenia Research*, *169*(1-3), 268–273. http://doi.org/10.1016/j.schres.2015.10.027
Bailey, M. T., & Coe, C. L. (1999). Maternal separation disrupts the integrity of the intestinal microflora in infant rhesus monkeys. *Developmental Psychobiology*, *35*(2), 146–155. http://doi.org/10.1002/(SICI)1098-2302(199909)35:2<146::AID-DEV7>3.0.CO;2-G
Bailey, M. T., Dowd, S. E., Galley, J. D., Hufnagle, A. R., Allen, R. G., & Lyte, M. (2011). Exposure to a social stressor alters the structure of the intestinal microbiota: implications for stressor-induced immunomodulation. *Brain Behavior and Immunity*, *25*(3), 397–407. http://doi.org/10.1016/j.bbi.2010.10.023
Bajaj, J. S., Ahluwalia, V., Steinberg, J. L., Hobgood, S., Boling, P. A., Godschalk, M., et al. (2016). Elderly patients have an altered gut-brain axis regardless of the presence of cirrhosis. *Scientific Reports*, 1–12. http://doi.org/10.1038/srep38481
Baker, L. D., Frank, L. L., Foster-Schubert, K., Green, P. S., Wilkinson, C. W., McTiernan, A., Cholerton, B. A., et al. (2010a). Aerobic Exercise Improves Cognition for Older Adults with Glucose Intolerance, A Risk Factor for Alzheimer's Disease. *Journal of Alzheimer's Disease*, *22*(2), 569–579. http://doi.org/10.3233/JAD-2010-100768
Baker, L. D., Frank, L. L., Foster-Schubert, K., Green, P. S., Wilkinson, C. W., McTiernan, A., Plymate, S. R., et al. (2010b). Effects of aerobic exercise on mild cognitive impairment: a controlled trial. *Archives of Neurology*, *67*(1), 71–79. http://doi.org/10.1001/archneurol.2009.307
Banati, M., Csecsei, P., Koszegi, E., Nielsen, H. H., Suto, G., Bors, L., et al. (2013). Antibody response against gastrointestinal antigens in demyelinating diseases of the central nervous system. *European Journal of Neurology*, *20*(11), 1492–1495. http://doi.org/10.1111/ene.12072
Bankston, A. N., Mandler, M. D., & Feng, Y. (2013). Oligodendroglia and neurotrophic factors in neurodegeneration. *Neuroscience Bulletin*, *29*(2), 216–228. http://doi.org/10.1007/s12264-013-1321-3
Barres, B. A. (2008). The Mystery and Magic of Glia: A Perspective on Their Roles in Health and Disease. *Neuron*, *60*(3), 430–440. http://doi.org/10.1016/j.neuron.2008.10.013
Bartzokis, G., Lu, P. H., Tishler, T. A., Fong, S. M., Oluwadara, B., Finn, J. P., et al. (2007). Myelin Breakdown and Iron Changes in Huntington's Disease: Pathogenesis and Treatment Implications. *Neurochemical Research*, *32*(10), 1655–1664. http://doi.org/10.1007/s11064-007-9352-7
Baumann, N., & Pham-Dinh, D. (2001). Biology of oligodendrocyte and myelin in the mammalian central nervous system. *Physiological Reviews*, *81*(2), 871–927. http://doi.org/10.1152/physrev.2001.81.2.871
Baxter, A. G. (2007). The origin and application of experimental autoimmune encephalomyelitis. *Nature Reviews Immunology*, *7*(11), 904–912.

http://doi.org/10.1038/nri2190
Bäckhed, F., Ding, H., Wang, T., Hooper, L. V., Koh, G. Y., Nagy, A., et al. (2004). The gut microbiota as an environmental factor that regulates fat storage. *Proceedings of the National Academy of Sciences*, *101*(44), 15718–15723. http://doi.org/10.1073/pnas.0407076101
Bäckhed, F., Ley, R. E., Sonnenburg, J. L., Peterson, D. A., & Gordon, J. I. (2005). Host-bacterial mutualism in the human intestine. *Science*, *307*(5717), 1915–1920. http://doi.org/10.1126/science.1104816
Bäckhed, F., Manchester, J. K., Semenkovich, C. F., & Gordon, J. I. (2007). Mechanisms underlying the resistance to diet-induced obesity in germ-free mice. *Proceedings of the National Academy of Sciences*, *104*(3), 979–984. http://doi.org/10.1073/pnas.0605374104
Bäckhed, F., Roswall, J., Peng, Y., Feng, Q., Jia, H., Kovatcheva-Datchary, P., et al. (2015). Dynamics and Stabilization of the Human Gut Microbiome during the First Year of Life. *Cell Host and Microbe*, *17*(5), 690–703. http://doi.org/10.1016/j.chom.2015.04.004
Bechler, M. E., Byrne, L., & ffrench-Constant, C. (2015). CNS Myelin Sheath Lengths Are an Intrinsic Property of Oligodendrocytes. *Current Biology*, *25*(18), 2411–2416. http://doi.org/10.1016/j.cub.2015.07.056
Bechler, M. E., Swire, M., & ffrench-Constant, C. (2017). Intrinsic and adaptive myelination-A sequential mechanism for smart wiring in the brain. *Developmental Neurobiology*, *138*, 4443–12. http://doi.org/10.1002/dneu.22518
Benaroya-Milshtein, N., Hollander, N., Apter, A., Kukulansky, T., Raz, N., Wilf, A., et al. (2004). Environmental enrichment in mice decreases anxiety, attenuates stress responses and enhances natural killer cell activity. *European Journal of Neuroscience*, *20*(5), 1341–1347. http://doi.org/10.1111/j.1460-9568.2004.03587.x
Bence, N. F. (2001). Impairment of the Ubiquitin-Proteasome System by Protein Aggregation. *Science*, *292*(5521), 1552–1555. http://doi.org/10.1126/science.292.5521.1552
Bengtsson, S. L., Nagy, Z., Skare, S., Forsman, L., Forssberg, H., & Ullén, F. (2005). Extensive piano practicing has regionally specific effects on white matter development. *Nature Neuroscience*, *8*(9), 1148–1150. http://doi.org/10.1038/nn1516
Benn, C. L., Slow, E. J., Farrell, L. A., Graham, R., Deng, Y., Hayden, M. R., & Cha, J. H. J. (2007). Glutamate receptor abnormalities in the YAC128 transgenic mouse model of Huntington's disease. *Neuroscience*, *147*(2), 354–372. http://doi.org/10.1016/j.neuroscience.2007.03.010
Bennett, E. J., Bence, N. F., Jayakumar, R., & Kopito, R. R. (2005). Global Impairment of the Ubiquitin-Proteasome System by Nuclear or Cytoplasmic Protein Aggregates Precedes Inclusion Body Formation. *Molecular Cell*, *17*(3), 351–365. http://doi.org/10.1016/j.molcel.2004.12.021
Benraiss, A., Wang, S., Herrlinger, S., Li, X., Chandler-Militello, D., Mauceri, J., et al. (2016). Human glia can both induce and rescue aspects of disease phenotype in Huntington disease. *Nature Communications*, *7*, 11758. http://doi.org/10.1038/ncomms11758
Bercik, P., Collins, S. M., & Verdu, E. F. (2012). Microbes and the gut-brain axis. *Neurogastroenterology & Motility*, *24*(5), 405–413.

http://doi.org/10.1111/j.1365-2982.2012.01906.x
Bercik, P., Denou, E., Collins, J., Jackson, W., Lu, J., Jury, J., et al. (2011). The Intestinal Microbiota Affect Central Levels of Brain-Derived Neurotropic Factor and Behavior in Mice. *Gastroenterology*, *141*(2), 599–609.e3. http://doi.org/10.1053/j.gastro.2011.04.052
Bercury, K. K., & Macklin, W. B. (2015). Dynamics and Mechanisms of CNS Myelination. *Developmental Cell*, *32*(4), 447–458. http://doi.org/10.1016/j.devcel.2015.01.016
Berer, K., Mues, M., Koutrolos, M., Rasbi, Z. A., Boziki, M., Johner, C., et al. (2011). Commensal microbiota and myelin autoantigen cooperate to trigger autoimmune demyelination. *Nature*, *479*(7374), 538–541. http://doi.org/10.1038/nature10554
Besten, den, G., van Eunen, K., Groen, A. K., Venema, K., Reijngoud, D.-J., & Bakker, B. M. (2013). The role of short-chain fatty acids in the interplay between diet, gut microbiota, and host energy metabolism. *Journal of Lipid Research*, *54*(9), 2325–2340. http://doi.org/10.1194/jlr.R036012
Binder, M. D., Cate, H. S., Prieto, A. L., Kemper, D., Butzkueven, H., Gresle, M. M., et al. (2008). Gas6 deficiency increases oligodendrocyte loss and microglial activation in response to cuprizone-induced demyelination. *The Journal of Neuroscience : the Official Journal of the Society for Neuroscience*, *28*(20), 5195–5206. http://doi.org/10.1523/JNEUROSCI.1180-08.2008
Björkqvist, M., Wild, E. J., Thiele, J., Silvestroni, A., Andre, R., Lahiri, N., et al. (2008). A novel pathogenic pathway of immune activation detectable before clinical onset in Huntington's disease. *The Journal of Experimental Medicine*, *205*(8), 1869–1877. http://doi.org/10.1084/jem.20080178
Bjørkøy, G., Lamark, T., Brech, A., Outzen, H., Perander, M., Øvervatn, A., et al. (2005). p62/SQSTM1 forms protein aggregates degraded by autophagy and has a protective effect on huntingtin-induced cell death. *The Journal of Cell Biology*, *171*(4), 603–614. http://doi.org/10.1083/jcb.200507002
Boggs, J. M. (2006). Myelin basic protein: a multifunctional protein. *Cellular and Molecular Life Sciences*, *63*(17), 1945–1961. http://doi.org/10.1007/s00018-006-6094-7
Bos, K., Zeanah, C. H., Fox, N. A., Drury, S. S., McLaughlin, K. A., & Nelson, C. A. (2011). Psychiatric outcomes in young children with a history of institutionalization. *Harvard Review of Psychiatry*, *19*(1), 15–24. http://doi.org/10.3109/10673229.2011.549773
Bourbon-Teles, J., Bells, S., Jones, D. K., Coulthard, E., Rosser, A., & Metzler-Baddeley, C. (2017). Myelin breakdown in human Huntingtonâ€™s disease: Multi-modal evidence from diffusion MRI and quantitative magnetization transfer, 1–14. http://doi.org/10.1016/j.neuroscience.2017.05.042
Bradford, J., Shin, J. Y., Roberts, M., Wang, C. E., Li, X. J., & Li, S. (2009). Expression of mutant huntingtin in mouse brain astrocytes causes age-dependent neurological symptoms. *Proceedings of the National Academy of Sciences*, *106*(52), 22480–22485. http://doi.org/10.1073/pnas.0911503106
Brandscheid, C., Schuck, F., Reinhardt, S., Schäfer, K.-H., Pietrzik, C. U.,

Grimm, M., et al. (2016). Altered Gut Microbiome Composition and Tryptic Activity of the 5xFAD Alzheimer's Mouse Model. *Journal of Alzheimer's Disease*, *56*(2), 775–788. http://doi.org/10.3233/JAD-160926

Braniste, V., Al-Asmakh, M., Kowal, C., Anuar, F., Abbaspour, A., Tóth, M., et al. (2014). The gut microbiota influences blood-brain barrier permeability in mice. *Science Translational Medicine*, *6*(263), 263ra158–263ra158. http://doi.org/10.1126/scitranslmed.3009759

Branton, W. G., Lu, J. Q., Surette, M. G., Holt, R. A., Lind, J., Laman, J. D., & Power, C. (2016). Brain microbiota disruption within inflammatory demyelinating lesions in multiple sclerosis, 1–10. http://doi.org/10.1038/srep37344

Bravo, J. A., Forsythe, P., Chew, M. V., Escaravage, E., Savignac, H. M., Dinan, T. G., et al. (2011). Ingestion of Lactobacillus strain regulates emotional behavior and central GABA receptor expression in a mouse via the vagus nerve. *Proceedings of the National Academy of Sciences of the United States of America*, *108*(38), 16050–16055. http://doi.org/10.1073/pnas.1102999108

Brenes, J. C., Rodríguez, O., & Fornaguera, J. (2008a). Differential effect of environment enrichment and social isolation on depressive-like behavior, spontaneous activity and serotonin and norepinephrine concentration in prefrontal cortex and ventral striatum. *Pharmacology Biochemistry and Behavior*, *89*(1), 85–93. http://doi.org/10.1016/j.pbb.2007.11.004

Brenes, J. C., Rodríguez, O., & Fornaguera, J. (2008b). Differential effect of environment enrichment and social isolation on depressive-like behavior, spontaneous activity and serotonin and norepinephrine concentration in prefrontal cortex and ventral striatum. *Pharmacology Biochemistry and Behavior*, *89*(1), 85–93. http://doi.org/10.1016/j.pbb.2007.11.004

Brenes, J., Padilla, M., & Fornaguera, J. (2009). A detailed analysis of open-field habituation and behavioral and neurochemical antidepressant-like effects in postweaning enriched rats. *Behavioural Brain Research*, *197*(1), 125–137. http://doi.org/10.1016/j.bbr.2008.08.014

Brinkmann, B. G., Agarwal, A., Sereda, M. W., Garratt, A. N., Müller, T., Wende, H., et al. (2008). Neuregulin-1/ErbB signaling serves distinct functions in myelination of the peripheral and central nervous system. *Neuron*, *59*(4), 581–595. http://doi.org/10.1016/j.neuron.2008.06.028

Brooks, S. P., & Dunnett, S. B. (2009). Tests to assess motor phenotype in mice: a user's guide. *Nature Publishing Group*, *10*(7), 519–529. http://doi.org/10.1038/nrn2652

Bujalka, H., Koenning, M., Jackson, S., Perreau, V. M., Pope, B., Hay, C. M., et al. (2013). MYRF Is a Membrane-Associated Transcription Factor That Autoproteolytically Cleaves to Directly Activate Myelin Genes. *PLoS Biology*, *11*(8), e1001625–15. http://doi.org/10.1371/journal.pbio.1001625

Butler, T. R., Carter, E., & Weiner, J. L. (2014). Adolescent Social Isolation Does Not Lead to Persistent Increases in Anxiety- Like Behavior or Ethanol Intake in Female Long-Evans Rats. *Alcoholism: Clinical and Experimental Research*, *38*(8), 2199–2207. http://doi.org/10.1111/acer.12476

Butt, A. M., Ibrahim, M., & Berry, M. (1998). Axon-myelin sheath relations of oligodendrocyte unit phenotypes in the adult rat anterior medullary velum. *Journal of Neurocytology*, *27*(4), 259–269.

Cacioppo, J. T., & Hawkley, L. C. (2009). Perceived social isolation and cognition. *Trends in Cognitive Sciences*, *13*(10), 447–454. http://doi.org/10.1016/j.tics.2009.06.005

Cacioppo, J. T., Hughes, M. E., Waite, L. J., Hawkley, L. C., & Thisted, R. A. (2006). Loneliness as a specific risk factor for depressive symptoms: cross-sectional and longitudinal analyses. *Psychology and Aging*, *21*(1), 140–151. http://doi.org/10.1037/0882-7974.21.1.140

Camilleri, M., Lasch, K., & Zhou, W. (2012). Irritable bowel syndrome: methods, mechanisms, and pathophysiology. The confluence of increased permeability, inflammation, and pain in irritable bowel syndrome. *American Journal of Physiology. Gastrointestinal and Liver Physiology*, *303*(7), G775–85. http://doi.org/10.1152/ajpgi.00155.2012

Cani, P. D., Everard, A., & Duparc, T. (2013). Gut microbiota, enteroendocrine functions and metabolism. *Current Opinion in Pharmacology*, *13*(6), 935–940. http://doi.org/10.1016/j.coph.2013.09.008

Cantarel, B. L., Waubant, E., Chehoud, C., Kuczynski, J., DeSantis, T. Z., Warrington, J., et al. (2015). Gut microbiota in multiple sclerosis: possible influence of immunomodulators. *Journal of Investigative Medicine : the Official Publication of the American Federation for Clinical Research*, *63*(5), 729–734. http://doi.org/10.1097/JIM.0000000000000192

Cao, M., Pu, T., Wang, L., Marshall, C., He, H., Hu, G., & Xiao, M. (2017). Early enriched physical environment reverses impairments of the hippocampus, but not medial prefrontal cortex, of socially-isolated mice, 1–12. http://doi.org/10.1016/j.bbi.2017.04.009

Carter, R. J., Hunt, M. J., & Morton, A. J. (2000). Environmental stimulation increases survival in mice transgenic for exon 1 of the Huntington's disease gene. *Movement Disorders*, *15*(5), 925–937.

Caviston, J. P., & Holzbaur, E. L. F. (2009). Huntingtin as an essential integrator of intracellular vesicular trafficking. *Trends in Cell Biology*, *19*(4), 147–155. http://doi.org/10.1016/j.tcb.2009.01.005

Câmara, J., Wang, Z., Nunes-Fonseca, C., Friedman, H. C., Grove, M., Sherman, D. L., et al. (2009). Integrin-mediated axoglial interactions initiate myelination in the central nervous system. *The Journal of Cell Biology*, *185*(4), 699–712. http://doi.org/10.1083/jcb.200807010

Cha, J. H., Kosinski, C. M., Kerner, J. A., Alsdorf, S. A., Mangiarini, L., Davies, S. W., et al. (1998). Altered brain neurotransmitter receptors in transgenic mice expressing a portion of an abnormal human huntington disease gene. *Proceedings of the National Academy of Sciences of the United States of America*, *95*(11), 6480–6485.

Chan, W. Y., Kohsaka, S., & Rezaie, P. (2007). The origin and cell lineage of microglia: new concepts. *Brain Research Reviews*, *53*(2), 344–354. http://doi.org/10.1016/j.brainresrev.2006.11.002

Chen, J., Chia, N., Kalari, K. R., Yao, J. Z., Novotna, M., Soldan, M. M. P., et al. (2016). Multiple sclerosis patients have a distinct gut microbiota compared to healthy controls. *Scientific Reports*, 1–10. http://doi.org/10.1038/srep28484

Cho, I., Yamanishi, S., Cox, L., Methé, B. A., Zavadil, J., Li, K., et al. (2012). Antibiotics in early life alter the murine colonic microbiome and adiposity.

Nature, *488*(7413), 621–626. http://doi.org/10.1038/nature11400
Chomiak, T., & Hu, B. (2009). What Is the Optimal Value of the g-Ratio for Myelinated Fibers in the Rat CNS? A Theoretical Approach. *PLoS ONE*, *4*(11), e7754–7. http://doi.org/10.1371/journal.pone.0007754
Chow, J., & Mazmanian, S. K. (2010). A pathobiont of the microbiota balances host colonization and intestinal inflammation. *Cell Host and Microbe*, *7*(4), 265–276. http://doi.org/10.1016/j.chom.2010.03.004
Chrast, R., Saher, G., Nave, K.-A., & Verheijen, M. H. G. (2011). Lipid metabolism in myelinating glial cells: lessons from human inherited disorders and mouse models. *Journal of Lipid Research*, *52*(3), 419–434. http://doi.org/10.1194/jlr.R009761
Christine K Fleissner, N. H. M. M. A. E.-B. G. L. S. K. M. B. (2010). Absence of intestinal microbiota does not protect mice from diet-induced obesity. *Doi.org*, 1–11. http://doi.org/10.1017/S0007114510001303
Chugani, H. T., Behen, M. E., Muzik, O., Juhász, C., Nagy, F., & Chugani, D. C. (2001). Local brain functional activity following early deprivation: a study of postinstitutionalized Romanian orphans. *NeuroImage*, *14*(6), 1290–1301. http://doi.org/10.1006/nimg.2001.0917
Ciarmiello, A., Cannella, M., Lastoria, S., Simonelli, M., Frati, L., Rubinsztein, D. C., & Squitieri, F. (2006). Brain white-matter volume loss and glucose hypometabolism precede the clinical symptoms of Huntington's disease. *Journal of Nuclear Medicine : Official Publication, Society of Nuclear Medicine*, *47*(2), 215–222.
Claesson, M. J., Cusack, S., O'Sullivan, O., Greene-Diniz, R., de Weerd, H., Flannery, E., et al. (2011). Composition, variability, and temporal stability of the intestinal microbiota of the elderly. *Proceedings of the National Academy of Sciences of the United States of America*, *108 Suppl 1*(Supplement_1), 4586–4591. http://doi.org/10.1073/pnas.1000097107
Clarke, G., Grenham, S., Scully, P., Fitzgerald, P., Moloney, R. D., Shanahan, F., et al. (2013). The microbiome-gut-brain axis during early life regulates the hippocampal serotonergic system in a sex-dependent manner. *Molecular Psychiatry*, *18*(6), 666–673. http://doi.org/10.1038/mp.2012.77
Clarke, L. E., Young, K. M., Hamilton, N. B., Li, H., Richardson, W. D., & Attwell, D. (2012). Properties and Fate of Oligodendrocyte Progenitor Cells in the Corpus Callosum, Motor Cortex, and Piriform Cortex of the Mouse. *Journal of Neuroscience*, *32*(24), 8173–8185. http://doi.org/10.1523/JNEUROSCI.0928-12.2012
Coelho, R. P., Yuelling, L. M., Fuss, B., & Sato-Bigbee, C. (2009). Neurotrophin-3 targets the translational initiation machinery in oligodendrocytes. *Glia*, *57*(16), 1754–1764. http://doi.org/10.1002/glia.20888
Constantinescu, C. S., Farooqi, N., O'Brien, K., & Gran, B. (2012). Experimental autoimmune encephalomyelitis (EAE) as a model for multiple sclerosis (MS). *British Journal of Pharmacology*, *164*(4), 1079–1106. http://doi.org/10.1111/j.1476-5381.2011.01302.x
Copray, S., Huynh, J. L., Sher, F., Casaccia-Bonnefil, P., & Boddeke, E. (2009). Epigenetic mechanisms facilitating oligodendrocyte development, maturation, and aging. *Glia*, *57*(15), 1579–1587.
Corrêa-Oliveira, R. C. E., Fachi, J. E. L. I. S., Vieira, A., Sato, F. T., & Vinolo,

M. A. E. L. R. (2016). Regulation of immune cell function by short-chain fatty acids, *5*(4), e73–8. http://doi.org/10.1038/cti.2016.17
http://doi.org/10.1002/glia.20881
Cox, L. M., Yamanishi, S., Sohn, J., Alekseyenko, A. V., Leung, J. M., Cho, I., et al. (2014). Altering the intestinal microbiota during a critical developmental window has lasting metabolic consequences. *Cell*, *158*(4), 705–721. http://doi.org/10.1016/j.cell.2014.05.052
Cox, M. A., Jackson, J., Stanton, M., Rojas-Triana, A., Bober, L., Laverty, M., et al. (2009). Short-chain fatty acids act as antiinflammatory mediatorsby regulating prostaglandin E2 and cytokines. *World Journal of Gastroenterology*, *15*(44), 5549–5557. http://doi.org/10.3748/wjg.15.5549
Coyle, J. T., & Schwarcz, R. (1976). Lesion of striatal neurons with kainic acid provides a model for Huntington's chorea. *Nature*, *263*(5574), 244–246. http://doi.org/10.1038/263244a0
Crofton, E. J., Zhang, Y., & Green, T. A. (2015). Inoculation stress hypothesis of environmental enrichment. *Neuroscience and Biobehavioral Reviews*, *49*, 19–31. http://doi.org/10.1016/j.neubiorev.2014.11.017
Crotti, A., Benner, C., Kerman, B. E., Gosselin, D., Lagier-Tourenne, C., Zuccato, C., et al. (2014). Mutant Huntingtin promotes autonomous microglia activation via myeloid lineage-determining factors. *Nature Neuroscience*, *17*(4), 513–521. http://doi.org/10.1038/nn.3668
Cruickshank, T. M., Thompson, J. A., Domínguez D, J. F., Reyes, A. P., Bynevelt, M., Georgiou-Karistianis, N., et al. (2015). The effect of multidisciplinary rehabilitation on brain structure and cognition in Huntington's disease: an exploratory study. *Brain and Behavior*, *5*(2), n/a–n/a. http://doi.org/10.1002/brb3.312
Cryan, J. F., & O'Mahony, S. M. (2011). The microbiome-gut-brain axis: from bowel to behavior. *Neurogastroenterology and Motility : the Official Journal of the European Gastrointestinal Motility Society*, *23*(3), 187–192. http://doi.org/10.1111/j.1365-2982.2010.01664.x
Cui, L., Jeong, H., Borovecki, F., Parkhurst, C. N., Tanese, N., & Krainc, D. (2006). Transcriptional Repression of PGC-1α by Mutant Huntingtin Leads to Mitochondrial Dysfunction and Neurodegeneration. *Cell*, *127*(1), 59–69. http://doi.org/10.1016/j.cell.2006.09.015
Czopka, T., ffrench-Constant, C., & Lyons, D. A. (2013). Individual Oligodendrocytes Have Only a Few Hours in which to Generate New Myelin Sheaths In Vivo. *Developmental Cell*, *25*(6), 599–609. http://doi.org/10.1016/j.devcel.2013.05.013
Dahlqvist, P., Rönnbäck, A., Bergström, S.-A., Söderström, I., & Olsson, T. (2004). Environmental enrichment reverses learning impairment in the Morris water maze after focal cerebral ischemia in rats. *European Journal of Neuroscience*, *19*(8), 2288–2298. http://doi.org/10.1111/j.0953-816X.2004.03248.x
Dai, X., Lercher, L. D., Clinton, P. M., Du, Y., Livingston, D. L., Vieira, C., et al. (2003). The trophic role of oligodendrocytes in the basal forebrain. *The Journal of Neuroscience : the Official Journal of the Society for Neuroscience*, *23*(13), 5846–5853.
Dangata, Y. Y., Findlater, G. S., & Kaufman, M. H. (1996). Postnatal

development of the optic nerve in (C57BL x CBA)F1 hybrid mice: general changes in morphometric parameters. *Journal of Anatomy*, *189 (Pt 1)*(Pt 1), 117–125. http://doi.org/10.1111/(ISSN)1469-7580
David, L. A., Maurice, C. F., Carmody, R. N., Gootenberg, D. B., Button, J. E., Wolfe, B. E., et al. (2014). Diet rapidly and reproducibly alters the human gut microbiome. *Nature*, *505*(7484), 559–563. http://doi.org/10.1038/nature12820
de Hoz, L., & Simons, M. (2014). The emerging functions of oligodendrocytes in regulating neuronal network behaviour. *BioEssays*, *37*(1), 60–69. http://doi.org/10.1002/bies.201400127
de Lartigue, G., La Serre, de, C. B., & Raybould, H. E. (2011). Vagal afferent neurons in high fat diet-induced obesity; intestinal microflora, gut inflammation and cholecystokinin. *Physiology & Behavior*, *105*(1), 100–105. http://doi.org/10.1016/j.physbeh.2011.02.040
DeCastro, M., Nankova, B. B., Shah, P., Patel, P., Mally, P. V., Mishra, R., & La Gamma, E. F. (2005). Short chain fatty acids regulate tyrosine hydroxylase gene expression through a cAMP-dependent signaling pathway. *Brain Research. Molecular Brain Research*, *142*(1), 28–38. http://doi.org/10.1016/j.molbrainres.2005.09.002
Desbonnet, L., Clarke, G., Shanahan, F., Dinan, T. G., & Cryan, J. F. (2014). Microbiota is essential for social development in the mouse. *Molecular Psychiatry*, *19*(2), 146–148. http://doi.org/10.1038/mp.2013.65
Dewhirst, F. E., Chien, C. C., Paster, B. J., Ericson, R. L., Orcutt, R. P., Schauer, D. B., & Fox, J. G. (1999). Phylogeny of the defined murine microbiota: altered Schaedler flora. *Applied and Environmental Microbiology*, *65*(8), 3287–3292.
Di Paola, M., Luders, E., Cherubini, A., Sanchez-Castaneda, C., Thompson, P. M., Toga, A. W., et al. (2012). Multimodal MRI Analysis of the Corpus Callosum Reveals White Matter Differences in Presymptomatic and Early Huntington's Disease. *Cerebral Cortex*, *22*(12), 2858–2866. http://doi.org/10.1093/cercor/bhr360
Diamond, M. C., Krech, D., & Rosenzweig, M. R. (1964). The effects of an enriched environment on the histology of the rat cerebral cortex. *Journal of Comparative Neurology*, *123*(1), 111–119. http://doi.org/10.1002/cne.901230110
DiFiglia, M. (1997). Aggregation of Huntingtin in Neuronal Intranuclear Inclusions and Dystrophic Neurites in Brain. *Science*, *277*(5334), 1990–1993. http://doi.org/10.1126/science.277.5334.1990
DiFiglia, M., Sapp, E., Chase, K., Schwarz, C., Meloni, A., Young, C., et al. (1995). Huntingtin is a cytoplasmic protein associated with vesicles in human and rat brain neurons. *Neuron*, *14*(5), 1075–1081.
DiGiulio, D. B. (2012). Diversity of microbes in amniotic fluid. *Seminars in Fetal & Neonatal Medicine*, *17*(1), 2–11. http://doi.org/10.1016/j.siny.2011.10.001
Dimou, L., Simon, C., Kirchhoff, F., Takebayashi, H., & Götz, M. (2008). Progeny of Olig2-expressing progenitors in the gray and white matter of the adult mouse cerebral cortex. *The Journal of Neuroscience : the Official Journal of the Society for Neuroscience*, *28*(41), 10434–10442. http://doi.org/10.1523/JNEUROSCI.2831-08.2008
Djordjevic, A., Adzic, M., Djordjevic, J., & Radojcic, M. B. (2009). Chronic

social isolation is related to both upregulation of plasticity genes and initiation of proapoptotic signaling in Wistar rat hippocampus. *Journal of Neural Transmission (Vienna, Austria : 1996)*, *116*(12), 1579–1589. http://doi.org/10.1007/s00702-009-0286-x

Domingues, H. S., Portugal, C. C., Socodato, R., & Relvas, J. B. (2016). Oligodendrocyte, Astrocyte, and Microglia Crosstalk in Myelin Development, Damage, and Repair. *Frontiers in Cell and Developmental Biology*, *4*(268), 89–16. http://doi.org/10.3389/fcell.2016.00071

Dong, H., & Csernansky, J. G. (2009). Effects of stress and stress hormones on amyloid-beta protein and plaque deposition. *Journal of Alzheimer's Disease : JAD*, *18*(2), 459–469. http://doi.org/10.3233/JAD-2009-1152

Donohoe, D. R., & Bultman, S. J. (2012). Metaboloepigenetics: interrelationships between energy metabolism and epigenetic control of gene expression. *Journal of Cellular Physiology*, *227*(9), 3169–3177. http://doi.org/10.1002/jcp.24054

Doulames, V. M., Vilcans, M., Lee, S., & Shea, T. B. (2015). Social interaction attenuates the extent of secondary neuronal damage following closed head injury in mice. *Frontiers in Behavioral Neuroscience*, *9*, 275. http://doi.org/10.3389/fnbeh.2015.00275

Drewnowski, A., & Popkin, B. M. (1997). The nutrition transition: new trends in the global diet. *Nutrition Reviews*, *55*(2), 31–43.

Drijkoningen, D., Caeyenberghs, K., Leunissen, I., Vander Linden, C., Leemans, A., Sunaert, S., et al. (2015). Training-induced improvements in postural control are accompanied by alterations in cerebellar white matter in brain injured patients. *Ynicl*, *7*(C), 240–251. http://doi.org/10.1016/j.nicl.2014.12.006

Du, X., Leang, L., Mustafa, T., Renoir, T., Pang, T. Y., & Hannan, A. J. (2012a). Environmental enrichment rescues female-specific hyperactivity of the hypothalamic-pituitary-adrenal axis in a model of Huntington's disease. *Translational Psychiatry*, *2*(7), e144–1. http://doi.org/10.1038/tp.2012.71

Du, X., Leang, L., Mustafa, T., Renoir, T., Pang, T. Y., & Hannan, A. J. (2012b). Environmental enrichment rescues female-specific hyperactivity of the hypothalamic-pituitary-adrenal axis in a model of Huntington's disease. *Translational Psychiatry*, *2*(7), e133–8. http://doi.org/10.1038/tp.2012.58

Dumas, E. M., van den Bogaard, S. J. A., Ruber, M. E., Reilmann, R., Stout, J. C., Craufurd, D., et al. (2011). Early changes in white matter pathways of the sensorimotor cortex in premanifest Huntington's disease. *Human Brain Mapping*, *33*(1), 203–212. http://doi.org/10.1002/hbm.21205

Dunah, A. W., Jeong, H., Griffin, A., Kim, Y.-M., Standaert, D. G., Hersch, S. M., et al. (2002). Sp1 and TAFII130 transcriptional activity disrupted in early Huntington's disease. *Science*, *296*(5576), 2238–2243. http://doi.org/10.1126/science.1072613

Duyao, M., Ambrose, C., Myers, R., Novelletto, A., Persichetti, F., Frontali, M., et al. (1993). Trinucleotide repeat length instability and age of onset in Huntington's disease. *Nature Genetics*, *4*(4), 387–392. http://doi.org/10.1038/ng0893-387

Egeland, B., Sroufe, L. A., & Erickson, M. (1983). The developmental

consequence of different patterns of maltreatment. *Child Abuse & Neglect*, *7*(4), 459–469.
Ehninger, D., & Kempermann, G. (2003). Regional effects of wheel running and environmental enrichment on cell genesis and microglia proliferation in the adult murine neocortex. *Cerebral Cortex*, *13*(8), 845–851.
Ehninger, D., Wang, L.-P., Klempin, F., Römer, B., Kettenmann, H., & Kempermann, G. (2011). Enriched environment and physical activity reduce microglia and influence the fate of NG2 cells in the amygdala of adult mice. *Cell and Tissue Research*, *345*(1), 69–86. http://doi.org/10.1007/s00441-011-1200-z
El-Ansary, A. K., Ben Bacha, A., & Kotb, M. (2012). Etiology of autistic features: the persisting neurotoxic effects of propionic acid. *Journal of Neuroinflammation*, *9*(1), 74. http://doi.org/10.1186/1742-2094-9-74
Eluvathingal, T. J., Chugani, H. T., Behen, M. E., Juhász, C., Muzik, O., Maqbool, M., et al. (2006). Abnormal brain connectivity in children after early severe socioemotional deprivation: a diffusion tensor imaging study. *Pediatrics*, *117*(6), 2093–2100. http://doi.org/10.1542/peds.2005-1727
Emery, B., Agalliu, D., Cahoy, J. D., Watkins, T. A., Dugas, J. C., Mulinyawe, S. B., et al. (2009). Myelin gene regulatory factor is a critical transcriptional regulator required for CNS myelination. *Cell*, *138*(1), 172–185. http://doi.org/10.1016/j.cell.2009.04.031
Erny, D., Hrabě de Angelis, A. L., Jaitin, D., Wieghofer, P., Staszewski, O., David, E., et al. (2015). Host microbiota constantly control maturation and function of microglia in the CNS. *Nature Neuroscience*, *18*(7), 965–977. http://doi.org/10.1038/nn.4030
Ettle, B., Schlachetzki, J. C. M., & Winkler, J. (2016). Oligodendroglia and Myelin in Neurodegenerative Diseases: More Than Just Bystanders? *Molecular Neurobiology*, 1–17. http://doi.org/10.1007/s12035-015-9205-3
Faherty, C. J., Raviie Shepherd, K., Herasimtschuk, A., & Smeyne, R. J. (2005). Environmental enrichment in adulthood eliminates neuronal death in experimental Parkinsonism. *Brain Research. Molecular Brain Research*, *134*(1), 170–179. http://doi.org/10.1016/j.molbrainres.2004.08.008
Faideau, M., Kim, J., Cormier, K., Gilmore, R., Welch, M., Auregan, G., et al. (2010). In vivo expression of polyglutamine-expanded huntingtin by mouse striatal astrocytes impairs glutamate transport: a correlation with Huntington's disease subjects. *Human Molecular Genetics*, *19*(15), 3053–3067. http://doi.org/10.1093/hmg/ddq212
Fan, M. M. Y., Fernandes, H. B., Zhang, L. Y. J., Hayden, M. R., & Raymond, L. A. (2007). Altered NMDA receptor trafficking in a yeast artificial chromosome transgenic mouse model of Huntington's disease. *The Journal of Neuroscience : the Official Journal of the Society for Neuroscience*, *27*(14), 3768–3779. http://doi.org/10.1523/JNEUROSCI.4356-06.2007
Fasano, A., Visanji, N. P., Liu, L. W. C., Lang, A. E., & Pfeiffer, R. F. (2015). Gastrointestinal dysfunction in Parkinson's disease. *The Lancet. Neurology*, *14*(6), 625–639. http://doi.org/10.1016/S1474-4422(15)00007-1
Fennema-Notestine, C., Archibald, S. L., Jacobson, M. W., Corey-Bloom, J., Paulsen, J. S., Peavy, G. M., et al. (2004). In vivo evidence of cerebellar

atrophy and cerebral white matter loss in Huntington disease. *Neurology*, *63*(6), 989–995.
Fields, R. D. (2008). White matter in learning, cognition and psychiatric disorders. *Trends in Neurosciences*, *31*(7), 361–370. http://doi.org/10.1016/j.tins.2008.04.001
Fisher, E. R., & Hayden, M. R. (2014). Multisource ascertainment of Huntington disease in Canada: prevalence and population at risk. *Movement Disorders*, *29*(1), 105–114. http://doi.org/10.1002/mds.25717
Flint Beal, M. (1994). Huntington's disease, energy, and excitotoxicity. *Neurobiology of Aging*, *15*(2), 275–276. http://doi.org/10.1016/0197-4580(94)90132-5
Fone, K. C. F., & Porkess, M. V. (2008). Behavioural and neurochemical effects of post-weaning social isolation in rodents—Relevance to developmental neuropsychiatric disorders. *Neuroscience and Biobehavioral Reviews*, *32*(6), 1087–1102. http://doi.org/10.1016/j.neubiorev.2008.03.003
Fontana, L., & Partridge, L. (2015). Promoting Health and Longevity through Diet: From Model Organisms to Humans. *Cell*, *161*(1), 106–118. http://doi.org/10.1016/j.cell.2015.02.020
Forbes, T. A., & Gallo, V. (2017). All Wrapped Up: Environmental Effects on Myelination. *Trends in Neurosciences*, *40*(9), 572–587. http://doi.org/10.1016/j.tins.2017.06.009
Forsythe, P., & Kunze, W. A. (2012). Voices from within: gut microbes and the CNS. *Cellular and Molecular Life Sciences*, *70*(1), 55–69. http://doi.org/10.1007/s00018-012-1028-z
Franciosi, S., Ryu, J. K., Shim, Y., Hill, A., Connolly, C., Hayden, M. R., et al. (2012). Age-dependent neurovascular abnormalities and altered microglial morphology in the YAC128 mouse model of Huntington disease. *Neurobiology of Disease*, *45*(1), 438–449. http://doi.org/10.1016/j.nbd.2011.09.003
Frank, D. N., & Pace, N. R. (2008). Gastrointestinal microbiology enters the metagenomics era. *Current Opinion in Gastroenterology*, *24*(1), 4–10. http://doi.org/10.1097/MOG.0b013e3282f2b0e8
Franklin, R. J. M., & ffrench-Constant, C. (2008). Remyelination in the CNS: from biology to therapy. *Nature Reviews Neuroscience*, *9*(11), 839–855. http://doi.org/10.1038/nrn2480
Franklin, R. J., & Hinks, G. L. (1999). Understanding CNS remyelination: clues from developmental and regeneration biology. *Journal of Neuroscience Research*, *58*(2), 207–213.
Fratiglioni, L., Paillard-Borg, S., & Winblad, B. (2004). An active and socially integrated lifestyle in late life might protect against dementia. *The Lancet. Neurology*, *3*(6), 343–353. http://doi.org/10.1016/S1474-4422(04)00767-7
Frazzitta, G., Maestri, R., Bertotti, G., Riboldazzi, G., Boveri, N., Perini, M., et al. (2015). Intensive rehabilitation treatment in early Parkinson's disease: a randomized pilot study with a 2-year follow-up. *Neurorehabilitation and Neural Repair*, *29*(2), 123–131. http://doi.org/10.1177/1545968314542981
Friede, R. L., & Miyagishi, T. (1972). Adjustment of the myelin sheath to

changes in axon caliber. *The Anatomical Record: Advances in Integrative Anatomy and Evolutionary Biology*, *172*(1), 1–14. http://doi.org/10.1002/ar.1091720101

Fritz, J. V., Desai, M. S., Shah, P., Schneider, J. G., & Wilmes, P. (2013). From meta-omics to causality: experimental models for human microbiome research. *Microbiome*, *1*(1), 14. http://doi.org/10.1186/2049-2618-1-14

Fuster, J. M. (1996). Frontal Lobe and the Cognitive Foundation of Behavioral Action. In *Neurobiology of Decision-Making* (pp. 47–61). Berlin, Heidelberg: Springer Berlin Heidelberg. http://doi.org/10.1007/978-3-642-79928-0_3

Fünfschilling, U., Supplie, L. M., Mahad, D., Boretius, S., Saab, A. S., Edgar, J., et al. (2012). Glycolytic oligodendrocytes maintain myelin and long-term axonal integrity. *Nature*, *280*, 1610–17. http://doi.org/10.1038/nature11007

Gabrielli, M., Bonazzi, P., Lauritano, E. C., Scarpellini, E., Bentivoglio, A., Soleti, F., et al. (2010). OC.09.5 PREVALENCE OF SMALL INTESTINAL BACTERIAL OVERGROWTH IN PARKINSON'S DISEASE. *Digestive and Liver Disease*, *42*, S92. http://doi.org/10.1016/S1590-8658(10)60087-4

Gacias, M., Gaspari, S., Santos, P.-M. G., Tamburini, S., Andrade, M., Zhang, F., et al. (2016). Microbiota-driven transcriptional changes in prefrontal cortex override genetic differences in social behavior. *eLife*, *5*, 1013. http://doi.org/10.7554/eLife.13442

Galani, R., Berthel, M.-C., Lazarus, C., Majchrzak, M., Barbelivien, A., Kelche, C., & Cassel, J.-C. (2007). The behavioral effects of enriched housing are not altered by serotonin depletion but enrichment alters hippocampal neurochemistry. *Neurobiology of Learning and Memory*, *88*(1), 1–10. http://doi.org/10.1016/j.nlm.2007.03.009

Garcia-Miralles, M., Hong, X., Tan, L. J., Caron, N. S., Huang, Y., To, X. V., et al. (2016). Laquinimod rescues striatal, cortical and white matter pathology and results in modest behavioural improvements in the YAC128 model of Huntington disease. *Scientific Reports*, *6*(1), 31652. http://doi.org/10.1038/srep31652

Gareau, M. G., Wine, E., Rodrigues, D. M., Cho, J. H., Whary, M. T., Philpott, D. J., et al. (2011). Bacterial infection causes stress-induced memory dysfunction in mice. *Gut*, *60*(3), 307–317. http://doi.org/10.1136/gut.2009.202515

Gatto, R. G., Chu, Y., Ye, A. Q., Price, S. D., Tavassoli, E., Buenaventura, A., et al. (2015). Analysis of YFP(J16)-R6/2 reporter mice and postmortem brains reveals early pathology and increased vulnerability of callosal axons in Huntington's disease. *Human Molecular Genetics*, *24*(18), 5285–5298. http://doi.org/10.1093/hmg/ddv248

Gauthier, L. R., Charrin, B. C., Borrell-Pagès, M., Dompierre, J. P., Rangone, H., Cordelières, F. P., et al. (2004). Huntingtin Controls Neurotrophic Support and Survival of Neurons by Enhancing BDNF Vesicular Transport along Microtubules. *Cell*, *118*(1), 127–138. http://doi.org/10.1016/j.cell.2004.06.018

Gautier, H. O. B., Evans, K. A., Volbracht, K., James, R., Sitnikov, S., Lundgaard, I., et al. (2015). Neuronal activity regulates remyelination via

glutamate signalling to oligodendrocyte progenitors. *Nature Communications*, *6*, 8518. http://doi.org/10.1038/ncomms9518
Gevers, D., Knight, R., Petrosino, J. F., Huang, K., McGuire, A. L., Birren, B. W., et al. (2012). The Human Microbiome Project: A Community Resource for the Healthy Human Microbiome. *PLoS Biology*, *10*(8), e1001377–6. http://doi.org/10.1371/journal.pbio.1001377
Ghosh, S., Sinha, J. K., & Raghunath, M. (2016). Epigenomic maintenance through dietary intervention can facilitate DNA repair process to slow down the progress of premature aging. *IUBMB Life*, *68*(9), 717–721. http://doi.org/10.1002/iub.1532
Gibson, E. M., Purger, D., Mount, C. W., Goldstein, A. K., Lin, G. L., Wood, L. S., et al. (2014). Neuronal Activity Promotes Oligodendrogenesis and Adaptive Myelination in the Mammalian Brain. *Science*, *344*(6183), 1252304–1252304. http://doi.org/10.1126/science.1252304
Goebbels, S., Wieser, G. L., Pieper, A., Spitzer, S., Weege, B., Yan, K., et al. (2017). A neuronal PI(3,4,5)P3-dependent program of oligodendrocyte precursor recruitment and myelination. *Nature Publishing Group*, *20*(1), 10–15. http://doi.org/10.1038/nn.4425
Goldberg, N. R. S., Haack, A. K., & Meshul, C. K. (2010). Enriched environment promotes similar neuronal and behavioral recovery in a young and aged mouse model of Parkinson's disease, 1–10. http://doi.org/10.1016/j.neuroscience.2010.09.062
Gomez de Agüero, M., Ganal-Vonarburg, S. C., Fuhrer, T., Rupp, S., Uchimura, Y., Li, H., et al. (2016). The maternal microbiota drives early postnatal innate immune development. *Science*, *351*(6279), 1296–1302. http://doi.org/10.1126/science.aad2571
Goodrich, J. K., Davenport, E. R., Beaumont, M., Jackson, M. A., Knight, R., Ober, C., et al. (2016). Genetic Determinants of the Gut Microbiome in UK Twins. *Cell Host and Microbe*, *19*(5), 731–743. http://doi.org/10.1016/j.chom.2016.04.017
Graeber, M. B., Li, W., & Rodriguez, M. L. (2011). Role of microglia in CNS inflammation. *FEBS Letters*, *585*(23), 3798–3805. http://doi.org/10.1016/j.febslet.2011.08.033
Gray, M., Shirasaki, D. I., Cepeda, C., Andre, V. M., Wilburn, B., Lu, X. H., et al. (2008). Full-Length Human Mutant Huntingtin with a Stable Polyglutamine Repeat Can Elicit Progressive and Selective Neuropathogenesis in BACHD Mice. *Journal of Neuroscience*, *28*(24), 6182–6195. http://doi.org/10.1523/JNEUROSCI.0857-08.2008
Grydeland, H., Walhovd, K. B., Tamnes, C. K., Westlye, L. T., & Fjell, A. M. (2013). Intracortical myelin links with performance variability across the human lifespan: results from T1- and T2-weighted MRI myelin mapping and diffusion tensor imaging. *The Journal of Neuroscience : the Official Journal of the Society for Neuroscience*, *33*(47), 18618–18630. http://doi.org/10.1523/JNEUROSCI.2811-13.2013
Gunawardena, S., Her, L.-S., Brusch, R. G., Laymon, R. A., Niesman, I. R., Gordesky-Gold, B., et al. (2003). Disruption of Axonal Transport by Loss of Huntingtin or Expression of Pathogenic PolyQ Proteins in Drosophila. *Neuron*, *40*(1), 25–40. http://doi.org/10.1016/S0896-6273(03)00594-4
Gurav, A., Sivaprakasam, S., Bhutia, Y. D., Boettger, T., Singh, N., &

Ganapathy, V. (2015). Slc5a8, a Na+-coupled high-affinity transporter for short-chain fatty acids, is a conditional tumour suppressor in colon that protects against colitis and colon cancer under low-fibre dietary conditions. *The Biochemical Journal*, *469*(2), 267–278. http://doi.org/10.1042/BJ20150242

Gutekunst, C. A., Li, S. H., Yi, H., Mulroy, J. S., Kuemmerle, S., Jones, R., et al. (1999). Nuclear and neuropil aggregates in Huntington's disease: relationship to neuropathology. *The Journal of Neuroscience : the Official Journal of the Society for Neuroscience*, *19*(7), 2522–2534.

Hackam, A. S., Singaraja, R., Wellington, C. L., Metzler, M., McCutcheon, K., Zhang, T., et al. (1998). The Influence of Huntingtin Protein Size on Nuclear Localization and Cellular Toxicity. *The Journal of Cell Biology*, *141*(5), 1097–1105. http://doi.org/10.1083/jcb.141.5.1097

Hahn, A. F., Whitaker, J. N., Kachar, B., & Webster, H. D. (1987). P2, P1, and P0 myelin protein expression in developing rat sixth nerve: a quantitative immunocytochemical study. *Journal of Comparative Neurology*, *260*(4), 501–512. http://doi.org/10.1002/cne.902600404

Haj, El, M., Jardri, R., Larøi, F., & Antoine, P. (2016). Hallucinations, loneliness, and social isolation in Alzheimer's disease. *Cognitive Neuropsychiatry*, *0*(0), 1–13. http://doi.org/10.1080/13546805.2015.1121139

Han, Y., Yang, H., Lv, Y.-T., Zhu, C.-Z., He, Y., Tang, H.-H., et al. (2009). Gray matter density and white matter integrity in pianists' brain: a combined structural and diffusion tensor MRI study. *Neuroscience Letters*, *459*(1), 3–6. http://doi.org/10.1016/j.neulet.2008.07.056

Hannan, A. J. (2014). Review: Environmental enrichment and brain repair: harnessing the therapeutic effects of cognitive stimulation and physical activity to enhance experience-dependent plasticity. *Neuropathology and Applied Neurobiology*, *40*(1), 13–25. http://doi.org/10.1111/nan.12102

Harris, J. J., & Attwell, D. (2012). The energetics of CNS white matter. *The Journal of Neuroscience : the Official Journal of the Society for Neuroscience*, *32*(1), 356–371. http://doi.org/10.1523/JNEUROSCI.3430-11.2012

Harte, M. K., Powell, S. B., Swerdlow, N. R., Geyer, M. A., & Reynolds, G. P. (2007). Deficits in parvalbumin and calbindin immunoreactive cells in the hippocampus of isolation reared rats. *Journal of Neural Transmission (Vienna, Austria : 1996)*, *114*(7), 893–898. http://doi.org/10.1007/s00702-007-0627-6

Havel, L. S., Wang, C.-E., Wade, B., Huang, B., Li, S., & Li, X.-J. (2011). Preferential accumulation of N-terminal mutant huntingtin in the nuclei of striatal neurons is regulated by phosphorylation. *Human Molecular Genetics*, *20*(7), 1424–1437. http://doi.org/10.1093/hmg/ddr023

Hebb, M. O., Denovan-Wright, E. M., & Robertson, H. A. (1999). Expression of the Huntington's disease gene is regulated in astrocytes in the arcuate nucleus of the hypothalamus of postpartum rats. *The FASEB Journal*, *13*(9), 1099–1106.

Hedreen, J. C. (2003). Neuronal Intranuclear Inclusions in Neostriatal Striosomes and Matrix in Huntington’s Disease. In *The Basal Ganglia VI* (Vol. 54, pp. 83–86). Boston, MA: Springer US. http://doi.org/10.1007/978-1-4615-0179-4_8

Heidbreder, C. A., Weiss, I. C., Domeney, A. M., Pryce, C., Homberg, J., Hedou, G., et al. (2000). Behavioral, neurochemical and endocrinological characterization of the early social isolation syndrome. *Neuroscience*, *100*(4), 749–768.

Heijtz, R. D., Wang, S., Anuar, F., Qian, Y., Bjorkholm, B., Samuelsson, A., et al. (2011). Normal gut microbiota modulates brain development and behavior. *Proceedings of the National Academy of Sciences*, *108*(7), 3047–3052. http://doi.org/10.1073/pnas.1010529108

Hellemans, K. G. C., Benge, L. C., & Olmstead, M. C. (2004). Adolescent enrichment partially reverses the social isolation syndrome. *Developmental Brain Research*, *150*(2), 103–115. http://doi.org/10.1016/j.devbrainres.2004.03.003

Henderson, N. D. (1973). Brain weight changes resulting from enriched rearing conditions: a diallel analysis. *Developmental Psychobiology*, *6*(4), 367–376. http://doi.org/10.1002/dev.420060410

Hermes, G., Li, N., Duman, C., & Duman, R. (2011). Post-weaning chronic social isolation produces profound behavioral dysregulation with decreases in prefrontal cortex synaptic-associated protein expression in female rats. *Physiology & Behavior*, *104*(2), 354–359. http://doi.org/10.1016/j.physbeh.2010.12.019

Herring, A., Blome, M., Ambrée, O., Sachser, N., Paulus, W., & Keyvani, K. (2010). Reduction of cerebral oxidative stress following environmental enrichment in mice with Alzheimer-like pathology. *Brain Pathology (Zurich, Switzerland)*, *20*(1), 166–175. http://doi.org/10.1111/j.1750-3639.2008.00257.x

Hicks, A. U., Hewlett, K., Windle, V., Chernenko, G., Ploughman, M., Jolkkonen, J., et al. (2007). Enriched environment enhances transplanted subventricular zone stem cell migration and functional recovery after stroke. *Neuroscience*, *146*(1), 31–40. http://doi.org/10.1016/j.neuroscience.2007.01.020

Hildebrand, C., Remahl, S., Persson, H., & Bjartmar, C. (1993). Myelinated nerve fibres in the CNS. *Progress in Neurobiology*, *40*(3), 319–384.

Hill, R. A., Patel, K. D., Medved, J., Reiss, A. M., & Nishiyama, A. (2013). NG2 cells in white matter but not gray matter proliferate in response to PDGF. *The Journal of Neuroscience : the Official Journal of the Society for Neuroscience*, *33*(36), 14558–14566. http://doi.org/10.1523/jneurosci.2001-12.2013

Hines, J. H., Ravanelli, A. M., Schwindt, R., Scott, E. K., & Appel, B. (2015). Neuronal activity biases axon selection for myelination in vivo. *Nature Publishing Group*, *18*(5), 683–689. http://doi.org/10.1038/nn.3992

Hoban, A. E., Moloney, R. D., Golubeva, A. V., Neufeld, K. A. M., O'Sullivan, O., Patterson, E., et al. (2016a). Behavioural and neurochemical consequences of chronic gut microbiota depletion during adulthood in the rat. *Neuroscience*, *339*(C), 463–477. http://doi.org/10.1016/j.neuroscience.2016.10.003

Hoban, A. E., Stilling, R. M., Ryan, F. J., Shanahan, F., Dinan, T. G., Claesson, M. J., et al. (2016b). Regulation of prefrontal cortex myelination by the microbiota, *6*(4), e774–9. http://doi.org/10.1038/tp.2016.42

Hobbs, N. Z., Henley, S. M. D., Ridgway, G. R., Wild, E. J., Barker, R. A., Scahill, R. I., et al. (2010). The progression of regional atrophy in premanifest and early Huntington's disease: a longitudinal voxel-based morphometry study. *Journal of Neurology, Neurosurgery & Psychiatry*, *81*(7), 756–763. http://doi.org/10.1136/jnnp.2009.190702

Hockly, E., Cordery, P. M., Woodman, B., Mahal, A., Van Dellen, A., Blakemore, C., et al. (2002). Environmental enrichment slows disease progression in R6/2 Huntington's disease mice. *Annals of Neurology*, *51*(2), 235–242. http://doi.org/10.1002/ana.10094

Hodges, A. (2006). Regional and cellular gene expression changes in human Huntington's disease brain. *Human Molecular Genetics*, *15*(6), 965–977. http://doi.org/10.1093/hmg/ddl013

Hodgson, J. G., Agopyan, N., Gutekunst, C.-A., Leavitt, B. R., LePiane, F., Singaraja, R., et al. (1999). A YAC Mouse Model for Huntington's Disease with Full-Length Mutant Huntingtin, Cytoplasmic Toxicity, and Selective Striatal Neurodegeneration. *Neuron*, *23*(1), 181–192. http://doi.org/10.1016/S0896-6273(00)80764-3

Hofer, S., & Frahm, J. (2006). Topography of the human corpus callosum revisited—Comprehensive fiber tractography using diffusion tensor magnetic resonance imaging. *NeuroImage*, *32*(3), 989–994. http://doi.org/10.1016/j.neuroimage.2006.05.044

Holmes, E., Li, J. V., Athanasiou, T., Ashrafian, H., & Nicholson, J. K. (2011). Understanding the role of gut microbiomeâ€"host metabolic signal disruption in health and disease. *Trends in Microbiology*, *19*(7), 349–359. http://doi.org/10.1016/j.tim.2011.05.006

Holwerda, T. J., Deeg, D. J. H., Beekman, A. T. F., van Tilburg, T. G., Stek, M. L., Jonker, C., & Schoevers, R. A. (2014). Feelings of loneliness, but not social isolation, predict dementia onset: results from the Amsterdam Study of the Elderly (AMSTEL). *Journal of Neurology, Neurosurgery & Psychiatry*, *85*(2), 135–142. http://doi.org/10.1136/jnnp-2012-302755

Holzer, P., Hassan, A. M., Jain, P., Reichmann, F., & Farzi, A. (2015). ScienceDirect Neuroimmune pharmacological approaches, 1–10. http://doi.org/10.1016/j.coph.2015.09.003

Hong, Y., Zhao, T., Li, X. J., & Li, S. (2016). Mutant Huntingtin Impairs BDNF Release from Astrocytes by Disrupting Conversion of Rab3a-GTP into Rab3a-GDP. *Journal of Neuroscience*, *36*(34), 8790–8801. http://doi.org/10.1523/JNEUROSCI.0168-16.2016

Hooper, L. V., Midtvedt, T., & Gordon, J. I. (2002). How host-microbial interactions shape the nutrient environment of the mammalian intestine. *Annual Review of Nutrition*, *22*(1), 283–307. http://doi.org/10.1146/annurev.nutr.22.011602.092259

Hooper, L. V., Wong, M. H., Thelin, A., Hansson, L., Falk, P. G., & Gordon, J. I. (2001). Molecular analysis of commensal host-microbial relationships in the intestine. *Science*, *291*(5505), 881–884. http://doi.org/10.1126/science.291.5505.881

Howng, S. Y. B., Avila, R. L., Emery, B., Traka, M., Lin, W., Watkins, T., et al. (2010). ZFP191 is required by oligodendrocytes for CNS myelination. *Genes & Development*, *24*(3), 301–311. http://doi.org/10.1101/gad.1864510

Hsiao, Y.-H., Chen, P. S., Chen, S.-H., & Gean, P.-W. (2011). The

involvement of Cdk5 activator p35 in social isolation-triggered onset of early Alzheimer's disease-related cognitive deficit in the transgenic mice. *Neuropsychopharmacology*, *36*(9), 1848–1858. http://doi.org/10.1038/npp.2011.69

Hsiao, Y.-H., Kuo, J.-R., Chen, S.-H., & Gean, P.-W. (2012). Amelioration of social isolation-triggered onset of early Alzheimer's disease-related cognitive deficit by N-acetylcysteine in a transgenic mouse model. *Neurobiology of Disease*, *45*(3), 1111–1120. http://doi.org/10.1016/j.nbd.2011.12.031

Hu, F. B. (2011, June). *Globalization of diabetes: the role of diet, lifestyle, and genes.* Presented at the Diabetes care. http://doi.org/10.2337/dc11-0442

Hu, Y., Geng, F., Tao, L., Hu, N., Du, F., Fu, K., & Chen, F. (2011). Enhanced white matter tracts integrity in children with abacus training. *Human Brain Mapping*, *32*(1), 10–21. http://doi.org/10.1002/hbm.20996

Huang, B., Wei, W., Wang, G., Gaertig, M. A., Feng, Y., Wang, W., et al. (2015a). Mutant Huntingtin Downregulates Myelin Regulatory Factor-Mediated Myelin Gene Expression and Affects Mature Oligodendrocytes. *Neuron*, *85*(6), 1212–1226. http://doi.org/10.1016/j.neuron.2015.02.026

Huang, H., Wang, L., Cao, M., Marshall, C., Gao, J., Xiao, N., et al. (2015b). Isolation Housing Exacerbates Alzheimer's Disease-Like Pathophysiology in Aged APP/PS1 Mice. *International Journal of Neuropsychopharmacology*, *18*(7), pyu116–pyu116. http://doi.org/10.1093/ijnp/pyu116

Hughes, E. G., Kang, S. H., Fukaya, M., & Bergles, D. E. (2013). Oligodendrocyte progenitors balance growth with self-repulsion to achieve homeostasis in the adult brain. *Nature Publishing Group*, *16*(6), 668–676. http://doi.org/10.1038/nn.3390

Hughes, G. L., Dodson, B. L., Johnson, R. M., Murdock, C. C., Tsujimoto, H., Suzuki, Y., et al. (2014). Native microbiome impedes vertical transmission of Wolbachia in Anopheles mosquitoes. *Proceedings of the National Academy of Sciences of the United States of America*, *111*(34), 12498–12503. http://doi.org/10.1073/pnas.1408888111

Hult Lundh, S., Nilsson, N., Soylu, R., Kirik, D., & Petersén, Å. (2013). Hypothalamic expression of mutant huntingtin contributes to the development of depressive-like behavior in the BAC transgenic mouse model of Huntington's disease. *Human Molecular Genetics*, *22*(17), 3485–3497. http://doi.org/10.1093/hmg/ddt203

Hult, S., Soylu, R., Björklund, T., Belgardt, B. F., Mauer, J., Brüning, J. C., et al. (2011). Mutant Huntingtin Causes Metabolic Imbalance by Disruption of Hypothalamic Neurocircuits. *Cell Metabolism*, *13*(4), 428–439. http://doi.org/10.1016/j.cmet.2011.02.013

Huuskonen, J., Suuronen, T., Nuutinen, T., Kyrylenko, S., & Salminen, A. (2004). Regulation of microglial inflammatory response by sodium butyrate and short-chain fatty acids. *British Journal of Pharmacology*, *141*(5), 874–880. http://doi.org/10.1038/sj.bjp.0705682

Ieraci, A., Mallei, A., & Popoli, M. (2016). Social Isolation Stress Induces Anxious-Depressive-Like Behavior and Alterations of Neuroplasticity-Related Genes in Adult Male Mice. *Neural Plasticity*, *2016*(18), 1–13.

http://doi.org/10.1155/2016/6212983
Innocenti, G. M. (1994). Some new trends in the study of the corpus callosum. *Behavioural Brain Research*, *64*(1-2), 1–8.
Iraporda, C., Errea, A., Romanin, D. E., Cayet, D., Pereyra, E., Pignataro, O., et al. (2015). Lactate and short chain fatty acids produced by microbial fermentation downregulate proinflammatory responses in intestinal epithelial cells and myeloid cells. *Immunobiology*, *220*(10), 1161–1169. http://doi.org/10.1016/j.imbio.2015.06.004
Ivanov, I. I., Atarashi, K., Manel, N., Brodie, E. L., Shima, T., Karaoz, U., et al. (2009). Induction of intestinal Th17 cells by segmented filamentous bacteria. *Cell*, *139*(3), 485–498. http://doi.org/10.1016/j.cell.2009.09.033
Jadavji, N. M., Kolb, B., & Metz, G. A. (2006). Enriched environment improves motor function in intact and unilateral dopamine-depleted rats. *Neuroscience*, *140*(4), 1127–1138. http://doi.org/10.1016/j.neuroscience.2006.03.027
Jangi, S., Gandhi, R., Cox, L. M., Li, N., Glehn, von, F., Yan, R., et al. (2016). Alterations of the human gut microbiome in multiple sclerosis. *Nature Communications*, *7*, 1–11. http://doi.org/10.1038/ncomms12015
Jankowsky, J. L., Melnikova, T., Fadale, D. J., Xu, G. M., Slunt, H. H., Gonzales, V., et al. (2005). Environmental enrichment mitigates cognitive deficits in a mouse model of Alzheimer's disease. *The Journal of Neuroscience : the Official Journal of the Society for Neuroscience*, *25*(21), 5217–5224. http://doi.org/10.1523/JNEUROSCI.5080-04.2005
Jiang, Z., Rompala, G. R., Zhang, S., Cowell, R. M., & Nakazawa, K. (2013). Social isolation exacerbates schizophrenia-like phenotypes via oxidative stress in cortical interneurons. *Biological Psychiatry*, *73*(10), 1024–1034. http://doi.org/10.1016/j.biopsych.2012.12.004
Jin, J., Peng, Q., Hou, Z., Jiang, M., Wang, X., Langseth, A. J., et al. (2015). Early white matter abnormalities, progressive brain pathology and motor deficits in a novel knock-in mouse model of Huntington's disease. *Human Molecular Genetics*, *24*(9), 2508–2527. http://doi.org/10.1093/hmg/ddv016
Johns, T. G., & Bernard, C. C. (1999). The structure and function of myelin oligodendrocyte glycoprotein. *Journal of Neurochemistry*, *72*(1), 1–9.
Kang, S. H., Fukaya, M., Yang, J. K., Rothstein, J. D., & Bergles, D. E. (2010). NG2+ CNS glial progenitors remain committed to the oligodendrocyte lineage in postnatal life and following neurodegeneration. *Neuron*, *68*(4), 668–681. http://doi.org/10.1016/j.neuron.2010.09.009
Karttunen, M. J., Czopka, T., Goedhar, M., Early, J. J., & Lyons, D. A. (2017). Regeneration of myelin sheaths of normal length and thickness in the zebrafish CNS correlates with growth of axons in caliber, *PLoS ONE*, *12(5): e0178058*. http://doi.org/10.1371/journal.pone.0178058
Kearney, J. (2010). Food consumption trends and drivers. *Philosophical Transactions of the Royal Society B: Biological Sciences*, *365*(1554), 2793–2807. http://doi.org/10.1098/rstb.2010.0149
Keiner, S., Niv, F., Neumann, S., Steinbach, T., Schmeer, C., Hornung, K., et al. (2017). Effect of skilled reaching training and enriched environment on generation of oligodendrocytes in the adult sensorimotor cortex and corpus callosum. *BMC Neuroscience*, 1–13.

http://doi.org/10.1186/s12868-017-0347-2
Keiner, S., Wurm, F., Kunze, A., Witte, O. W., & Redecker, C. (2008). Rehabilitative therapies differentially alter proliferation and survival of glial cell populations in the perilesional zone of cortical infarcts. *Glia*, *56*(5), 516–527. http://doi.org/10.1002/glia.20632
Kelly, C. J., Zheng, L., Campbell, E. L., Saeedi, B., Scholz, C. C., Bayless, A. J., et al. (2015). Crosstalk between Microbiota-Derived Short-Chain Fatty Acids and Intestinal Epithelial HIF Augments Tissue Barrier Function. *Cell Host and Microbe*, *17*(5), 662–671. http://doi.org/10.1016/j.chom.2015.03.005
Kempermann, G., Kuhn, H. G., & Gage, F. H. (1997). More hippocampal neurons in adult mice living in an enriched environment. *Nature*, *386*(6624), 493–495. http://doi.org/10.1038/386493a0
Khan, F., Amatya, B., & Turner-Stokes, L. (2011). Symptomatic therapy and rehabilitation in primary progressive multiple sclerosis. *Neurology Research International*, *2011*(3), 740505–22. http://doi.org/10.1155/2011/740505
Khan, F., Turner-Stokes, L., Ng, L., Abrahamson, S., & Kilpatrick, T. (1996). Multidisciplinary rehabilitation for adults with multiple sclerosis. (F. Khan, Ed.) (Vol. 55). Chichester, UK: John Wiley & Sons, Ltd. http://doi.org/10.1002/14651858.CD006036
Kim, J. S., & Sampson, H. A. (2012). Food allergy: a glimpse into the inner workings of gut immunology. *Current Opinion in Gastroenterology*, *28*(2), 99–103. http://doi.org/10.1097/MOG.0b013e32834e7b60
Kim, Y. J., Yi, Y., Sapp, E., Wang, Y., Cuiffo, B., Kegel, K. B., et al. (2001). Caspase 3-cleaved N-terminal fragments of wild-type and mutant huntingtin are present in normal and Huntington's disease brains, associate with membranes, and undergo calpain-dependent proteolysis. *Proceedings of the National Academy of Sciences of the United States of America*, *98*(22), 12784–12789. http://doi.org/10.1073/pnas.221451398
Klaissle, P., Lesemann, A., Huehnchen, P., Hermann, A., Storch, A., & Steiner, B. (2012). Physical activity and environmental enrichment regulate the generation of neural precursors in the adult mouse substantia nigra in a dopamine-dependent manner. *BMC Neuroscience*, *13*(1), 132. http://doi.org/10.1186/1471-2202-13-132
Klugmann, M., Schwab, M. H., Pühlhofer, A., Schneider, A., Zimmermann, F., Griffiths, I. R., & Nave, K.-A. (1997). Assembly of CNS Myelin in the Absence of Proteolipid Protein. *Neuron*, *18*(1), 59–70. http://doi.org/10.1016/S0896-6273(01)80046-5
Koenning, M., Jackson, S., Hay, C. M., Faux, C., Kilpatrick, T. J., Willingham, M., & Emery, B. (2012). Myelin Gene Regulatory Factor Is Required for Maintenance of Myelin and Mature Oligodendrocyte Identity in the Adult CNS. *Journal of Neuroscience*, *32*(36), 12528–12542. http://doi.org/10.1523/JNEUROSCI.1069-12.2012
Komitova, M., Perfilieva, E., Mattsson, B., Eriksson, P. S., & Johansson, B. B. (2006). Enriched environment after focal cortical ischemia enhances the generation of astroglia and NG2 positive polydendrocytes in adult rat neocortex. *Experimental Neurology*, *199*(1), 113–121. http://doi.org/10.1016/j.expneurol.2005.12.007

Kruska, D. C. T. (2005). On the evolutionary significance of encephalization in some eutherian mammals: effects of adaptive radiation, domestication, and feralization. *Brain, Behavior and Evolution*, *65*(2), 73–108. http://doi.org/10.1159/000082979

Kuperman, A. A., & Koren, O. (2016). Antibiotic use during pregnancy: how bad is it? *BMC Medicine*, *14*(1), 207. http://doi.org/10.1186/s12916-016-0636-0

Küspert, M., Hammer, A., Bösl, M. R., & Wegner, M. (2011). Olig2 regulates Sox10 expression in oligodendrocyte precursors through an evolutionary conserved distal enhancer. *Nucleic Acids Research*, *39*(4), 1280–1293. http://doi.org/10.1093/nar/gkq951

Lakhan, S. E., & Kirchgessner, A. (2010). Gut inflammation in chronic fatigue syndrome. *Nutrition & Metabolism*, *7*(1), 79. http://doi.org/10.1186/1743-7075-7-79

Lander, S. S., Linder-Shacham, D., & Gaisler-Salomon, I. (2017). Differential effects of social isolation in adolescent and adult mice on behavior and cortical gene expression. *Behavioural Brain Research*, *316*, 245–254. http://doi.org/10.1016/j.bbr.2016.09.005

Langbehn, D. R., Brinkman, R. R., Falush, D., Paulsen, J. S., Hayden, M. R., International Huntington's Disease Collaborative Group. (2004). A new model for prediction of the age of onset and penetrance for Huntington's disease based on CAG length. *Clinical Genetics*, *65*(4), 267–277. http://doi.org/10.1111/j.1399-0004.2004.00241.x

Larson, V. A., Zhang, Y., & Bergles, D. E. (2016). Electrophysiological properties of NG2(+) cells: Matching physiological studies with gene expression profiles. *Brain Research*, *1638*(Pt B), 138–160. http://doi.org/10.1016/j.brainres.2015.09.010

Lauder, A. P., Roche, A. M., Sherrill-Mix, S., Bailey, A., Laughlin, A. L., Bittinger, K., et al. (2016). Comparison of placenta samples with contamination controls does not provide evidence for a distinct placenta microbiota. *Microbiome*, *4*(1), 29. http://doi.org/10.1186/s40168-016-0172-3

Lauer, K. (2010). Environmental risk factors in multiple sclerosis. *Expert Review of Neurotherapeutics*, *10*(3), 421–440. http://doi.org/10.1586/ern.10.7

Lavasani, S., Dzhambazov, B., Nouri, M., Fåk, F., Buske, S., Molin, G., et al. (2010). A Novel Probiotic Mixture Exerts a Therapeutic Effect on Experimental Autoimmune Encephalomyelitis Mediated by IL-10 Producing Regulatory T Cells. *PLoS ONE*, *5*(2), e9009–11. http://doi.org/10.1371/journal.pone.0009009

Lawhorn, C., Smith, D. M., & Brown, L. L. (2008). Striosome-matrix pathology and motor deficits in the YAC128 mouse model of Huntington's disease. *Neurobiology of Disease*, *32*(3), 471–478. http://doi.org/10.1016/j.nbd.2008.08.006

Lazic, S. E., Grote, H. E., Blakemore, C., Hannan, A. J., Van Dellen, A., Phillips, W., & Barker, R. A. (2006). Neurogenesis in the R6/1 transgenic mouse model of Huntington's disease: effects of environmental enrichment. *European Journal of Neuroscience*, *23*(7), 1829–1838. http://doi.org/10.1111/j.1460-9568.2006.04715.x

Le Bihan, D., Breton, E., Lallemand, D., Grenier, P., Cabanis, E., & Laval-

Jeantet, M. (1986). MR imaging of intravoxel incoherent motions: application to diffusion and perfusion in neurologic disorders. *Radiology*, *161*(2), 401–407. http://doi.org/10.1148/radiology.161.2.3763909
Lee, Y. K., Menezes, J. S., Umesaki, Y., & Mazmanian, S. K. (2011). Proinflammatory T-cell responses to gut microbiota promote experimental autoimmune encephalomyelitis. *Proceedings of the National Academy of Sciences of the United States of America*, *108 Suppl 1*(Supplement_1), 4615–4622. http://doi.org/10.1073/pnas.1000082107
Lee, Y., Morrison, B. M., Li, Y., Lengacher, S., Farah, M. H., Hoffman, P. N., et al. (2012). Oligodendroglia metabolically support axons and contribute to neurodegeneration. *Nature*, *487*(7408), 443–448. http://doi.org/10.1038/nature11314
Leger, M., Paizanis, E., Dzahini, K., Quiedeville, A., Bouet, V., Cassel, J.-C., et al. (2015). Environmental Enrichment Duration Differentially Affects Behavior and Neuroplasticity in Adult Mice. *Cerebral Cortex*, *25*(11), 4048–4061. http://doi.org/10.1093/cercor/bhu119
Levine, J. B., Youngs, R. M., MacDonald, M. L., Chu, M., Leeder, A. D., Berthiaume, F., & Konradi, C. (2007). Isolation rearing and hyperlocomotion are associated with reduced immediate early gene expression levels in the medial prefrontal cortex. *Neuroscience*, *145*(1), 42–55. http://doi.org/10.1016/j.neuroscience.2006.11.063
Levine, J. M., Stincone, F., & Lee, Y.-S. (1993). Development and differentiation of glial precursor cells in the rat cerebellum. *Glia*, *7*(4), 307–321. http://doi.org/10.1002/glia.440070406
Ley, R. E., Peterson, D. A., & Gordon, J. I. (2006). Ecological and evolutionary forces shaping microbial diversity in the human intestine. *Cell*, *124*(4), 837–848. http://doi.org/10.1016/j.cell.2006.02.017
Li, H., Lu, Y., Smith, H. K., & Richardson, W. D. (2007). Olig1 and Sox10 interact synergistically to drive myelin basic protein transcription in oligodendrocytes. *The Journal of Neuroscience : the Official Journal of the Society for Neuroscience*, *27*(52), 14375–14382. http://doi.org/10.1523/JNEUROSCI.4456-07.2007
Li, W., Serpell, L. C., Carter, W. J., Rubinsztein, D. C., & Huntington, J. A. (2006). Expression and characterization of full-length human huntingtin, an elongated HEAT repeat protein. *The Journal of Biological Chemistry*, *281*(23), 15916–15922. http://doi.org/10.1074/jbc.M511007200
Ligon, K. L., Fancy, S. P. J., Franklin, R. J. M., & Rowitch, D. H. (2006). Olig gene function in CNS development and disease. *Glia*, *54*(1), 1–10. http://doi.org/10.1002/glia.20273
Linden, J. R., Ma, Y., Zhao, B., Harris, J. M., Rumah, K. R., Schaeren-Wiemers, N., & Vartanian, T. (2015). Clostridium perfringensEpsilon Toxin Causes Selective Death of Mature Oligodendrocytes and Central Nervous System Demyelination. *mBio*, *6*(3), e02513–14–13. http://doi.org/10.1128/mBio.02513-14
Lione, L. A., Carter, R. J., Hunt, M. J., Bates, G. P., Morton, A. J., & Dunnett, S. B. (1999). Selective discrimination learning impairments in mice expressing the human Huntington's disease mutation. *Journal of Neuroscience*, *19*(23), 10428–10437.

Liu, J., Dietz, K., DeLoyht, J. M., Pedre, X., Kelkar, D., Kaur, J., et al. (2012). Impaired adult myelination in the prefrontal cortex of socially isolated mice. *Nature Neuroscience*, *15*(12), 1621–1623. http://doi.org/10.1038/nn.3263

Liu, J., Dupree, J. L., Gacias, M., Frawley, R., Sikder, T., Naik, P., & Casaccia, P. (2016). Clemastine Enhances Myelination in the Prefrontal Cortex and Rescues Behavioral Changes in Socially Isolated Mice. *Journal of Neuroscience*, *36*(3), 957–962. http://doi.org/10.1523/JNEUROSCI.3608-15.2016

Liu, K.-Y., Shyu, Y.-C., Barbaro, B. A., Lin, Y.-T., Chern, Y., Thompson, L. M., et al. (2014). Disruption of the nuclear membrane by perinuclear inclusions of mutant huntingtin causes cell-cycle re-entry and striatal cell death in mouse and cell models of Huntington's disease. *Human Molecular Genetics*, *24*(6), 1602–1616. http://doi.org/10.1093/hmg/ddu574

Liu, Y., & Zhou, J. (2013). Oligodendrocytes in neurodegenerative diseases. *Frontiers in Biology*, *8*(2), 127–133. http://doi.org/10.1007/s11515-013-1260-4

Lloyd-Price, J., Abu-Ali, G., & Huttenhower, C. (2016). The healthy human microbiome. *Genome Medicine*, 1–11. http://doi.org/10.1186/s13073-016-0307-y

Lu, Q. R., Sun, T., Zhu, Z., Ma, N., Garcia, M., Stiles, C. D., & Rowitch, D. H. (2002). Common Developmental Requirement for Olig Function Indicates a Motor Neuron/Oligodendrocyte Connection. *Cell*, *109*(1), 75–86. http://doi.org/10.1016/S0092-8674(02)00678-5

Luckey, T. D. (1963). Theory and General Aspects of Germfree Life and Gnotobiology. In *Germfree Life and Gnotobiology* (pp. 1–33). Elsevier. http://doi.org/10.1016/B978-0-12-395585-2.50007-0

Lunkes, A., & Mandel, J. L. (1998). A cellular model that recapitulates major pathogenic steps of Huntington's disease. *Human Molecular Genetics*, *7*(9), 1355–1361.

Luthi-Carter, R. (2000). Decreased expression of striatal signaling genes in a mouse model of Huntington's disease. *Human Molecular Genetics*, *9*(9), 1259–1271. http://doi.org/10.1093/hmg/9.9.1259

Lyte, M. (2013). Microbial endocrinology in the microbiome-gut-brain axis: how bacterial production and utilization of neurochemicals influence behavior. *PLoS Pathogens*, *9*(11), e1003726. http://doi.org/10.1371/journal.ppat.1003726

Macdonald, M. (1993). A novel gene containing a trinucleotide repeat that is expanded and unstable on Huntington's disease chromosomes. *Cell*, *72*(6), 971–983. http://doi.org/10.1016/0092-8674(93)90585-E

Mackey, A. P. (2012). Experience-dependent plasticity in white matter microstructure: reasoning training alters structural connectivity, 1–9. http://doi.org/10.3389/fnana.2012.00032/abstract

Maes, M., Kubera, M., Leunis, J.-C., & Berk, M. (2012). Increased IgA and IgM responses against gut commensals in chronic depression: further evidence for increased bacterial translocation or leaky gut. *Journal of Affective Disorders*, *141*(1), 55–62. http://doi.org/10.1016/j.jad.2012.02.023

Magalon, K., Cantarella, C., Monti, G., Cayre, M., & Durbec, P. (2007).

Enriched environment promotes adult neural progenitor cell mobilization in mouse demyelination models. *European Journal of Neuroscience*, *25*(3), 761–771. http://doi.org/10.1111/j.1460-9568.2007.05335.x
Makinodan, M., Ikawa, D., Miyamoto, Y., Yamauchi, J., Yamamuro, K., Yamashita, Y., et al. (2016). Social isolation impairs remyelination in mice through modulation of IL-6. *The FASEB Journal*, *30*(12), 4267–4274. http://doi.org/10.1096/fj.201600537R
Makinodan, M., Rosen, K. M., Ito, S., & Corfas, G. (2012). A Critical Period for Social Experience-Dependent Oligodendrocyte Maturation and Myelination. *Science*, *337*(6100), 1357–1360. http://doi.org/10.1126/science.1220845
Maldonado, P. P., & Angulo, M. C. (2015). Multiple Modes of Communication between Neurons and Oligodendrocyte Precursor Cells. *The Neuroscientist*, *21*(3), 266–276. http://doi.org/10.1177/1073858414530784
Mangiarini, L., Sathasivam, K., Seller, M., Cozens, B., Harper, A., Hetherington, C., et al. (1996). Exon 1 of the HD gene with an expanded CAG repeat is sufficient to cause a progressive neurological phenotype in transgenic mice. *Cell*, *87*(3), 493–506.
Marchesi, J., & Shanahan, F. (2007). The normal intestinal microbiota. *Current Opinion in Infectious Diseases*, *20*(5), 508–513. http://doi.org/10.1097/QCO.0b013e3282a56a99
Marder, K., Zhao, H., Myers, R. H., Cudkowicz, M., Kayson, E., Kieburtz, K., et al. (2000). Rate of functional decline in Huntington's disease. Huntington Study Group. *Neurology*, *54*(2), 452–458.
Marin-Husstege, M., Muggironi, M., Liu, A., & Casaccia-Bonnefil, P. (2002). Histone deacetylase activity is necessary for oligodendrocyte lineage progression. *The Journal of Neuroscience : the Official Journal of the Society for Neuroscience*, *22*(23), 10333–10345.
Markham, J. A., Herting, M. M., Luszpak, A. E., Juraska, J. M., & Greenough, W. T. (2009). Myelination of the corpus callosum in male and female rats following complex environment housing during adulthood. *Brain Research*, *1288*, 9–17. http://doi.org/10.1016/j.brainres.2009.06.087
Martinez-Vicente, M., Talloczy, Z., Wong, E., Tang, G., Koga, H., Kaushik, S., et al. (2010). Cargo recognition failure is responsible for inefficient autophagy in Huntington's disease. *Nature Neuroscience*, *13*(5), 567–576. http://doi.org/10.1038/nn.2528
Matarese, G., Di Giacomo, A., Sanna, V., Lord, G. M., Howard, J. K., Di Tuoro, A., et al. (2001). Requirement for leptin in the induction and progression of autoimmune encephalomyelitis. *The Journal of Immunology*, *166*(10), 5909–5916. http://doi.org/10.4049/jimmunol.166.10.5909
Matarese, G., Moschos, S., & Mantzoros, C. S. (2005). Leptin in immunology. *The Journal of Immunology*, *174*(6), 3137–3142. http://doi.org/10.4049/jimmunol.174.6.3137
Matricon, J., Meleine, M., Gelot, A., Piche, T., Dapoigny, M., Muller, E., & Ardid, D. (2012). Review article: Associations between immune activation, intestinal permeability and the irritable bowel syndrome. *Alimentary Pharmacology & Therapeutics*, *36*(11-12), 1009–1031.

http://doi.org/10.1111/apt.12080
Matsui, J. T., Vaidya, J. G., Johnson, H. J., Magnotta, V. A., Long, J. D., Mills, J. A., et al. (2013). Diffusion weighted imaging of prefrontal cortex in prodromal huntington's disease. *Human Brain Mapping*, *35*(4), 1562–1573. http://doi.org/10.1002/hbm.22273
Matsui, J. T., Vaidya, J. G., Wassermann, D., Kim, R. E., Magnotta, V. A., Johnson, H. J., et al. (2015). Prefrontal cortex white matter tracts in prodromal Huntington disease. *Human Brain Mapping*, *36*(10), 3717–3732. http://doi.org/10.1002/hbm.22835
Matsumoto, K., Nomura, H., Murakami, Y., Taki, K., Takahata, H., & Watanabe, H. (2003). Long-term social isolation enhances picrotoxin seizure susceptibility in mice: up-regulatory role of endogenous brain allopregnanolone in GABAergic systems. *Pharmacology Biochemistry and Behavior*, *75*(4), 831–835.
Matsumoto, K., Pinna, G., Puia, G., Guidotti, A., & Costa, E. (2005). Social isolation stress-induced aggression in mice: a model to study the pharmacology of neurosteroidogenesis. *Stress (Amsterdam, Netherlands)*, *8*(2), 85–93. http://doi.org/10.1080/10253890500159022
Matsumoto, M., Kibe, R., Ooga, T., Aiba, Y., Kurihara, S., Sawaki, E., et al. (2012). Impact of Intestinal Microbiota on Intestinal Luminal Metabolome. *Scientific Reports*, *2*(1), 59–11. http://doi.org/10.1038/srep00233
Matthews, M. A., & Duncan, D. (1971). A quantitative study of morphological changes accompanying the initiation and progress of myelin production in the dorsal funiculus of the rat spinal cord. *Journal of Comparative Neurology*, *142*(1), 1–22. http://doi.org/10.1002/cne.901420102
Matthieu, J. M., Quarles, R. H., Brady, R. O., & Webster, H. de F. (1973). Variation of proteins, enzyme markers and gangliosides in myelin subfractions. *Biochimica Et Biophysica Acta*, *329*(2), 305–317.
Mayer, E. A., Tillisch, K., & Gupta, A. (2015). Gut/brain axis and the microbiota. *Journal of Clinical Investigation*, *125*(3), 926–938. http://doi.org/10.1172/JCI76304
Maynard, C. J., Böttcher, C., Ortega, Z., Smith, R., Florea, B. I., Díaz-Hernández, M., et al. (2009). Accumulation of ubiquitin conjugates in a polyglutamine disease model occurs without global ubiquitin/proteasome system impairment. *Proceedings of the National Academy of Sciences of the United States of America*, *106*(33), 13986–13991. http://doi.org/10.1073/pnas.0906463106
Mazmanian, S. K., Liu, C. H., Tzianabos, A. O., & Kasper, D. L. (2005). An immunomodulatory molecule of symbiotic bacteria directs maturation of the host immune system. *Cell*, *122*(1), 107–118. http://doi.org/10.1016/j.cell.2005.05.007
McEwen, B. S. (2013). The Brain on Stress. *Perspectives on Psychological Science*, *8*(6), 673–675. http://doi.org/10.1177/1745691613506907
McKenzie, I. A., Ohayon, D., Li, H., Paes de Faria, J., Emery, B., Tohyama, K., & Richardson, W. D. (2014). Motor skill learning requires active central myelination. *Science*, *346*(6207), 318–322. http://doi.org/10.1126/science.1254960
McLean, P. G., Bergonzelli, G. E., Collins, S. M., & Bercik, P. (2012). Targeting the microbiota-gut-brain axis to modulate behavior: which bacterial strain will translate best to humans? *Proceedings of the*

National Academy of Sciences of the United States of America, *109*(4), E174–author reply E176. http://doi.org/10.1073/pnas.1118626109
Mehta, M. A., Golembo, N. I., Nosarti, C., Colvert, E., Mota, A., Williams, S. C. R., et al. (2009). Amygdala, hippocampal and corpus callosum size following severe early institutional deprivation: the English and Romanian Adoptees study pilot. *Journal of Child Psychology and Psychiatry, and Allied Disciplines*, *50*(8), 943–951. http://doi.org/10.1111/j.1469-7610.2009.02084.x
Mei, F., Wang, H., Liu, S., Niu, J., Wang, L., He, Y., et al. (2013). Stage-specific deletion of Olig2 conveys opposing functions on differentiation and maturation of oligodendrocytes. *The Journal of Neuroscience : the Official Journal of the Society for Neuroscience*, *33*(19), 8454–8462. http://doi.org/10.1523/JNEUROSCI.2453-12.2013
Melendez, R. I., Gregory, M. L., Bardo, M. T., & Kalivas, P. W. (2004). Impoverished rearing environment alters metabotropic glutamate receptor expression and function in the prefrontal cortex. *Neuropsychopharmacology*, *29*(11), 1980–1987. http://doi.org/10.1038/sj.npp.1300507
Menalled, L., El-Khodor, B. F., Patry, M., Suárez-Fariñas, M., Orenstein, S. J., Zahasky, B., et al. (2009). Systematic behavioral evaluation of Huntington's disease transgenic and knock-in mouse models. *Neurobiology of Disease*, *35*(3), 319–336. http://doi.org/10.1016/j.nbd.2009.05.007
Mensch, S., Baraban, M., Almeida, R., Czopka, T., Ausborn, J., Manira, El, A., & Lyons, D. A. (2015). Synaptic vesicle release regulates myelin sheath number of individual oligodendrocytes in vivo. *Nature Publishing Group*, *18*(5), 628–630. http://doi.org/10.1038/nn.3991
Merlino, D. J., Blomain, E. S., Aing, A. S., & Waldman, S. A. (2014). Gut-Brain Endocrine Axes in Weight Regulation and Obesity Pharmacotherapy. *Journal of Clinical Medicine*, *3*(3), 763–794. http://doi.org/10.3390/jcm3030763
Micheva, K. D., Wolman, D., Mensh, B. D., Pax, E., Buchanan, J., Smith, S. J., & Bock, D. D. (2016). A large fraction of neocortical myelin ensheathes axons of local inhibitory neurons. *eLife*, *5*, 3347. http://doi.org/10.7554/eLife.15784
Millard, A. L., Mertes, P. M., Ittelet, D., Villard, F., Jeannesson, P., & Bernard, J. (2002). Butyrate affects differentiation, maturation and function of human monocyte-derived dendritic cells and macrophages. *Clinical & Experimental Immunology*, *130*(2), 245–255. http://doi.org/10.1046/j.0009-9104.2002.01977.x
Miller, B. R., & Bezprozvanny, I. (2010). Corticostriatal circuit dysfunction in Huntington’s disease: intersection of glutamate, dopamine and calcium. *Future Neurology*, *5*(5), 735–756. http://doi.org/10.2217/fnl.10.41
Miller, D. J., Duka, T., Stimpson, C. D., Schapiro, S. J., Baze, W. B., McArthur, M. J., et al. (2012). Prolonged myelination in human neocortical evolution. *Proceedings of the National Academy of Sciences of the United States of America*, *109*(41), 16480–16485. http://doi.org/10.1073/pnas.1117943109
Miller, E. K., & Cohen, J. D. (2001). An integrative theory of prefrontal cortex

function. *Annual Review of Neuroscience*, *24*(1), 167–202. http://doi.org/10.1146/annurev.neuro.24.1.167
Min, Y., Kristiansen, K., Boggs, J. M., Husted, C., Zasadzinski, J. A., & Israelachvili, J. (2009). Interaction forces and adhesion of supported myelin lipid bilayers modulated by myelin basic protein. *Proceedings of the National Academy of Sciences of the United States of America*, *106*(9), 3154–3159. http://doi.org/10.1073/pnas.0813110106
Minot, S., Sinha, R., Chen, J., Li, H., Keilbaugh, S. A., Wu, G. D., et al. (2011). The human gut virome: Inter-individual variation and dynamic response to diet. *Genome Research*, *21*(10), 1616–1625. http://doi.org/10.1101/gr.122705.111
Minter, M. R., Zhang, C., Leone, V., Ringus, D. L., Zhang, X., Oyler-Castrillo, P., Musch, M. W., Liao, F., Ward, J. F., Holtzman, D. M., Chang, E. B., Tanzi, R. E., & Sisodia, S. S. (2017). Antibiotic-induced perturbations in gut microbial diversity influences neuro-inflammation and amyloidosis in a murine model of Alzheimer's disease. *Scientific Reports*, 1–12. http://doi.org/10.1038/srep30028
Mirochnic, S., Wolf, S., Staufenbiel, M., & Kempermann, G. (2009). Age effects on the regulation of adult hippocampal neurogenesis by physical activity and environmental enrichment in the APP23 mouse model of Alzheimer disease. *Hippocampus*, *19*(10), 1008–1018. http://doi.org/10.1002/hipo.20560
Mitew, S., Hay, C. M., Peckham, H., Xiao, J., Koenning, M., & Emery, B. (2014). Mechanisms regulating the development of oligodendrocytes and central nervous system myelin. *Neuroscience*, *276*(C), 29–47. http://doi.org/10.1016/j.neuroscience.2013.11.029
Mitra, S., Tsvetkov, A. S., & Finkbeiner, S. (2009). Single neuron ubiquitin-proteasome dynamics accompanying inclusion body formation in huntington disease. *The Journal of Biological Chemistry*, *284*(7), 4398–4403. http://doi.org/10.1074/jbc.M806269200
Mo, C., Hannan, A. J., & Renoir, T. (2015a). Environmental factors as modulators of neurodegeneration: Insights from gene–environment interactions in Huntington's disease. *Neuroscience and Biobehavioral Reviews*, *52*, 178–192. http://doi.org/10.1016/j.neubiorev.2015.03.003
Mo, C., Pang, T. Y., Ransome, M. I., Hill, R. A., Renoir, T., & Hannan, A. J. (2014a). High stress hormone levels accelerate the onset of memory deficits in male Huntington's disease mice. *Neurobiology of Disease*, *69*(C), 248–262. http://doi.org/10.1016/j.nbd.2014.05.004
Mo, C., Renoir, T., & Hannan, A. J. (2014b). Effects of chronic stress on the onset and progression of Huntington's disease in transgenic mice. *Neurobiology of Disease*, *71*(C), 81–94. http://doi.org/10.1016/j.nbd.2014.07.008
Mo, C., Renoir, T., & Hannan, A. J. (2014c). Ethological endophenotypes are altered by elevated stress hormone levels in both Huntington's disease and wildtype mice. *Behavioural Brain Research*, *274*, 118–127. http://doi.org/10.1016/j.bbr.2014.07.044
Mo, C., Renoir, T., & Hannan, A. J. (2015b). What's wrong with my mouse cage? Methodological considerations for modeling lifestyle factors and gene–environment interactions in mice. *Journal of Neuroscience Methods*, 1–10. http://doi.org/10.1016/j.jneumeth.2015.08.008

Mo, C., Renoir, T., Pang, T. Y. C., & Hannan, A. J. (2013). Short-term memory acquisition in female Huntington's disease mice is vulnerable to acute stress. *Behavioural Brain Research*, *253*, 318–322. http://doi.org/10.1016/j.bbr.2013.07.041

Morrison, P. J. (2012). Prevalence estimates of Huntington disease in Caucasian populations are gross underestimates. *Movement Disorders*, *27*(13), 1707–8– author reply 1708–9. http://doi.org/10.1002/mds.25266

Mosaferi, B., Babri, S., Ebrahimi, H., & Mohaddes, G. (2015). Enduring effects of post-weaning rearing condition on depressive- and anxiety-like behaviors and motor activity in male rats. *Physiology & Behavior*, *142*(C), 131–136. http://doi.org/10.1016/j.physbeh.2015.02.015

Mount, C. W., & Monje, M. (2017). Wrapped to Adapt: Experience-Dependent Myelination, 1–14. http://doi.org/10.1016/j.neuron.2017.07.009

Moya, A., & Ferrer, M. (2016). Functional Redundancy- Induced Stability of Gut Microbiota Subjected to Disturbance. *Trends in Microbiology*, *24*(5), 402–413. http://doi.org/10.1016/j.tim.2016.02.002

Nakatani, H., Martin, E., Hassani, H., Clavairoly, A., Maire, C. L., Viadieu, A., et al. (2013). Ascl1/Mash1 promotes brain oligodendrogenesis during myelination and remyelination. *The Journal of Neuroscience : the Official Journal of the Society for Neuroscience*, *33*(23), 9752–9768. http://doi.org/10.1523/JNEUROSCI.0805-13.2013

Nankova, B. B., Agarwal, R., MacFabe, D. F., & La Gamma, E. F. (2014). Enteric bacterial metabolites propionic and butyric acid modulate gene expression, including CREB-dependent catecholaminergic neurotransmission, in PC12 cells--possible relevance to autism spectrum disorders. *PLoS ONE*, *9*(8), e103740. http://doi.org/10.1371/journal.pone.0103740

Nave, K.-A. (2010). Myelination and support of axonal integrity by glia. *Nature*, *468*(7321), 244–252. http://doi.org/10.1038/nature09614

Nave, K.-A., & Werner, H. B. (2014). Myelination of the Nervous System: Mechanisms and Functions. *Annual Review of Cell and Developmental Biology*, *30*(1), 503–533. http://doi.org/10.1146/annurev-cellbio-100913-013101

Neufeld, K. M., Kang, N., Bienenstock, J., & Foster, J. A. (2011). Reduced anxiety-like behavior and central neurochemical change in germ-free mice. *Neurogastroenterology and Motility : the Official Journal of the European Gastrointestinal Motility Society*, *23*(3), 255–64– e119. http://doi.org/10.1111/j.1365-2982.2010.01620.x

Nguyen, G. D., Gokhan, S., Molero, A. E., & Mehler, M. F. (2013). Selective Roles of Normal and Mutant Huntingtin in Neural Induction and Early Neurogenesis. *PLoS ONE*, *8*(5), e64368. http://doi.org/10.1371/journal.pone.0064368

Nishida, C., Uauy, R., Kumanyika, S., & Shetty, P. (2004). The joint WHO/FAO expert consultation on diet, nutrition and the prevention of chronic diseases: process, product and policy implications. (Vol. 7, pp. 245–250). Presented at the Public health nutrition.

Nishiyama, A., Boshans, L., Goncalves, C. M., Wegrzyn, J., & Patel, K. D. (2016). Lineage, fate, and fate potential of NG2-glia, 1–13.

http://doi.org/10.1016/j.brainres.2015.08.013
Nishiyama, A., Komitova, M., Suzuki, R., & Zhu, X. (2009). Polydendrocytes (NG2 cells): multifunctional cells with lineage plasticity. *Nature Reviews Neuroscience*, *10*(1), 9–22. http://doi.org/10.1038/nrn2495
Nishiyama, A., Lin, X. H., Giese, N., Heldin, C. H., & Stallcup, W. B. (1996). Interaction between NG2 proteoglycan and PDGF alpha-receptor on O2A progenitor cells is required for optimal response to PDGF. *Journal of Neuroscience Research*, *43*(3), 315–330. http://doi.org/10.1002/(SICI)1097-4547(19960201)43:3<315::AID-JNR6>3.0.CO;2-M
Nithianantharajah, J., & Hannan, A. J. (2006). Enriched environments, experience-dependent plasticity and disorders of the nervous system. *Nature Reviews Neuroscience*, *7*(9), 697–709. http://doi.org/10.1038/nrn1970
Nithianantharajah, J., Barkus, C., Murphy, M., & Hannan, A. J. (2008). Gene–environment interactions modulating cognitive function and molecular correlates of synaptic plasticity in Huntington's disease transgenic mice. *Neurobiology of Disease*, *29*(3), 490–504. http://doi.org/10.1016/j.nbd.2007.11.006
Noble, M., Murray, K., Stroobant, P., Waterfield, M. D., & Riddle, P. (1988). Platelet-derived growth factor promotes division and motility and inhibits premature differentiation of the oligodendrocyte/type-2 astrocyte progenitor ceil. *Nature*, *333*(6173), 560–562. http://doi.org/10.1038/333560a0
Norin, E., & Midtvedt, T. (2010). Intestinal microflora functions in laboratory mice claimed to harbor a "normal" intestinal microflora. Is the SPF concept running out of date? *Anaerobe*, *16*(3), 311–313. http://doi.org/10.1016/j.anaerobe.2009.10.006
Novak, M. J. U., Seunarine, K. K., Gibbard, C. R., Hobbs, N. Z., Scahill, R. I., Clark, C. A., & Tabrizi, S. J. (2014). White matter integrity in premanifest and early Huntington's disease is related to caudate loss and disease progression. *Cortex*, *52*(C), 98–112. http://doi.org/10.1016/j.cortex.2013.11.009
Novitch, B. G., Chen, A. I., & Jessell, T. M. (2001). Coordinate Regulation of Motor Neuron Subtype Identity and Pan-Neuronal Properties by the bHLH Repressor Olig2. *Neuron*, *31*(5), 773–789. http://doi.org/10.1016/S0896-6273(01)00407-X
Novkovic, T., Mittmann, T., & Manahan-Vaughan, D. (2015). BDNF contributes to the facilitation of hippocampal synaptic plasticity and learning enabled by environmental enrichment. *Hippocampus*, *25*(1), 1–15. http://doi.org/10.1002/hipo.22342
Nucifora, F. C., Jr. (2001). Interference by Huntingtin and Atrophin-1 with CBP-Mediated Transcription Leading to Cellular Toxicity. *Science*, *291*(5512), 2423–2428. http://doi.org/10.1126/science.1056784
Ohland, C. L., Pankiv, E., Barkema, H., Thiesen, A., & Madsen, K. (2013). Tu2109 A Diet High in Fat and Refined Carbohydrate Decreases Anxiety and Exploratory Behaviour Under Normal but Not Inflammatory Conditions. *Gastroenterology*, *144*(5), S–931. http://doi.org/10.1016/S0016-5085(13)63464-2
Okada, R., Fujiwara, H., Mizuki, D., Araki, R., Yabe, T., & Matsumoto, K.

(2015). Involvement of dopaminergic and cholinergic systems in social isolation-induced deficits in social affiliation and conditional fear memory in mice. *Neuroscience*, *299*(C), 134–145. http://doi.org/10.1016/j.neuroscience.2015.04.064

Okuda, H., Tatsumi, K., Makinodan, M., Yamauchi, T., Kishimoto, T., & Wanaka, A. (2009). Environmental enrichment stimulates progenitor cell proliferation in the amygdala. *Journal of Neuroscience Research*, *87*(16), 3546–3553. http://doi.org/10.1002/jnr.22160

Olsson, I. A. S., & Dahlborn, K. (2002). Improving housing conditions for laboratory mice: a review of "environmental enrichment". *Laboratory Animals*, *36*(3), 243–270. http://doi.org/10.1258/002367702320162379

Orr, A. L., Li, S., Wang, C.-E., Li, H., Wang, J., Rong, J., et al. (2008). N-terminal mutant huntingtin associates with mitochondria and impairs mitochondrial trafficking. *The Journal of Neuroscience : the Official Journal of the Society for Neuroscience*, *28*(11), 2783–2792. http://doi.org/10.1523/JNEUROSCI.0106-08.2008

Osso, L. A., & Chan, J. R. (2017). ScienceDirect Architecting the myelin landscape, 1–7. http://doi.org/10.1016/j.conb.2017.06.005

Ouchi, H., Ono, K., Murakami, Y., & Matsumoto, K. (2013). Social isolation induces deficit of latent learning performance in mice: a putative animal model of attention deficit/hyperactivity disorder. *Behavioural Brain Research*, *238*, 146–153. http://doi.org/10.1016/j.bbr.2012.10.029

Pang, T. Y. C., & Hannan, A. J. (2012). Enhancement of cognitive function in models of brain disease through environmental enrichment and physical activity, 1–14. http://doi.org/10.1016/j.neuropharm.2012.06.029

Pang, T. Y. C., Du, X., Zajac, M. S., Howard, M. L., & Hannan, A. J. (2008). Altered serotonin receptor expression is associated with depression-related behavior in the R6/1 transgenic mouse model of Huntington's disease. *Human Molecular Genetics*, *18*(4), 753–766. http://doi.org/10.1093/hmg/ddn385

Parras, C. M., Hunt, C., Sugimori, M., Nakafuku, M., Rowitch, D., & Guillemot, F. (2007). The Proneural Gene Mash1 Specifies an Early Population of Telencephalic Oligodendrocytes. *Journal of Neuroscience*, *27*(16), 4233–4242. http://doi.org/10.1523/JNEUROSCI.0126-07.2007

Pell, M. D., Cheang, H. S., & Leonard, C. L. (2006). The impact of Parkinson's disease on vocal-prosodic communication from the perspective of listeners. *Brain and Language*, *97*(2), 123–134. http://doi.org/10.1016/j.bandl.2005.08.010

Penders, J., Stobberingh, E. E., van den Brandt, P. A., & Thijs, C. (2007). The role of the intestinal microbiota in the development of atopic disorders. *Allergy*, *62*(11), 1223–1236. http://doi.org/10.1111/j.1398-9995.2007.01462.x

Peña, Y., Prunell, M., Dimitsantos, V., Nadal, R., & Escorihuela, R. M. (2006). Environmental enrichment effects in social investigation in rats are gender dependent. *Behavioural Brain Research*, *174*(1), 181–187. http://doi.org/10.1016/j.bbr.2006.07.007

Peña, Y., Prunell, M., Rotllant, D., Armario, A., & Escorihuela, R. M. (2009). Enduring effects of environmental enrichment from weaning to adulthood on pituitary-adrenal function, pre-pulse inhibition and learning in male

and female rats. *Psychoneuroendocrinology*, *34*(9), 1390–1404. http://doi.org/10.1016/j.psyneuen.2009.04.019
Pereda-Pérez, I., Popović, N., Otalora, B. B., Popović, M., Madrid, J. A., Rol, M. A., & Venero, C. (2013). Long-term social isolation in the adulthood results in CA1 shrinkage and cognitive impairment. *Neurobiology of Learning and Memory*, *106*, 31–39. http://doi.org/10.1016/j.nlm.2013.07.004
Perez-Burgos, A., Wang, B., Mao, Y.-K., Mistry, B., McVey Neufeld, K.-A., Bienenstock, J., & Kunze, W. (2013). Psychoactive bacteria Lactobacillus rhamnosus (JB-1) elicits rapid frequency facilitation in vagal afferents. *American Journal of Physiology. Gastrointestinal and Liver Physiology*, *304*(2), G211–20. http://doi.org/10.1152/ajpgi.00128.2012
Peters, Y. M., & O'Donnell, P. (2005). Social isolation rearing affects prefrontal cortical response to ventral tegmental area stimulation. *Biological Psychiatry*, *57*(10), 1205–1208. http://doi.org/10.1016/j.biopsych.2005.02.011
Pfeiffer, S. E., Warrington, A. E., & Bansal, R. (1993). The oligodendrocyte and its many cellular processes. *Trends in Cell Biology*, *3*(6), 191–197.
Pham-Dinh, D., Mattei, M. G., Nussbaum, J. L., Roussel, G., Pontarotti, P., Roeckel, N., et al. (1993). Myelin/oligodendrocyte glycoprotein is a member of a subset of the immunoglobulin superfamily encoded within the major histocompatibility complex. *Proceedings of the National Academy of Sciences*, *90*(17), 7990–7994.
Phillips, O., Squitieri, F., Sanchez-Castaneda, C., Elifani, F., Caltagirone, C., Sabatini, U., & Di Paola, M. (2014). Deep White Matter in Huntington's Disease. *PLoS ONE*, *9*(10), e109676–11. http://doi.org/10.1371/journal.pone.0109676
Piira, A., van Walsem, M. R., Mikalsen, G., Nilsen, K. H., Knutsen, S., & Frich, J. C. (2013). Effects of a One Year Intensive Multidisciplinary Rehabilitation Program for Patients with Huntington's Disease: a Prospective Intervention Study. *PLoS Currents*, 1–11. http://doi.org/10.1371/currents.hd.9504af71e0d1f87830c25c394be47027
Poirier, M. A., Jiang, H., & Ross, C. A. (2005). A structure-based analysis of huntingtin mutant polyglutamine aggregation and toxicity: evidence for a compact beta-sheet structure. *Human Molecular Genetics*, *14*(6), 765–774. http://doi.org/10.1093/hmg/ddi071
Polak, S., & Saini, M. (2015). Children Resisting Contact With a Parent Postseparation: Assessing This Phenomenon Using an Ecological Systems Framework. *Journal of Divorce & Remarriage*, *56*(3), 220–247. http://doi.org/10.1080/10502556.2015.1012698
Popkin, B. M. (2001). Nutrition in transition: the changing global nutrition challenge. *Asia Pacific Journal of Clinical Nutrition*, *10 Suppl*, S13–8.
Popkin, B. M., Adair, L. S., & Ng, S. W. (2012). Global nutrition transition and the pandemic of obesity in developing countries. *Nutrition Reviews*, *70*(1), 3–21. http://doi.org/10.1111/j.1753-4887.2011.00456.x
Porter, J. R., & Rettger, L. F. (1940). Influence of Diet on the Distribution of Bacteria in The Stomach, Small Intestine and Cecum of the White Rat. *Journal of Infectious Diseases*, *66*(2), 104–110. http://doi.org/10.1093/infdis/66.2.104
Potter, M. C., Yuan, C., Ottenritter, C., Mughal, M., & van Praag, H. (2010).

Exercise is not beneficial and may accelerate symptom onset in a mouse model of Huntington's disease. *PLoS Currents*, *2*, RRN1201–19. http://doi.org/10.1371/currents.RRN1201

Poudel, G. R., Stout, J. C., Domínguez D, J. F., Churchyard, A., Chua, P., Egan, G. F., & Georgiou-Karistianis, N. (2015). Longitudinal change in white matter microstructure in Huntington's disease: The IMAGE-HD study. *Neurobiology of Disease*, *74*, 406–412. http://doi.org/10.1016/j.nbd.2014.12.009

Pouladi, M. A., Graham, R. K., Karasinska, J. M., Xie, Y., Santos, R. D., Petersen, A., & Hayden, M. R. (2008). Prevention of depressive behaviour in the YAC128 mouse model of Huntington disease by mutation at residue 586 of huntingtin. *Brain*, *132*(4), 919–932. http://doi.org/10.1093/brain/awp006

Pouladi, M. A., Morton, A. J., & Hayden, M. R. (2013a). Choosing an animal model for the study of Huntington's disease. *Nature Reviews Neuroscience*, *14*(10), 708–721. http://doi.org/10.1038/nrn3570

Pouladi, M. A., Morton, A. J., & Hayden, M. R. (2013b). Choosing an animal model for the study of Huntington's disease. *Nature Publishing Group*, *14*(10), 708–721. http://doi.org/10.1038/nrn3570

Pouladi, M. A., Xie, Y., Skotte, N. H., Ehrnhoefer, D. E., Graham, R. K., Kim, J. E., et al. (2010). Full-length huntingtin levels modulate body weight by influencing insulin-like growth factor 1 expression. *Human Molecular Genetics*, *19*(8), 1528–1538. http://doi.org/10.1093/hmg/ddq026

Powers, B. E., Sellers, D. L., Lovelett, E. A., Cheung, W., Aalami, S. P., Zapertov, N., et al. (2013). Remyelination reporter reveals prolonged refinement of spontaneously regenerated myelin. *Proceedings of the National Academy of Sciences of the United States of America*, *110*(10), 4075–4080. http://doi.org/10.1073/pnas.1210293110

Pöllinger, B., Krishnamoorthy, G., Berer, K., Lassmann, H., Bösl, M. R., Dunn, R., et al. (2009). Spontaneous relapsing-remitting EAE in the SJL/J mouse: MOG-reactive transgenic T cells recruit endogenous MOG-specific B cells. *The Journal of Experimental Medicine*, *206*(6), 1303–1316. http://doi.org/10.1084/jem.20090299

Pringle, N. P., & Richardson, W. D. (1993). A singularity of PDGF alpha-receptor expression in the dorsoventral axis of the neural tube may define the origin of the oligodendrocyte lineage. *Development*, *117*(2), 525–533.

Psachoulia, K., Jamen, F., Young, K. M., & Richardson, W. D. (2009). Cell cycle dynamics of NG2 cells in the postnatal and ageing brain. *Neuron Glia Biology*, *5*(3-4), 57–67. http://doi.org/10.1017/S1740925X09990354

Puhl, N. J., Uwiera, R. R. E., Yanke, L. J., Selinger, L. B., & Inglis, G. D. (2012). Antibiotics conspicuously affect community profiles and richness, but not the density of bacterial cells associated with mucosa in the large and small intestines of mice. *Anaerobe*, *18*(1), 67–75. http://doi.org/10.1016/j.anaerobe.2011.12.007

Qi, Y., Cai, J., Wu, Y., Wu, R., Lee, J., Fu, H., et al. (2001). Control of oligodendrocyte differentiation by the Nkx2.2 homeodomain transcription factor. *Development*, *128*(14), 2723–2733.

Qin, J., Li, R., Raes, J., Arumugam, M., Burgdorf, K. S., Manichanh, C., et al.

(2010). A human gut microbial gene catalogue established by metagenomic sequencing. *Nature*, *464*(7285), 59–65. http://doi.org/10.1038/nature08821

Qiu, X., Huang, C.-X., Lu, W., Yang, S., Li, C., Shi, X.-Y., et al. (2012). Effects of a 4month enriched environment on the hippocampus and the myelinated fibers in the hippocampus of middle-aged rats. *Brain Research*, *1465*, 26–33. http://doi.org/10.1016/j.brainres.2012.05.025

Quinn, L., Busse, M., Carrier, J., Fritz, N., Harden, J., Hartel, L., et al. (2017). Physical therapy and exercise interventions in Huntington's disease. *JBI Database of Systematic Reviews and Implementation Reports*, *15*(7), 1783–1799. http://doi.org/10.11124/JBISRIR-2016-003274

Raff, M. C., Miller, R. H., & Noble, M. (1983). A glial progenitor cell that develops in vitro into an astrocyte or an oligodendrocyte depending on culture medium. *Nature*, *303*(5916), 390–396.

Rakoff-Nahoum, S., Paglino, J., Eslami-Varzaneh, F., Edberg, S., & Medzhitov, R. (2004). Recognition of commensal microflora by toll-like receptors is required for intestinal homeostasis. *Cell*, *118*(2), 229–241. http://doi.org/10.1016/j.cell.2004.07.002

Ransome, M. I., & Hannan, A. J. (2013). Impaired basal and running-induced hippocampal neurogenesis coincides with reduced Akt signaling in adult R6/1 HD mice. *Molecular and Cellular Neurosciences*, *54*, 93–107. http://doi.org/10.1016/j.mcn.2013.01.005

Raybaud, C. (2010). The corpus callosum, the other great forebrain commissures, and the septum pellucidum: anatomy, development, and malformation. *Neuroradiology*, *52*(6), 447–477. http://doi.org/10.1007/s00234-010-0696-3

Reddy, P. H., Williams, M., Charles, V., Garrett, L., Pike-Buchanan, L., Whetsell, W. O., et al. (1998). Behavioural abnormalities and selective neuronal loss in HD transgenic mice expressing mutated full-length HD cDNA. *Nature Genetics*, *20*(2), 198–202. http://doi.org/10.1038/2510

Reetz, K., Werner, C. J., & Schiefer, J. (2015). Clinical diagnosis and management in early Huntington's disease: a review. *Degenerative Neurological and Neuromuscular Disease*, 37–14. http://doi.org/10.2147/DNND.S49135

Reikvam, D. H., Erofeev, A., Sandvik, A., Grcic, V., Jahnsen, F. L., Gaustad, P., et al. (2011). Depletion of Murine Intestinal Microbiota: Effects on Gut Mucosa and Epithelial Gene Expression. *PLoS ONE*, *6*(3), e17996–13. http://doi.org/10.1371/journal.pone.0017996

Reiner, A., Albin, R. L., Anderson, K. D., D'Amato, C. J., Penney, J. B., & Young, A. B. (1988). Differential loss of striatal projection neurons in Huntington disease. *Proceedings of the National Academy of Sciences*, *85*(15), 5733–5737.

Renner, M. J., & Rosenzweig, M. R. (1987). The golden-mantled ground squirrel (Spermophilus lateralis) as a model for the effects of environmental enrichment in solitary animals. *Developmental Psychobiology*, *20*(1), 19–24. http://doi.org/10.1002/dev.420200106

Renoir, T., Pang, T. Y. C., Mo, C., Chan, G., Chevarin, C., Lanfumey, L., & Hannan, A. J. (2012). Differential effects of early environmental enrichment on emotionality related behaviours in Huntington's disease transgenic mice. *The Journal of Physiology*, *591*(1), 41–55.

http://doi.org/10.1113/jphysiol.2012.239798
Ringel, Y., & Maharshak, N. (2013). Intestinal microbiota and immune function in the pathogenesis of irritable bowel syndrome. *American Journal of Physiology. Gastrointestinal and Liver Physiology*, *305*(8), G529–41. http://doi.org/10.1152/ajpgi.00207.2012
Rivers, L. E., Young, K. M., Rizzi, M., Jamen, F., Psachoulia, K., Wade, A., et al. (2008). PDGFRA/NG2 glia generate myelinating oligodendrocytes and piriform projection neurons in adult mice. *Nature Publishing Group*, *11*(12), 1392–1401. http://doi.org/10.1038/nn.2220
Roberts, L., & Greene, J. R. T. (2003). Post-weaning social isolation of rats leads to a diminution of LTP in the CA1 to subiculum pathway. *Brain Research*, *991*(1-2), 271–273.
Rodrigues, H. G., Takeo Sato, F., Curi, R., & Vinolo, M. A. R. (2016). Fatty acids as modulators of neutrophil recruitment, function and survival. *European Journal of Pharmacology*, *785*, 50–58. http://doi.org/10.1016/j.ejphar.2015.03.098
Rosas, H. D., Koroshetz, W. J., Chen, Y. I., Skeuse, C., Vangel, M., Cudkowicz, M. E., et al. (2003). Evidence for more widespread cerebral pathology in early HD: an MRI-based morphometric analysis. *Neurology*, *60*(10), 1615–1620.
Rosas, H. D., Tuch, D. S., Hevelone, N. D., Zaleta, A. K., Vangel, M., Hersch, S. M., & Salat, D. H. (2006). Diffusion tensor imaging in presymptomatic and early Huntington's disease: Selective white matter pathology and its relationship to clinical measures. *Movement Disorders*, *21*(9), 1317–1325. http://doi.org/10.1002/mds.20979
Rosenberg, S. S., Kelland, E. E., Tokar, E., la Torre, De, A. R., & Chan, J. R. (2008). The geometric and spatial constraints of the microenvironment induce oligodendrocyte differentiation. *Proceedings of the National Academy of Sciences of the United States of America*, *105*(38), 14662–14667. http://doi.org/10.1073/pnas.0805640105
Ross, C. A., & Tabrizi, S. J. (2011). Huntington's disease: from molecular pathogenesis to clinical treatment. *The Lancet. Neurology*, *10*(1), 83–98. http://doi.org/10.1016/S1474-4422(10)70245-3
Round, J. L., & Mazmanian, S. K. (2009). The gut microbiota shapes intestinal immune responses during health and disease. *Nature Reviews Immunology*, *9*(5), 313–323. http://doi.org/10.1038/nri2515
Rumah, K. R., Linden, J., Fischetti, V. A., & Vartanian, T. (2013). Isolation of Clostridium perfringens Type B in an Individual at First Clinical Presentation of Multiple Sclerosis Provides Clues for Environmental Triggers of the Disease. *PLoS ONE*, *8*(10), e76359–9. http://doi.org/10.1371/journal.pone.0076359
Rushton, W. A. H. (1951). A theory of the effects of fibre size in medullated nerve. *The Journal of Physiology*, *115*(1), 101–122. http://doi.org/10.1111/(ISSN)1469-7793
Saab, A. S., Tzvetanova, I. D., & Nave, K.-A. (2013). The role of myelin and oligodendrocytes in axonal energy metabolism. *Current Opinion in Neurobiology*, *23*(6), 1065–1072. http://doi.org/10.1016/j.conb.2013.09.008
Sakakibara, H., Suzuki, A., Kobayashi, A., Motoyama, K., Matsui, A.,

Sayama, K., et al. (2012). Social isolation stress induces hepatic hypertrophy in C57BL/6J mice. *The Journal of Toxicological Sciences*, *37*(5), 1071–1076.
Salazar, N., Arboleya, S., Valdés, L., Stanton, C., Ross, P., Ruiz, L., et al. (2014). The human intestinal microbiome at extreme ages of life. Dietary intervention as a way to counteract alterations. *Frontiers in Genetics*, *5*(237ra265), 406. http://doi.org/10.3389/fgene.2014.00406
Salonen, A., Salojärvi, J., Lahti, L., & de Vos, W. M. (2012). The adult intestinal core microbiota is determined by analysis depth and health status. *Clinical Microbiology and Infection : the Official Publication of the European Society of Clinical Microbiology and Infectious Diseases*, *18 Suppl 4*, 16–20. http://doi.org/10.1111/j.1469-0691.2012.03855.x
Sampson, T. R., Debelius, J. W., Thron, T., Janssen, S., Shastri, G. G., Ilhan, Z. E., et al. (2016). Gut Microbiota Regulate Motor Deficits and Neuroinflammation in a Model of Parkinson's Disease, 1–25. http://doi.org/10.1016/j.cell.2016.11.018
Sanna, V., Di Giacomo, A., La Cava, A., Lechler, R. I., Fontana, S., Zappacosta, S., & Matarese, G. (2003). Leptin surge precedes onset of autoimmune encephalomyelitis and correlates with development of pathogenic T cell responses. *Journal of Clinical Investigation*, *111*(2), 241–250. http://doi.org/10.1172/JCI16721
Sapp, E., Ge, P., Aizawa, H., Bird, E., Penney, J., Young, A. B., et al. (1995). Evidence for a preferential loss of enkephalin immunoreactivity in the external globus pallidus in low grade Huntington's disease using high resolution image analysis. *Neuroscience*, *64*(2), 397–404.
Sapp, E., Kegel, K. B., Aronin, N., Hashikawa, T., Uchiyama, Y., Tohyama, K., et al. (2001). Early and Progressive Accumulation of Reactive Microglia in the Huntington Disease Brain. *Journal of Neuropathology & Experimental Neurology*, *60*(2), 161–172. http://doi.org/10.1093/jnen/60.2.161
Sathasivam, K., Neueder, A., Gipson, T. A., Landles, C., Benjamin, A. C., Bondulich, M. K., et al. (2013). Aberrant splicing of HTT generates the pathogenic exon 1 protein in Huntington disease. *Proceedings of the National Academy of Sciences of the United States of America*, *110*(6), 2366–2370. http://doi.org/10.1073/pnas.1221891110
Savignac, H. M., Kiely, B., Dinan, T. G., & Cryan, J. F. (2014). Bifidobacteria exert strain-specific effects on stress-related behavior and physiology in BALB/c mice. *Neurogastroenterology and Motility : the Official Journal of the European Gastrointestinal Motility Society*, *26*(11), 1615–1627. http://doi.org/10.1111/nmo.12427
Sánchez, M. M., Hearn, E. F., Do, D., Rilling, J. K., & Herndon, J. G. (1998). Differential rearing affects corpus callosum size and cognitive function of rhesus monkeys. *Brain Research*, *812*(1-2), 38–49.
Scaccianoce, S., Del Bianco, P., Paolone, G., Caprioli, D., Modafferi, A. M. E., Nencini, P., & Badiani, A. (2006). Social isolation selectively reduces hippocampal brain-derived neurotrophic factor without altering plasma corticosterone. *Behavioural Brain Research*, *168*(2), 323–325. http://doi.org/10.1016/j.bbr.2005.04.024
Schilling, G., Savonenko, A. V., Coonfield, M. L., Morton, J. L., Vorovich, E., Gale, A., et al. (2004). Environmental, pharmacological, and genetic

modulation of the HD phenotype in transgenic mice. *Experimental Neurology*, *187*(1), 137–149. http://doi.org/10.1016/j.expneurol.2004.01.003

Schmithorst, V. J., & Wilke, M. (2002). Differences in white matter architecture between musicians and non-musicians: a diffusion tensor imaging study. *Neuroscience Letters*, *321*(1-2), 57–60.

Scholz, J., Klein, M. C., Behrens, T. E. J., & Johansen-Berg, H. (2009). Training induces changes in white-matter architecture. *Nature Publishing Group*, *12*(11), 1370–1371. http://doi.org/10.1038/nn.2412

Schrag, A., Jahanshahi, M., & Quinn, N. P. (2001). What contributes to depression in Parkinson's disease? *Psychological Medicine*, *31*(1), 65–73.

Segovia, G., Delarco, A., Deblas, M., Garrido, P., & Mora, F. (2008). Effects of an enriched environment on the release of dopamine in the prefrontal cortex produced by stress and on working memory during aging in the awake rat. *Behavioural Brain Research*, *187*(2), 304–311. http://doi.org/10.1016/j.bbr.2007.09.024

Severance, E. G., Gressitt, K. L., Stallings, C. R., Origoni, A. E., Khushalani, S., Leweke, F. M., et al. (2013). Discordant patterns of bacterial translocation markers and implications for innate immune imbalances in schizophrenia. *Schizophrenia Research*, *148*(1-3), 130–137. http://doi.org/10.1016/j.schres.2013.05.018

Shaffer, J. J., Ghayoor, A., Long, J. D., Kim, R. E.-Y., Lourens, S., O'Donnell, L. J., et al. (2017). Longitudinal diffusion changes in prodromal and early HD: Evidence of white-matter tract deterioration. *Human Brain Mapping*, *38*(3), 1460–1477. http://doi.org/10.1002/hbm.23465

Shah, Parul, Nankova, B. B., Parab, S., & La Gamma, E. F. (2006). Short chain fatty acids induce TH gene expression via ERK-dependent phosphorylation of CREB protein. *Brain Research*, *1107*(1), 13–23. http://doi.org/10.1016/j.brainres.2006.05.097

Shen, S., Li, J., & Casaccia-Bonnefil, P. (2005). Histone modifications affect timing of oligodendrocyte progenitor differentiation in the developing rat brain. *The Journal of Cell Biology*, *169*(4), 577–589. http://doi.org/10.1083/jcb.200412101

Shi, J., Marinovich, A., & Barres, B. A. (1998). Purification and characterization of adult oligodendrocyte precursor cells from the rat optic nerve. *Journal of Neuroscience*, *18*(12), 4627–4636.

Shin, J.-Y., Fang, Z.-H., Yu, Z.-X., Wang, C.-E., Li, S.-H., & Li, X.-J. (2005). Expression of mutant huntingtin in glial cells contributes to neuronal excitotoxicity. *The Journal of Cell Biology*, *171*(6), 1001–1012. http://doi.org/10.1083/jcb.200508072

Shirendeb, U. P., Calkins, M. J., Manczak, M., Anekonda, V., Dufour, B., McBride, J. L., et al. (2011). Mutant huntingtin“s interaction with mitochondrial protein Drp1 impairs mitochondrial biogenesis and causes defective axonal transport and synaptic degeneration in Huntington”s disease. *Human Molecular Genetics*, *21*(2), 406–420. http://doi.org/10.1093/hmg/ddr475

Silva, C. S. D., Lindau, T. A., & Giacheti, C. M. (2015). Comportamento, competência social e qualidade de vida na Doença de Huntington.

Revista CEFAC, *17*(6), 1792–1801. http://doi.org/10.1590/1982-0216201517621414
Simon, C., Götz, M., & Dimou, L. (2011). Progenitors in the adult cerebral cortex: cell cycle properties and regulation by physiological stimuli and injury. *Glia*, *59*(6), 869–881. http://doi.org/10.1002/glia.21156
Simonetti, T., Lee, H., Bourke, M., Leamey, C. A., & Sawatari, A. (2009). Enrichment from Birth Accelerates the Functional and Cellular Development of a Motor Control Area in the Mouse. *PLoS ONE*, *4*(8), e6780–9. http://doi.org/10.1371/journal.pone.0006780
Simons, M., & Nave, K.-A. (2015). Oligodendrocytes: Myelination and Axonal Support. *Cold Spring Harbor Perspectives in Biology*, *8*(1), a020479. http://doi.org/10.1101/cshperspect.a020479
Singh, N., Thangaraju, M., Prasad, P. D., Martin, P. M., Lambert, N. A., Boettger, T., et al. (2010). Blockade of dendritic cell development by bacterial fermentation products butyrate and propionate through a transporter (Slc5a8)-dependent inhibition of histone deacetylases. *The Journal of Biological Chemistry*, *285*(36), 27601–27608. http://doi.org/10.1074/jbc.M110.102947
Singhal, G., Jaehne, E. J., Corrigan, F., & Baune, B. T. (2014). Cellular and molecular mechanisms of immunomodulation in the brain through environmental enrichment. *Frontiers in Cellular Neuroscience*, *8*(e64208), 165. http://doi.org/10.3389/fncel.2014.00097
Sipione, S., Rigamonti, D., Valenza, M., Zuccato, C., Conti, L., Pritchard, J., et al. (2002). Early transcriptional profiles in huntingtin-inducible striatal cells by microarray analyses. *Human Molecular Genetics*, *11*(17), 1953–1965.
Skillings, E. A., Wood, N. I., & Morton, A. J. (2014). Beneficial effects of environmental enrichment and food entrainment in the R6/2 mouse model of Huntington's disease. *Brain and Behavior*, *4*(5), 675–686. http://doi.org/10.1002/brb3.235
Slow, E. J., van Raamsdonk, J., Rogers, D., Coleman, S. H., Graham, R. K., Deng, Y., et al. (2003). Selective striatal neuronal loss in a YAC128 mouse model of Huntington disease. *Human Molecular Genetics*, *12*(13), 1555–1567.
Smith, K., McCoy, K. D., & Macpherson, A. J. (2007). Use of axenic animals in studying the adaptation of mammals to their commensal intestinal microbiota. *Seminars in Immunology*, *19*(2), 59–69. http://doi.org/10.1016/j.smim.2006.10.002
Snaidero, N., & Simons, M. (2014). Myelination at a glance. *Journal of Cell Science*, *127*(Pt 14), 2999–3004. http://doi.org/10.1242/jcs.151043
Snell, R. G., MacMillan, J. C., Cheadle, J. P., Fenton, I., Lazarou, L. P., Davies, P., et al. (1993). Relationship between trinucleotide repeat expansion and phenotypic variation in Huntington's disease. *Nature Genetics*, *4*(4), 393–397. http://doi.org/10.1038/ng0893-393
Sommer, I., & Schachner, M. (1981). Monoclonal antibodies (O1 to O4) to oligodendrocyte cell surfaces: An immunocytological study in the central nervous system. *Developmental Biology*, *83*(2), 311–327. http://doi.org/10.1016/0012-1606(81)90477-2
Soundarapandian, M. M., Selvaraj, V., Lo, U.-G., Golub, M. S., Feldman, D. H., Pleasure, D. E., & Deng, W. (2011). Zfp488 promotes

oligodendrocyte differentiation of neural progenitor cells in adult mice after demyelination. *Scientific Reports*, *1*(1), 2. http://doi.org/10.1038/srep00002

Southwell, A. L., Ko, J., & Patterson, P. H. (2009). Intrabody Gene Therapy Ameliorates Motor, Cognitive, and Neuropathological Symptoms in Multiple Mouse Models of Huntington's Disease. *Journal of Neuroscience*, *29*(43), 13589–13602. http://doi.org/10.1523/JNEUROSCI.4286-09.2009

Spires, T. L. (2004). Environmental Enrichment Rescues Protein Deficits in a Mouse Model of Huntington's Disease, Indicating a Possible Disease Mechanism. *Journal of Neuroscience*, *24*(9), 2270–2276. http://doi.org/10.1523/JNEUROSCI.1658-03.2004

Steelman, A. J., Thompson, J. P., & Li, J. (2012). Demyelination and remyelination in anatomically distinct regions of the corpus callosum following cuprizone intoxication. *Neuroscience Research*, *72*(1), 32–42. http://doi.org/10.1016/j.neures.2011.10.002

Steffan, J. S., Bodai, L., Pallos, J., Poelman, M., McCampbell, A., Apostol, B. L., et al. (2001). Histone deacetylase inhibitors arrest polyglutamine-dependent neurodegeneration in Drosophila. *Nature*, *413*(6857), 739–743. http://doi.org/10.1038/35099568

Steiner, B., Winter, C., Hosman, K., Siebert, E., Kempermann, G., Petrus, D. S., & Kupsch, A. (2006). Enriched environment induces cellular plasticity in the adult substantia nigra and improves motor behavior function in the 6-OHDA rat model of Parkinson's disease. *Experimental Neurology*, *199*(2), 291–300. http://doi.org/10.1016/j.expneurol.2005.11.004

Stilling, R. M., Dinan, T. G., & Cryan, J. F. (2013). Microbial genes, brain & behaviour - epigenetic regulation of the gut-brain axis. *Genes, Brain and Behavior*, *13*(1), 69–86. http://doi.org/10.1111/gbb.12109

Stolt, C. C. (2004). Transcription factors Sox8 and Sox10 perform non-equivalent roles during oligodendrocyte development despite functional redundancy. *Development*, *131*(10), 2349–2358. http://doi.org/10.1242/dev.01114

Stolt, C. C., Rehberg, S., Ader, M., Lommes, P., Riethmacher, D., Schachner, M., et al. (2002). Terminal differentiation of myelin-forming oligodendrocytes depends on the transcription factor Sox10. *Genes & Development*, *16*(2), 165–170. http://doi.org/10.1101/gad.215802

Stranahan, A. M., Khalil, D., & Gould, E. (2006). Social isolation delays the positive effects of running on adult neurogenesis. *Nature Neuroscience*, *9*(4), 526–533. http://doi.org/10.1038/nn1668

Sturrock, R. R. (1980). Myelination of the mouse corpus callosum. *Neuropathology and Applied Neurobiology*, *6*(6), 415–420.

Sudo, N., Chida, Y., Aiba, Y., Sonoda, J., Oyama, N., Yu, X.-N., et al. (2004). Postnatal microbial colonization programs the hypothalamic-pituitary-adrenal system for stress response in mice. *The Journal of Physiology*, *558*(Pt 1), 263–275. http://doi.org/10.1113/jphysiol.2004.063388

Sugimori, M., Nagao, M., Parras, C. M., Nakatani, H., Lebel, M., Guillemot, F., & Nakafuku, M. (2008). Ascl1 is required for oligodendrocyte development in the spinal cord. *Development*, *135*(7), 1271–1281. http://doi.org/10.1242/dev.015370

Sun, M., Choi, E. Y., Magee, D. J., Stets, C. W., During, M. J., & Lin, E.-J. D. (2014). Metabolic Effects of Social Isolation in Adult C57BL/6 Mice. *International Scholarly Research Notices*, *2014*(2), 1–9. http://doi.org/10.1155/2014/690950

Svaren, J. (2014). MicroRNA and transcriptional crosstalk in myelinating glia. *Neurochemistry International*, *77*, 50–57. http://doi.org/10.1016/j.neuint.2014.06.010

Szebenyi, G., Morfini, G. A., Babcock, A., Gould, M., Selkoe, K., Stenoien, D. L., et al. (2003). Neuropathogenic forms of huntingtin and androgen receptor inhibit fast axonal transport. *Neuron*, *40*(1), 41–52. http://doi.org/10.1038/nrn1268

Tabrizi, S. J., Langbehn, D. R., Leavitt, B. R., Roos, R. A., Durr, A., Craufurd, D., et al. (2009). Articles Biological and clinical manifestations of Huntington's disease in the longitudinal TRACK-HD study: cross-sectional analysis of baseline data. *The Lancet. Neurology*, *8*(9), 791–801. http://doi.org/10.1016/S1474-4422(09)70170-X

Tabrizi, S. J., Scahill, R. I., Owen, G., Durr, A., Leavitt, B. R., Roos, R. A., et al. (2013). Predictors of phenotypic progression and disease onset in premanifest and early-stage Huntington's disease in the TRACK-HD study: analysis of 36-month observational data. *The Lancet. Neurology*, *12*(7), 637–649. http://doi.org/10.1016/S1474-4422(13)70088-7

Tai, Y. F., Pavese, N., Gerhard, A., Tabrizi, S. J., Barker, R. A., Brooks, D. J., & Piccini, P. (2007). Microglial activation in presymptomatic Huntington's disease gene carriers. *Brain*, *130*(7), 1759–1766. http://doi.org/10.1093/brain/awm044

Tajiri, N., Yasuhara, T., Shingo, T., Kondo, A., Yuan, W., Kadota, T., et al. (2010). Exercise exerts neuroprotective effects on Parkinson's disease model of rats. *Brain Research*, *1310*(C), 200–207. http://doi.org/10.1016/j.brainres.2009.10.075

Takada, N., Kucenas, S., & Appel, B. (2010). Sox10 is necessary for oligodendrocyte survival following axon wrapping. *Glia*, *58*(8), 996–1006. http://doi.org/10.1002/glia.20981

Takeuchi, H., Sekiguchi, A., Taki, Y., Yokoyama, S., Yomogida, Y., Komuro, N., et al. (2010). Training of Working Memory Impacts Structural Connectivity. *Journal of Neuroscience*, *30*(9), 3297–3303. http://doi.org/10.1523/JNEUROSCI.4611-09.2010

Tang, Y. Y., Lu, Q., Fan, M., Yang, Y., & Posner, M. I. (2012). Mechanisms of white matter changes induced by meditation. *Proceedings of the National Academy of Sciences*, *109*(26), 10570–10574. http://doi.org/10.1073/pnas.1207817109

Taubert, M., Lohmann, G., Margulies, D. S., Villringer, A., & Ragert, P. (2011). Long-term effects of motor training on resting-state networks and underlying brain structure. *NeuroImage*, *57*(4), 1492–1498. http://doi.org/10.1016/j.neuroimage.2011.05.078

Taveggia, C., Thaker, P., Petrylak, A., Caporaso, G. L., Toews, A., Falls, D. L., et al. (2007). Type III neuregulin-1 promotes oligodendrocyte myelination. *Glia*, *56*(3), 284–293. http://doi.org/10.1002/glia.20612

Teicher, M. H., Dumont, N. L., Ito, Y., Vaituzis, C., Giedd, J. N., & Andersen, S. L. (2004). Childhood neglect is associated with reduced corpus callosum area. *Biological Psychiatry*, *56*(2), 80–85.

http://doi.org/10.1016/j.biopsych.2004.03.016
Teo, R. T. Y., Hong, X., Yu-Taeger, L., Huang, Y., Tan, L. J., Xie, Y., et al. (2016). Structural and molecular myelination deficits occur prior to neuronal loss in the YAC128 and BACHD models of Huntington disease. *Human Molecular Genetics*, *25*(13), 2621–2632. http://doi.org/10.1093/hmg/ddw122
Thompson, J. A., Cruickshank, T. M., Penailillo, L. E., Lee, J. W., Newton, R. U., Barker, R. A., & Ziman, M. R. (2013). The effects of multidisciplinary rehabilitation in patients with early-to-middle-stage Huntington's disease: a pilot study. *European Journal of Neurology*, *20*(9), 1325–1329. http://doi.org/10.1111/ene.12053
Tillerson, J. L., Caudle, W. M., Reverón, M. E., & Miller, G. W. (2003). Exercise induces behavioral recovery and attenuates neurochemical deficits in rodent models of Parkinson's disease. *Neuroscience*, *119*(3), 899–911.
Tomassy, G. S., Berger, D. R., Chen, H.-H., Kasthuri, N., Hayworth, K. J., Vercelli, A., et al. (2014). Distinct profiles of myelin distribution along single axons of pyramidal neurons in the neocortex. *Science*, *344*(6181), 319–324. http://doi.org/10.1126/science.1249766
Tomassy, G. S., Dershowitz, L. B., & Arlotta, P. (2016). Diversity Matters: A Revised Guide to Myelination. *Trends in Cell Biology*, *26*(2), 135–147. http://doi.org/10.1016/j.tcb.2015.09.002
Tomlinson, L., Leiton, C. V., & Colognato, H. (2016a). Behavioral experiences as drivers of oligodendrocyte lineage dynamics and myelin plasticity. *Neuropharmacology*, *110*, 548–562. http://doi.org/10.1016/j.neuropharm.2015.09.016
Tomlinson, L., Leiton, C. V., & Colognato, H. (2016b). Behavioral experiences as drivers of oligodendrocyte lineage dynamics and myelin plasticity. *Neuropharmacology*, *110*, 548–562. http://doi.org/10.1016/j.neuropharm.2015.09.016
Tong, X., Ao, Y., Faas, G. C., Nwaobi, S. E., Xu, J., Haustein, M. D., et al. (2014). Astrocyte Kir4.1 ion channel deficits contribute to neuronal dysfunction in Huntington's disease model mice. *Nature Neuroscience*, *17*(5), 694–703. http://doi.org/10.1038/nn.3691
Tsai, P. P., Pachowsky, U., Stelzer, H. D., & Hackbarth, H. (2016). Impact of environmental enrichment in mice. 1: Effect of housing conditions on body weight, organ weights and haematology in different strains. *Laboratory Animals*, *36*(4), 411–419. http://doi.org/10.1258/002367702320389071
Tsai, P. P., Stelzer, H. D., Hedrich, H. J., & Hackbarth, H. (2003). Are the effects of different enrichment designs on the physiology and behaviour of DBA/2 mice consistent? *Laboratory Animals*, *37*(4), 314–327. http://doi.org/10.1258/002367703322389889
Tsigos, C., & Chrousos, G. P. (2002). Hypothalamic-pituitary-adrenal axis, neuroendocrine factors and stress. *Journal of Psychosomatic Research*, *53*(4), 865–871.
Turnbaugh, P. J., Ley, R. E., Hamady, M., Fraser-Liggett, C. M., Knight, R., & Gordon, J. I. (2007). The Human Microbiome Project. *Nature*, *449*(7164), 804–810. http://doi.org/10.1038/nature06244

Valero, J., España, J., Parra-Damas, A., Martín, E., Rodríguez-Álvarez, J., & Saura, C. A. (2011). Short-Term Environmental Enrichment Rescues Adult Neurogenesis and Memory Deficits in APPSw,Ind Transgenic Mice. *PLoS ONE*, *6*(2), e16832. http://doi.org/10.1371/journal.pone.0016832

Vallès, Y., Artacho, A., Pascual-García, A., Ferrús, M. L., Gosalbes, M. J., Abellán, J. J., & Francino, M. P. (2014). Microbial succession in the gut: directional trends of taxonomic and functional change in a birth cohort of Spanish infants. *PLoS Genetics*, *10*(6), e1004406. http://doi.org/10.1371/journal.pgen.1004406

Vallès, Y., Gosalbes, M. J., de Vries, L. E., Abellán, J. J., & Francino, M. P. (2012). Metagenomics and development of the gut microbiota in infants. *Clinical Microbiology and Infection : the Official Publication of the European Society of Clinical Microbiology and Infectious Diseases*, *18 Suppl 4*, 21–26. http://doi.org/10.1111/j.1469-0691.2012.03876.x

Valny, M., Honsa, P., Kriska, J., & Anderova, M. (2017). Multipotency and therapeutic potential of NG2 cells, 1–14. http://doi.org/10.1016/j.bcp.2017.05.008

van Dellen, A., Blakemore, C., Deacon, R., York, D., & Hannan, A. J. (2000). Delaying the onset of Huntington's in mice. *Nature*, *404*(6779), 721–722. http://doi.org/10.1038/35008142

Van Dellen, A., Cordery, P. M., Spires, T. L., Blakemore, C., & Hannan, A. J. (2008). Wheel running from a juvenile age delays onset of specific motor deficits but does not alter protein aggregate density in a mouse model of Huntington's disease. *BMC Neuroscience*, *9*(1), 34–12. http://doi.org/10.1186/1471-2202-9-34

van der Marck, M. A., & Bloem, B. R. (2014). How to organize multispecialty care for patients with Parkinson's disease. *Parkinsonism and Related Disorders*, *20 Suppl 1*, S167–73. http://doi.org/10.1016/S1353-8020(13)70040-3

van der Marck, M. A., Munneke, M., Mulleners, W., Hoogerwaard, E. M., Borm, G. F., Overeem, S., et al. (2013). Integrated multidisciplinary care in Parkinson's disease: a non-randomised, controlled trial (IMPACT). *The Lancet. Neurology*, *12*(10), 947–956. http://doi.org/10.1016/S1474-4422(13)70196-0

van Oostrom, J. C. H., Sijens, P. E., Roos, R. A. C., & Leenders, K. L. (2007). 1H magnetic resonance spectroscopy in preclinical Huntington disease. *Brain Research*, *1168*, 67–71. http://doi.org/10.1016/j.brainres.2007.05.082

Van Raamsdonk, J. M., Pearson, J., Murphy, Z., Hayden, M. R., & Leavitt, B. R. (2006). Wild-type huntingtin ameliorates striatal neuronal atrophy but does not prevent other abnormalities in the YAC128 mouse model of Huntington disease. *BMC Neuroscience*, *7*(1), 80. http://doi.org/10.1186/1471-2202-7-80

Van Raamsdonk, J. M., Pearson, J., Slow, E. J., Hossain, S. M., Leavitt, B. R., & Hayden, M. R. (2005). Cognitive dysfunction precedes neuropathology and motor abnormalities in the YAC128 mouse model of Huntington's disease. *The Journal of Neuroscience : the Official Journal of the Society for Neuroscience*, *25*(16), 4169–4180. http://doi.org/10.1523/JNEUROSCI.0590-05.2005

Veenhuizen, R. B., Kootstra, B., Vink, W., Posthumus, J., van Bekkum, P.,

Zijlstra, M., & Dokter, J. (2011). Coordinated multidisciplinary care for ambulatory Huntington's disease patients. Evaluation of 18 months of implementation. *Orphanet Journal of Rare Diseases*, *6*(1), 77. http://doi.org/10.1186/1750-1172-6-77

Viganò, F., & Dimou, L. (2016). The heterogeneous nature of NG2-glia, 1–9. http://doi.org/10.1016/j.brainres.2015.09.012

Viganò, F., Möbius, W., Götz, M., & Dimou, L. (2013). Transplantation reveals regional differences in oligodendrocyte differentiation in the adult brain. *Nature Publishing Group*, *16*(10), 1370–1372. http://doi.org/10.1038/nn.3503

Vinolo, M. A. R., Rodrigues, H. G., Nachbar, R. T., & Curi, R. (2011). Regulation of inflammation by short chain fatty acids. *Nutrients*, *3*(10), 858–876. http://doi.org/10.3390/nu3100858

Viola, G. G., Rodrigues, L., Américo, J. C., Hansel, G., Vargas, R. S., Biasibetti, R., et al. (2009). Morphological changes in hippocampal astrocytes induced by environmental enrichment in mice. *Brain Research*, *1274*(C), 47–54. http://doi.org/10.1016/j.brainres.2009.04.007

Vonsattel, J. P. G. (2007). Huntington disease models and human neuropathology: similarities and differences. *Acta Neuropathologica*, *115*(1), 55–69. http://doi.org/10.1007/s00401-007-0306-6

Wade, A., Jacobs, P., & Morton, A. J. (2008). Atrophy and degeneration in sciatic nerve of presymptomatic mice carrying the Huntington's disease mutation. *Brain Research*, *1188*, 61–68. http://doi.org/10.1016/j.brainres.2007.06.059

Wake, H., Lee, P. R., & Fields, R. D. (2011). Control of Local Protein Synthesis and Initial Events in Myelination by Action Potentials. *Science*, *333*(6049), 1647–1651. http://doi.org/10.1126/science.1206998

Wake, H., Ortiz, F. C., Woo, D. H., Lee, P. R., Angulo, M. I. A. C., & Fields, R. D. (2015). Nonsynaptic junctions on myelinating glia promote preferential myelination of electrically active axons. *Nature Communications*, *6*, 1–9. http://doi.org/10.1038/ncomms8844

Walhovd, K. B., Johansen-Berg, H., & Káradóttir, R. T. (2014). Review unraveling the secrets of white matter – bridging the gap between cellular, animal and human imaging studies. *Neuroscience*, *276*(C), 2–13. http://doi.org/10.1016/j.neuroscience.2014.06.058

Walker, F. O. (2007). Huntington's disease. *Lancet (London, England)*, *369*(9557), 218–228. http://doi.org/10.1016/S0140-6736(07)60111-1

Waly, El, B., Macchi, M., Cayre, M., & Durbec, P. (2014). Oligodendrogenesis in the normal and pathological central nervous system. *Frontiers in Neuroscience*, *8*(147), 145. http://doi.org/10.3389/fnins.2014.00145

Wang, L., Lin, F., Wang, J., Wu, J., Han, R., Zhu, L., et al. (2012). Expression of mutant N-terminal huntingtin fragment (htt552-100Q) in astrocytes suppresses the secretion of BDNF. *Brain Research*, *1449*, 69–82. http://doi.org/10.1016/j.brainres.2012.01.077

Wang, S., & Young, K. M. (2014). Review white matter plasticity in adulthood. *Neuroscience*, *276*(C), 148–160. http://doi.org/10.1016/j.neuroscience.2013.10.018

Wang, Y., & Kasper, L. H. (2014). The role of microbiome in central nervous

system disorders, 1–12. http://doi.org/10.1016/j.bbi.2013.12.015
Watkins, T. A., Emery, B., Mulinyawe, S., & Barres, B. A. (2008). Distinct stages of myelination regulated by gamma-secretase and astrocytes in a rapidly myelinating CNS coculture system. *Neuron*, *60*(4), 555–569. http://doi.org/10.1016/j.neuron.2008.09.011
Waxman, S. G. (1980). Determinants of conduction velocity in myelinated nerve fibers. *Muscle & Nerve*, *3*(2), 141–150. http://doi.org/10.1002/mus.880030207
Wellington, C. L., Ellerby, L. M., Gutekunst, C.-A., Rogers, D., Warby, S., Graham, R. K., et al. (2002). Caspase cleavage of mutant huntingtin precedes neurodegeneration in Huntington's disease. *The Journal of Neuroscience : the Official Journal of the Society for Neuroscience*, *22*(18), 7862–7872.
Wellington, C. L., Leavitt, B. R., & Hayden, M. R. (2000). Huntington disease: new insights on the role of huntingtin cleavage. *Journal of Neural Transmission. Supplementum*, (58), 1–17.
Werner, H. B., Krämer-Albers, E.-M., Strenzke, N., Saher, G., Tenzer, S., Ohno-Iwashita, Y., et al. (2013). A critical role for the cholesterol-associated proteolipids PLP and M6B in myelination of the central nervous system. *Glia*, *61*(4), 567–586. http://doi.org/10.1002/glia.22456
Westlye, L. T., Walhovd, K. B., Dale, A. M., Bjornerud, A., Due-Tonnessen, P., Engvig, A., et al. (2010). Life-Span Changes of the Human Brain White Matter: Diffusion Tensor Imaging (DTI) and Volumetry. *Cerebral Cortex*, *20*(9), 2055–2068. http://doi.org/10.1093/cercor/bhp280
Wexler, N. S., Collett, L., Wexler, A. R., Rawlins, M. D., Tabrizi, S. J., Douglas, I., et al. (2016). Incidence of adult Huntington's disease in the UK: a UK-based primary care study and a systematic review. *BMJ Open*, *6*(2), e009070. http://doi.org/10.1136/bmjopen-2015-009070
Whitman, W. B., Coleman, D. C., & Wiebe, W. J. (1998). Prokaryotes: The unseen majority. *Proceedings of the National Academy of Sciences*, *95*(12), 6578–6583. http://doi.org/10.1073/pnas.95.12.6578
Wiggins, R. C. (1986). Myelination: a critical stage in development. *Neurotoxicology*, *7*(2), 103–120.
Wild, E., Magnusson, A., Lahiri, N., Krus, U., Orth, M., Tabrizi, S. J., & Björkqvist, M. (2011). Abnormal peripheral chemokine profile in Huntington’s disease. *PLoS Currents*, *3*, RRN1231. http://doi.org/10.1371/currents.RRN1231
Wilkins, A., Majed, H., Layfield, R., Compston, A., & Chandran, S. (2003). Oligodendrocytes promote neuronal survival and axonal length by distinct intracellular mechanisms: a novel role for oligodendrocyte-derived glial cell line-derived neurotrophic factor. *The Journal of Neuroscience : the Official Journal of the Society for Neuroscience*, *23*(12), 4967–4974.
Wilson, R. S., Krueger, K. R., Arnold, S. E., Schneider, J. A., Kelly, J. F., Barnes, L. L., et al. (2007). Loneliness and risk of Alzheimer disease. *Archives of General Psychiatry*, *64*(2), 234–240. http://doi.org/10.1001/archpsyc.64.2.234
Wood, N. I., Carta, V., Milde, S., Skillings, E. A., McAllister, C. J., Ang, Y. L. M., et al. (2010). Responses to Environmental Enrichment Differ with Sex and Genotype in a Transgenic Mouse Model of Huntington's Disease. *PLoS ONE*, *5*(2), e9077–16. http://doi.org/10.1371/journal.pone.0009077

Wood, N. I., Glynn, D., & Morton, A. J. (2011). â€œBrain trainingâ€ improves cognitive performance and survival in a transgenic mouse model of Huntington's disease. *Neurobiology of Disease*, *42*(3), 427–437. http://doi.org/10.1016/j.nbd.2011.02.005

Wostmann, B. S. (1981). The Germfree Animal in Nutritional Studies. *Annual Review of Nutrition*, *1*(1), 257–279. http://doi.org/10.1146/annurev.nu.01.070181.001353

Xiang, Z., Valenza, M., Cui, L., Leoni, V., Jeong, H. K., Brilli, E., et al. (2011). Peroxisome-Proliferator-Activated Receptor Gamma Coactivator 1 Contributes to Dysmyelination in Experimental Models of Huntington's Disease. *Journal of Neuroscience*, *31*(26), 9544–9553. http://doi.org/10.1523/JNEUROSCI.1291-11.2011

Xiao, L., Ohayon, D., McKenzie, I. A., Sinclair-Wilson, A., Wright, J. L., Fudge, A. D., et al. (2016). Rapid production of new oligodendrocytes is required in the earliest stages of motor-skill learning. *Nature Neuroscience*, *19*(9), 1210–1217. http://doi.org/10.1038/nn.4351

Xin, M., Yue, T., Ma, Z., Wu, F.-F., Gow, A., & Lu, Q. R. (2005). Myelinogenesis and axonal recognition by oligodendrocytes in brain are uncoupled in Olig1-null mice. *The Journal of Neuroscience : the Official Journal of the Society for Neuroscience*, *25*(6), 1354–1365. http://doi.org/10.1523/jneurosci.3034-04.2005

Yanai, A., Huang, K., Kang, R., Singaraja, R. R., Arstikaitis, P., Gan, L., et al. (2006). Palmitoylation of huntingtin by HIP14 is essential for its trafficking and function. *Nature Neuroscience*, *9*(6), 824–831. http://doi.org/10.1038/nn1702

Yang, S., Li, C., Qiu, X., Zhang, L., Lu, W., Chen, L., et al. (2013). Effects of an enriched environment on myelin sheaths in the white matter of rats during normal aging: A stereological study. *Neuroscience*, *234*(C), 13–21. http://doi.org/10.1016/j.neuroscience.2013.01.003

Yang, Y., Raine, A., Colletti, P., Toga, A. W., & Narr, K. L. (2009). Abnormal temporal and prefrontal cortical gray matter thinning in psychopaths. *Molecular Psychiatry*, *14*(6), 561–2– 555. http://doi.org/10.1038/mp.2009.12

Yano, H., Baranov, S. V., Baranova, O. V., Kim, J., Pan, Y., Yablonska, S., et al. (2014). Inhibition of mitochondrial protein import by mutant huntingtin. *Nature Neuroscience*, *17*(6), 822–831. http://doi.org/10.1038/nn.3721

Yeung, M. S. Y., Zdunek, S., Bergmann, O., Bernard, S., Salehpour, M., Alkass, K., et al. (2014). Dynamics of Oligodendrocyte Generation and Myelination in the Human Brain. *Cell*, *159*(4), 766–774. http://doi.org/10.1016/j.cell.2014.10.011

Yi, C.-X., & Tschöp, M. H. (2012). Brain-gut-adipose-tissue communication pathways at a glance. *Disease Models & Mechanisms*, *5*(5), 583–587. http://doi.org/10.1242/dmm.009902

Yi, P., & Li, L. (2012). The germfree murine animal: an important animal model for research on the relationship between gut microbiota and the host. *Veterinary Microbiology*, *157*(1-2), 1–7. http://doi.org/10.1016/j.vetmic.2011.10.024

Yin, X., Crawford, T. O., Griffin, J. W., Tu, P. H., Lee, V. M., Li, C., et al. (1998). Myelin-associated glycoprotein is a myelin signal that modulates

the caliber of myelinated axons. *Journal of Neuroscience*, *18*(6), 1953–1962.
Yokote, H., Miyake, S., Croxford, J. L., Oki, S., Mizusawa, H., & Yamamura, T. (2010). NKT Cell-Dependent Amelioration of a Mouse Model of Multiple Sclerosis by Altering Gut Flora. *The American Journal of Pathology*, *173*(6), 1714–1723. http://doi.org/10.2353/ajpath.2008.080622
Young, K. M., Psachoulia, K., Tripathi, R. B., Dunn, S.-J., Cossell, L., Attwell, D., et al. (2013). Oligodendrocyte Dynamics in the Healthy Adult CNS: Evidence for Myelin Remodeling. *Neuron*, *77*(5), 873–885. http://doi.org/10.1016/j.neuron.2013.01.006
Yuan, P., & Raz, N. (2014). Prefrontal cortex and executive functions in healthy adults: a meta-analysis of structural neuroimaging studies. *Neuroscience and Biobehavioral Reviews*, *42*, 180–192. http://doi.org/10.1016/j.neubiorev.2014.02.005
Zatorre, R. J., Fields, R. D., & Johansen-Berg, H. (2012). Plasticity in gray and white: neuroimaging changes in brain structure during learning. *Nature Neuroscience*, *15*(4), 528–536. http://doi.org/10.1038/nn.3045
Zeron, M. M., Hansson, O., Chen, N., Wellington, C. L., Leavitt, B. R., Brundin, P., et al. (2002). Increased Sensitivity to N-Methyl-D-Aspartate Receptor-Mediated Excitotoxicity in a Mouse Model of Huntington's Disease. *Neuron*, *33*(6), 849–860. http://doi.org/10.1016/S0896-6273(02)00615-3
Zhang, J., & Jiao, J. (2015). Review Article Molecular Biomarkers for Embryonic and Adult Neural Stem Cell and Neurogenesis. *BioMed Research International*, 1–14. http://doi.org/10.1155/2015/727542
Zhao, Y.-Y., Shi, X.-Y., Qiu, X., Lu, W., Yang, S., Li, C., et al. (2012). Enriched Environment Increases the Myelinated Nerve Fibers of Aged Rat Corpus Callosum. *The Anatomical Record: Advances in Integrative Anatomy and Evolutionary Biology*, *295*(6), 999–1005. http://doi.org/10.1002/ar.22446
Zhao, Y.-Y., Shi, X.-Y., Qiu, X., Zhang, L., Lu, W., Yang, S., et al. (2011). Enriched environment increases the total number of CNPase positive cells in the corpus callosum of middle-aged rats. *Acta Neurobiologiae Experimentalis*, *71*(3), 322–330.
Zheng, J., Ding, W., Li, B., & Yang, Y. (2017). Enriched environment promotes remyelination and motor function recovery through modulation of HDAC1/2 in mice. *Neuroscience Letters*, 1–31. http://doi.org/10.1016/j.neulet.2017.06.039
Zhu, B., Wang, X., & Li, L. (2010). Human gut microbiome: the second genome of human body. *Protein & Cell*, *1*(8), 718–725. http://doi.org/10.1007/s13238-010-0093-z
Zhu, X., Hill, R. A., Dietrich, D., Komitova, M., Suzuki, R., & Nishiyama, A. (2011). Age-dependent fate and lineage restriction of single NG2 cells. *Development*, *138*(4), 745–753. http://doi.org/10.1242/dev.047951
Zhu, X.-R., Maskri, L., Herold, C., Bader, V., Stichel, C. C., Güntürkün, O., & Lübbert, H. (2007). Non-motor behavioural impairments in parkin-deficient mice. *European Journal of Neuroscience*, *26*(7), 1902–1911. http://doi.org/10.1111/j.1460-9568.2007.05812.x
Zinzi, P., Salmaso, D., De Grandis, R., Graziani, G., Maceroni, S.,

Bentivoglio, A., et al. (2007). Effects of an intensive rehabilitation programme on patients with Huntington's disease: a pilot study. *Clinical Rehabilitation*, *21*(7), 603–613. http://doi.org/10.1177/0269215507075495

Zuccato, C., & Cattaneo, E. (2009). Brain-derived neurotrophic factor in neurodegenerative diseases. *Nature Reviews Neurology*, *5*(6), 311–322. http://doi.org/10.1038/nrneurol.2009.54

Zuchero, J. B., & Barres, B. A. (2015). Glia in mammalian development and disease. *Development*, *142*(22), 3805–3809. http://doi.org/10.1242/dev.129304

Appendix

Appendix A. Solutions

Paraformaldehyde (PFA)

1L of 1xPBS was placed in a 65^{o}C water bath for 20-30min. For tissue staining purposes, 4% PFA, 40g of PFA and 3 pieces of NaOH (to aid clarification) was added to 1L of PBS. Otherwise, for TEM purposes, 2.5% paraformaldehyde (PFA, see Appendix xxxx) and 2.5% glutaraldehyde (GlutAH), and 3 pieces of NaOH were added to 1L of PBS. The solution was stirred for ~30min under a fume hood until solution temperature reached 60^{o}C. The solution was then placed on ice for 15 minutes, after which the pH is measured and adjusted to 7.4 using HCl. Finally, the PFA solution was filtered using a filter pump.

Hydrochloric acid (HCl)

Using a normality and molarity calculator, the stock solution of HCl was calculated to be 12.178 N based on a density of 1.2 g/mL, a formula weight of 36.46 g/mol, and a concentration of 37% w/w. Depending on the desired concentration (1N or 2N) the stock solution (8.212 mL for 1N, and 16.423 mL for 2N) was slowly added to 25 mL deionized water. The final volume of solution was adjusted to 100 mL with deionized water.

Appendix B. Western blots

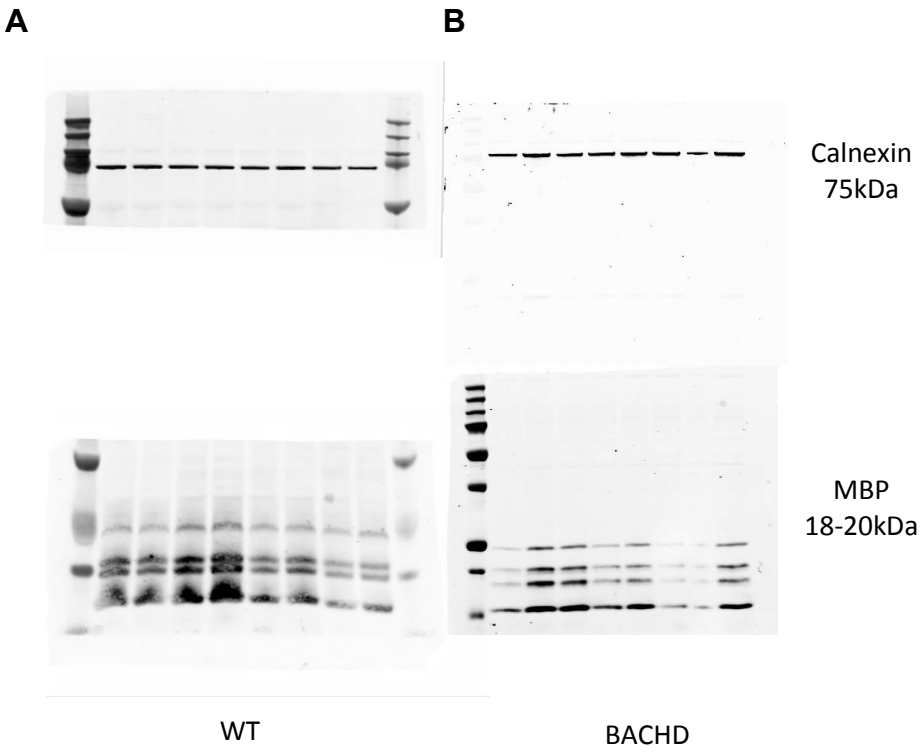

With reference to figure 5.11.

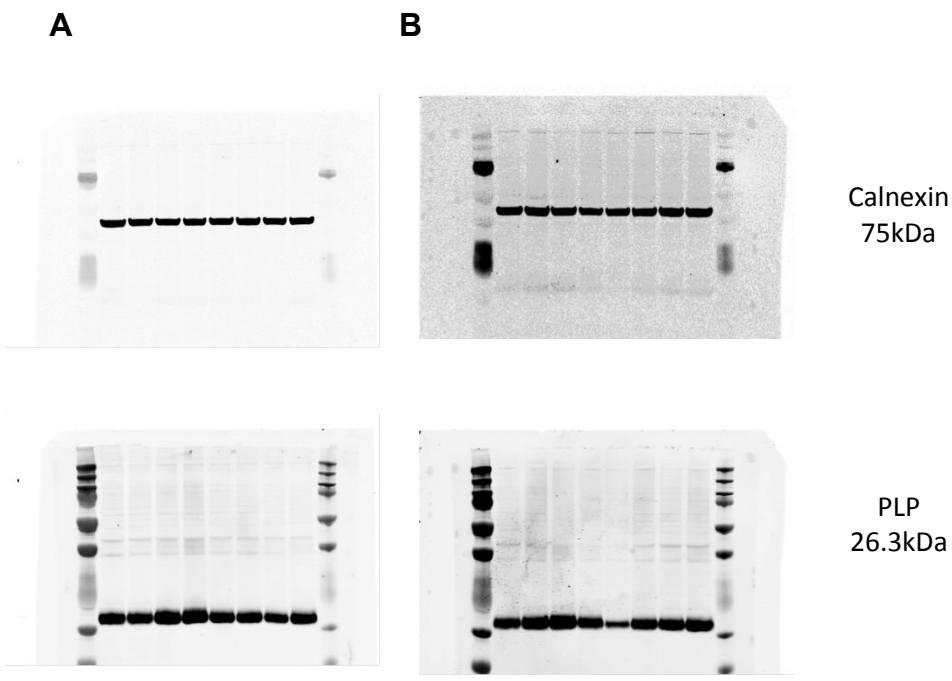

With reference to figure 5.12

“When it all goes quiet behind my eyes, I see everything that made me lying around in invisible pieces. When I look too hard, it goes away. And when it all goes quiet, I see they are right here. I see that I'm a little piece in a big, big universe. And that makes things right. When I die, the scientists of the future, they're gonna find it all.” - Hushpuppy, Beasts of the Southern Wild (Benh Zeitlin, 2012)